Exploring the role of pipecolic acid in defence priming and inducible immunity in *Arabidopsis thaliana* (L.) Heynh.

Inaugural-Dissertation

zur Erlangung des Doktorgrades
der Mathematisch-Naturwissenschaftlichen Fakultät
der Heinrich-Heine-Universität Düsseldorf

vorgelegt von

Anne-Christin Döring

aus Aschersleben

Düsseldorf, Mai 2015

aus dem Institut für molekulare Ökophysiologie der Pflanzen
der Heinrich-Heine-Universität Düsseldorf

Gedruckt mit der Genehmigung der
Mathematisch-Naturwissenschaftlichen Fakultät der
Heinrich-Heine-Universität Düsseldorf

Referent: Prof. Dr. Jürgen Zeier

Korreferent: Prof. Dr. Michael Feldbrügge

Tag der mündlichen Prüfung: 4. September 2015

Table of contents

List of figures

List of tables

Supplemental figures

Abbrevations

Aad	*α*-Aminoadipic acid
ABA	Abscisic acid
AGO	Argonaute
ALD1	*AGD2-LIKE DEFENCE RESPONSE PROTEIN 1*
Arg	Arginine
AS	Anthranilate synthase
Asp	Aspartic acid
Avr	Avirulence
BABA	*ß*-Aminobutyric acid
BAK	*BRASSINOSTEROID INSENSITIVE 1-ASSOCIATED KINASE*
Bc	*Botrytis cinerea*
BIK	*BOTRYTIS-INDUCED KINASE*
BRI	*BRASSINOSTEROID-INSENSITIVE*
BSA	Bovine serumalbumine
BSMT	*SAM-dependent carboxyl methyltransferase*
BTH	Benzothiadiazole-7-carbothioc acid S-methylester
°C	Degree Celsius
Ca^{2+}	Calcium^{2+} ion
CaMV	Cauliflower mosaic virus
CC	Coiled-coil
cDNA	Complementary DNA
CEV1	*CONSTITUTIVE EXPRESSION OF VSP 1*
CFA	Coronafacic acid
cfu	Colony forming units
CM	Chorismate mutase
CMA	Coronamic acid
COI	*CORONATINE INSENSITIVE*
COR	Coronatine
cp	Conidiophores
Ct	Cycle threshold
DAMP	Damage-associated molecular pattern
DEX	Dexamethasone
dpi	days post infection
DSP	Dual specificity phosphatase
DTT	Dithiothreitol
E	Efficiency
EDR	*ENHANCED DISEASE RESISTANCE*
EDS	*ENHANCED DISEASE SUSCEPTIBILITY*
EDTA	Ethylendiaminetetraacetic acid
EFR	Elongation factor Tu receptor
EF-Tu	Elongation factor Tu
EGTA	Ethylene glycol tetraacetic acid
EIL1	*ETHYLENE INSENSENSITIVE-LIKE1*
EIN	*ETHYLENE INSENSITIVE*
elf18	EF-Tu epitope 18

ET	Ethylene
ETI	Effector-triggered immunity
ETR	*ETHYLENE RECEPTOR*
ETS	Effector-triggered susceptibility
FAD	Flavin adenine dinucleotide
flg22	Flagellin epitope 22
FLS2	*FLAGELLIN SENSING 2*
FMO1	*FLAVIN-DEPENDENT MONOOXYGENASE 1*
FW	Fresh weight
GABA	*γ*-Aminobutyric acid
gl1	*Glabra1*
Go	*Golovinomyces orontii*
GS/GOGAT	Glutamine synthetase/glutamate synthase
GST	Gluthathione S-transferase
h	Hours
HAC1	*HISTONE ACETYLTRANSFERASE1*
Hpa	*Hyaloperonospora arabidopsidis*
hpi	Hours post inoculation
HR	Hypersensitive response
hy	Hyphae
IAA	Indole acetic acid
IAN	Indole-3-acetonitrile
IAOx	Indole-3-acetaldoxime
ICA	Indole-3-carboxylic acid
ICS1	*ISOCHORISMATE SYNTHASE 1*
INA	2,6-Dichloroisonicotinic acid
IPA	Indolepropionic acid
IR	Induced resistance
ISR	Induced systemic resistance
JA	Jasmonic acid
JA-Ile	Jasmonate-Isoleucine
JAZ	Jasmonate ZIM domain
Leu	Leucine
LKR	Lysine ketoglutarate reductase
LPS	Lipopolysaccharides
LRR	Leucine-rich repeat
Lys	Lysine
M	Mol l^{-1}
MAMP	Microbe-associated molecular pattern
MAP	Mitogen-activated protein
MAPK	MAP kinase
MeJA	Methyl jasmonate
MeSA	Methylsalicylate
MKKK/MEK	MAP kinase kinase kinase
mRNA	Messenger RNA
MS	Murashige & Skoog
NADPH	Nicotinamide adenine dinucleotide phosphate

NB	Nucleotide-binding site domain
NB-LRR	Nucleotide-binding – leucine rich repeats
NDR1	*NON RACE SPECIFIC DISEASE RESISTANCE 1*
NIMIN	*NON-INDUCIBLE IMMUNITY 1 (NIM1-) INTERACTING*
NPR1	*NON-EXPRESSOR OF PR GENES1*
OD	Optical density
oo	Oospores
Orn	Ornithine
PAD	*PHYTOALEXIN DEFICIENT*
PAL	*PHENYLALANINE AMMONIA-LYASE*
PAMP	Pathogen-associated molecular pattern
PBS3	*AvrPphB SUSCEPTIBLE 3*
PCD	Programmed cell death
PCR	Polymerase chain reaction
PDF1.2	Plant defensin
PEN2	*PENETRATION2*
PGN	Peptidoglycan
Pip	Pipecolic acid
PR-1	*PATHOGENESIS-RELATED PROTEIN1*
PRR	Pattern recognition receptors
Psm	*Pseudomonas syringae* pv. *maculicola* ES4326
Psm avrRpm1	*Psm* carrying the avirulence gene pLAFR3::avrRpm1
Pst	*Pseudomonas syringae* pv. *tomato*
PTI	PAMP-triggered immunity
PTP	Protein tyrosine phosphatase
qPCR	Quantitative Real-Time PCR
R	Resistance
RIN4	*RPM1-INTERACTING PROTEIN 4*
RIPK	*RPM1 INDUCED PROTEIN KINASE*
RK	Receptor kinase
RLK	Receptor-like kinase
RLP	Receptor-like proteins
RNAi	RNA interference
ROS	Reactive oxygen species
rpm	Revolutions per minute
RPP	*RESISTANCE TO PERONOSPORA PARASITICA*
RPW	*RESISTANCE TO POWDERY MILDEW*
RT	Retention time
SA	Salicylic acid
SAG	Glycosylated form of SA
SAR	Systemic acquired resistance
SD	Standard deviation
SDH	Saccharopine dehydrogenase
SDS-PAGE	Sodium dodecyl sulfate-polyacrylamide gelelectrophoresis
Ser	Serine
SID	*SALICYLIC ACID INDUCTION DEFICIENT*
sRNA	Small RNA

TAE	Tris-acetate-ethylenediamine tetraacetic acid
TB	Lactophenol/trypanblue
T-DNA	Transfer DNA
Thr	Threonine
TTSS	Type-III secretion system
Tyr	Tyrosine
UDP	Uridine diphosphate
WT	Wild type
1°	Local inoculated tissue
2°	Systemic inoculated tissue

1 Summary

Plants are capable to defend themselves against diverse microbial pathogens and can also establish a long-lasting protection of the whole plant body, called systemic acquired resistance (SAR), which provides elevated immunity against a variety of pathogens and primes plants for subsequent attacks. In this work, the molecular mechanisms of defence priming and its role in SAR, as well as the importance of pipecolic acid (Pip) in plant priming and immunity, were analysed in *Arabidopsis thaliana*. Evidence is provided that accumulation of the non-protein amino acid Pip, whose biosynthesis is catalyzed by the *AGD2-LIKE DEFENCE RESPONSE PROTEIN 1* (*ALD1*), and its activation by the flavin-dependent monooxygenase FMO1 is essential for defence priming, as priming of gene expression is almost completely abolished in *ald1* and *fmo1* mutant lines. Moreover, a large number of genes primed for enhanced expression was found to be independent of salicylic acid (SA)-mediated signalling and could be classified according to their role in detoxification, defence signalling, defence metabolism, and cell wall-related processes. Pip was furthermore shown to be essential for primed expression of SA-dependent and -independent genes. Mitogen-activated protein (MAP) kinase signalling was previously implied as being essential for defence priming and SAR, but SAR, as well as Pip-induced resistance, and priming of gene expression were not significantly impaired in *mpk3, mpk6*, and *mpk3 mpk6* mutant plants infected with *Pseudomonas syringae* pv. *maculicola* (*Psm*) bacteria. This thesis provides proof that Pip not only accumulates upon bacterial infection, but also after infection with the fungi *Botrytis cinerea* and *Golovinomyces orontii*, as well as the oomycete *Hyaloperonospora arabidopsidis*. Analysis of these diverse plant-microbe interactions led to the discovery of a number of so far unknown or uncommon metabolites, whose accumulation seemed to be in part very specific for each interaction. Furthermore, metabolite profiles differed strongly depending on the lifestyle of the infecting microbe. This work also shows that exogenously applied Pip is able to induce resistance in Col-0 and *ald1* against the necrotrophic fungus *B. cinerea* and the biotrophic downy mildew *H. arabidopsidis*, but not the biotrophic powdery mildew *G. orontii*.

2 Zusammenfassung

Pflanzen sind nicht nur in der Lage, sich in Folge eines Angriffs durch verschiedene pathogene Mikroorganismen gegen diese zu verteidigen, sie können auch einen lang anhaltenden Schutz aufbauen, der sich auf den gesamten Pflanzenkörper erstreckt. Dieser Schutz wird als systemisch erworbene Resistenz (systemic acquired resistance; SAR) bezeichnet und rüstet die Pflanze gegen eine Vielfalt von Pathogenen. In dieser Arbeit wurden die Mechanismen des „defence priming“ und dessen Rolle in der SAR, sowie die Bedeutung der Pipecolinsäure (Pip) für dieses priming und die pflanzliche Abwehr untersucht. Es wird gezeigt, dass die *ALD1*-vermittelte Akkumulation der nicht-proteinogenen Aminosäure Pip und ihre Aktivierung durch die Flavin-abhängige Monooxygenase FMO1 essentiell für „defence priming“ ist, da das Priming der Genexpression in den Mutantenlinien *ald1* und *fmo1* fast komplett ausbleibt. Eine große Anzahl der Gene, die Priming zeigten, erwies sich in ihrer Expression als unabhängig von der Akkumulation von Salicylsäure (SA) und konnte außerdem den Kategorien „Detoxifizierung“, „Signalprozesse der Verteidigung“, „Aufbau von Verteidigungsrelevanten Metaboliten“, und „in Zellwand-Prozesse involviert“ zugeordnet werden. Außerdem konnte demonstriert werden, dass für ausgewählte SA-abhängige und –unabhängige Gene die Akkumulation von Pip unerlässlich für geprimte Expression ist. In einigen Veröffentlichungen wurde den Mitogen-aktivierten Protein (MAP) Kinase Signalkaskaden eine wichtige Rolle in der SAR und im Priming zugesprochen, jedoch zeigt diese Arbeit, dass die Mutantenlinien *mpk3, mpk6*, und *mpk3 mpk6* weder in der SAR-Antwort, der Pip-induzierten Resistenz, oder der Primingantwort behindert sind, wenn sie mit *P. syringae* pv. *maculicola* Bakterien infiziert werden. Diese Dissertation liefert außerdem Beweise, dass Pip nicht nur nach Infektion mit Bakterien, sondern auch nach Infektion mit den Pilzen *B. cinerea* und *G. orontii* und dem Oomyceten *H. arabidopsidis* in infizierten Blättern akkumuliert. Pipecolinsäure ist ebenfalls fähig, Verteidigungsmechanismen gegen *B. cinerea* und *H. arabidopsidis*, jedoch nicht gegen *G. orontii,* zu aktivieren. Metabolitenanalysen nach Infektion von *Arabidopsis* Pflanzen mit diesen Pathogenen führte zur Entdeckung teils unbekannter Metabolite, deren Akkumulation relativ spezifisch für die einzelnen Interaktionen schienen. Auch ist das Profil der Metabolitenakkumulation stark abhängig vom Lebensstil des infizierenden Mikroorganismus.

3 Introduction

3.1 Plant life –surviving in an adverse environment

Plants are very important life-forms on our planet, converting energy from the sun into chemical energy and thus representing a fundamental food source for humans and animals alike. As sessile organisms, they are subject to a great number of environmental influences, including abiotic factors –like light and water availability– and biotic factors –for example interactions with insects and microbes in the soil. Because plants are not able to flee in case of danger, they have evolved a complex system to perceive possible sources of peril and are by no means defenceless in the event of an attack. Upon closer inspection of a plant´s environment, it is surprising that despite being surrounded by a multitude of different microbe species, only a very small number of these microbes are pathogenic towards plants and able to use the plants´ resources for their own benefit. This is due to structural and chemical defence features of plants that a pathogen has to overcome and adapt to. Structural, or preformed, barriers include trichomes on stem and leaves of the plant, antimicrobial enzymes, secondary metabolites, and the presence of a distinct cuticle, a layer of wax on aerial parts of the plant, and additionally plant cells can be reinforced with callose (Thordal-Christensen, 2003; Spoel and Dong, 2012; Figure 1). These structural barriers are mostly directed against insect and herbivore threats to the aerial parts of plants, but can also be effective against microbial pathogens. For a number of pathogens it was shown previously that they need to detect particular components in the composition of the plant cuticle to recognize their host. If they fail to perceive plant chemical or topographical cues and thus do not differentiate, plant colonisation is not possible (Thordal-Christensen, 2003; Figure 1). For example, the barley pathogen *Blumeria graminis*, a fungus that can also infect maize, detects its host by the presence of very-long-chain aldehydes in cuticular waxes and is not able to infect mutated maize plants with these aldehydes missing (Hansjakob *et al*., 2011). In addition to preformed barriers, active defence responses can also be induced upon perception of a possible threat. Plants are able to recognize microbial elicitors, for example peptidoglycan, lipopolysaccharides, chitin and bacterial flagellin (Spoel and Dong, 2012). Recognition of these microbe-associated molecular patterns (MAMPs) by pattern recognition receptors (PRRs) induces pattern-triggered immunity (PTI), which can be elicited by nonhost and host pathogens alike and is distinguished by a medium-strong defence reaction of the plant (Thordal-Christensen, 2003; Jones and Dangl, 2006; Spoel and Dong, 2012; Figure 2; Figure 3). A number of biotrophic pathogens have to establish close interactions with plant cells to gain nutrients and have to be able to repress these plant defence reactions in order to survive (Figure 1).

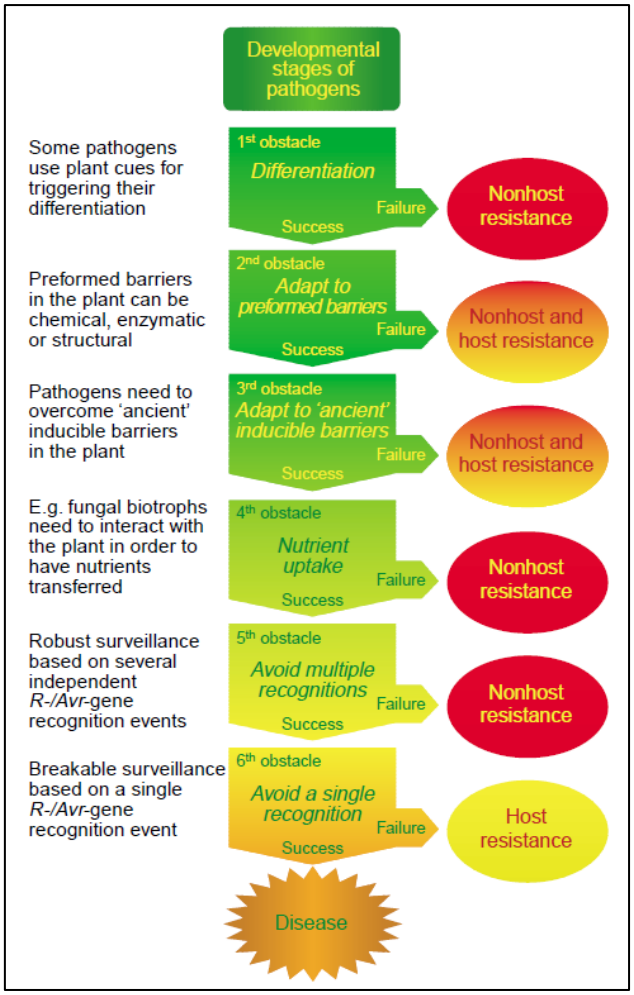

Figure 1. Schematic overview of challenges a pathogen has to overcome to cause plant infection.

In order to infect a plant, the attacking microbe has to overcome different layers of preformed and inducible plant resistance mechanisms (Thordal-Christensen, 2003).

To be able to overcome PTI, pathogens deliver effectors into plant cells to suppress defence reactions. In the course of co-evolution, plants have developed intracellular immune receptors, so called R proteins, that are able to recognize these effectors and initiate defence responses (Thordal-Christensen, 2003; Jones and Dangl, 2006; Spoel and Dong, 2012). Detection of bacterial effectors by these "avirulence" proteins, for instance, activates effector-triggered immunity (ETI), which leads to a hypersensitive response (HR) and programmed cell death of affected cells (Spoel and Dong, 2012). Only if the pathogen is able to overcome all defence lines, it will be able to infect the plant and exploit it for nutrients.

3.2 Molecular principles of innate immunity

To understand molecular mechanisms of plant immunity, *Arabidopsis thaliana* is prominently used as a model plant. Plants are able to detect extracellular MAMPs, pathogen associated molecular patterns (PAMPs), and damage associated molecular patterns (DAMPs) that accumulate after attack by cell wall-degrading enzymes, as well as extracellular pathogen-

derived effectors (Figure 3). These molecules are detected by membrane-localised PRRs and activation of these receptors invokes a signalling cascade inside the cell that leads to induction of gene expression and often to HR-mediated cell death.

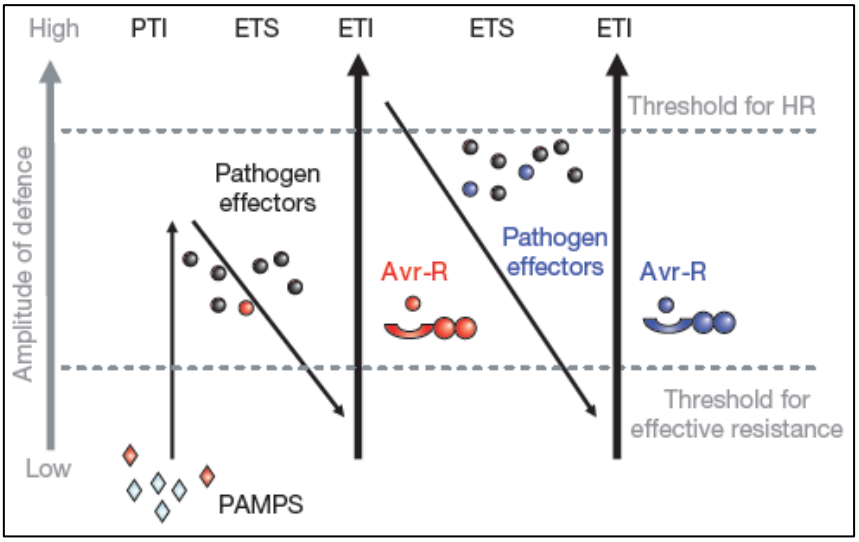

Figure 2. Zig-zag model of plant defence responses.

MAMPs or PAMPs are detected by receptors and induce PTI. Pathogens deliver effectors into plant cells to suppress PTI and induce ETS, detection of these effectors by R-proteins leads to ETI-mediated defence responses. PTI, pattern-triggered immunity; ETS, effector-triggered susceptibility; ETI, effector-triggered immunity; HR, hypersensitive response; PAMPS, pathogen-associated molecular patterns; Avr-R, avirulence protein (Jones and Dangl, 2006).

One well studied example of MAMP detection is perception of flagellin by the leucine-rich repeat transmembrane receptor kinase FLAGELLIN SENSITIVE2 (FLS2), which leads to very fast complex formation consisting of the receptor kinases FLS2 and BRI1-ASSOCIATED KINASE 1 (BAK1) and the receptor-like kinase BOTRYTIS-INDUCED KINASE 1 (BIK1) (Gómez-Gómez and Boller, 2000; Chinchilla *et al*, 2006; Chinchilla *et al*., 2007; Heese *et al*., 2007). This causes phosphorylation of BIK1 by BAK1 (Lin *et al*., 2014) and is followed by activation of a signalling network comprising Ca^{2+}- and mitogen-activated protein kinase (MAPK) signalling, which induces expression of defence-related genes, formation of reactive oxygen species (ROS) and results in HR, destroying infected cells and the revealed attackers with them. To evade detection, phytopathogens have evolved effectors to manipulate host defences and induce effector-triggered susceptibilty (Jones and Dangl, 2006; Figure 2). For bacteria, most of these effectors are introduced by a type III secretion system (TTSS) into plant cells (Bender, 1999; Da Cunha *et al*., 2006; Figure 3). It was shown recently that genes encoding the TTSS system are expressed in *Pseudomonas syringae* shortly after perception of plant-derived signals and that mutated strains without a functioning TTSS are not fully virulent (Anderson *et al*., 2014). Up to 100 different effectors can be secreted into plant cells by a single bacterium (Da Cunha *et al*., 2006), but if only one

of them is detected by a matching “avirulence” protein in the plant, ETI is induced, leading to disease and often results in a HR reaction (Jones and Dangl, 2006).

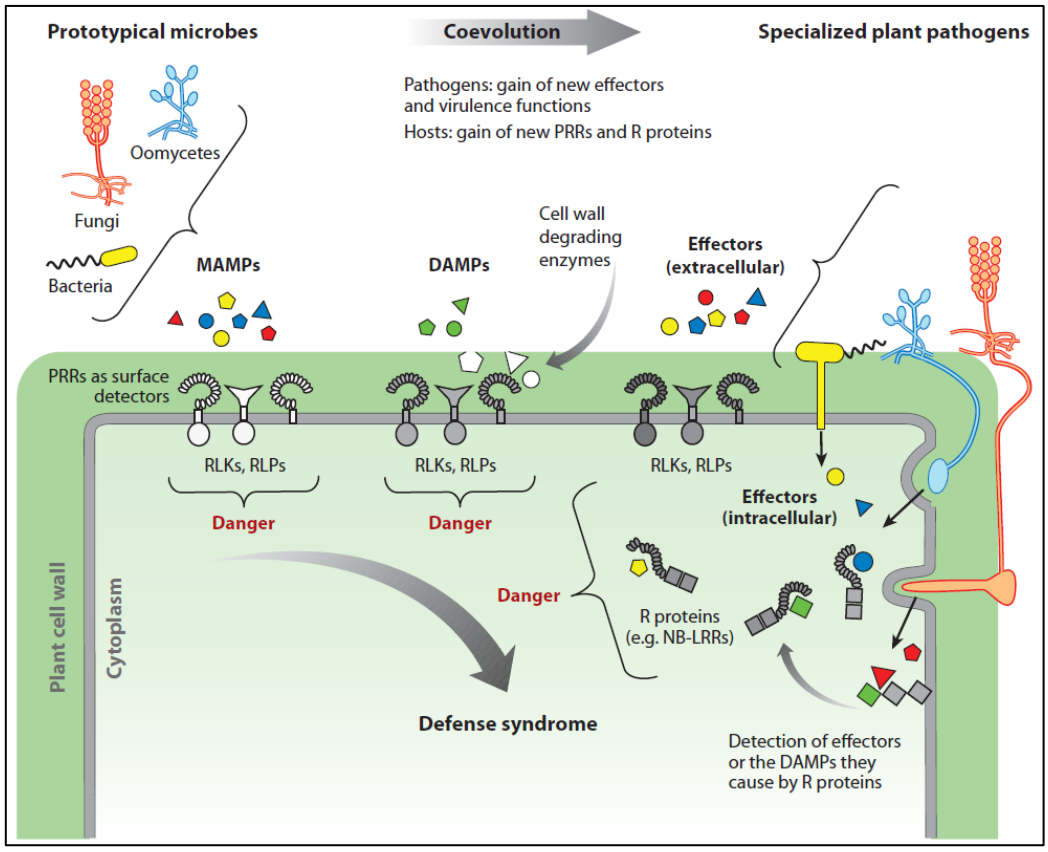

Figure 3. Microbial pattern recognition by plants.

Membrane-located pattern recognition receptors (PRRs) detect microbe-derived MAMPs and plant-derived DAMPs, while cytoplasm-located R-proteins perceive effectors introduced into plant cells by pathogens to repress plant resistance mechanisms. MAMPs, microbe associated molecular patterns; DAMPs, damage associated molecular patterns; RLKs, receptor-like kinases; RLPs, receptor-like proteins; PRRs, pattern recognition receptors; NB-LRR, nucleotide binding-site–leucine-rich repeat (Boller and Felix, 2009).

In the process of co-evolution, pathogens became able to get rid of effectors that are recognized by plants and develop new effectors to repress plant immune responses (Jones and Dangl, 2006; Figure 2). Known *P. syringae*-derived effector proteins are for example AvrRpm1, AvrB, and AvrRpt2 that are perceived by RPM1 and RPS2, respectively, as well as Hop effectors (Underwood *et al*., 2007; Spoel and Dong, 2012; Li *et al*., 2014). Pathogens not only use effectors to actively suppress the HR-reaction in plants, but also to manipulate signalling in infected cells by targeting transcription factors (HopD1; Block *et al*., 2013) and members of signalling cascade pathways, e.g. by actively dephosphorylating MAP kinases (HopAI1; Meng and Zhang, 2013). Effectors are also used by pathogenic microbes to repress callose deposition in plant cells (HopAO1; Underwood *et al*., 2007), prevent stomatal closure (Spoel and Dong, 2012), and severely disturb hormone homeostasis (AvrRpt2; Cui *et al*., 2013; Mutka *et al*., 2013) to facilitate infection. In more recent studies evidence accumulated that extended Flor´s hypothesis of gene-for-gene resistance (Flor, 1942) to the

so-called “guard model” (Figure 4). For instance, the avirulence proteins RPM1 and RPS2 both exhibit interaction with RPM1-INTERACTING PROTEIN4 (RIN4), which is targeted by three different effectors (AvrB, AvrRpm1, AvrRpt2; Axtell and Staskawicz, 2003; Spoel and Dong, 2012). In unchallenged cells, the physical contact of RIN4 with either inactive RPM1 or RPS2 suppresses effector-triggered immunity (Figure 4).

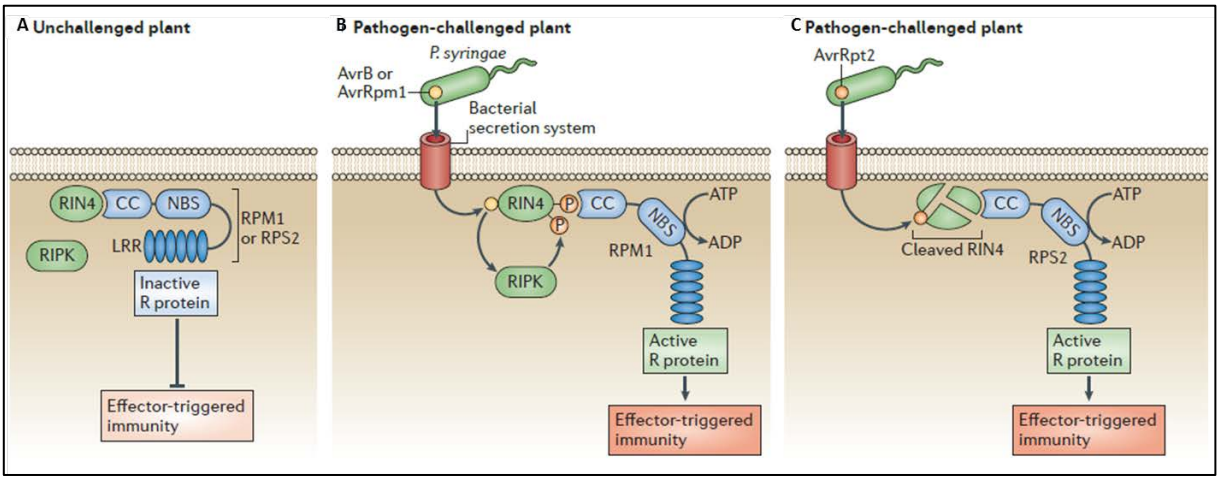

Figure 4. Schematic depiction of the guard model hypothesis.

(A) In naive plants, R proteins containing a CC–NBS–LRR domain structure interact with unmodified RIN4 protein, keeping the R proteins in an inactive state. (B) Upon infection with *P. syringae* bacteria that introduce AvrB or AvrRpm1 effectors into the plant the RIN4 protein is phosphorylated by RPM1 INDUCED PROTEIN KINASE (RIPK), which leads to detection of modified RIN4 by RPM1. Detection of conformational changes in RIN4 induces activation of RPM1 protein and subsequent induction of effector-triggered immunity. (C) Infection with a *P. syringae* strain that injects AvrRpt2 effectors into plant cells leads to degradation of RIN4 protein and subsequent activation of RPS2, which induces effector-triggered immunity (modified from Spoel and Dong, 2012).

In plants infected with *P. syringae* strains producing effector proteins AvrB or ArvRpm1, respectively, the RIN4 protein is targeted by these effectors and subsequently phosphorylated by a RPM1-INDUCED PROTEIN KINASE. This change in phosphorylation status of RIN4 is detected by RPM1 and leads to induction of ETI responses (Spoel and Dong, 2012; Figure 4b). Infection of plants with a *P. syringae* strain carrying the AvrRpt2 effector leads to cleavage of RIN4 protein by AvrRpt2 (Figure 4c). RIN4 physically interacts with RPS2 and RIN4 disappearance subsequently activates RPS2-mediated ETI responses (Axtell and Staskawicz, 2003). Considering the large number of effectors found in *Pseudomonas*, as well as other pathogens, it makes sense for the plant to monitor pathogen-mediated changes in proteins targeted by several different effectors, rather than having RPPs for every effector introduced by pathogens. *P. syringae* not only inserts effectors into plant cells to favour successful infection, but also toxins. These phytotoxins usually induce chlorosis (coronatine, phaseolotoxin, and tabtoxin) or necrosis (syringomycin and syringopeptin) (Bender *et al*., 1999) and despite not being required for infection of plants, act as virulence factors and can severely increase disease. One of these toxins –coronatine, which is composed of the polyketide coronafacic acid (CFA) and coronamic acid (CMA), an

ethylcyclopropyl amino acid derived from isoleucine– was found to be of special interest, as it resembles jasmonate-isoleucine, the bioactive form of jasmonic acid (JA), and is perceived by the JA-receptor CORONATINE INSENSITIVE1 (COI1) (Katsir *et al.*, 2008; Koo *et al.*, 2009; Figure 10).

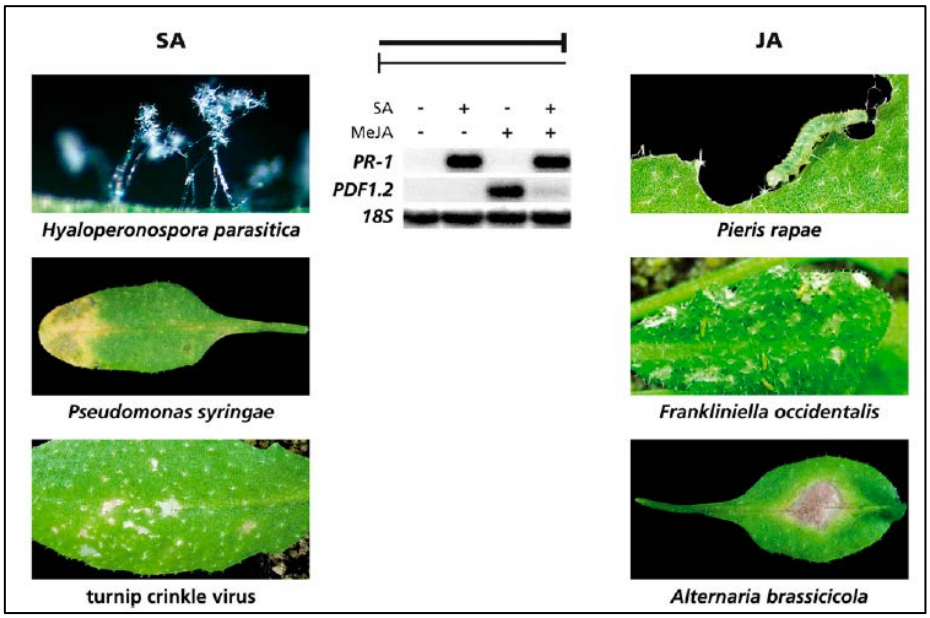

Figure 5. Reciprocal antagonism in SA- and JA-signalling.

SA-mediated defences were described to be effective against (hemi-) biotrophic pathogens like *H. arabidopsidis, P. syringae*, and the turnip crinkle virus. JA-mediated defences are predominantly effective against herbivorous insects and necrotrophic pathogens like *A. brassicicola*. As an indicator for SA- and JA-mediated responses in plants respective gene expression of *PR-1* and *PDF1.2* is typically analysed. Figure modified from Koorneef and Pieterse, 2008.

Activation of the JA-signalling pathway was shown to repress salicylic acid (SA)-mediated signalling (Figure 5), which is effective against (hemi-) biotrophic pathogens and this provides clear evidence that *P. syringae* actively manipulates plant hormone pathways to enable infection.

3.3 Systemic acquired resistance and defence signalling

Besides triggering innate immunity in plant cells, perception of host and nonhost microbes leads to accumulation of defence-related gene products and metabolites. This sets in motion a strongly regulated series of (feedback-) amplification loops and crosstalk between different metabolite pathways and often induces systemic acquired resistance (SAR; Durrant and Dong, 2004), a defence mechanism, which confers broad spectrum resistance to the whole plant foliage after an initial localised leaf infection. SAR is characterised as a combination of preactivated defence reactions and enhanced alertness. Plants in the SAR state demonstrate the ability to react faster and more strongly to subsequent threats by accumulation of active defence compounds or precursors thereof, preactivation of defence signalling pathways, and priming of gene expression. As a central regulator for innate

immunity and SAR, the non-protein amino acid pipecolic acid (Pip) was identified (Návarová *et al.,* 2012). Pip is a lysine derivative, whose biosynthesis is catalysed by the aminotransferase ALD1 (Figure 7) and which is found in locally *P.* syringae-infected leaves as well as in leaves distal from the infection site. Pip regulates plant resistance in locally infected leaves by amplifying defence responses that lead to the accumulation of important defence compounds like SA and the phytoalexin camalexin (Návarová *et al*., 2012). This non-protein amino acid was also found in significant amounts in petiole exudates and accumulates to comparably high levels in distal leaves.

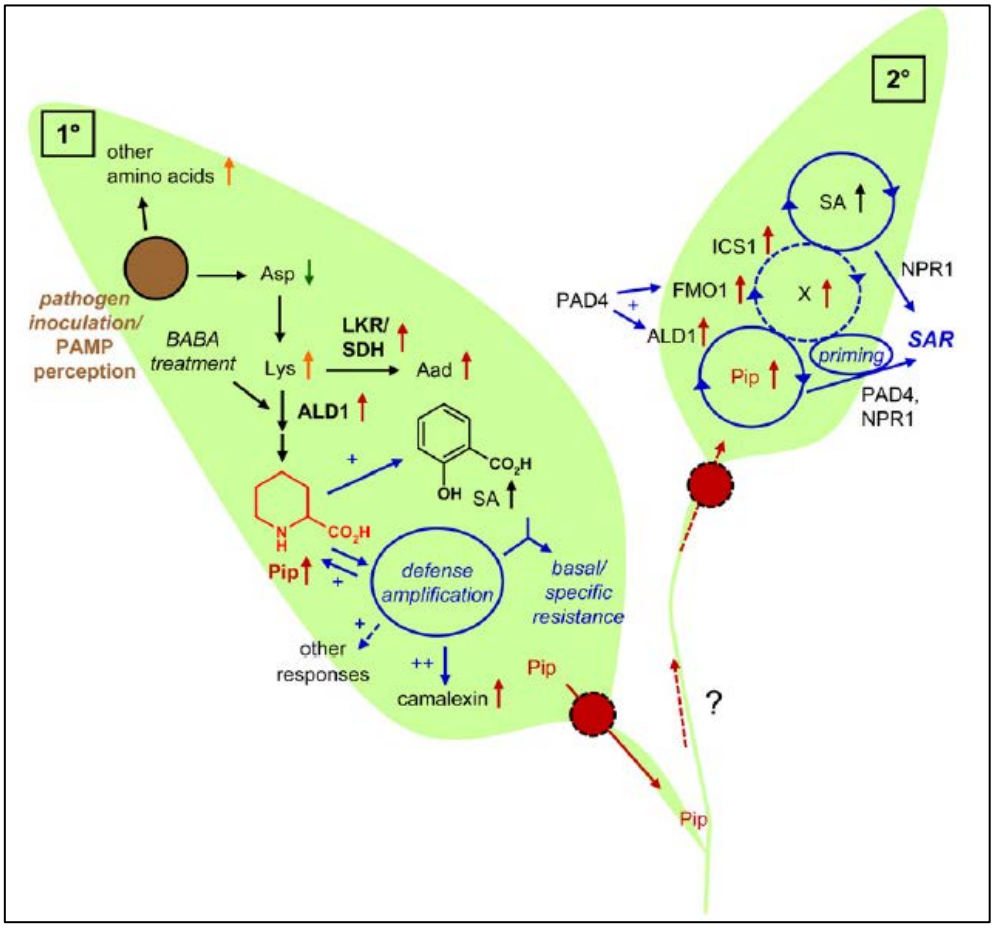

Figure 6. Induction of basal resistance and SAR in *Arabidopsis thaliana*.

Infection with a pathogen or perception of PAMPs leads to a decrease of Asp and an increase in Lys levels, which serves as precursor for Pip and Aad. Rising Pip-levels induce a defence amplification mechanism by upregulating Pip biosynthesis via enhanced *ALD1* expression, as well as induction of SA and camalexin accumulation. Pip is further actively transported out of infected leaves and travels via the phloem to leaves distal of the infection site. In distal leaves the arriving Pip induces a feedback amplification mechanism consisting of *ALD1, FMO1*, and *ICS1* expression and accumulation of Pip and SA in distal leaves, which eventually results in activation of SAR and defence priming in plants (Návarová *et al.*, 2012).

In the current model, local Pip-production initiates an amplification module that increases gene expression of *ALD1, FMO1*, and *ICS1* in distal leaves, thereby inducing an increase in Pip- and SA-levels systemically (Figure 6). Results from our laboratory point to a modification of Pip by the FLAVIN-DEPENDENT MONOOXYGENASE1 (FMO1) necessary for proper

Pip-signalling, as the SAR response could be restored in SAR-deficient *ald1* mutant plants treated with exogenously applied Pip, but not in likewise SAR-deficient *fmo1* plants (Návarová *et al*., 2012). Flavin-dependent monooxygenases are enzymes first described in animals but also found in bacteria, yeast, and plants (Ziegler and Pettit, 1964; Bartsch *et al.,* 2006). They catalyse oxygenation of their substrates, which contain nucleophilic nitrogen, phosphorous, sulfur, or selenium, by binding flavin adenine dinucleotide (FAD) as a cofactor and using NADPH as reduction equivalent (Bartsch *et al*., 2006; Schlaich, 2007). In mammals, FMO enzymes play an important role in the detoxification of xenobiotics by hydroxylation of hydrophobic pharmaceuticals in liver tissue, thus adding water-soluble groups to facilitate a quick excretion of this substance (Lawton *et al*., 1994; Cashman, 2004; Koch *et al*., 2006). The yeast FMO was shown to be involved in regulation of the redox status of the cell by oxidizing thiols (Suh *et al*., 1999) and an insect FMO was shown to deactivate a plant toxin (Naumann *et al*., 2002).

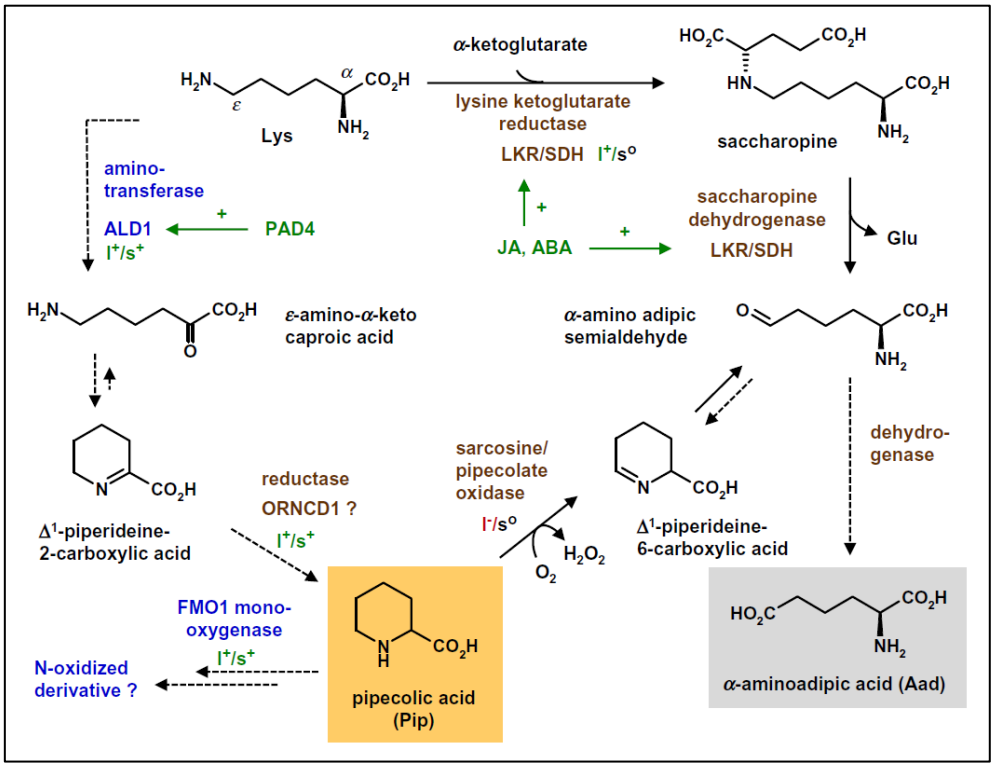

Figure 7. Current model of Pip-biosynthesis.

Lysine is converted to *ε*-amino-*α*-keto-caproic acid by the amino transferase ALD1. *ε*-amino-*α*-keto-caproic acid can spontaneously react to Δ1-piperideine-2-carboxylic acid, which yields Pip after a reduction step catalysed by a reductase. Pip is thought to be a possible substrate for FMO1, which converts it to a N-oxidized Pip-derivative. The amino acid lysine also serves as a precursor molecule for *α*-aminoadipic acid, which was previously thought to be the precursor for Pip. In *α*-aminoadipic acid biosynthesis, Lys is reduced by LKR/SDH to saccharopine, further dehydrogenated to *α*-amino adipic semialdehyde and yields *α*-aminoadipic acid in a last dehydrogenase-catalysed step. Pip can also be converted to Δ1-piperideine-6-carboxylic acid, which can serve as precursor for *α*-amino adipic semialdehyde and can add to *α*-aminoadipic acid content in plant cells (Zeier, 2013).

The *Arabidopsis FMO1* gene product is crucial for development of the SAR response after pathogen attack, as deletions in this gene abolish plant defence against the bacterium

Pseudomonas syringae pv. *maculicola* (*Psm*) and the downy mildew agent *Hyaloperonospora arabidopsidis* (*Hpa*) in systemic, but not in locally infected leaves (Bartsch *et al*., 2006; Mishina and Zeier, 2006).

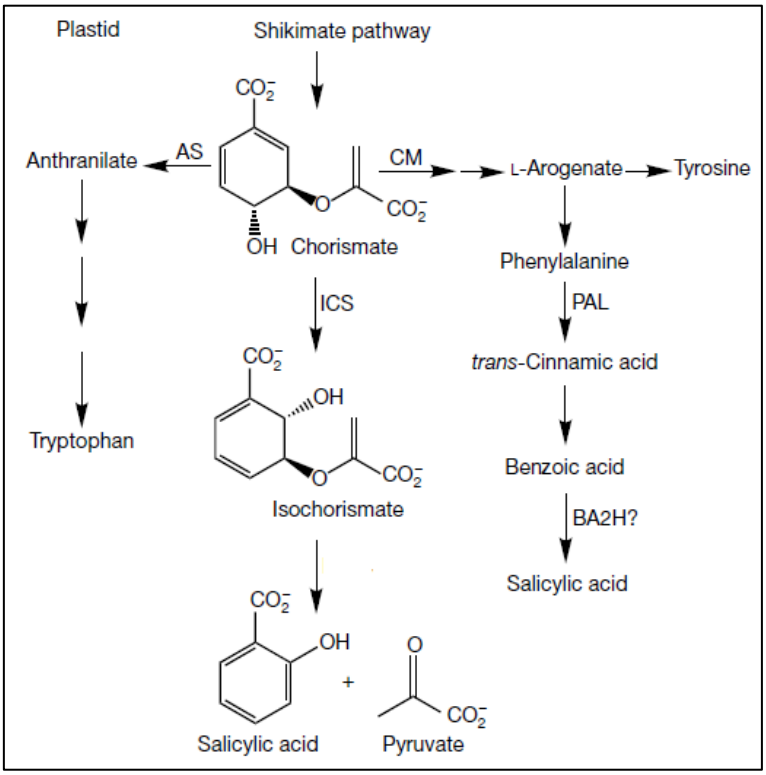

Figure 8. Proposed scheme of SA-biosynthesis in *A. thaliana* via ISOCHORISMATE SYNTHASE1 (ICS1).

Also shown is the previously described SA-biosynthesis pathway via PAL, which was shown to be irrelevant for accumulation of SA upon pathogen infection. AS, anthranilate synthase; CM, chorismate mutase. Modified from Wildermuth *et al*., 2001.

FMO1 expression in locally infected leaves was shown to be independent of SA-accumulation, whereas in systemic leaves *FMO1* expression and establishment of SAR were SA-dependent (Mishina and Zeier, 2006). A transgenic line, overexpressing *FMO1* under control of the *35S CaMV* promoter, featured enhanced basal resistance against *Psm* and *Hpa* (Koch *et al.,* 2006) supporting a role for *FMO1* in the regulation of defence responses in systemic leaves by participating in the potentiation of defence responses (Mishina and Zeier, 2006). Increasing SA-levels are necessary for a full SAR response, albeit an attenuated SAR was observed in *sid2* (*salicylic acid induction-deficient2*) mutant plants, which are impaired in SA-biosynthesis (Nawrath and Métraux, 1999). Gene products of *ALD1, FMO1, NPR1*, and *PAD4* participate in induction of the SAR response, as mutant lines for these genes are impaired in SAR-establishment. Most interestingly, plants of these mutant lines show a wild type-like accumulation of SA in locally infected, but not in distal leaves (Mishina and Zeier, 2006; Attaran *et al*., 2009). SA is synthesized from chorismate via isochorismate, a reaction

catalysed by ICS1 (ISOCHORISMATE SYNTHASE1; Wildermuth *et al.*, 2001; Figure 8). The *ICS1* knockout line, *sid2* does not accumulate SA upon bacterial infection, is more susceptible to virulent and avirulent *Psm* bacteria, and demonstrates only a very weak SAR reaction (Nawrath and Métraux, 1999; Wildermuth *et al.*, 2001). It was previously hypothesised that SA represents the mobile signal for SAR-induction by being converted to the methylated form in local leaves and back to free SA in distal leaves after travelling as methylsalicylate (MeSA) via the phloem. Research, however, has shown that SA is not the transported SAR signal in plants, as for instance in grafting experiments transgenic tobacco rootstocks, unable to generate SA, induced a SAR reaction in nontransgenic scions (Vernooij *et al.*, 1994).

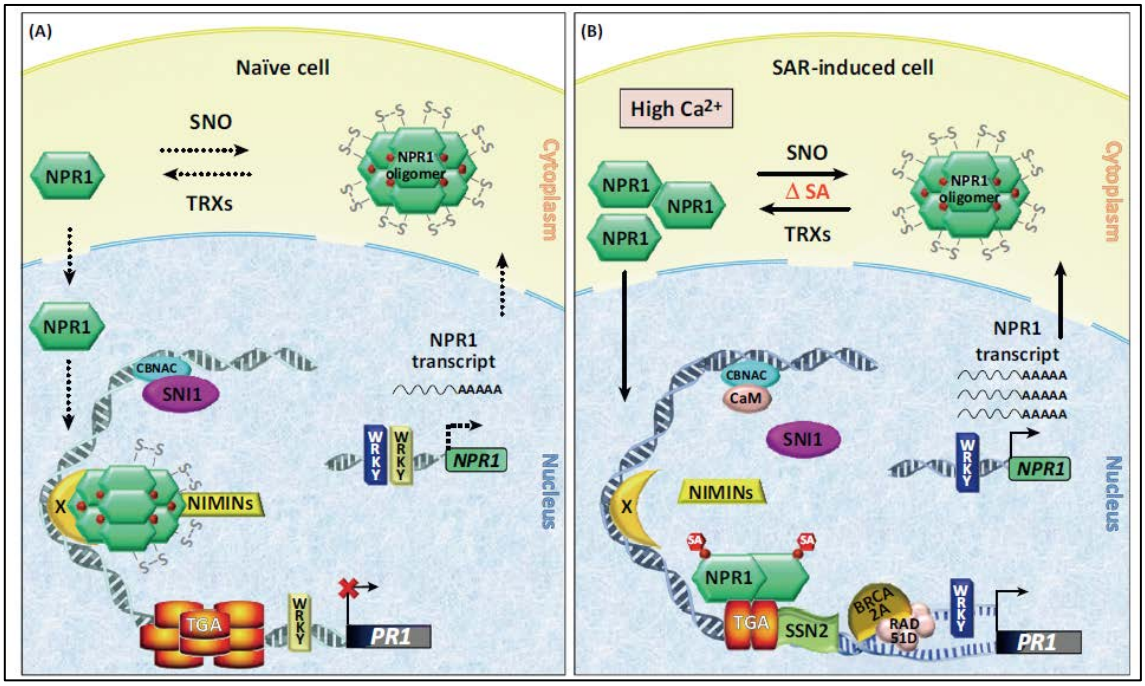

Figure 9. NPR1 mediates SA-signalling.

(A) In uninfected cells the NPR1 protein is present mostly in large oligomeric complexes in the cytosol, with only a small number of monomeric NPR1 able to enter the nucleus where it interacts with the repressor protein NON-INDUCIBLE IMMUNITY 1 (NIM1)-INTERACTING (NIMIN). This repressor complex and other repression mechanisms prevent the expression of *PR-1*. (B) Upon infection with a bacterial pathogen, SA-levels in the cell increase and allow dissociation of larger numbers of NPR1 protein from the oligomeric complex and enables NPR1 monomers to enter the nucleus. Inside the nucleus, assembly of a TGA-NPR1-SA complex together with additional transcription factors, enables transcription of *PR-1* followed by induction of defence responses (Pajerowska-Mukhtar *et al.*, 2013).

Another experiment proved that SA is synthesised *de novo* in distal leaves and that MeSA, proposed to be the dislocated form of SA, cannot be the transport form, as most of the highly volatile MeSA evaporates from leaves and mutant plant lines with a defect in the SA methyl transferase gene *BSMT1* (SAM-dependent carboxyl methyltransferase) exhibit a WT-like SAR response (Attaran *et al.*, 2009). An increase in SA-levels is mandatory for basal

resistance and elicitation of SAR, however, as SA-mediated signalling is responsible for expression of a large number of defence-related genes and transcription factors, as well as regulation of signalling and hormone networks to economically allocate resources. A central part in SA-mediated signalling plays NONEXPRESSOR OF PR-1 (NPR1), a protein that is found mostly in oligomeric form in the cytosol of non-infected plant cells (Figure 9). A small amount of NPR1 is present in monomeric form and can enter the nucleus, where it interacts with NON-INDUCIBLE IMMUNITY 1 (NIM1-) INTERACTING (NIMIN), a repressor upstream of the coding region for *PR-1* (Mou *et al*., 2003; Figure 9). Accumulation of SA in infected plant cells leads to changes in redox potential in the cell and subsequent reduction of NPR1 to its monomeric form. Consequently, more monomeric NPR1 is able to enter the nucleus, where association of NPR1 with a complex consisting of transcription factors and transcriptional regulators as well as SA enables transcription of *PR* genes followed by induction of SAR (Mou *et al*., 2003; Da Cunha *et al.,* 2006; Figure 9).

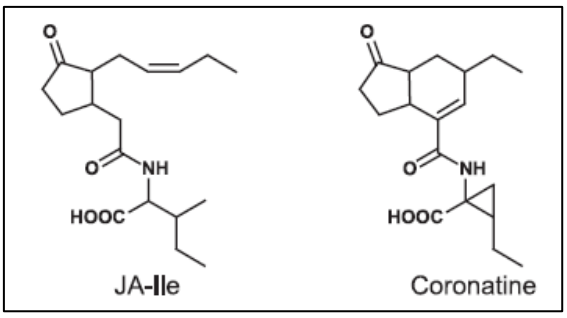

Figure 10. Comparison of Ja-Ile and coronatine.

The toxin coronatine introduced into plant cells by *Psm* has a structure very similar to jasmonate-isoleucine, the bioactive form of JA (Katsir *et al*., 2008).

It was recently shown that additionally to its role in SA-signalling described above, NPR1, as well as its paralogues NPR3 and NPR4, is able to bind SA and functions as SA-receptor (Wu *et al*., 2012; Fu *et al*., 2012; Yan and Dong, 2014). In further experiments, NPR1 not only activated a large number of defence-related genes, but also downregulated genes involved in basic cell processes, for instance photosynthesis, in order to prioritise defence reactions over growth in the plant (Spoel and Dong, 2012). Furthermore, SA is not only involved in controlling expression of defence-related genes in SAR, but also regulates cell-to-cell signalling by induction of plasmodesmata closure upon perception of PAMPs (Wang *et al*., 2013 b) and defence signalling by actively repressing JA- and ethylene (ET)-responsive genes (Vlot *et al*., 2009). Similar to other compounds in plants, SA can be toxic in higher doses and needs to be conjugated with other compounds for inactivation. Glucosylation by UDP-glucosyltransferases on either of its two hydroxyl groups converts SA into the

corresponding glycosylated (SAG) form, which is the abundant inactive form of SA and is stored in plant vacuoles (Dempsey *et al*., 2011).

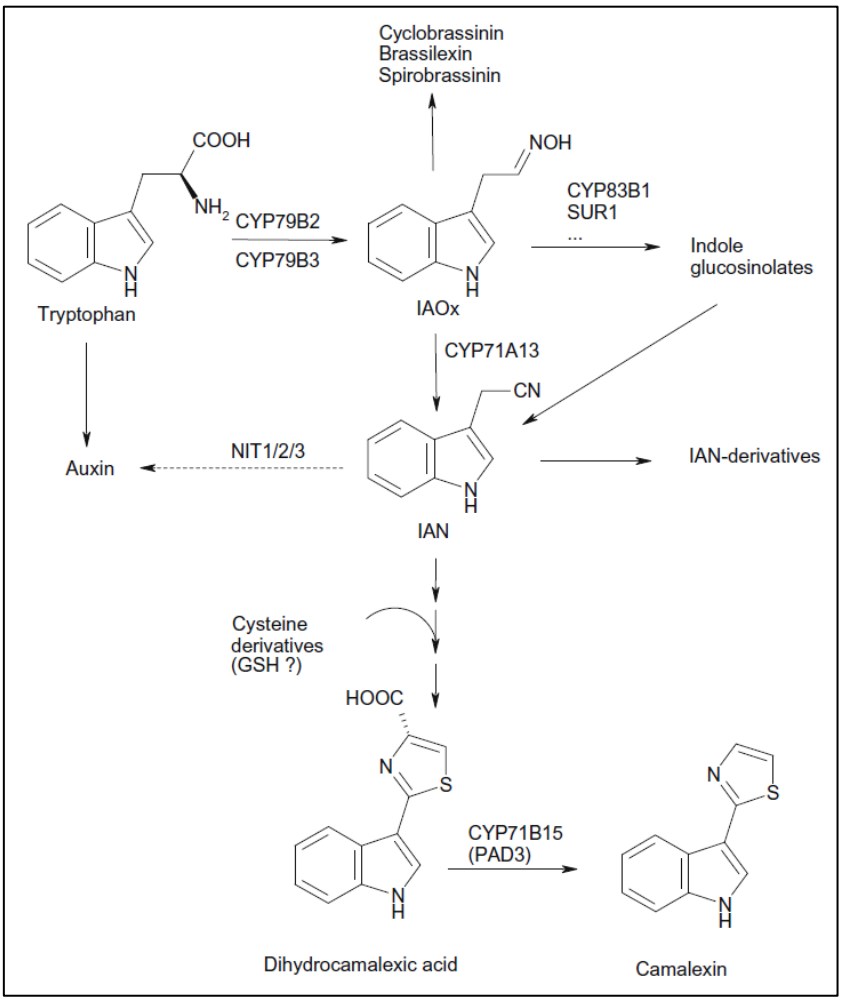

Figure 11. Biosynthesis of camalexin and other indolic compounds in *A. thaliana*.

Cytochrome P450s CYP79B2 and CYP79B3 catalyse the conversion of tryptophan to indole-3-acetaldoxime (IAOx), the substrate for CYP71A13 to generate indole-3-acetonitrile (IAN), which is converted in further steps to the phytoalexin camalexin (Rauhut and Glawischnig, 2009).

As described earlier, conversion of SA to its methylester by BSMT1 exceedingly increases volatility and leads to a rapid evaporation from leaves (Attaran *et al*., 2009; Dempsey *et al*., 2011). Production of MeSA is another possibility for the plant to dispose of excess SA, but this reaction is also used by pathogenic bacteria to suppress SA-mediated defence responses (Attaran *et al*., 2009). It is known from other signalling metabolites that they can achieve bioactivity after receiving some kind of modification, one example being JA, which in its bioactive form is conjugated to the amino acid isoleucine and perceived by the receptor COI1 (Katsir *et al*., 2008; Koo *et al*., 2009; Yan *et al*., 2009). SA can hypothetically be conjugated to amino acids by GH3-like phytohormone amino acid synthetases, one of these

conjugates could be for instance the aspartate conjugate SA-Asp (Staswick *et al*., 2002; Zhang *et al*., 2007; Dempsey *et al*., 2011). Overexpression of the amino acid synthetase GH3.5, showing activity on indole acetic acid (IAA) and SA in vitro with a preference for IAA as a substrate, resulted in increased levels of SA-Asp after pathogen infection (Zhang *et al*., 2007). But, as in a *gh3.5* null mutant no differences were observed for levels of SA, SAG, or SA-Asp, and increased susceptibility could also be credited to disturbances in auxin homeostasis, activation of SA by conjugation to amino acids seems a very unlikely hypothesis (Park *et al.,* 2007; Zhang *et al*., 2007). SA-mediated defence responses are active against biotrophic and hemibiotrophic pathogens and JA- and ET-mediated defence responses were found to be most effective against necrotrophic pathogens (Glazebrook, 2005). Research showed a closely regulated crosstalk between SA- and JA/ET-mediated signalling in plant defence with prioritization of SA- over JA-mediated responses and strong NPR1-dependent repression of JA-regulated genes by SA (Gupta *et al*., 2000; Spoel *et al*., 2003; Vlot *et al*., 2009). In *Arabidopsis* mutants with reduced SA-levels, responses to JA were much stronger than in WT plants upon infection with the bacterial pathogen *P. syringae* (Gupta *et al*., 2000; Spoel *et al*., 2003). This negative crosstalk between SA and JA is often exploited by pathogens to facilitate infection, for instance the effector coronatine from *Psm* has a structure very similar to Ja-Ile, the bioactive form of JA (Figure 10). The necrotrophic fungus *Botrytis cinerea*, on the other hand, facilitates infection by manipulating the plant to increase SA-levels, which represses JA-mediated signalling that would be effective against this fungus (La Camera *et al*., 2011). Upon infection with different pathogens, *A. thaliana* plants also accumulate camalexin, a phytoalexin derived from tryptophan, in the vicinity of the infection site (Glawischnig, 2007; Figure 11). This phytoalexin also accumulated after treatment with several abiotic stresses that induce formation of ROS, for example application of heavy metal ions, UV-B irradiation, and the toxin fusaric acid (Glawischnig, 2007). Camalexin was shown to disrupt bacterial membranes *in vitro*, although the high concentrations needed for an antibacterial effect would have a strong toxic effect in plant cells. For phytopathogenic fungi, on the other hand, a tenfold lower concentration of camalexin was shown to be sufficient for an antimicrobial effect (Glawischnig, 2007). The importance of camalexin in plant defence against necrotrophic fungi is further emphasized by phytoalexin-deficient mutants, notably *pad2* and *pad3*, which are only slightly impaired in resistance against the hemibiotroph *Psm*, but exhibit enhanced susceptibility towards the necrotrophic fungi *B. cinerea* and *A. brassicicola* (Glazebrook and Ausubel, 1994; Zhou *et al*., 1999; Glawischnig, 2007).

3.4 Mitogen-activated protein kinase signalling in plants

MAP kinase signalling cascades are found ubiquitiously in eukaryotes and are necessary to translate extracellular stimuli into intracellular responses (Figure 15). Signal perception by a membrane-localised receptor leads to activation of MAPKK kinases (MAPKKK or MEKK) that phosphorylate MAPK kinases (MAPKK or MEK) on two Ser/Thr residues in a Ser/Thr-X_{3-5}-Ser/Thr motif of the MAPKK activation loop. In turn, activation of MAPKK leads to phosphorylation of a Thr and a Tyr residue in the Thr-X-Tyr activation motif of MAP kinases downstream in the signalling cascade. The activated MAP kinase is able to phosphorylate transcription factors that in turn activate gene expression (Widmann *et al*., 1999; Meng and Zhang, 2013; Figure 12).

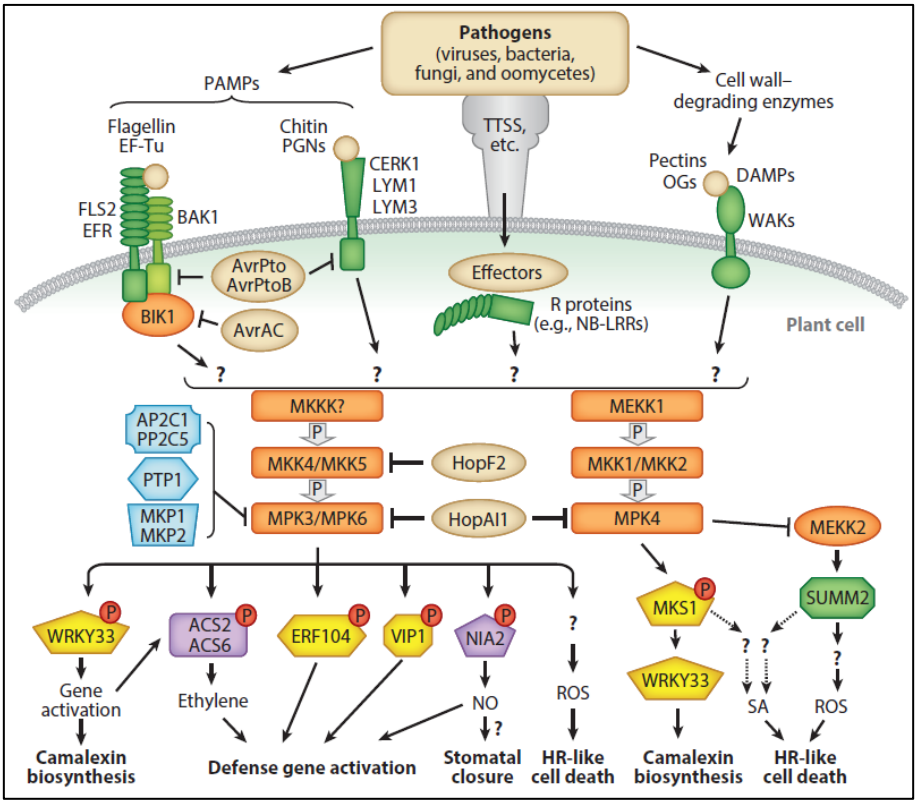

Figure 12. MAP kinase signalling in *Arabidopsis* innate immunity.

Perception of an elicitor by a LRR receptor (e.g. FLS2) activates a MAPK signalling cascade, which results in activation of transcription factors to induce expression of defence-related genes. Activation of the MAPK signalling network is one of the earliest events after pathogen perception and can modulate homeostasis of hormone and metabolism networks. NB-LRRs, nucleotide-binding site–leucine-rich repeat proteins; NO, nitric oxide; OGs, oligogalacturonic acids; PGNs, peptidoglycans; ROS, reactive oxygen species; SA, salicylic acid; TTSS, type three secretion system; WAKs, wall-associated kinases (Meng and Zhang, 2013).

In plants, MAPK signalling cascades play important roles in the regulation of development and responses to different stresses like pathogen infection, wounding, temperature, drought, osmolarity, UV-irradiation, and ROS (Ichimura *et al*., 2002; Pedley and Martin, 2005; Zhang, 2008; Pitzschke *et al*., 2009; Rodriguez *et al*., 2010; Tena *et al*., 2011; Meng and Zhang,

2013). In the *Arabidopsis* genome, sequences for 20 MAPKs, 10 MAPKKs, and close to 60 MAPKKKs were found, suggesting a high grade of functional redundancy in MAPK signalling (Ichimura *et al*., 2002; Hamel *et al*., 2006). One example for a MAPK cascade reportedly involved in defence signalling is the perception of the MAMP flg22 by its PRR receptor FLS2, which induces heterodimer formation with BIK1 and activation of a phosphorylation-activation cascade comprising MEKK1, MKK4 and MKK5, as well as MPK3 and MPK6 (Asai *et al*., 2002; Meng and Zhang, 2013). This phosphorylation cascade provides a robust means to amplify the perceived signal and enables gene expression via activation of transcription factors (Conrath, 2011; Meng and Zhang, 2013). Several effectors introduced into plant cells by pathogenic bacteria or fungi directly target the MAPK network in plants to prevent this signal amplification mechanism (Meng and Zhang, 2013). To inactivate MAPKs, dephosphorylation of either Thr- or Tyr-residue is sufficient and is needed to control the extent, duration, and physiological outcome of MAPK activation. Inactivation of MAPKs is attained by Ser/Thr phosphatases (PP2C family), protein Tyr phosphatases (PTPs), or dual specificity phosphatases (DSPs) (Wang *et al*., 2007; Meng and Zhang, 2013). To ensure signalling specificity of MAPK cascades, *MPK3, MPK6*, and *MPK4* show different expression levels in diverse tissues, for instance higher expression levels in guard cells that control aperture of stomata, the major entranceway for bacterial pathogens like *P. syringae* (Petersen *et al*., 2000; Zeng *et al*., 2010; Meng and Zhang, 2013).

3.5 Chemical inducers of plant pathogen resistance

Several chemical compounds were discovered that are able to induce resistance to a number of pathogens after exogenous application. Treating plants with SA or the SA-analogues benzo-(1,2,3,)-thiadiazole-7-carbothioc acid S-methylester (BTH) and 2,6-dichloroisonicotinic acid (INA), induces local *PR-1* gene expression, a marker for SA-signalling in plants (Kessmann *et al*., 1994; Sticher *et al*., 1997). Using SA and its analogues for induction of plant resistance is not optimal though, because resistance induction by exogenously applied SA, BTH, or INA was found to be restricted to treated tissue, the applied SA was swiftly converted to its glycoside and inactivated in this way, and it is also a fine line between SA-efficacy and -toxicity (Kessmann *et al*., 1994). The non-protein amino acid *ß*-aminobutyric acid (BABA) does not occur naturally in *A. thaliana*, but is able to induce resistance against different pathogens, including the oomycete pathogens *Hyaloperonospora arabidopsidis* and *Phythopthora infestans,* the bacterium *Pseudomonas syringae*, and the fungus *Botrytis cinerea* (Zimmerli *et al*., 2001; Cohen, 2002; Tsai *et al.,* 2011), as well as several abiotic stresses (Ton *et al*., 2005). BABA is effective against a wide array of biotrophic and necrotrophic pathogens and results gained from recent studies hinted at

priming of plant defences via BABA, enabling the plant to react faster and stronger to a threat (see below; Ton *et al*., 2005).

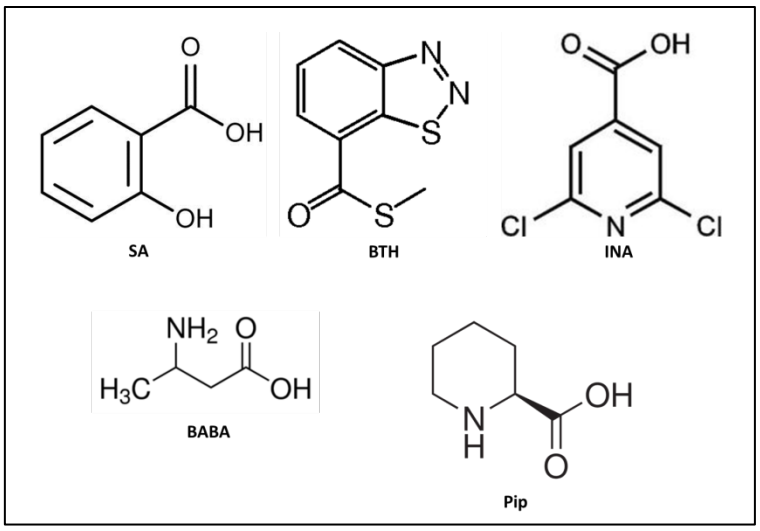

Figure 13. Chemicals shown to induce resistance against pathogens.

Exogenous application of SA and the SA-analogues benzo (1,2,3,) thiadiazole-7-carbothioc acid S-methylester (BTH) and 2,6-dichloroisonicotinic acid (INA), as well as the non-protein amino acids *ß*-aminobutyric acid (BABA) and Pip, were shown to induce resistance in plants.

Interestingly, BABA-treatment induced resistance in already infected plants up to three days post infection, while other chemical inducers of resistance were shown to be effective only prior to infection (Cohen, 2002). The defence regulator Pip also induces resistance to virulent and avirulent *Psm* strains by activating *ALD1* expression and increasing Pip-levels throughout the plant in this way (Návarová *et al*., 2012). Pip has a strong priming effect on camalexin and its own biosynthesis and on expression of defence-related genes as well. Results from our laboratory suggest that BABA-induced resistance in *Arabidopsis* is dependent on Pip-mediated responses in plants rather than a BABA-specific pathway (Návarová *et al*., 2012).

3.6 Mechanisms of priming in systemic acquired and chemical-induced resistance

A key mechanism in SAR and chemically induced resistance is priming of plant responses, which enables primed plants to react faster and stronger to a threat compared to non-primed plants (Conrath *et al*., 2001; Bruce *et al*., 2007; Figure 13). Priming, or sensitation, of plant defence responses, was first described by Chester in 1933 as an important mechanism for SAR (Chester, 1933; Conrath, 2011).

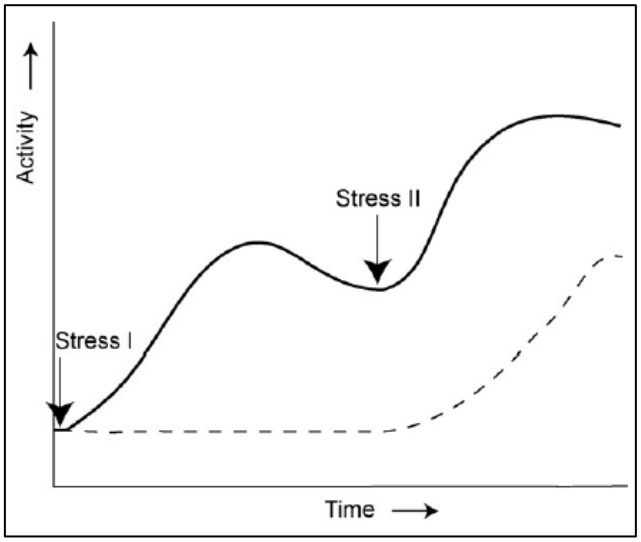

Figure 14. Simplified representation of defence gene expression in a non-primed and primed plant.

The primed plant experiences two stress events, whereas the non-primed plant is only exposed to stress II. Gene expression of certain genes in primed plants is higher than in non-primed plants upon stress event II. non-primed (--); primed (-) (Bruce *et al.,* 2007).

Priming of plant cells becomes apparent only in the moment of a challenge to the primed tissue and it was shown that primed cells not only show greater sensitivity to pathogens, but also to abiotic stresses (Sticher *et al*., 1997). Interestingly, repetetive mild abiotic stresses (heat, cold, drought) were shown to prime *Arabidopsis* plants for enhanced resistance against *Psm* by enrichment of epigenetic marks on defence-related genes in environmentally stressed plants (Singh *et al*., 2014). In 1973, Skipp and Deverall showed that infection of bean hypocotyls by *Colletotrichum lindemuthianum* protected plants from further infections by the same pathogen and also induced a necrosis after a mild heat shock, leading to the conclusion that the shift of sensitivity in primed cells causes alterations in the plant´s reactions to its biotic and abiotic environment (Skipp and Deverall, 1973; Sticher *et al*., 1997). Experiments with carnation (*Dianthus caryophyllus*) provided strong evidence that priming is an important mechanism in induced systemic resistance (ISR) as well as in SAR. ISR is invoked by beneficial microbes, for instance rhizobia that are able to colonise plant roots and form symbioses with the plant. In carnation plants with roots colonised by the non-pathogenic rhizobacterium *Pseudomonas fluorescens* WCS417, phytoalexin levels increased faster upon challenge infection with the pathogenic fungus *Fusarium oxysporum* f. sp. *dianthi* compared to plants without root colonisation (van Peer *et al.*, 1991; Conrath *et al.*, 2001).

It is also possible to prime plant tissue by exogenously applied chemicals. In parsley cell cultures, for example, treatment with SA or its analogue INA enhanced the capability of these cells to synthesise coumarins in response to an elicitor derived from *Phytophthora megasperma* f. sp. *glycinea* (Kauss *et al*., 1992; Sticher *et al*., 1997). In further experiments with this cell culture system it was shown that cells primed by SA, INA, or BTH also enhanced the elicitation of the oxidative burst, secretion of cell wall phenolics, phytoalexin

production, and expression of defence genes (Kauss *et al.*, 1992; Kauss *et al.*, 1993; Kauss and Jeblick, 1995; Mur *et al.*, 1996; Thulke and Conrath, 1998; Zimmerli *et al.*, 2001).

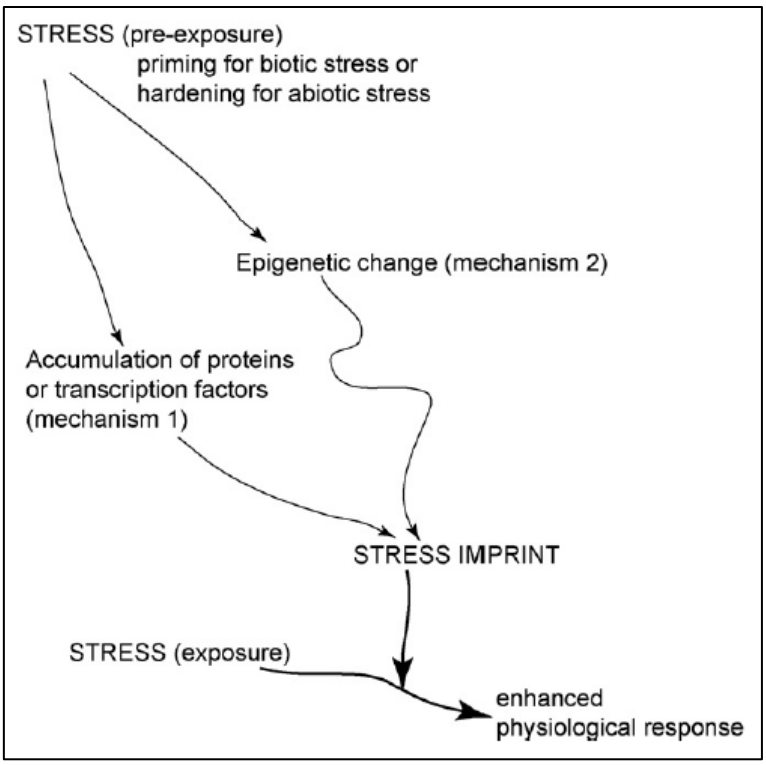

Figure 15. Schematic model to explain the generation of stress imprint following priming.

Stress imprint could be generated by accumulation of (preformed) proteins and/or transcription factors in cells (mechanism 1) on the one hand and epigenetic changes (mechanism 2) on the other hand. A combination of both mechanisms to achieve an enhanced physiological response in primed plants is possible, too (Bruce *et al*., 2007).

Mur *et al*. (1996) provided evidence that SA is able to enhance the expression of SA-independent genes, which are induced after pathogen attack or wounding (Mur *et al*., 1996; Sticher *et al*., 1997). The non-protein amino acid BABA was shown to heighten the expression of the defence-related *PR-1* gene in response to attack by virulent bacteria and also enabled the plant to activate *PR-1* expression much faster than in control plants (Zimmerli *et al*., 2000). This amino acid also induced resistance against the biotrophic oomycete *Hpa* and the necrotrophic fungus *B. cinerea* (Zimmerli *et al*., 2000; Zimmerli *et al*., 2001) and was shown to protect plants against osmotic stress (Ton *et al*., 2004; Ton *et al.*, 2005). An endogenously produced non-protein amino acid, Pip, was shown to not only induce defence against *Psm* after exogenous application, but also potentiated expression of a number of defence-related genes as well as accumulation of the phytoalexin camalexin after challenge infection with *Psm* (Návarová *et al*., 2012). Other chemical inducers of priming include the nine-carbon dicarboxylic acid azelaic acid, which was shown to prime SA-accumulation upon infection with the bacterial pathogen *Psm* (Jung *et al*., 2009);

thiamine that potentiated *PR-1* expression in response to *Psm* (Ahn *et al*., 2007); and several amino acids including D-phenylalanine, D-alanine, and DL-tryptophan, which primed apple trees against scab (Kuc *et al*., 1957; Kuc *et al*., 1959), and D-serine, D-threonine, and L-threo-β-phenylserine that induced resistance in cucumber against the pathogen *Cladosporium cucumerinum* (van Andel, 1958). An obvious advantage in enabling the plant to react faster and more efficiently to a threat by priming, compared to the constitutive activation of defence responses, is a cost-efficient management of energy resources (Bruce *et al*., 2007).

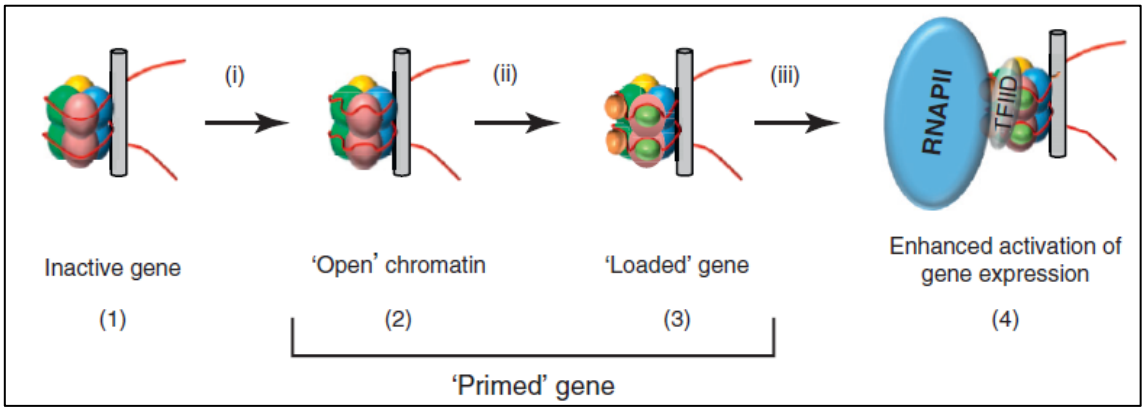

Figure 16. Chromatin modifications as a possible mechanism for priming of gene expression.

In inactive genes the chromatin structure is tightly packed with genomic DNA wrapped around histone proteins (1), Genes primed for expression show characteristics of a more open chromatin structure (2). This is achieved by modifications to Lys-residues in histone proteins, which decrease ionic interactions between proteins and DNA. These modifications might also offer ´docking sites´ for transcription co-activators, chromatin remodelling factors, and other proteins (3). Perception of an additional stimulus enables this ´loaded´ gene to be transcribed immediately, leading to enhanced activation of gene expression (4) (Conrath, 2011).

Two possible mechanisms of stress-imprint in order to prime plants were proposed. One possibility would be the accumulation of proteins and/or transcription factors after a first exposure to stress and in this way a preactivation of defence signalling pathways (Bruce *et al*., 2007; Figure 15). One example for preactivated biosynthesis pathways in the plant´s priming reaction is the biosynthesis of the phytoalexin camalexin. Genes encoding enzymes involved in camalexin biosynthesis, *CYP71A13* and *PAD3*, were shown to be preactivated in systemic leaves, leading to a partial pathway activation by ensuring key biosynthetic enzymes are already present before a second pathogen infection. This mechanism would also be a possibility to manage defence more cost-effectively, as fewer components of camalexin biosynthesis have to be synthesised *de novo* (Gruner *et al*., 2013). Another example is the activation of the MAPK signalling network. It was shown that a signalling cascade involving MAP kinases 3 and 6 (MPK3, MPK6) is activated in plants infected with *Psm* or treated with flg22 (Asai *et al*., 2002). Also, proteins of MPK3 and MPK6 accumulated in the cytoplasm of BTH-treated *Arabidopsis* cells, but appeared to be inactive until

perception of an additional stress signal. Upon treatment with a biotic or an abiotic stress challenge, these proteins showed stronger activity in primed compared to non-primed plants (Beckers *et al*., 2009). The second possibility to confer priming to a plant is epigenetic changes, for instance by modifying the chromatin structure via acetylation or methylation of histone proteins associated with DNA (Bruce *et al*., 2007). Chromatin modifications do not change the DNA sequence, but by acetylation of lysine residues of histone proteins, for example, the ionic interactions between histones and DNA become much weaker (Conrath, 2011). Acetylation of histones is associated with gene activation, as the “open” chromatin structure and the acetylated residues provide space and possible docking sites for transcriptional co-activators and other proteins and thus enhances expression of genes marked in this way (Conrath, 2011; Figure 16). Methylation of amino acid residues is a more complicated matter, because lysine and arginine residues can be methylated and single-, double-, and triple-methylation are possible. Moreover, triple-methylation of Lys-residues is associated with both active and repressed gene activity, whereas the activation state of single- and double-methylated Lys-residues is still unclear (Jaskiewicz *et al*., 2011). Nevertheless, chromatin modifications would provide a means of a longer-term stress-imprint compared to accumulation of gene products and metabolites in plant tissues (Bruce *et al*., 2007). It is possible that plants experiencing an episode of biotic or abiotic stress and being primed during this stress are able to confer this primed state to the next generation. Luna *et al.* have shown in 2012 that progeny from plants infected with either *Psm* or *Hpa* exhibited primed activation of SA-inducible defence genes and were more resistant towards infection with these pathogens. This priming of defence responses was preserved over one stress-free generation and suggests a strong role for epigenetic changes in transgenerational priming.

3.7 The grey mould disease agent *Botrytis cinerea*

The fungus *Botrytis cinerea* is responsible for the grey mould disease of plants and can infect more than 200 different plant species. This broad host spectrum makes this fungus a very dangerous pathogen to agriculture all over the world. In accordance with its necrotrophic lifestyle, *B. cinerea* has to kill plant tissue to be able to feed on its resources (Glazebrook, 2005). After germination of *Botrytis* spores, an appressorium is formed which enables fungal hyphae to invade plant cells and grow through the whole plant to achieve a necrotrophic colonisation (Figure 17). Infection of *Arabidopsis* plants with this fungus induces expression of JA- and ET-dependent genes, for instance the plant defensin gene *PDF1.2*, and accumulation of camalexin in tissues in close proximity to the infection site (Thomma *et al*., 1999; Govrin and Levine, 2002). Camalexin was shown to be very effective against *B.*

cinerea and mutant plants impaired in camalexin biosynthesis, especially *pad2* and *pad3,* show more severe disease symptoms than WT plants (Ferrari *et al.*, 2003).

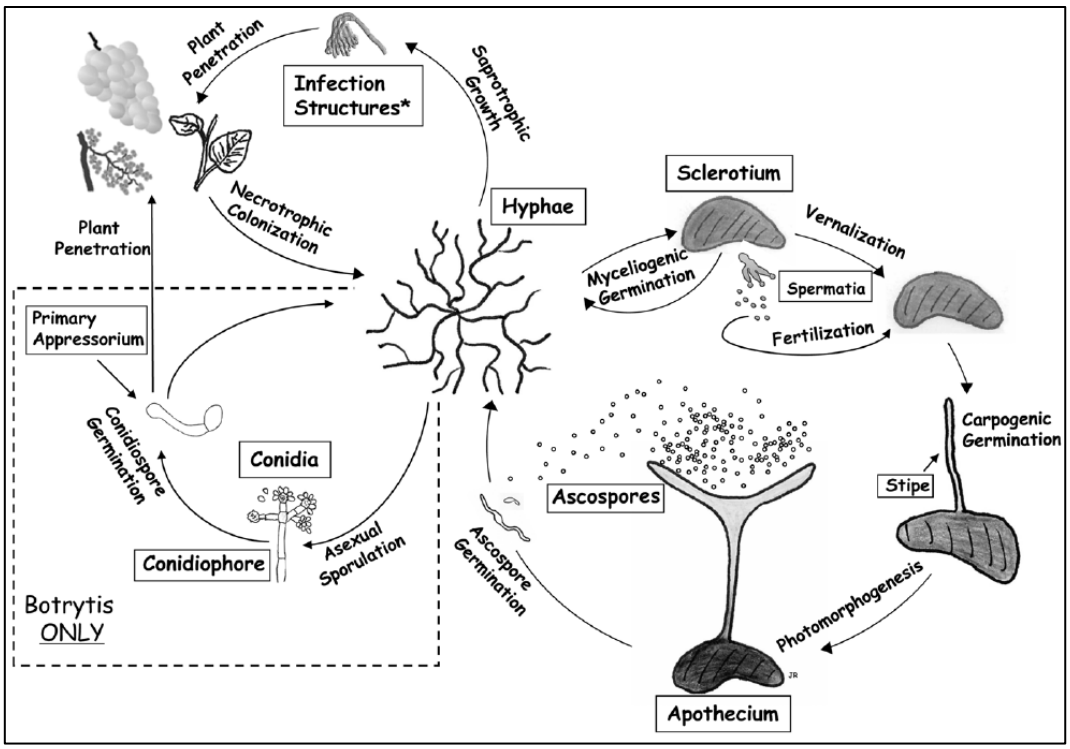

Figure 17. Infection cycle of the necrotrophic fungal pathogens *Sclerotinia sclerotiorum* and *Botrytis cinerea*.

Depicted are different stages of sexual and asexual development (Amselem *et al.*, 2011).

Several *Botrytis* strains were described to be able to tolerate camalexin by actively transporting it out of fungal cells via an ABC transporter (Rauhut and Glawischnig, 2009; Amselem, *et al.* 2011). *B. cinerea* manipulates plant defence in several different ways in order to facilitate infection. For instance, it actively triggers ROS-development and the HR response in order to further plant infection and the severity of infection was found to be directly proportionate to the level of ROS-generation (Govrin and Levine, 2000; Amselem *et al*., 2011). This fungus also exploits the SA-mediated signalling pathway via the glutaredoxin GRXS13 to suppress JA-mediated defence responses, enabling development of more severe disease symptoms (La Camera *et al*., 2011). An additional strategy to facilitate cell death in plants is the introduction of toxins into plant cells, for instance the sesquiterpene botrydial and related compounds, as well as botcinic acid and its derivatives (Amselem *et al*., 2011). Another highly interesting way for repression and manipulation of plant defence responses by *B. cinerea* is the introduction of small RNAs (sRNA), about 20-24 nucleotides in length, into plant cells. These sRNAs guide plant Argonaute (AGO) nucleases to targeted mRNAs, including mRNAs derived from defence-related genes, in order to silence those

genes via the plants´ own RNA interference machinery, leading to a more severe disease development (Baulcombe, 2013; Weiberg *et al*., 2013; Figure 18).

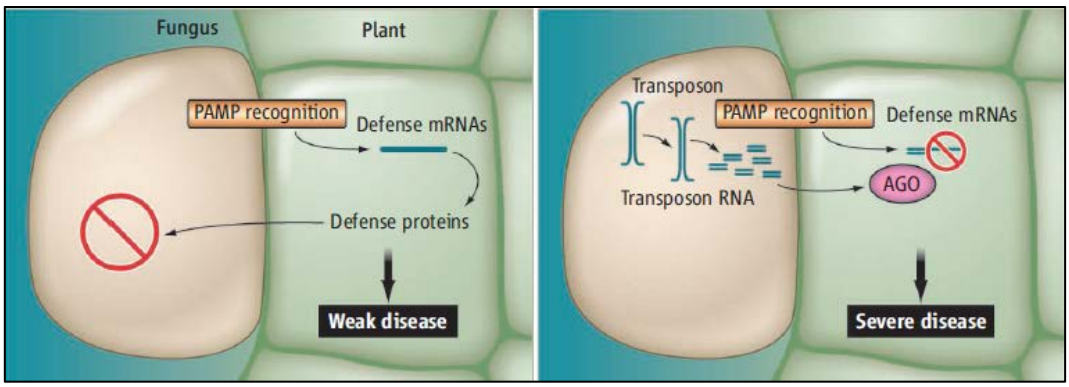

Figure 18. *B. cinerea* introduces sRNAs into plant cells to facilitate infection.
As described by Baulcombe, 2013.

In experiments using plant *ago* mutants or *B. cinerea* strains no longer capable of sRNA production, disease symptoms were much weaker than in interactions between wild type plants and pathogens (Weiberg *et al*., 2013).

3.8 Resistance against the powdery mildew fungus *Golovinomyces orontii*

The powdery mildew fungus *Golovinomyces orontii* follows an obligate biotrophic lifestyle and adapted its metabolism closely to its host in order to do so. After germination of a conidiospore on the leaf surface, the fungus penetrates an epidermal cell and at approximately 1 dpi establishes the haustorial complex, a feeding structure, inside the cell (Micali *et al*., 2008; Chandran *et al*., 2013; Figure 19). *G. orontii* then shows extensive hyphal growth on the leaf surface and develops asexual reproductive structures (conidiophores) at 3 dpi and later. In *Arabidopsis*, non-host resistance against non-adapted powdery mildew strains is dependent on the myrosinase PEN2 and SA-mediated defence signalling (Lipka *et al*., 2005; Bednarek *et al*., 2009; Chandran *et al*., 2013). In addition to SA-mediated defence signalling, other defence hormone pathways like ET- or JA-signalling seem to be of importance, too. Research showed that mutations in *PAD4, EDS5, ICS1*, and *NPR1*, genes involved in SA-mediated signalling, resulted in higher susceptibility of plants towards powdery mildew pathogens (Reuber *et al*., 1998; Wildermuth *et al*., 2001; Chandran *et al*., 2013). ET- and JA-signalling pathways are not typically activated after infection with *G. orontii*, but mutants showing constitutive activation of these signalling pathways, for instance *cev1* (*constitutive expression of vsp1*; constitutively activated JA-signalling) and an *EFR1* (*ETHYLENE RESPONSE FACTOR 1*) overexpressor line, are more resistant to powdery

mildews (Ellis and Turner, 2001; Gu *et al*., 2002; Chandran *et al*., 2013). In order to gain nutrients for the widespread hyphal growth and reproduction of the fungus, extensive modulations of plant gene expression are necessary (Fabro *et al*., 2008; Chandran *et al*., 2013). Similar to other obligate biotrophic pathogens, plant cell death was shown to be a very potent mechanism in resistance against *G. orontii* as well (Micali *et al*., 2008). Powdery mildew infection also induces callose deposition, a (1,3)-*ß*-glucan polymer, in the form of papillae at the penetration site (Nishimura *et al*., 2003).

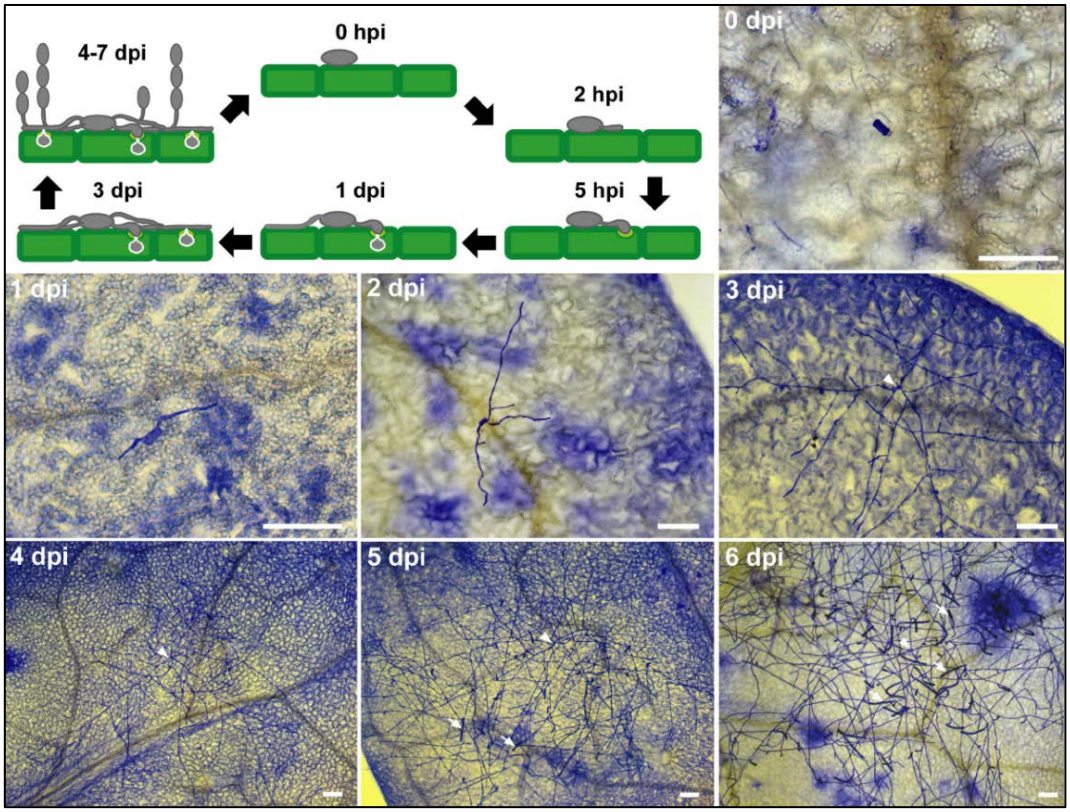

Figure 19. Infection cycle of *Golovinomyces orontii*.

After germination of conidiospores an appressorium is formed followed by haustorium formation. In the course of infection, several more appressoria develop in cells adjacent to the first invaginated plant cell. The infection cycle is completed by establishment of conidiophores carrying conidiospores at 4 to 7 days post infection (Weßling and Panstruga, 2012).

There are conflicting reports regarding this callose deposition after fungal penetration: On the one hand, in plants deficient in pathogen-induced callose deposition, resistance was higher compared to WT plants and it was speculated that the fungus might use callose deposition by the plant as a “cloaking device” to mask its presence and protect its haustoria (Nishimura *et al*., 2003; Maor and Shirasu, 2005). On the other hand, recent experiments have shown that elevated amounts of callose, deposited at an early time point in infection with powdery mildews, indeed confers penetration resistance (Ellinger *et al.,* 2013). In *Arabidopsis* plants resistant to *Golovinomyces orontii*, multiple copies of the *R* genes *RPW8.1* and *RPW8.2* were detected (Xiao *et al*., 2003). These resistance genes engage the SA-signalling

pathway, including SA, *EDS1*, the NB-LRR gene signalling components *PAD4, EDS5*, and *NPR1* in order to activate HR and induce resistance (Xiao *et al*., 2005). Recent studies provided evidence that RPW8 proteins are targeted and translocated specifically to the extrahaustorial membrane of *G. orontii* and induce broad-spectrum resistance against powdery mildew pathogens (Wang *et al*., 2013).

3.9 The biotrophic oomycete *Hyaloperonospora arabidopsidis* specialised on *Arabidopsis thaliana*

The downy mildew *Hyaloperonospora arabidopsidis* is one of various pathogens responsible for foliage blight and is closely adapted to its host *Arabidopsis thaliana*. Phylogenetically, this pathogen does not belong to the group of fungi, as described in the past, but to the oomycetes. Oomycetes show a morphological similarity to some fungal pathogens in their infection structures such as appressoria, infection hyphae and haustoria, but they belong to the kingdom of Stramenophiles and are thus more closely related to brown algae and diatoms (Coates and Beynon, 2010). Unlike fungi, oomycete cell walls are mostly cellulose based and contain little to no chitin. The hyphae of oomycetes are structured in a coenotic way, which means that no septa are present to subdivide the hyphae.

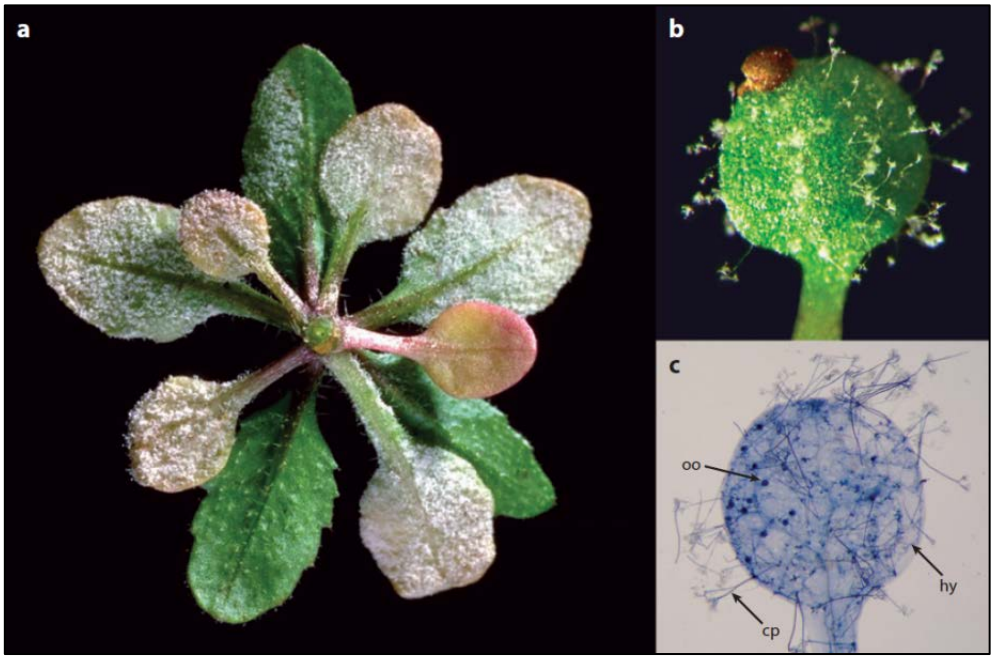

Figure 20. *A. thaliana* plants infected with the oomycete *H. arabidopsidis*.

(A) *Arabidopsis* plant heavily infected on the underside of leaves. (B) *Arabidopsis* cotyledon supporting clearly visible conidiophores. (C) Lactophenol/trypanblue-stained cotyledon (7 dpi) showing the leaf pervaded by oomycete hyphae (hy) and the leaf surface covered in conidiophores (cp) and sexual oospores (oo), respectively (Coates and Beynon, 2010).

3.9 The biotrophic oomycete *Hyaloperonospora arabidopsidis* specialized on *A. thaliana*

In contrast to fungi, which exhibit haploid or dikaryotic vegetative nuclei, oomycete vegetative nuclei are present in a diploid state. Compared to fungi, there are also some differences in biochemical pathways and in the production of motile biflagellated zoospores by oomycetes (Coates and Beynon, 2010). The downy mildew *Hpa* is very closely adapted to its host *A. thaliana*. In the compatible interaction, an asexual conidiospore that landed on a leaf germinates and forms an appressorium to enable the oomycete to gain access to plant cells (Figure 21).

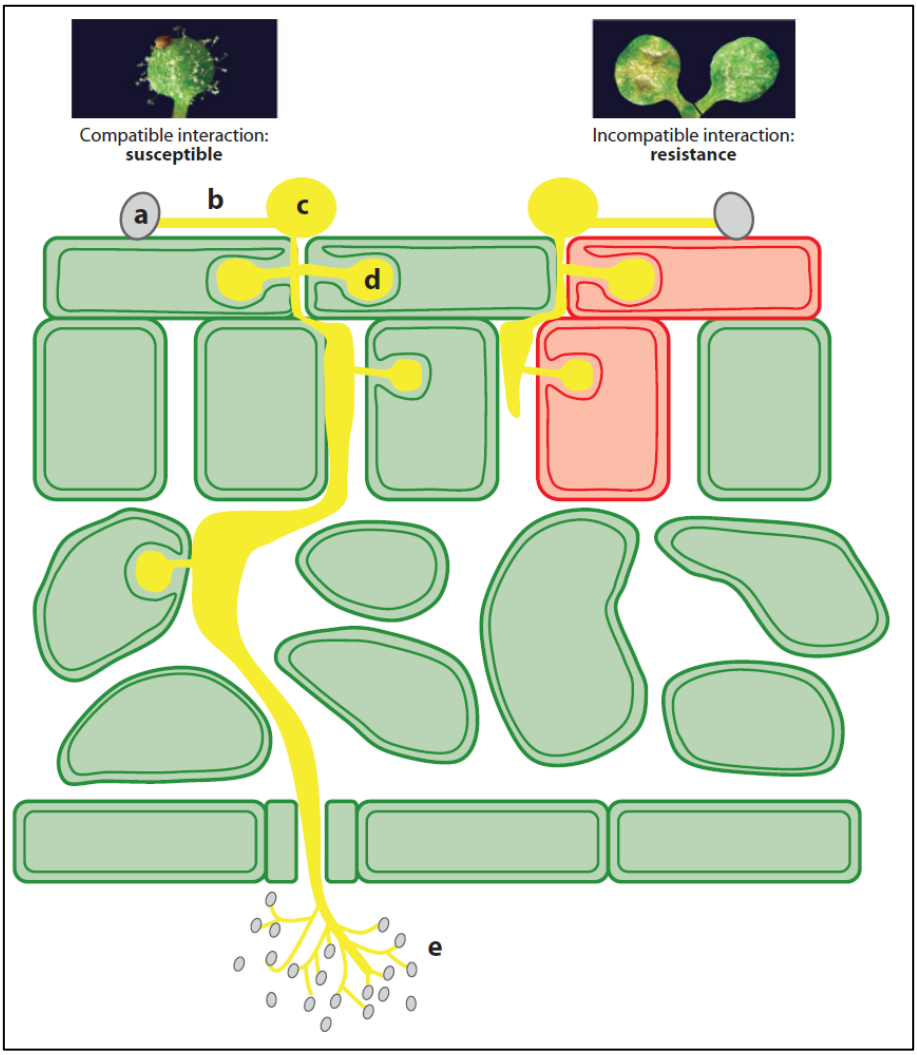

Figure 21. Schematic model of compatible and incompatible interactions of *A. thaliana* with *Hpa*.

In the compatible interaction the spore landing on the leaf (a) is able to germinate and form a germ tube (b) as well as appressorium (c) and haustoria (d), respectively. Hyphae grow intercellularly until exiting the leaf through stomata and producing conidiophores, which carry the asexual conidiospores (E). The incompatible interaction between plants and oomycetes is characterised by recognition of *Hpa* effectors and induction of a HR response (Coates and Beynon, 2010).

The oomycete then enters the leaf by producing a penetration hypha that is able to move between the anticlinal walls of neighbouring epidermal cells. Into these epidermal cells haustoria are inserted before the oomycete hyphae branch out into the mesophyll tissue, inserting haustoria into mesophyll cells on the way. Conidiophores are produced that egress

from stomata and bear asexual conidiospores (Figure 20; Figure 21). Approximately one week after infection, sexual oospores are formed by intertwining of hyphae that differentiate into oogonia and paragynous antheridia: karyogamy occurs and enables sexual reproduction of the oomycete. Oospores are able to survive during winter on plant debris and infect roots of new plants in favourable conditions, growing intercellularly through the plant and complete the pathogen´s lifecycle with production of new conidiospores and oospores (Glazebrook, 2005; Coates and Beynon, 2010). As *Hpa* is an obligate biotroph, the plant stays alive during the whole infection process (Glazebrook, 2005). In order to prompt the host to produce nutrients needed by the oomycete and to repress defence responses, *Hpa* introduces effector proteins into plant cells (Birch *et al*., 2006; Figure 22). These effectors share a conserved RXLR motif (Arg, any amino acid, Leu, Arg) and are delivered into plant cells in a two-step process, the secretion into the extrahaustorial space followed by translocation into the plant cell mediated by the RXLR motif and plant chaperone proteins (Birch *et al*., 2006; Morgan and Kamoun, 2007).

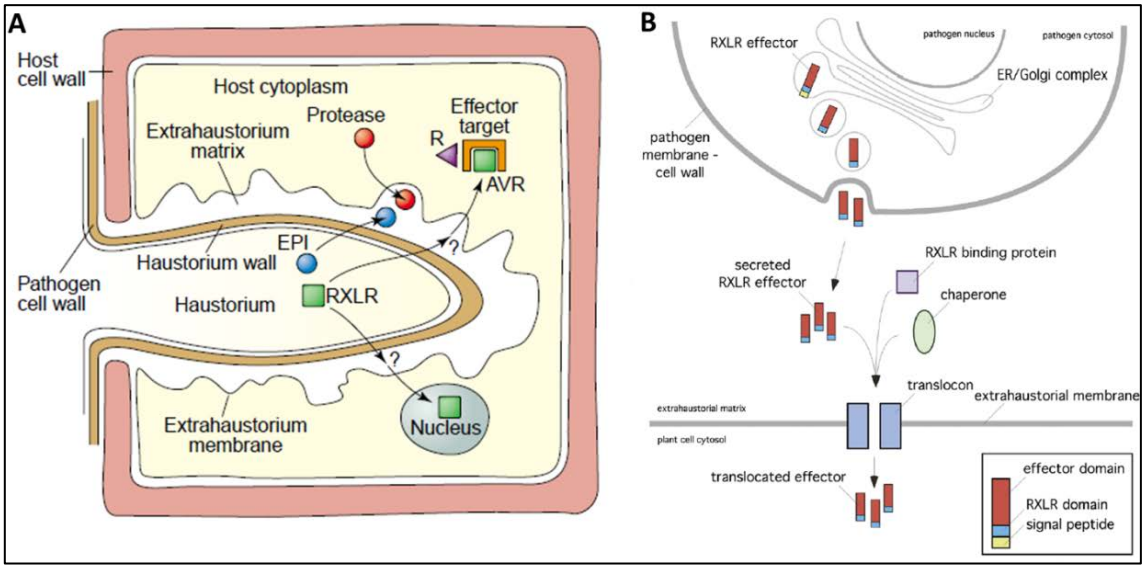

Figure 22. *Hpa* introduces effectors into plant cells to repress defence responses.

(A) *Hpa* effectors with a conserved RXLR motif (Arg, any amino acid, Leu, Arg) are translocated from the pathogen via the haustorial membrane and wall into the extrahaustorial matrix and introduced into the plant cell to manipulate defence responses (Birch *et al*., 2006). (B) RXLR effectors were shown to have a signal peptide to target the proteins for secretion into the extrahaustorial space. Translocation into the plant cell is mediated by RXLR binding proteins as well as chaperones (Morgan and Kamoun, 2007).

Recent results have shown that effectors introduced into plants by *Hpa* and other oomycetes not only function in repression of plant defence responses, but also lead to global molecular reprogramming of plant metabolism in order to accomplish parasitic colonisation (Birch *et al.,* 2006; Stuttmann *et al*., 2011). The most effective defence strategy against this biotrophic pathogen is HR-mediated death of infected cells (Glazebrook, 2005). Effectors introduced into plant cells are detected by cytoplasmatically located RPP proteins (RESISTANCE TO PERONOSPORA PARASITICA), which induce *EDS1/PAD4*-mediated and SA-dependent

responses culminating in programmed death of the infected cell (Feys *et al*., 2001; Rehmany *et al*., 2005; Coates and Beynon, 2010; Figure 21). Plants affected in this signalling pathway show enhanced susceptibility towards *Hpa*. In *eds1* plants, for instance, HR-establishment is no longer possible and the plant becomes fully susceptible, and in *pad4* plants the HR was shown to be much slower than in WT plants, resulting in hyphal spread of the oomycete before a trailing necrosis and sparse sporulation (Feys *et al*., 2001; Glazebrook, 2005). SA-dependent responses are a major way of the plant to defend itself against *Hpa*, nevertheless other defence mechanisms were shown to be effective against this oomycete as well. Bartsch *et al*. (2006) have shown that there is strong evidence for a SA-independent defence mechanism involving *FMO1*, as well as *EDS1* and *PAD4*. In *sid2-1 fmo1-1* double mutants, loss of resistance against the avirulent *Hpa* strain Cala2 was significantly more severe than in *sid2-1* or *fmo1-1* alone, leading to the conclusion that SA-dependent and –independent defence mechanisms are important for full resistance against *Hpa* (Bartsch *et al*., 2006). JA- and ET-mediated defence responses do not seem to be usually involved in this interaction, but are effective if induced prior to infection, for instance by continous exposure to JA (Thomma *et al*., 1998; Zimmerli *et al*., 2004; Glazebrook, 2005). It was also shown in previous experiments that mutations resulting in disturbances of the plant´s amino acid homeostasis lead to enhanced resistance against *Hpa* (Van Damme *et al*., 2009; Stuttmann *et al*., 2011), demonstrating the close adaption of this oomycete to its host. Upon analysis of the *Hpa* genome it became evident that it lacks several genes, for example for nitrogen-assimilation and -fixation, and therefore strongly depends on the plant resources to ascertain a sufficient nitrogen and amino acid supply (Baxter *et al*., 2010).

4 Aim of the thesis

This work was focussed on the elucidation of the molecular principles of plant innate immunity and defence priming, using molecular and biochemical analyses and detection methods. A very important role in SAR and defence priming was shown for the non-protein amino acid Pip. One major aim of this thesis was to analyse the role of Pip in *Psm*-induced priming as well as the mechanisms of priming of gene expression and accumulation of defence-related metabolites by exogenously applied Pip. Furthermore, the characteristics of genes showing primed expression were studied, for instance their SA-dependency, their role in plant physiology, and the interplay of Pip- and SA-signalling in their regulation. Another important aspect of this work was to gain deeper insight into the role of mitogen-activated protein kinase signalling in SAR, Pip-induced resistance, and priming via metabolite and gene expression analyses. To test wether Pip confers a broad-spectrum resistance comparable to BABA, its effect on interactions of *A. thaliana* with the fungi *B. cinerea* and *G. orontii*, as well as the oomycete *H. arabidopsidis* was also analysed. These analyses included comparative metabolite profiling of plants infected with these pathogens and impaired in different defence signalling or defence metabolite biosynthetic pathways. Furthermore, an important aim was to test the ability of Pip to induce resistance against these pathogens of different lifestyles and phylogenetic groups.

5 Materials and methods

5.1 Plant material

For analysis of defence priming, the *A. thaliana* mutant lines *ald1* (SALK_007673) and *fmo1* (SALK_026163) were used. In addition, the EMS generated line *sid2-1* (Nawrath and Métraux, 1999) and the *sid2-1 ald1-6* double mutant, created by Dr Friederike Bernsdorff (Dr F. Bernsdorff, PhD thesis), were used for analysis of SA-dependency of primed genes. Analysis of MAPK involvement in SAR priming was conducted with the T-DNA insertion lines *mpk3-1* (SALK_151594), *mpk6-2* (SALK_073907), and the *mpk3-1 mpk6-2* (+/-) double mutant, for which seeds were kindly provided by Dr Ken Tsuda (MPIZ Cologne). Pip-induced resistance against *B. cinerea* was tested in Col-0, *ald1, fmo1, sid2, coi1, pad2-1* (EMS mutant obtained from NASC), *pad3, ein2* (diepoxybutane mutant, NASC), *ein2-1* (EMS mutant, NASC), and *etr1-1* (EMS mutant; NASC). For analysis of the *Arabidopsis-Hpa* interaction in addition to Col-0, *ald1, sid2, fmo1*, and *sid2-1 ald1-6,* the lines *npr1, eds5,* and *ics1 ics2* were used. All lines were in the Col-0 background and this accession was used as control. In order to analyse the avirulent interaction between the *Hpa* isolate Cala2, Col-0, and lines in the Col-0 background, the *A. thaliana* accession Ler-0, which is a natural host for *Hpa* Cala2, was used to propagate oomycete spores.

5.2 Primer used for quantitative real-time PCR

Name	**3´ -> 5´**	**5´-> 3´**
2OGD1 / K3	ACCAAATGCAGGTCATAAGC	TGAAGGGAAATAGAAAGTCGG
2OGD2	TGATATCTGCAGGAATGAAACG	CGAATCGAGCCCATAAAGAG
ACD11L	CGTTACACAACATTCTTGACC	TCAGATCTAAACCTTGTCTCAC
AGP5	CTACTGAATCTCCACCAGCTC	GAGGGAGACTCTGCTAACTG
AIG1	AGCAGTGACACCAGAAGGCCCT	GCGTGTAGCCCTCCATCCGC
ALD1	GTGCAAGATCCTACCTTCCCGGC	CGGTCCTTGGGGTCATAGCCAGA
ANAC042	CTCAACAAGCAGAGGTATGG	TGTGGTCGGAATCTAAGCTG
ARD	AGAGATCCGTTACTGCCT	GCCTTCATATAGTTGTCCGAG
ASK7	GATTGAAGAAGAGACCGCAC	CGATCACCATCTCAAGAATCTC
AT1G03660	ATTTAGGCATCACAGGTTTGG	GTATCAGAGGAATATCACCCAG
AT1G26420	TCTGTGCCATTTGTCATTCTC	TTATGTGCCCTCCTACTCCT

Name	**3´ -> 5´**	**5´-> 3´**
AT3G57460	TAAGTCTTTCGGACAATGGT	GTACAGTCACCTTGACAACG
AT5G39090	GAGTTACACCCATTAGTCCC	TAAGTGAGCCCAAGATTTGAG
ATPase1	AGAGGAAGATGAAGAGGAGG	ACTACAAGCTGACCATAACC
BAHD1	ATTGTGGGTGCTAAGTATGTC	TTCCATCTACCAATTCTGTCAC
BGLU31	TTGGTTCGAGCCATATGACAGTGC	TGGATAGTCTCCGAAAACTAGAGGGC
BGLU45	TACCTAGAGGAAGATTTGGAGAG	CGTCACAAATGGTTTAATCCC
BP/KNAT1	CAATCCTGATGGGAAGAGTG	TTCAGCAAATGGTTCTTGAG
BSMT1	ACTTTGAAGCAGGACGCAAT	CTGCAGTTGGCATGTTGAGT
C2D1	CCAACATTATATCCGCTAACCT	TACTCGCACAAAGACCTCTG
CHI1	CTGCTGTTTCACTAGAAGGA	TCAATGTAACACATGAACCC
COBL4	TTACCTGCACATACTCACAG	GAATCTTAGAATCAGCCTTGAC
CXE17	GCCGTTAAAGCCCGTTGCGTC	GGGAGACGGTGTTCAGGGGC
CXE20	GTTTGTCCTCCCATAGTCAC	TCACTTTCCATCTCAACCGT
CYP710A1	AGAGTAAGAGAAGAAGTAGCC	GCCTGTATCTAATGACCTCAC
CYP71A13	ATGAAGAAACTCCAAGACGA	GATTATCACCTCTGTCCCTG
CYP81G1	GAAGTTCGGAAGCTGATTAGG	AAGCAACATCACCTGTACGA
EXP10	AACAGATGACTCTTCTTCGT	CTGAACCTCTTCTCTTATTCCT
EXP12	CAGCATGAAATGAAGCAGAC	TCCCTAGAAGACACAATCCA
EXP13	GTTAGTCACTCACAGAGAAGGA	GTACATGATACCATCTTGACCA
FMO1	TCTTCTGCGTGCCGTAGTTTC	CGCCATTTGACAAGAAGCATAG
FRK1	ACAACAAAGAGGTACACTTGG	CTTGTTCTCCATTTATGACACC
GH3.3	TGACCGTTGATTCAGCTCTGCGA	GCCTTCACGTCCTTAGTGGACGG
GH3.4	AGGTGGGTTACCGGCTCGTCC	GACGCTGTCTGAATCCGACGTCC
GPAT5	CGAAACGGATGTTGATCAGTC	TGCATGAATATGCTCCTCAC
GRX480	CTTGAGATTGATGAGGAGAGG	GAGATATGAGTAGCCATAACCC
GRXS13	GGTTGAGATTGGTGAAGAAGAC	GCCATTAATATGAGCAGCCA

Name	**3´ -> 5´**	**5´-> 3´**
GSTU1	TCGATGACCAGATCCTAACAC	ATACTTCCTGCGATCATGTC
GSTU4	CTTCCTCAAGATCCTTACGA	CAACCTCTACTCCCTTCTC
HSP70	ATGAACCCTACCAACACC	ACTGTTTCTCCTCTCCCT
HSP83	TTTGGTGTTGGTTTCTACTCTG	GTATTCAAGCTGATCGTCCT
IPT7	CAAGCAATCTCGAAACTCTCAG	GGAGTTAAGTACGGGTAAGGA
KTI1	CTGTCATCCGTGGCCGAGGC	GGACATGGCTGCCCACCG
LAC7	CATCTTATTTGGTGAATGGTGG	GCGAAGTAAGTATCTCTTTCCT
LHY	TTCACAAAGTTGGAGAAAGAGG	TGCTGATGATACTTGAGAGG
MAPKKK18	GGGTCGGATATTTAGGTGAG	ACGGATGGTTTAGTAGTTGAC
MRP7	TGAATAGAGCTTCTACAGACC	CAGGGATGAAGACGATAAGG
MYB122	CGGTTGGCGAACCCTTCCGG	TCCTCGTCTTGGCTAAACTCTCCACG
NAR2	CCAATCTCTTCAGCGTTCAG	GCCTTCCTCTTCTCATTGAC
NCED5	CGGCACTTTCGTGAATTCGGCG	TTCAAGCTGGCTCCCACCGC
NIA1	GCCTGAATACATAATCAACGAG	TACCTCCTCCAGAATAAGCG
NIA2	AGTATCTAACACCAGACCAC	TTATACCACCAACCTTCTTCG
NPR1	TCTATCAGAGGCACTTATTGG	GCTTCATACAAGCTTTACCAC
NPR3	AAACAGTTGAGACTGGTCGA	TGGACATCATCCTTAAGCTCTC
NPR4	ATATCTACACTGGGAGGTTAAAGC	GAAGCTTCCGCTGAAATGAC
PAD3/ CYP71B15	GGCTGAAGCGGTCATAAGAG	TCCAGGCTTAAGATGCTCGT
PBS3	TGCCTGCTCGAGTCGCAACC	TGGACTAAGCCACAGAGCAAATGGC
PER58	TGTCCCGGAGTTGTCTCTTGTGCT	GTCCGCACGGATCGCTGTCC
PMEa	ATGTTGAGAGGTGATGGTATAGG	TGATCCCACGAGCTATAAACC
PMEIa	CACAGGATCTCAAAGACCAG	GTACATCCAAAGCAGCACTC
PR-1	GTGCTCTTGTTCTTCCCTCG	GCCTGGTTGTGAACCCTTAG
PR-3	CATGAAACTACAGGTGGATGG	AGACCGTAATTGTAGTTCCAC
PRB1	GACTATGTAAATGCTCACAACC	CCACTCTTTGCCAAGTTCTC

Name	3´ -> 5´	5´-> 3´
PTB	GATCTGAATGTTAAGGCTTTTAGCG	GGCTTAGATCAGGAAGTGTATAGTCTCTG
RABA1i	GATCGTCAAGGCTCAAATATGG	CTAAGCTCCTTTAGCCATCTC
RBOHA	GTTGCTTCTTCTGTTTCTTCGT	CGATTTCATCCCTATACATTCACC
RKL1-12	TGAAAGCTCATAAGTCTCCAG	GATACACTGTTCCAAAGCCT
SAG13	GCGACAACATAAGGACGA	CTTCATTTGCTTCTCCAACAC
SBT3.3	TCACTACAGCTTGGAGAACAG	AACCAGCAGAACATAAGTAGAG
SBT3.5	GAAACTTGCTGATTCTCCTG	CTCCTGTGTCAATAAAGCCA
SDR4	CTTAGGCAAGTATTGGATGG	CTCTTCTTGTATGTCCACGA
STZ	ATCAAGATCCGATTTCCACC	TGTAGCTCAACTTCTCCACC
TAT3	CTAACTCTTACGCACCCAG	CTATCACGATCTCTATGGCT
TIR2	TGCTTATAGACAAACCTCTCCA	ACTCTGCCATAACTCCTTCC
TPPD	GACTATGACGGTACATTATCCC	TCTACGAACCTTATCACGGC
UGT73B2	TTCCGGTACAAGTTTCATTTGG	TGCCCATCCTCTTATTATCATACC
UGT73B3	AACAGATAGCAGACCGTGAC	TCAGCCTTCTCCTCAAATCC
UGT73D1	TCCCGAGGATCGTGTTCCATGGA	AGGGAATGGCTCTACGGCCGA
UGT74E2	AAAGTTGTTGAAATGGGTCC	ATAGACAACAGAATTAGGCTCC
UGT76B1	CTTTACAAGAGACTAAGGCAG	CACACCTATCTGTAACTTATCCC
UGT85A1	CTTTACTCTTGATGTTGCGG	GTCTTCTAAGTACTCCTTCGTC
VQ2	TCAACCTAATCATCAACACCAC	ATTTCACTTTCCCTCTTCCA
WRKY38	CTGCTAAACCAGAAACCGA	GAATCGTCCCTCCAATTCTC
XHT10	TGTCCTCAGATCAGCCTAACCGGG	CGCGGTTATCAAGTCCCTCGGC
ZCF37	ACAGAGGAAATCAAGAACACAG	AACACAAGAACCAAGATCACAG

5.3 Plant cultivation

Arabidopsis seeds were sterilized in ethanol and sown out on 0.5 x MS agar plates (Murashige and Skoog, 1962). After 10-14 days the seedlings were transferred to 120 ml pots in soil (Klasmann-Deilmann, Substrat BP3) mixed with vermiculite and sand (eight parts

soil, one part vermiculite and sand, respectively). The plants were grown in climate chambers with 50-60 % air humidity and a photoperiod of ten hours light at 22 °C and 14 hours dark at 18 °C, respectively. For the experiments 5-6 week old, unstressed plants with a uniform appearance were used. For experiments with *Hpa,* seeds were sown out directly on soil and seedlings used after two to three weeks.

5.4 Cultivation of pathogens and inoculation of plants

5.4.1 Cultivation of *Pseudomonas syringae* pv. *maculicola*

Pseudomonas syringae pv. *maculicola* ES4326 strains were grown on King´s medium B (King *et al*., 1954) agar plates containing appropriate concentrations of antibiotics (50 µg ml^{-1} rifampicin for the virulent *Psm* strain; 50 µg ml^{-1} rifampicin and 15 µg ml^{-1} tetracycline for the avirulent strain *Psm avrRpm1*; and 50 µg ml^{-1} rifampicin and 25 µg ml^{-1} kanamycin for the *Psm lux* strain [Fan *et al*., 2008]) for 2 days at 28 °C.

5.4.2 Inoculation of *A. thaliana* plants with *P. syringae* pv*. maculicola*

For inoculation of leaves with *Psm*, the bacteria were grown over night in 2-3 ml liquid King´s medium B with the appropriate amount of antibiotics at 28 °C and 240 rpm. The log phase culture was washed three times with 10 mM $MgCl_2$ and diluted to the desired OD_{600}. The bacterial solution was pressure infiltrated into the abaxial side of *Arabidopsis* leaves using a 1 ml syringe without a needle; infiltration of 10 mM $MgCl_2$ was used as a control treatment.

5.4.3 Cultivation of *Botrytis cinerea*

B. cinerea B05.10 (provided by Dr P. Tudszynski, University of Münster) was grown on sabour and maltose agar plates (S & M plates; 1 % [w/v] peptone; 4 % [w/v] maltose; 1.5-2 % [w/v] agar) for 10-14 days at 22 °C and a photoperiod of 10 hours light and 14 hours darkness, respectively (modified from Ferrari *et al*., 2003). The spores were harvested by washing the spores off the plate with 10-20 ml of distilled water and filtering the solution through 1 layer of Miracloth (Calbiochem).

5.4.4 Inoculation of *A. thaliana* plants with *B. cinerea*

B. cinerea spores were germinated in 4 % S & M medium (1 % [w/v] peptone; 4 % [w/v] maltose) for 1.5 hours prior to inoculation. Four to six 3 µl droplets of 5 x 10^4 spores ml^{-1} were put on both sides of the middle vein on the adaxial side of *Arabidopsis* leaves and a transparent lid was put on the tray and taped shut to ensure high air humidity. After three days the leaves were harvested for metabolite analysis, measurement of lesion size and scoring of disease symptoms; for time course experiments, leaves were harvested at given time points.

5.4.5 Cultivation of *Hyaloperonospora arabidopsidis*

Spores of *Hpa* isolates Noco2 (provided by Dr B. Mauch-Mani, Université de Neuchâtel) and Cala2 (provided by Dr T. Griebel, Dr J. Parker group, MPIZ Cologne) were propagated every week on *A. thaliana* ecotypes Col-0 and Ler-0, respectively. Conidiospores of *Hpa* were harvested from infected leaves by cutting the plants above soil level and placing them into a 50 ml Falcon tube filled with 25-30 ml of distilled water. The spores were loosened from the leaves by strongly shaking the tube for a short time. The spore solution was filtered through Miracloth (Calbiochem) into a clean 50 ml Falcon tube and spores were counted using a Neubauer Improved Haemocytometer. The spore concentration was adjusted to 4 x 10^4 spores ml^{-1} for optimal sporulation and sprayed onto 2-3 week old *A. thaliana* seedlings. The seedlings were put under a water-misted transparent lid, which was taped shut to ensure high air humidity.

5.4.6 Inoculation of *A. thaliana* plants with *H. arabidopsidis*

Hpa spores were harvested as described above and sprayed onto either two to three week old or five to six week old plants, respectively. The plants were put under a transparent lid and leaves were harvested after 7 days for metabolite analyses, as well as scoring of disease symptoms; for time course experiments leaves were harvested at the indicated time points.

5.4.7 Cultivation and inoculation of *Golovinomyces orontii*

The powdery mildew strain *G. orontii* MGH (Spanu *et al*., 2010) was grown on 5-week old *A. thaliana* plants. For infection of plants, spores of *G. orontii* were brushed off the leaves of heavily infected plants onto new plants. The leaves were harvested at given time points for metabolite analysis and scoring of disease symptoms.

5.5 Assessment of systemic acquired resistance

To assess SAR in *A. thaliana*, plants were infiltrated with an inoculum of *Psm* ES4326 (OD_{600}=0.005) in three leaves with uniform appearance; as a control treatment a solution of 10 mM $MgCl_2$ was used. Two days after first infection, upper leaves were infiltrated with a lower inoculum (OD_{600}=0.001) of *Psm* ES4326 *lux*, carrying a luxCDABE cassette (Fan *et al*., 2008). Two and a half days after the second infiltration, leaf discs were cut out of 2° infiltrated leaves and luminescence was measured with a Luminometer (Sirius FB12, Berthold detection systems). In addition to Luminometer measurements, bacteria were also plated in appropriate dilutions (40,000 x and 80,000 x) and colonies counted after incubating the plates for two days at 28 °C. Samples for the determination of local and systemic responses were harvested at 24 hpi and 48 hpi, respectively. For SAR experiments with *Hpa* Noco2 used for challenge infection, plants were first inoculated as described above. Two days after the first inoculation, plants were sprayed with 5 x 10^4 spores ml^{-1} of the virulent *Hpa* isolate

Noco2, placed in high air humidity for seven days, and scored for development of SAR by microscopy analysis of lactophenol/trypanblue-stained leaves and counting of conidiospores.

5.6 Analysis of defence priming and Pip-induced priming

For the analysis of defence priming during SAR, lower leaves of *A. thaliana* plants were infiltrated with either *Psm* (OD_{600}=0.005) or a solution of 10 mM $MgCl_2$. Two days after treatment of 1° leaves, upper leaves were infiltrated with *Psm* (OD_{600}=0.005) or a solution of 10 mM $MgCl_2$, respectively; samples for analysis of metabolites and gene expression were taken 10 hours after the second infiltration. To test Pip-induced priming, plants were either watered with 10 ml water or with 10 ml 1 mM (10 µmol) D,L-Pip (S47167; Sigma-Aldrich), respectively, one day prior to infiltration with *Psm* (OD_{600}=0.005) or a solution of 10 mM $MgCl_2$ as a control treatment. Samples for the analysis of metabolites and gene expression were taken ten hours after infiltration.

5.7 Pipecolic acid-induced resistance

To test Pip-induced resistance against different pathogens, plants were treated with 10 ml water or 1 mM (10 µmol) Pip (S47167; Sigma-Aldrich) in a soil drench one day prior to infection. Symptoms were scored after 2 days in the case of Pip-IR against *Psm lux* by measuring bacterial growth in the Luminometer and plating bacteria, respectively. Plants infected with *B. cinerea* after Pip-treatment were analysed 3 days after infection by measuring lesion size. Pip-IR in plants infected with *Hpa* was analysed seven days after infection by counting conidiospores and analysing cell death and hyphal growth by lactophenol/trypanblue-staining of leaves. Pip-induced resistance against *G. orontii* was measured at 7 dpi by quantification of conidiophore number per microcolony.

5.8 Analysis of gene expression by quantitative real-time PCR analysis

5.8.1 Extraction of plant RNA

Total plant RNA was isolated from frozen tissue by using the peqGOLD TriFast (PEQLAB) extraction reagent following the manufacturer´s instructions. Briefly, 80-100 mg of frozen plant tissue were homogenized in a tissue homogenizer (TissueLyser II, Qiagen), treated with 1 ml PeqGold TriFast reagent and mixed thoroughly till thawed. Samples were treated with 200 µl chloroform, vortexed strongly to form a homogenous suspension and centrifuged at 12,000 x g for 5 minutes. The upper organic phase was pipetted into a reaction tube containing 500 µl isopropanol; RNA was precipitated by incubating the samples at -20 °C for 15-20 minutes. After spinning the samples down (12,000 x g, 10 minutes) the resulting pellet was washed twice with 75 % ethanol and dried in the SpeedVac (Concentrater plus, eppendorf). RNA was dissolved in 44 µl of RNAse-free water at 65 °C, RNA purity was

checked on a 1 % agarose gel and RNA concentration determined by measuring absorption at 260 nm (BioPhotometer plus, Eppendorf). One microgram of RNA was treated with DNase for 30 minutes at 37 °C to remove genomic DNA. DNase was inactivated by adding 25 mM EDTA and incubating the samples at 70 °C for 15 minutes. RNA was transcribed to cDNA by adding 10 µM Oligo dTs, 10 mM dNTPs, 10 x reaction buffer and 3 units reverse transcriptase and incubating the samples at 42 °C for 60 minutes. To stop the reaction, samples were incubated at 70 °C for 15 minutes; the samples were diluted 1:10 with RNAse-free water prior to use in quantitative real-time PCR.

5.8.2 Quantitative real-time PCR analysis

To analyse gene expression, cDNA was amplified in a 10 µl reaction volume with 0.75 µM gene specific primers and 5 µl of SYBR-Green reaction mix. The qPCR was performed in triplicates with a cycling programme of a two minute activation step at 95 °C and 35 to 40 cycles of 5 s at 95 °C to denaturate the DNA strands and 30 s at 60 °C to amplify the new DNA strands. As a housekeeping gene the *POLYPYRIMIDINE TRACT-BINDING* (*PTB*) *PROTEIN1* (*At3g01150*) (Czechowski *et al*., 2005) was used. The qPCR data was analysed using the Rotorgene Q 2.0.2 software, with a threshold for normalized fluorescence set to 0.05. The resulting Ct and amplification values were used to calculate the relative mRNA abundance; gene expression of genes of interest were normalized to the expression of the housekeeping gene and expressed as fold-change expression relative to the $MgCl_2$-treated WT control sample.

5.9 Lactophenol/trypanblue-staining

Lactophenol/trypanblue (TB)-staining (Keogh *et al*., 1980) was used to visualize dead plant cells as well as fungal and oomycete hyphae. Leaves were covered with TB-staining solution (10 g phenol, 10 ml glycerol, 10 ml lactic acid, 10 ml water, and 0.02 g of trypan blue dye; mixed with 96 % ethanol; 1:2 [v/v]) and boiled for 1-5 minutes. The staining solution was removed and the leaves were destained in chloral hydrate (2 kg chloralhydrate dissolved in 1l water); the destaining solution was changed every day until no more blue background was visible on the leaves. The destained leaves were kept in 50 % (v/v) glycerol and mounted onto glass slides for analysis via light microscope.

5.10 Analyses of plant metabolites

To extract and analyse metabolites from *A. thaliana*, a modified Vapour Phase Extraction method (Schmelz *et al*., 2004) was used. Briefly, 150 to 200 mg of frozen leaf material were homogenized and the samples were mixed vigorously after adding 600 µl of extraction buffer (H_2O:1-propanol:HCl-1:2:0.005 [v:v:v]). After adding 30 µl of a standard solution (D4-salicylic acid, dihydro-jasmonic acid, indolepropionic acid [IPA]; 3.33 ng / µl each) and 1 ml of

dichloromethane (GC ultra-grade, Roth), the samples were mixed strongly and centrifugalized for 1 minute at 14,000 rpm. The lower organic phase was dried via water-free Na_2SO_4 and 2 µl of 2 M trimethylsilyldiazomethane (Sigma-Aldrich) in hexane was added to the samples to convert carboxylic acid groups into their corresponding methyl esters. The reaction was stopped after 5 minutes by adding 2 µl of 2 M acetic acid in hexane to each sample and incubating the samples another 5 minutes. The metabolites were evaporated at 70 °C and collected in a volatile collector trap packed with Porapak-Q absorbent (VCT-1/4X3-POR-Q, Analytical Research Systems), with a final evaporation step at 200 °C for 2 minutes. The samples were eluted from the collector trap with 1 ml of dichloromethane, reduced to 30 µl in a stream of gaseous nitrogen and subjected to GC/MS-analysis. For extraction of glycosidic bound forms of SA, 30 µl of standard solution (D4-salicylic acid, dihydro-jasmonic acid, indolepropionic acid; 3.33 ng / µl each) and 1 ml of 0.1 N HCl were added to the upper hydrous phase and the pellet resulting after the centrifugation step and heated at 100 °C for 30 minutes. After cooling down, the samples were subjected to solvent extraction by adding 2 ml of dichloromethane and shaking vigorously; the organic layer was transferred into a new glass vial and the step was repeated two times. The samples were dried via water-free sodium sulfate and the solvent completely removed in a gentle gaseous nitrogen flow. After adding 300 µl of dichloromethane and 60 µl of methanol, the samples were mixed briefly and subjected to vapour phase extraction as described above. Four microliters of sample mixture were separated in a gas chromatograph (GC 7890 A, Agilent Technologies) equipped with a fused silica capillary column (ZB-5MS 30 m x 0.25 mm, Zebron, Phenomenex), combined with a 5975C (EI) mass spectrometric detector (Agilent). Initiation injection was at 250 °C and afterwards the metabolites were separated according to the following temperature programme and under a constant flow of helium with 1.2 ml/min: 3 minutes at 50 °C followed by an increase to 240 °C in 8 °C per minute steps and a further increase in temperature to 320 °C in 20 °C per minute steps; the final temperature of 320 °C was maintained for 3 minutes. For the quantitative analysis of metabolites, peaks originating from selected ion chromatograms were integrated. The peak area of a substance was related to the peak area of the corresponding internal standard and experimentally determined correction factors for each substance and standard pair were used in the calculation of the substance amount: SA (m/z 120) –D4-salicylic acid (m/z 124); jasmonic acid (m/z 224) –dihydrojasmonic acid (m/z 156), camalexin (m/z 200) –indolepropionic acid (m/z 130), indole-3-carboxylic acid (m/z 144) –indolepropionic acid (m/z 130). In cases with no available correction factor, for example for unknown substances, a correction factor of 1 was used and the internal standard chosen according to retention time.

Calculation:

$Area_{m/z}$ (substance) * 100 * correction factor/ $Area_{m/z}$ (internal standard) * FW

5.11 Extraction of free amino acids

For the extraction and analysis of free physiological amino acids from plants, the EZ:faast free amino acid analysis kit for GC/MS (Phenomenex) was used. In short, 50-100 mg of leaf material were homogenized and 500 µl of extraction buffer (25 % acetonitrile in 0.01 N HCl) were added to each sample. After shaking the samples thoroughly for 15 minutes, free amino acids were extracted following the manufacturer´s instructions. In this method, free physiological amino acids were adsorbed to a SPE sorbent tip, eluted after a washing step, and treated with propyl chloroformate (Kugler *et al*., 2006) which lead to highly stable derivatisation of both the amine and carboxyl groups of amino acids. The dry residue after evaporating the solvent was re-dissolved in 30 µl dichloromethane and subjected to GC/MS analysis. Three microliters of each sample mixture were separated on a silica capillary column (ZB-AAA 10 m x 0.25 mm, Zebron, Phenomenex) with an initiation injection at 250 °C and a separation of amino acids according to the following programme and under a constant flow of helium with 1.2 ml/min: 3 minutes at 70 °C followed by an increase to 240 °C in 8 °C per minute steps and a further increase in temperature to 320 °C in 20 °C per two minutes steps; the final temperature of 320 °C was maintained for 2 minutes. To quantify amino acid levels, peaks originating from selected ion chromatograms were integrated: Gly (m/z 116), Ala (m/z 130), Val (m/z 158), β-Ala (m/z 116), Leu (m/z 172), Ile (m/z 172), GABA (m/z 130), Ser (m/z 146), Thr (m/z 101), Pro (m/z 156), Pip (m/z 170), Aad (m/z 244), Asp (m/z 216), Glu (m/z 84), Asn (m/z 69), Gln (m/z 84), Cys (m/z 248), Orn (m/z 156), Lys (m/z 170), His (m/z 282), Phe (m/z 148), Tyr (m/z 107), and Trp (m/z 130). The peak area of a substance was related to the peak area of the internal standard norvalin (m/z 158; included in reagent 1) and experimentally determined correction factors for each substance were used in the calculation of the substance amount. In cases with no available correction factor, for example for unknown substances, a correction factor of 1 was used and the relative amount per gram fresh weight calculated.

Calculation:

$Area_{m/z}$ (substance) * 11.7 * correction factor/ $Area_{m/z}$ (internal standard) * FW

5.12 MAP kinase activity assay

In order to analyse MAPK activity, samples were homogenized and 150 µl extraction buffer (50 mM Tris-Cl, ph 7.6; 5 mM EDTA; 5 mM EGTA; 2 mM DTT; 1 tablet of protein

phosphatase inhibitor for 10 ml buffer; 1 tablet of protease inhibitor cocktail for 10 ml buffer) were added to each sample. After shaking for 10 minutes at RT, the samples were spun down (6000 rpm, 10-15 minutes, 4 °C) and the supernatant was transferred to a new reaction tube. Protein concentrations were determined in a Bradford assay (Bradford, 1976) using a BSA protein calibration curve. For separation of proteins on a SDS-PAGE, equal amounts of protein were loaded onto the PAGE and blotted onto a PVDF membrane after electrophoresis. The blot was washed with TBST for 45 min, before the first antibody (anti-P42, 44; Tsuda *et al.*, 2013) was added and the blot incubated at 4 °C overnight. After washing the blot three times for 5 minutes each, the second antibody was added and the blot incubated for two to three hours. The signal was detected by ECL after washing the blot again three times for 5 minutes each.

5.13 Reproducibility of experiments and statistical analyses

The presented data shown in figures resulted from a single biological experiment. Unless otherwise stated, the results were similar in at least two biologically independent experiments. Statistical analyses were performed using Student´s two-tailed *t* test.

6 Results

6.1 *ALD1* and *FMO1* are necessary regulators of defence priming in *Arabidopsis thaliana*

In previous experiments strong evidence was revealed of an essential role for defence priming in SAR (Návarová *et al*., 2012). These data not only demonstrated that priming is a necessary mechanism for SAR-development, but also that Pip-accumulation is necessary as well as sufficient for the induction of SAR priming. As only a small selection of defence responses was analysed in previous experiments (primed accumulation of Pip and camalexin, primed expression of defence-related genes *ALD1* and *FMO1*; Návarová *et al.*, 2012) an expansion of this study was necessary to gain better insight into the principles of SAR priming. The crucial question for this study was if expression of all defence-related genes is primed during SAR or only a certain subset of these genes. In order to answer this question and get a more detailed understanding of defence-related gene priming, genome-wide microarray analyses were carried out (Gruner *et al*., 2013) and genes grouped in functional categories (SA-independent, partially SA-dependent, and SA-dependent). From these categories, a number of 67 genes were chosen for deeper analysis regarding their role in defence priming in Col-0, *ald1*, and *fmo1* (for full list of chosen genes, see table 1). Besides SA-dependency, other criteria for analysis of this set of genes were their induction in local and/or systemic leaves and their inducibility by exogenously applied Pip. Furthermore, among the studied genes were not only known defence-related genes, but also genes involved in metabolic processes (e.g. *TPPD,* involved in trehalose metabolism), signalling (e.g. *LHY*, a core regulator of the circadian clock), or transport (e.g. *ATPase1*). In this study, plants were treated as follows: lower leaves (1°) were infiltrated with either 10 mM $MgCl_2$ or *Psm* (OD_{600}=0.005), two days after 1° infiltration upper, distal leaves (2°) were infiltrated with either 10 mM $MgCl_2$ or *Psm* (OD_{600}=0.005) and scored for gene expression 10 hours post inoculation. We found in previous experiments that at 10 hpi, plants already show a clear priming response for both gene expression and metabolite accumulation (Návarová *et al*., 2012). Using the described mode of infiltration, four different cases could be distinguished: a control situation (1° $MgCl_2$/2° $MgCl_2$), a systemic response to the pathogen stimulus (1° *Psm*/2° $MgCl_2$), a local response to the pathogen stimulus (1° $MgCl_2$/2° *Psm*), and a combination of both local and systemic responses (1° *Psm*/2° *Psm*; SAR state). As mentioned earlier, SAR can be described as a combination of preactivated defence signalling pathways and enhanced alertness in the plant. Defence priming contributes in a major way to both by preactivation of defence metabolite biosynthesis pathways and marking defence-related genes for fast expression. We defined priming of a plant response as the response to

the combined local and systemic pathogen stimuli being significantly stronger than the sum of the individual local and systemic responses (Figure 23).

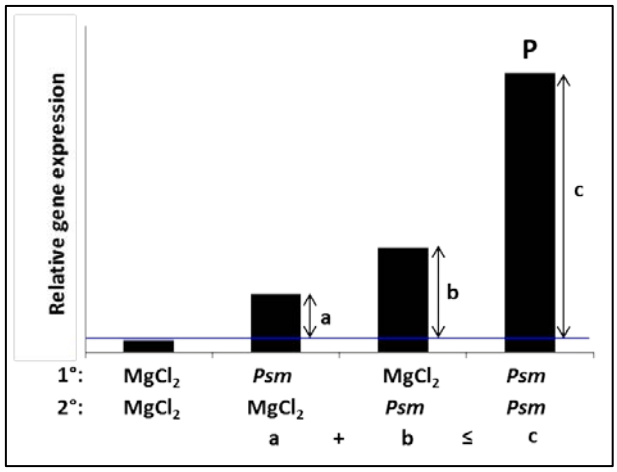

Figure 23. Priming of gene expression.

Plants were double inoculated to analyse defence priming of gene expression during SAR. Plants were treated in lower (1°) leaves with either 10 mM $MgCl_2$ or *Psm* (OD_{600}=0.005); 2 days later, upper leaves (2°) were infiltrated with either 10 mM $MgCl_2$ or *Psm* and scored for gene expression analysis at 10 hpi. Four different cases, a control situation (1° $MgCl_2$/2° $MgCl_2$), a systemic response (a; 1° *Psm*/2°$MgCl_2$), a local response (b; 1° $MgCl_2$/2° *Psm*), and a combination of systemic and local responses (SAR state) to the pathogen (c), can be discerned with this experimental setup. If the response in the SAR state of the plant (c) is significantly higher than the sum of local and systemic responses, expression of the analysed gene is considered as primed.

Analysis of gene expression in Col-0, *ald1* and *fmo1* showed a vast array of genes whose expression was primed upon biological SAR induction (Table 1). A very clear priming response was seen for the defence-related genes *ALD1* (Figure 24 A), and *FMO1* (Figure 24 B) in Col-0, which both belong to the group of SA-independent genes. The *ALD1* gene was not expressed in the *ald1* mutant and showed no priming of expression in *fmo1* plants. Similarly, the *FMO1* gene was not expressed in *fmo1* plants and showed no priming of expression in *ald1* plants (Figure 24 A, Figure 24 B). Moderate priming of gene expression demonstrated the likewise SA-independent genes *CHI1*, encoding a cell wall-located chitinase (Figure 24 C), and *TPPD,* which is involved in trehalose metabolism (Figure 24 D). These two genes exhibited very low expression in *ald1* plants and lower than WT expression in *fmo1* (Figure 24 C, Figure 24 D), but in the case of *TPPD*, a weak priming response was observable in *fmo1* (Figure 24 D). Among SA-independent genes were also several genes not showing primed expression during SAR, for instance the glutathione S-transferase gene *GSTU1* (Figure 24 E) and *At1g26420*, whose gene product is involved in ROS generation (Figure 24 F). *GSTU1* expression was slightly lower in *ald1* than in Col-0 plants, especially after the local pathogen stimulus (1° $MgCl_2$/2° *Psm*), but surprisingly this gene demonstrated primed expression in *fmo1* (Figure 24 E). Expression of *At1g26420* in *ald1* and *fmo1* was comparable to Col-0, with the exception of expression after a systemic pathogen stimulus (1° *Psm*/2° $MgCl_2$).

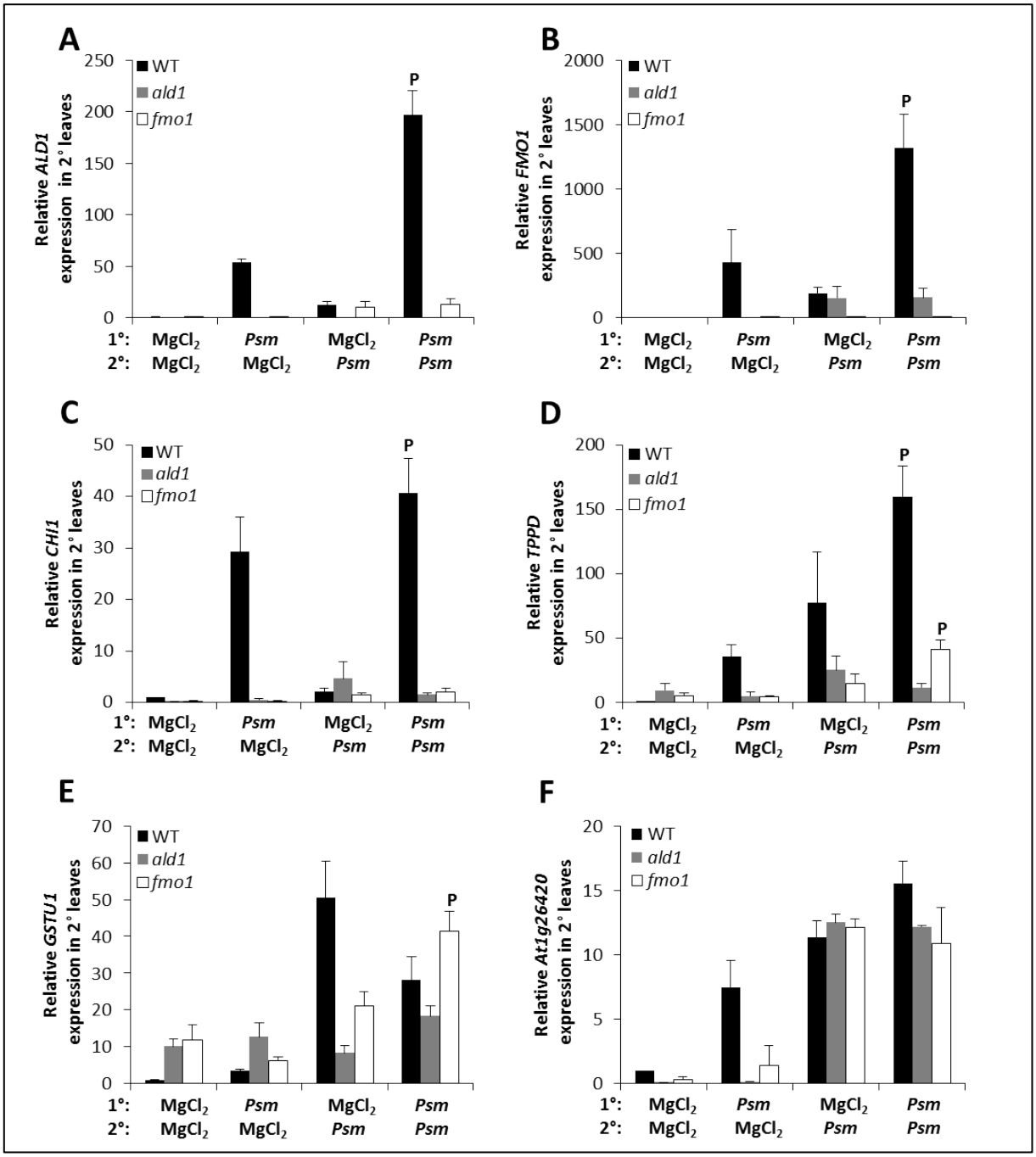

Figure 24. Defence priming of SA-independent genes.

Plants were double inoculated to analyse defence priming during SAR in Col-0, *ald1* and *fmo1*. Plants were treated in lower (1°) leaves with either 10 mM $MgCl_2$ or *Psm* (OD_{600}=0.005); 2 days later, upper leaves (2°) were infiltrated with either 10 mM $MgCl_2$ or *Psm* (OD_{600}=0.005) and scored for gene expression analysis at 10 hpi. Four different cases, a control situation (1° $MgCl_2$/2° $MgCl_2$), a systemic response (1° *Psm*/2°$MgCl_2$), a local response (1° $MgCl_2$/2° *Psm*), and a combination of systemic and local responses to the pathogen (SAR), can be discerned with this experimental setup. Relative expression of *ALD1* (A), *FMO1* (B), *CHI1* (C), *TPPD* (D), *GSTU1* (E), and *At1g26420* (F) at 10 hours after 2° treatment. Transcript levels were determined by quantitative real-time PCR analysis, are given as means ±SD of three replicate samples, and are expressed relative to the respective mock control value. Statistical differences in transcript abundance upon 2° *Psm* infection between SAR-noninduced and SAR-induced plants were analysed using two-tailed *t* test (P, primed gene). Due to the large number of genes analysed, the experiment was done one time.

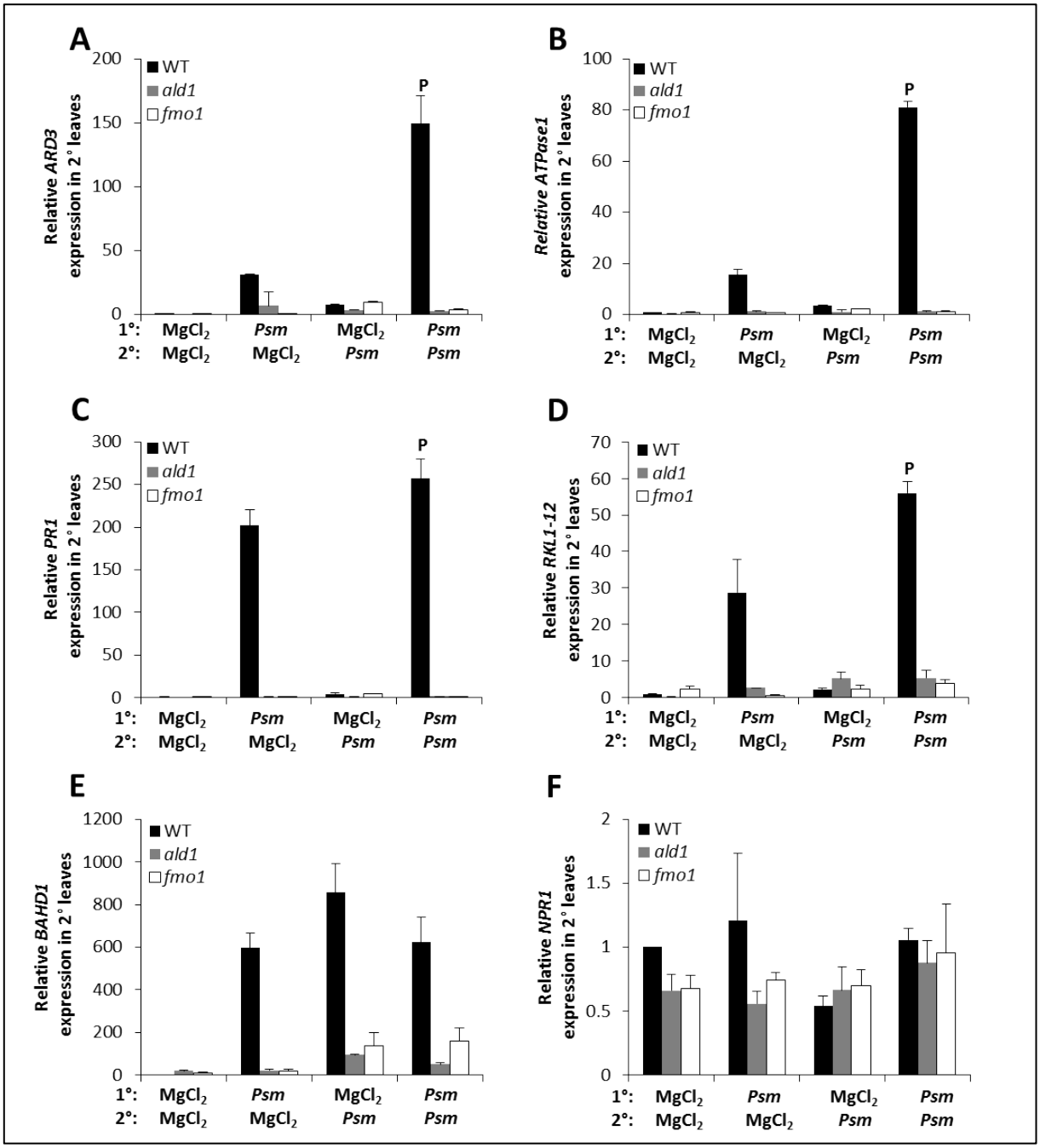

Figure 25. Defence priming of SA-dependent genes.

Plants were inoculated and samples analysed as described in figure 24. Relative expression of *ARD3* (A), *ATPase1* (B), *PR-1* (C), *RKL1-12* (D), *BAHD1* (E), and *NPR1* (F) at 10 hours after 2° treatment. This experiment was done once due to the large number of genes analysed.

Among the group of SA-dependent genes, primed expression in Col-0 demonstrated, amongst others, *ARD3* (Figure 25 A), encoding an acireductone dioxygenase involved in the methionine cycle, the transporter *ATPase1* (Figure 25 B), the defence-related *PR-1* gene (Figure 25 C), and *RKL1-12*, which encodes a leucine-rich repeat protein kinase involved in cell signalling (Figure 25 D). These four genes displayed very low expression in *ald1* and *fmo1* plants and additionally exhibited no primed expression (Figure 25 A-D). Non-primed genes in WT plants in this group were for example *BAHD1* (Figure 25 E), whose gene product plays a role in cell metabolism, and *NPR1,* a SA-receptor involved in SA-mediated signalling (Figure 25 F). Expression for *BAHD1* was again very low in *ald1* and *fmo1* and also not primed (Figure 25 E), but *NPR1* expression in these mutant lines was comparable to Col-0 WT plants (Figure 25 F).

In the group of partially SA-dependent genes, *PER58*, encoding a cell wall-located peroxidase (Figure 26 A), and the transcription factor involved in glucosinolate biosynthesis encoded by *MYB122* (Figure 26 B), showed a strong priming response in Col-0. In *ald1* and *fmo1*, expression of *PER58* in local leaves was comparable to Col-0, but this gene exhibited no expression in distal leaves and was also not primed in these lines (Figure 26 A). Expression of *MYB122* in *ald1* and *fmo1* was very low and likewise not primed (Figure 26 B). A weaker priming of expression was observed for *AGP5*, which encodes an arabinogalactan protein and is involved in cell wall biosynthesis (Figure 26 C), the oxidoreductase-encoding gene *2OGD1* (Figure 26 D), as well as *MRP7* (Figure 26 E), which encodes a transporter protein involved in SA-biosynthesis. This group of genes showed comparatively low expression in *ald1* and moderate, but lower than WT, expression in *fmo1*. In both plant lines expression of these genes was not primed. The likewise partially SA-dependent gene *ASK7*, which encodes a protein with ubiquitin-protein ligase activity that is involved in catabolism and signalling, demonstrated a very weak expression in Col-0, comparatively strong expression in mock-treated and local *Psm*-treated leaves of *fmo1*, and a surprisingly strong priming response in *ald1* (Figure 26 F). As this experiment was done one time so far, this strong priming response in *ald1* will have to be verified in further experiments.

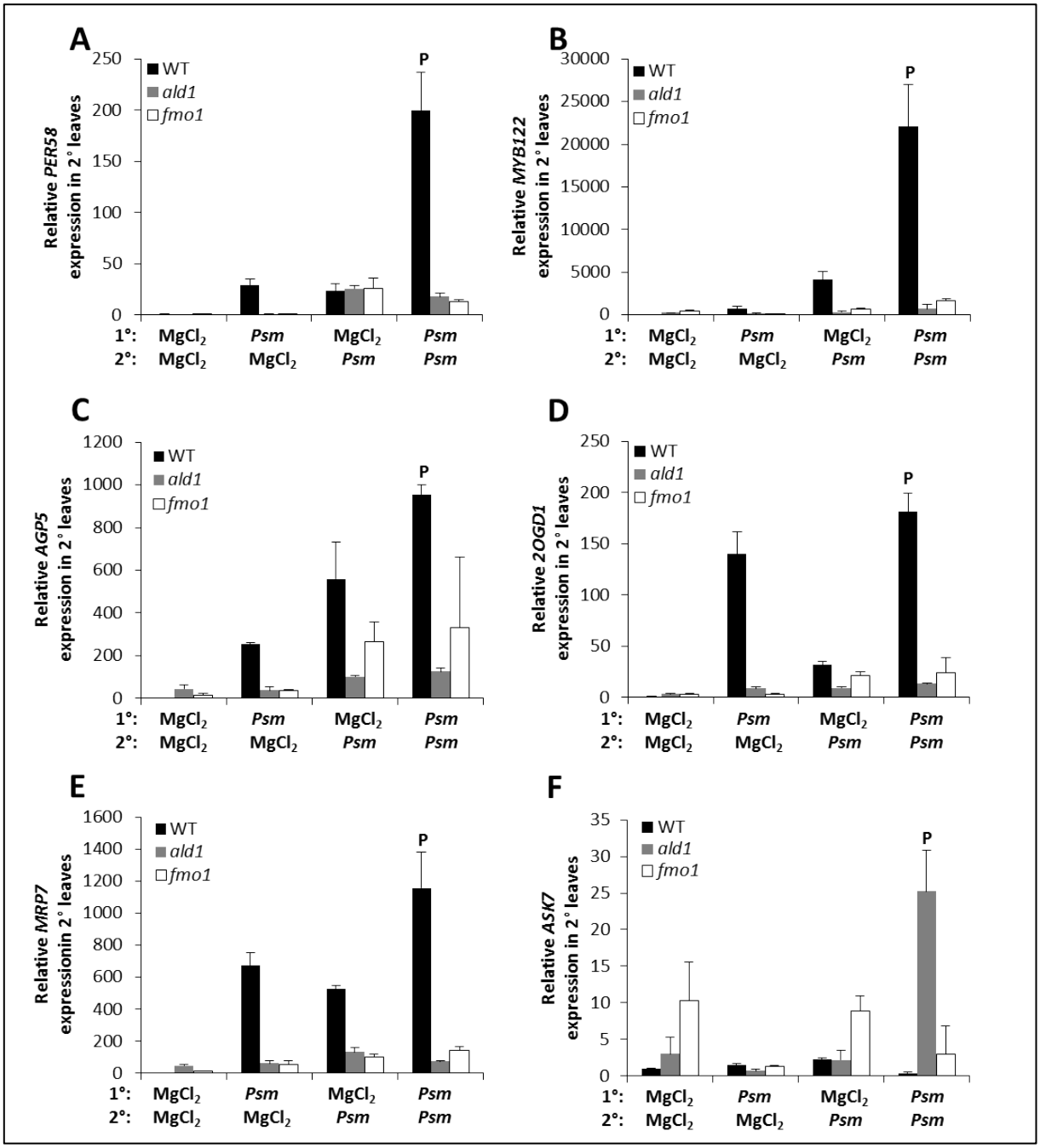

Figure 26. Defence priming of partially SA-dependent genes.

Plants were inoculated and samples analysed as described in figure 24. Relative expression of *PER58* (A), *MYB122* (B), *AGP5* (C), *2OGD1* (D), *MRP7* (E), and *ASK7* (F) at 10 hours after 2° treatment. This analysis was done one time due to the large number of genes analysed.

Table 1. Overview of gene expression in defence priming.

Plants were double inoculated to analyse defence priming during SAR in Col-0, *ald1* and *fmo1*. Plants were treated as described in figure 24. Genes were chosen after careful analysis of a set of microarray data (Gruner *et al*., 2013) and grouped into SA-independent, SA-dependent, and partially SA-dependent gene categories. Further criteria for chosen genes were their expression induction by exogenously applied Pip, local pathogen stimulus, and systemic pathogen stimulus (SAR), respectively. Corresponding gene expression data for genes presented in this table can be found in supplemental figures 1 to 8. P, gene primed; np, not primed.

Gene	Locus	Function/ involved in	Functional category	Expression induced by	SA-dependency	Col 0	*ald1*	*fmo1*
2OGD1	*At4g10500*	oxidoreductase	detoxification	ex. Pip; *Psm* local; SAR	partially SA-dependent	P	np	np
2OGD2	*At3g13610*	scopoletin biosynthesis	detoxification	*Psm* local; weak SAR	SA-independent	P	np	np
ACD11L	*At4g39670*	glycolipid transfer protein	detoxification/ abiotic stress	ex. Pip; *Psm* local; weak SAR	SA-independent	P	np	np
AGP5	*At1g35230*	arabinogalactan protein	cell wall	ex. Pip; *Psm* local; SAR	partially SA-dependent	P	np	np
AIG1	*At1g33960*	protein induced by *Psm avrRpt2*	defence signalling	ex. Pip; *Psm* local; SAR	SA-independent	P	np	np

6.1 *ALD1* and *FMO1* are necessary regulators of defence priming in *A. thaliana*

Gene	Locus	Function/ involved in	Functional category	Expression induced by	SA-dependency	Col 0	*ald1*	*fmo1*
ALD1	*At2g13810*	aminotransferase; Pipecolic acid biosynthesis	defence metabolism defence signalling	ex. Pip; *Psm* local; SAR	SA-independent	P	np	np
ANAC042	*At2g43000*	NAC transcription factor; senescence	defence metabolism	ex. Pip; *Psm* local; SAR	SA-independent	P	np	np
ARD3	*At2g26400*	acireductone dioxygenase 3	metabolism	*Psm* local; SAR	SA-dependent	P	np	np
ASK7	*At3g21840*	ubiquitin-protein ligase activity	catabolism/ signalling	ex. Pip; *Psm* local	partially SA-dependent	np	P	np
At1g03660	*At1g03660*	ankyrin-repeat containing protein	unknown	ex. Pip; *Psm* local; SAR	SA-dependent	np	np	np
At1g26420	*At1g26420*	oxidoreductase activity	ROS generation	ex. Pip; *Psm* local; SAR	SA-independent	np	np	np
At5g39090	*At5g39090*	HXXXD-type acyl-transferase family protein	metabolism	ex. Pip; *Psm* local; weak SAR	SA-independent	np	np	np

Gene	Locus	Function/ involved in	Functional category	Expression induced by	SA-dependency	Col 0	*ald1*	*fmo1*
ATPase1	*At3g28510*	AAA-type ATPase family protein	transporter	ex. Pip; *Psm* local; SAR	SA-dependent	P	np	np
BAHD1	*At5g42830*	BAHD transferase family protein	metabolism	ex. Pip; *Psm* local; SAR	SA-dependent	np	np	np
BGLU31	*At5g24540*	beta-glucosidase	detoxification/ biotic+abiotic stress	*Psm* local	partially SA-dependent	P	np	np
BGLU45	*At1g61810*	beta-glucosidase; lignin biosynthesis	secondary metabolism	*Psm* local	SA-independent	P	np	np
BSMT1	*At3g11480*	benzoic acid/ Salicylic acid-methyltransferase	secondary metabolism	ex. Pip; *Psm* local	SA-independent	np	np	np
C2D1	*At4g00700*	Ca^{2+}/lipid-binding phosphoribosyl-transferase	signalling	ex. Pip; *Psm* local; SAR	partially SA-dependent	np	np	np
CHI1	*At2g43570*	chitinase	defence	ex. Pip; *Psm* local; SAR	SA-independent	P	np	np

6.1 *ALD1* and *FMO1* are necessary regulators of defence priming in *A. thaliana*

Gene	Locus	Function/ involved in	Functional category	Expression induced by	SA-dependency	Col 0	*ald1*	*fmo1*
COBL4	*At5g15630*	secondary cell wall biosynthesis	cell wall	/	partially SA-dependent	np	np	np
CXE17	*At5g16080*	carboxyesterase	metabolism/ cell wall	*Psm* local	SA-independent	P	np	np
CXE20	*At5g62180*	carboxyesterase	cell wall	*Psm* local	SA-independent	P	np	np
CYP710A1	*At2g34500*	cytochrome P450; C22-sterol desaturase activity	defence metabolism	*Psm* local	SA-independent	P	np	np
CYP71A13	*At2g30770*	cytochrome P450; camalexin biosynthesis	defence metabolism	*Psm* local; weak SAR	SA-independent	P	np	np
CYP81G1	*At5g67310*	cytochrome P450	detoxification	*Psm* local	SA-independent	P	np	np
FMO1	*At1g19250*	flavin-dependent monooxygenase; SAR response	defence metabolism/ defence signalling	*Psm* local; SAR	SA-independent	P	np	np

6.1 *ALD1* and *FMO1* are necessary regulators of defence priming in *A. thaliana*

Gene	Locus	Function/ involved in	Functional category	Expression induced by	SA-dependency	Col 0	*ald1*	*fmo1*
FRK1	*At2g19190*	FLG22 INDUCED RECEPTOR KINASE1; early defence signalling	defence signalling	ex. Pip; *Psm* local; SAR	SA-dependent	P	np	np
GH3.3	*At2g23170*	IAA-amido synthase; conjugates amino acids to auxin	metabolism	/	SA-independent	P	np	np
GH3.4	*At1g59500*	IAA-amido synthase; conjugates amino acids to auxin	metabolism	*Psm* local	SA-independent	np	np	np
GPAT5	*At3g11430*	glycerol-3-phosphate acyltransferase; suberin biosynthesis	secondary metabolism	ex. Pip; *Psm* local	SA-independent	np	np	np
GRXS13	*At1g03850*	glutaredoxin; facilitates *B.cinerea* infection of *A.thaliana*	detoxification/ defence signalling	ex. Pip; *Psm* local; SAR	SA-dependent	P	np	np
GSTU1	*At2g29490*	glutathione s-transferase	detoxification	ex. Pip; *Psm* local	SA-independent	np	np	P
IPT7	*At3g23630*	isopentenyl transferase; cytokinin biosynthesis	metabolism	*Psm* local	SA-dependent	np	np	np

Gene	Locus	Function/ involved in	Functional category	Expression induced by	SA-dependency	Col 0	*ald1*	*fmo1*
KNAT1	*At4g08150*	class I knotted 1-like homeobox gene family	development	ex. Pip	SA-dependent	np	np	np
KTI1	*At1g73260*	trypsin inhibitor; modulates PCD in plant-pathogen interactions	cell death	/	SA-independent	P	np	np
LAC7	*At3g09220*	laccase	metabolism	*Psm* local	SA-dependent	np	np	np
LHY	*At1g01060*	myb-related transcription factor; circadian clock	signalling	ex. Pip	SA-independent	np	np	np
MAPKKK18	*At1g05100*	mitogen activated protein kinase kinase kinase	cell signalling	/	SA-independent	P	np	np
MRP7	*At3g13100*	multidrug resistance-associated protein; SA biosynthesis	transporter	ex. Pip; *Psm* local; SAR	partially SA-dependent	np	np	np
MYB122	*At1g74080*	transcription factor of the R2R3 factor gene family	defence metabolism	*Psm* local	partially SA-dependent	P	np	np

6.1 *ALD1* and *FMO1* are necessary regulators of defence priming in *A. thaliana*

Gene	Locus	Function/ involved in	Functional category	Expression induced by	SA-dependency	Col 0	*ald1*	*fmo1*
NCED5	*At1g30100*	9-*cis*-epoxycarotenoid dioxygenase	metabolism	*Psm* local	partially SA-dependent	np	np	np
NPR1	*At1g64280*	key regulator of SA-mediated SAR pathway	signalling	ex. Pip; SAR	SA-dependent	np	np	np
NPR3	*At5g45110*	SA-receptor	signalling	ex. Pip; *Psm* local; SAR	SA-dependent	np	np	np
NPR4	*At4g19660*	required for basal resistance in *A.thaliana*; SA-receptor	defence signalling	SAR	SA-dependent	np	np	np
PAD3	*At3g26830*	camalexin biosynthesis	defence metabolism	ex. Pip; *Psm* local; SAR	SA-independent	P	np	np
PBS3	*At5g13320*	conjugates amino acids to 4-substituted benzoates	signalling/ defence metabolism	ex. Pip; *Psm* local; SAR	SA-independent	np	np	np
PER58	*At5g19880*	peroxidase	biotic+abiotic stress	*Psm* local	partially SA-dependent	P	np	np

6.1 *ALD1* and *FMO1* are necessary regulators of defence priming in *A. thaliana*

Gene	Locus	Function/ involved in	Functional category	Expression induced by	SA-dependency	Col 0	*ald1*	*fmo1*
PMEa	*At2g45220*	invertase/pectin methylesterase inhibitor superfamily	cell wall	*Psm* local	SA-independent	P	np	np
PMEIa	*At5g46960*	invertase/pectin methylesterase inhibitor family protein	cell wall	*Psm* local	SA-independent	P	np	np
PR1	*At2g14610*	signalling in the SAR response; SA-responsive	defence signalling	ex. Pip; *Psm* local; SAR	SA-dependent	P	np	np
PR3	*At3g12500*	basic chitinase	defence signalling	*Psm* local	SA-independent	P	np	np
PRB1	*At2g14580*	basic PR1-like protein; repressed by SA	signalling	ex. Pip; *Psm* local	SA-dependent	np	np	np
RABA1i	*At1g28550*	RAB GTPase homolog	cell wall	/	SA-independent	np	np	np
RBOHA	*At5g07390*	NADPH oxidase; oxidative burst	ROS generation	*Psm* local	SA-dependent	np	np	np

6.1 *ALD1* and *FMO1* are necessary regulators of defence priming in *A. thaliana*

Gene	Locus	Function/ involved in	Functional category	Expression induced by	SA-dependency	Col 0	*ald1*	*fmo1*
RKL1-12	*At1g51860*	leucine-rich repeat protein kinase	signalling	ex. Pip; *Psm* local	SA-dependent	P	np	np
SAG13	*At2g29350*	short-chain alcohol dehydrogenase; senescence process	senescence/ cell death	*Psm* local; SAR	SA-independent	P	np	np
SDR4	*At3g29250*	short-chain dehydrogenase reductase	signalling	ex. Pip; *Psm* local	SA-dependent	np	np	np
TPPD	*At1g35910*	trehalose-6-phosphate phosphatase	metabolism	ex. Pip; *Psm* local	SA-independent	P	np	P
UGT73B2	*At4g34131*	UDP-glucosyltransferase	ROS generation	ex. Pip; *Psm* local; SAR	partially SA-dependent	P	np	np
UGT73B3	*At4g34135*	UDP-glucosyltransferase	ROS generation	ex. Pip; *Psm* local; SAR	partially SA-dependent	P	np	np
UGT73D1	*At3g53150*	glucosyltransferase - like protein	metabolism	ex. Pip; *Psm* local; SAR	SA-dependent	np	np	np

6.1 *ALD1* and *FMO1* are necessary regulators of defence priming in *A. thaliana*

Gene	Locus	Function/ involved in	Functional category	Expression induced by	SA-dependency	Col 0	*ald1*	*fmo1*
UGT74E2	*At1g05680*	indole-3-acetate beta-glucosyltransferase	abiotic stress	*Psm* local	SA-independent	P	np	np
UGT76B1	*At3g11340*	glucosyltransferase; conjugates isoleucic acid	defence signalling	ex. Pip; *Psm* local; SAR	SA-dependent	P	np	np
UGT85A1	*At1g22400*	UDP-glucose glucosyltransferase	defence signalling/ defence metabolism	*Psm* local; SAR	SA-independent	P	P	np
WRKY38	*At5g22570*	member of WRKY Transcription Factor; Group III	signalling	ex. Pip; *Psm* local; SAR	SA-dependent	np	np	np
XHT10	*At2g14620*	endoxyloglucan glycosyltransferase	cell wall	SAR	SA-dependent	P	np	np
ZCF37	*At1g59590*	unknown	unknown	ex. Pip; *Psm* local; SAR	SA-independent	P	np	np

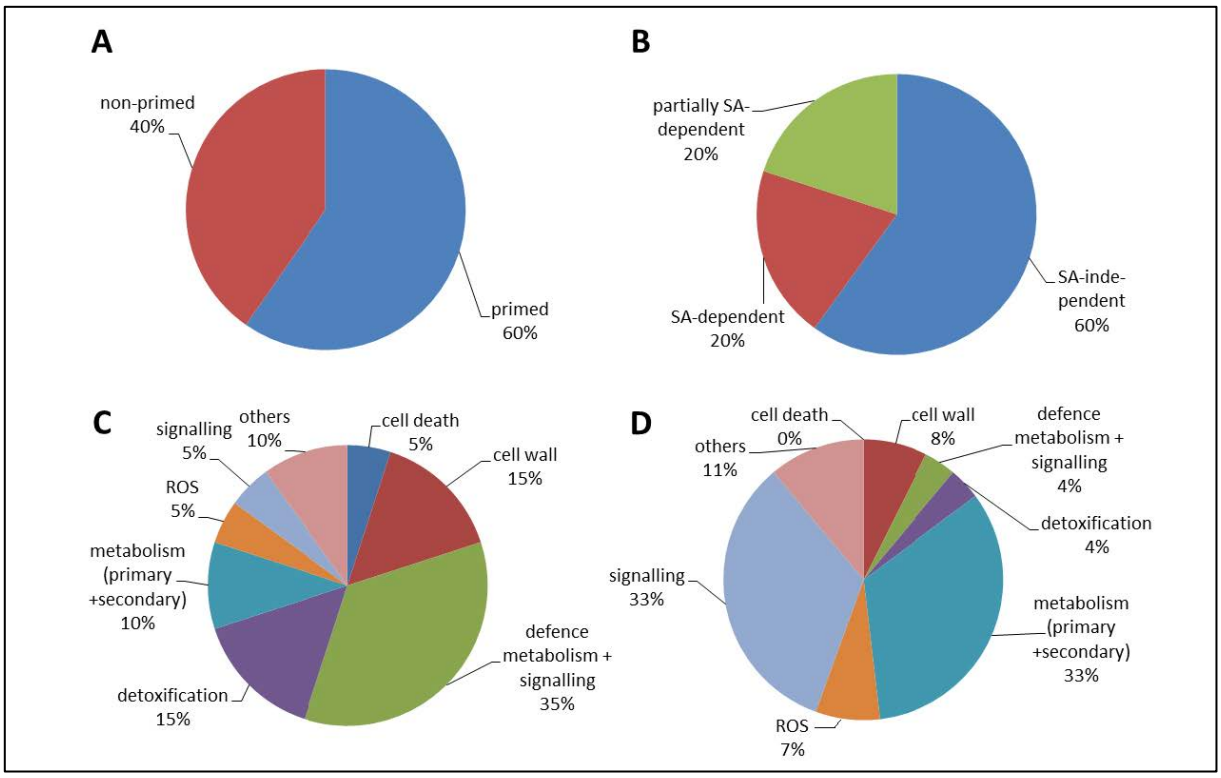

Figure 27. Categorisation of genes showing primed expression during SAR.

The 67 chosen genes (see table 1) were analysed with respect to their SA-dependency and priming of expression during SAR. (A) Of the 67 analysed genes, 60 % (n=40) showed primed expression and 40 % (n=27) were not primed. (B) The majority of genes showing primed expression was SA-independent (60 %, n=24) and 20 % were SA-dependent or partially SA-dependent, respectively (n=8). (C) The majority of primed genes were involved in defence signalling and metabolism, detoxification, and cell wall-related processes. (D) Genes not showing primed expression in defence were mostly involved in cell signalling and metabolism processes (primary and secondary metabolism).

Gene expression analysis of the 67 genes used in this study showed that a large number of genes exhibiting primed expression belonged to the group of SA-independent genes (Table 1; Figure 27 A). This is due in part to the majority of chosen genes showing SA-independent expression from the start (see Supplemental figure 9). More importantly, proteins encoded by genes with primed expression were found to be primarily involved in detoxification, defence signalling, defence metabolism, cell wall-related processes, cell death, and ROS generation or detoxification (Table 1; Figure 27 C). Gene products of non-primed genes, on the other hand, chiefly participate in metabolism and signalling processes of non-stressed plants (Table 1; Figure 27 D). One conclusion that can be drawn from this study is that a majority of genes exhibiting primed expression belong to the group of SA-independent genes. Another conclusion is that *ALD1* and *FMO1* play an essential role in defence priming, as only a very small number of genes showed primed expression in the *ald1* (*ASK7, UGT85A1*) and *fmo1* (*GSTU1, TPPD*) mutant lines.

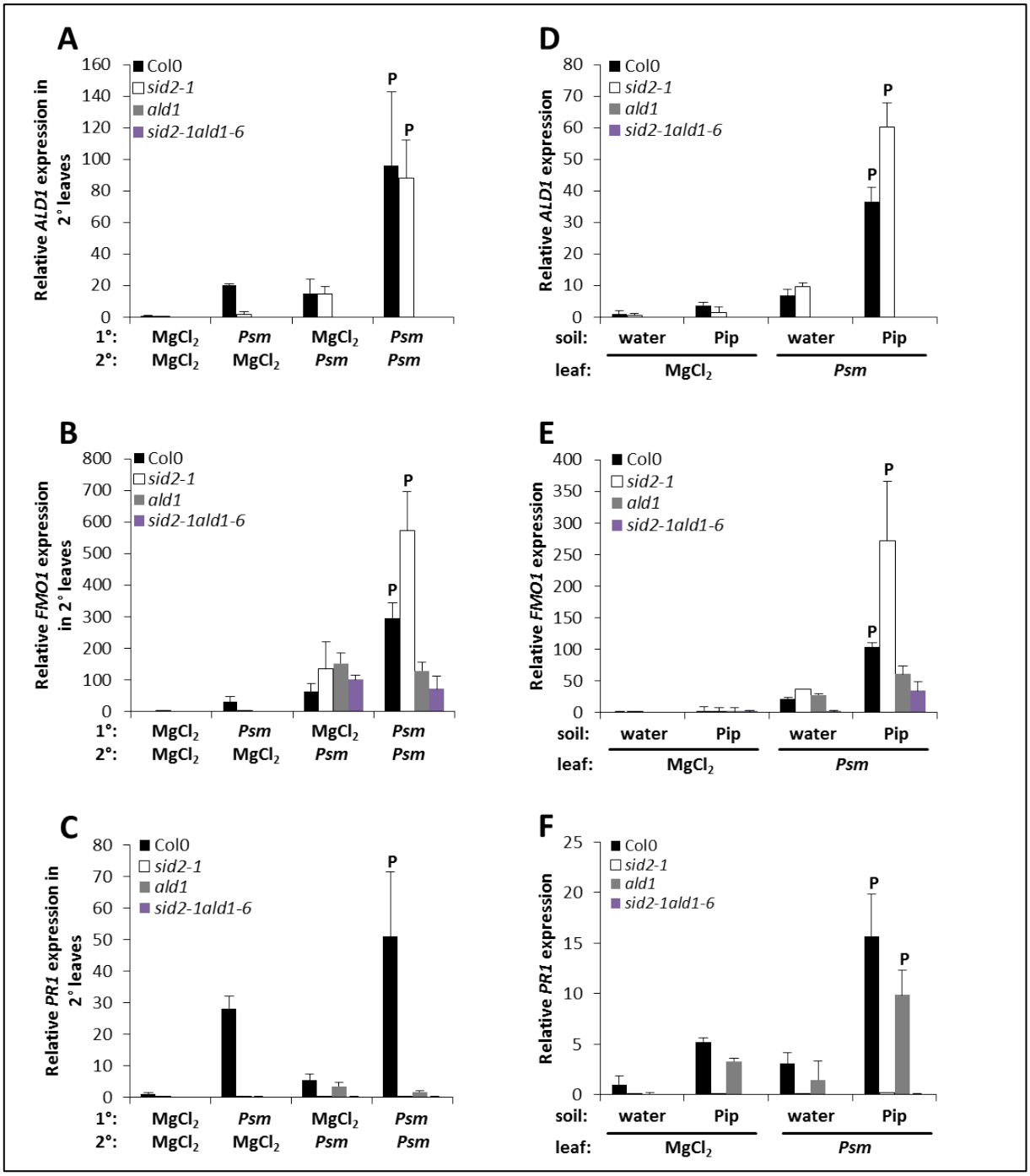

Figure 28. Regulation of SAR-associated defence priming.

(A) to (C) SAR priming and (D) to (F) Pip-induced priming of defence gene expression in Col-0, *ald1, sid2*, and *sid2 ald1*. (A) to (C) Plants were double inoculated to analyse defence priming during SAR in Col-0, *ald1, sid2*, and *sid2 ald1* as described in the legend to figure 24. (D) to (F) Water or 10 µmol Pip were applied to plants via soil drench. Leaves were infiltrated 1 day later with either 10 mM $MgCl_2$ or *Psm* (OD_{600}=0.005) and scored for gene expression analysis at 10 hpi. Relative *ALD1* (A) and (D), *FMO1* (B) and (E), and *PR-1* (C) and (F) gene expression was analysed as described in figure 24 (P, primed gene expression). This set of experiments was done in collaboration with Dr Friederike Bernsdorff.

We found in previous experiments a partial, SA-independent, SAR response in *sid2* (Bernsdorff, Döring, Gruner, Bräutigam, Schuck & Zeier, submitted to The Plant Cell) and in order to study this phenomenon in more detail, a double mutant unable to synthesize Pip and SA termed *sid2-1 ald1-6* was generated (*sid2 ald1*; Dr F. Bernsdorff, PhD thesis; Bernsdorff

et al., submitted to The Plant Cell). This mutant line, along with the parental lines *sid2* and *ald1* and Col-0 as WT control, was used to further dissect defence priming and SA-dependency of gene expression in priming (Figure 28; Bernsdorff *et al*., submitted to The Plant Cell). In a biological priming experiment gene expression of the SA-independent defence-related genes *ALD1* and *FMO1* was strongly primed in Col-0 and *sid2*, but not in *ald1* or *sid2 ald1* (Figure 28 A; Figure 28 B). In Col-0 and *sid2* the same level of transcript abundance for *ALD1* was determined (Figure 28 A), for *FMO1*, gene expression was about twice as high in *sid2* than in Col-0 (Figure 28 B). Expression of the SA-dependent gene *PR-1* was primed only in Col-0, and not in *sid2* or the double mutant *sid2 ald1* (Figure 28 C). From these results it can be deduced that for priming of SA-independent genes the presence of SA is not necessary, but for SA-dependent genes SA is essential.

6.2 Regulation of Pip-induced priming of gene expression

We were able to show in earlier experiments that exogenous application of Pip to plants one day prior to infection with *Psm* can prime gene expression in inoculated leaves (Návarová *et al.,* 2012). To analyse the relationship between Pip and SA and the SA-dependency of primed gene expression in more detail, Col-0, *ald1, sid2*, and *sid2 ald1* plants were treated with 10 ml 1 mM (=10 µmol) Pip one day before infiltrating leaves with 10 mM $MgCl_2$ or *Psm* (OD_{600}=0.005) and scoring gene expression 10 hours later. In plants treated in this manner, a strong priming response of *ALD1* and *FMO1* expression was observed in Col-0, with even stronger priming of these genes in *sid2* (Figure 28 D; Figure 28 E). *ALD1* expression was completely abolished in *ald1* and *sid2 ald1* (Figure 28 D), and *FMO1* expression was below WT-levels in these mutants (Figure 28 E). Treatment with Pip prior to infection lead to strong priming of *PR-1* expression in Col-0 and even restored priming of this gene to almost WT-levels in *ald1* (Figure 28 F). The priming response of this SA-dependent gene was abolished in *sid2* and *sid2 ald1* even after treating the plant with Pip prior to infection (Figure 28 F). The exogenously applied Pip seemed to be not sufficient to induce primed expression of the SA-independent gene *FMO1* in *ald1*, whereas primed expression of the SA-dependent gene *PR-1* could be observed very well in this line. This hints at different priming thresholds for SA-dependent and -independent genes.

As treatment of *Arabidopsis* plants with Pip before inoculation in part restored priming of *PR-1* expression in *ald1*, the effect of exogenously applied Pip on priming of gene expression in *fmo1* was analysed. Expression of the SA-independent genes *ALD1* and *SAG13*, as well as expression of the SA-dependent *PR-1*, was primed by exogenously supplied Pip in Col-0, but not in *fmo1* (Figure 29 A-C). Priming of camalexin accumulation by Pip-treatment was observed in Col-0, as described previously (Návarová *et al.*, 2012), but was completely abolished in *fmo1* (Figure 29 D).

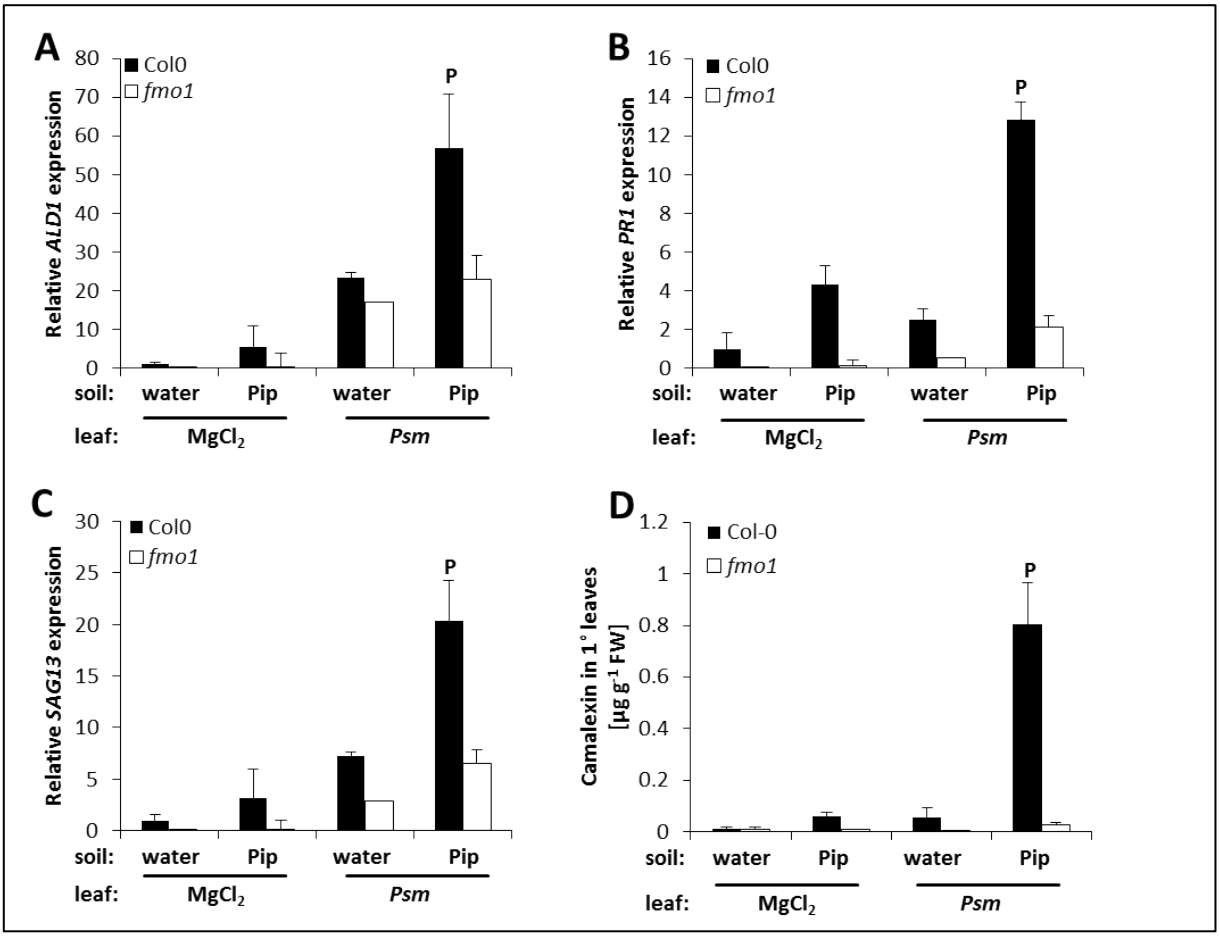

Figure 29. Pip-treatment of *Arabidopsis* leads to priming of gene expression and camalexin accumulation in WT plants, but not in *fmo1.*

Plants were supplied with either water or Pip via soil drench 1 day before infiltration with 10 mM $MgCl_2$ or *Psm* (OD_{600}=0.005), respectively. Relative expression of *ALD1* (A), *PR-1* (B), and *SAG13* (C) at 10 hpi. Transcript abundance was ascertained and analysed as described in figure 24 (P, primed gene expression). Accumulation of camalexin (D) at 10 h post inoculation in infiltrated leaves. Bars represent the mean ±SD of three replicate samples; P, primed response. This experiment was done in collaboration with Dr Friederike Bernsdorff.

This experiment shows that processing of the signal given by Pip via *FMO1* is necessary for Pip-induced priming of gene expression and camalexin accumulation.

6.3 A role for MAP kinase signalling cascades in defence priming?

Mitogen-activated protein kinases (MAP kinases; MAPKs) are more and more discussed as playing a central role in plant defence and particularly in defence-related priming (Beckers *et al.*, 2009). To further investigate the role of MAPKs in defence, the ability of *mpk3,* and *mpk6*, as well as the double mutant *mpk3 mpk6*, to establish SAR was tested. The *mpk3* line was previously described as being impaired in SAR (Beckers *et al.*, 2009) and as MPK3 and MPK6 were shown to be partly redundant, the *mpk3* (+/-) *mpk6* (-/-) double mutant was also used for experiments. This line is only available in a heterozygous form for *mpk3*, as a null mutant of both genes proved to be embryo lethal (Wang *et al.*, 2007 b). As shown in Figure

30 A, the SAR response in MAPK mutants was not impaired to the extent previously described (Beckers *et al*., 2009).

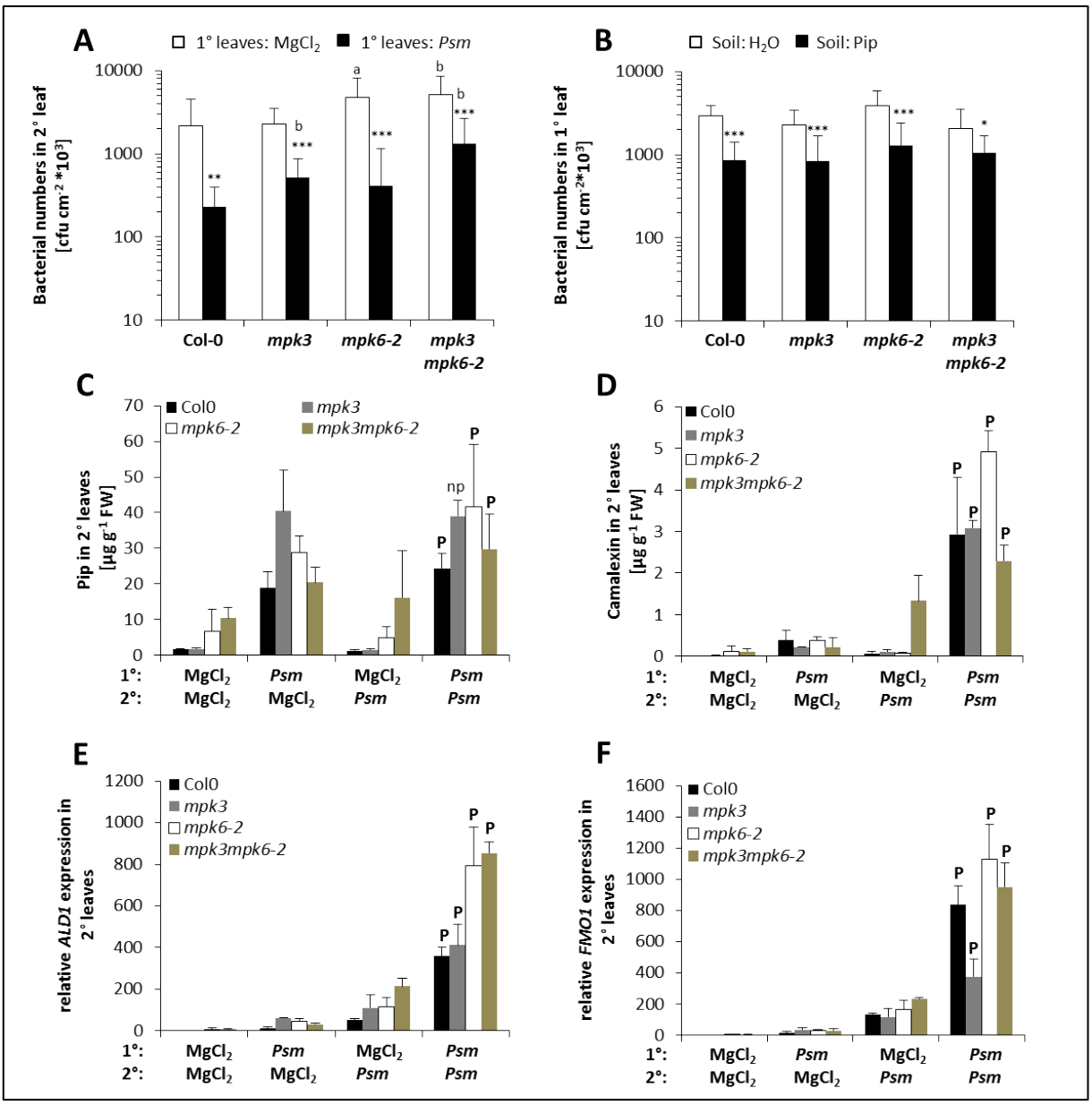

Figure 30. Role of MPK3 and MPK6 in Pip-induced resistance and SAR-associated defence priming.

(A) Analysis of SAR in Col-0, *mpk3, mpk6*, and *mpk3 mpk6*. Lower leaves of *Arabidopsis* plants were infiltrated with 10 mM $MgCl_2$ or *Psm* (OD_{600}=0.005), respectively. Two days later, upper leaves were challenge infected with *Psm* (OD_{600}=0.001) and disease symptoms scored by measuring bacterial growth in 2° leaves 3 days post inoculation. Asterisks above the bars signify statistical differences between $MgCl_2$-treated and *Psm*-treated plants, letters above the bars indicate statistical differences between the Col-0 WT and mutant plants (two-tailed *t* test; *a, P<0.05; **b, P<0.01; ***c, P<0.001). (B) Pip-induced resistance against *Psm* in Col-0, *mpk3, mpk6,* and *mpk3 mpk6.* Plants were treated as described in figure 28 (D)-(F). Asterisks above the bars denote statistically significant differences between water-treated and Pip-treated plants (two-tailed *t* test; *, P<0.05; **, P<0.01; ***, P<0.001). Accumulation of Pip (C) and camalexin (D) at 10 hpi in 2° leaves. Samples were treated as described in figure 24 and analysed as described in figure 29 (D); P, primed response; np, not primed. Relative *ALD1* (E) and *FMO1* (F) expression in 2° treated leaves, at 10 hpi. Plants were treated and gene expression analysed as described in figure 24; P, primed gene expression. Seeds for *mpk3, mpk6*, and *mpk3 mpk6* were kindly provided by Dr Ken Tsuda (MPIZ Cologne).

6.3 A role for MAPK signalling cascades in defence priming?

The SAR response was slightly reduced in *mpk3* and *mpk3 mpk6* compared to Col-0 plants, nevertheless bacterial growth was significantly inhibited in SAR-induced leaves (Figure 30 A). In addition to SAR, the impact of exogenously applied Pip on resistance in *mpk3, mpk6*, and *mpk3 mpk6* was tested. Supplying plants with 10 µmol Pip via the root system one day prior to inoculation with *Psm* (OD_{600}=0.005) induced resistance against infection with no significant differences between Col-0 and *mpk* mutants (Figure 30 B). As a next step biological priming of defence metabolites in MAPK mutant lines was tested. A high Pip-accumulation was observed in *mpk3* and *mpk6* in systemic leaves (1° *Psm*/2° $MgCl_2$), Pip-levels in these mutants were found to be higher than in Col-0 (Figure 30 C). The double mutant *mpk3 mpk6* exhibited WT-levels of Pip in systemic leaves and a rather high accumulation in local leaves (1° $MgCl_2$/2° *Psm*). In the shown experiment, *mpk3* did not show priming of Pip-accumulation due to already high levels in systemic tissue, but Pip-accumulation was found to be primed in a second experiment (Supplemental figure 11). Both *mpk6* as well as the double mutant *mpk3 mpk6* showed priming of Pip-accumulation. Most interestingly, these two mutant lines already show high Pip-levels in the mock/mock control situation. Accumulation of camalexin, a very important defence-related metabolite primed in Col-0, was also biologically primed in the three studied MAPK mutant lines (Figure 30 D). Camalexin levels in *mpk3* were similar to those in Col-0, in *mpk6* levels were even higher than in WT and in the *mpk3 mpk6* double mutant camalexin levels were somewhat less than in Col-0 (Figure 30 D). For the double mutant, very high camalexin levels were also detected in local leaves. Moreover, camalexin accumulation was also primed in this line (Figure 30 D). Defence priming of *ALD1* and *FMO1* gene expression was studied in the MAPK mutants as well. A strong priming of *ALD1* expression was observed in Col-0 and comparable transcript abundance was found in *mpk3* (Figure 30 E). The *mpk6* and the *mpk3 mpk6* double mutant exhibited an even stronger priming of *ALD1* expression compared to Col-0. For expression of *FMO1,* a strong priming response was observed in Col-0, *mpk6*, and the double mutant (Figure 30 F). In the mutant line *mpk3,* priming of *FMO1* expression was not as pronounced as in Col-0 or the other studied MAPK mutants. This tendency was not confirmed in a second experiment, which showed strongly primed expression of *FMO1* in *mpk3* (Supplemental figure 11).

The next step in studying the involvement of MAPKs in innate immunity was to test MAPK activity in Col-0, *ald1* and *fmo1* after infection with a virulent and an avirulent strain of *Psm*. Five week old *Arabidopsis* plants were infiltrated with either 10 mM $MgCl_2$, *Psm* (OD_{600}=0.005), or *Psm avrRpm1* (OD_{600}=0.005) and inoculated as well as distal leaves were harvested 6 and 48 hours post infiltration. MAPK activity was tested by separating total protein by SDS PAGE, gelblotting (western blot) and immunodetection with an anti-p44/42 MAPK polyclonal antibody (Tsuda *et al*., 2013).

6.3 A role for MAPK signalling cascades in defence priming?

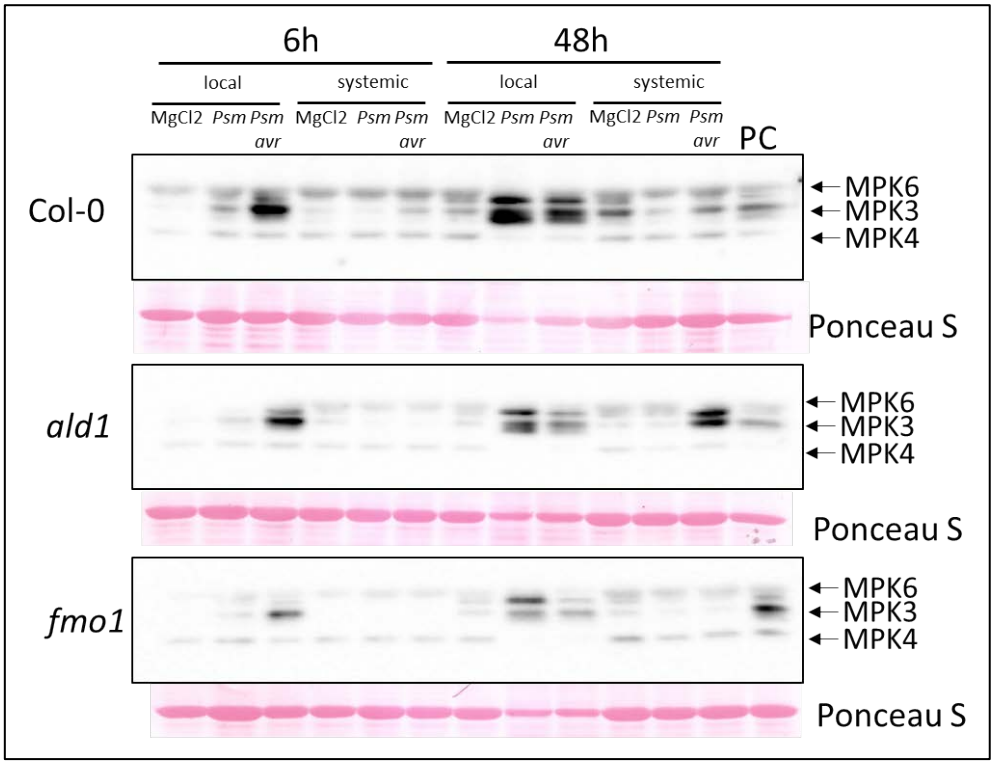

Figure 31. Reduced activity of MPK3 and MPK6 in *ald1* and *fmo1* upon infection with *Psm.*

Three leaves of 5 week old *Arabidopsis* plants were infiltrated with 10 mM $MgCl_2$, *Psm* (OD_{600}=0.005), or *Psm avrRpm1* (OD_{600}=0.005), respectively, and samples taken for analysis of MAPK activity in local and systemic leaves at 6 hpi and 48 hpi. Total protein was extracted, proteins were separated using SDS-PAGE, and MAPKs detected with an anti-p42/44 antibody. The MAPK assay was performed in cooperation with Dr Yiming Wang (MPIZ Cologne); the experiment was done one time so far. PC, positive control flg22-treated Col-0, 3 h post treatment.

Six hours after infiltration, activity for MPK3 was observed in Col-0, *ald1* and *fmo1* leaves treated with *Psm avrRpm1*, with a weaker signal in the mutant lines (Figure 31). No MAPK activity was detected in systemic leaves at 6 hpi. Forty-eight hours post infiltration activation was detected for MPK6 and MPK3 in local samples of Col-0 treated with both *Psm* and *Psm avrRpm1*. Again, MAPK activation in *ald1* and *fmo1* seemed to be weaker than in Col-0 (Figure 31). No MAPK activation was found in systemic leaves of Col-0 and *fmo1*, neither with the virulent nor the avirulent *Psm* strain, after 48 hours. In *ald1,* an activation signal for MPK6 and MPK3 was detected in leaves treated with *Psm avrRpm1*. This experiment was done one time so far and has to be repeated to allow for more robust conclusions.

DEX-inducible *MKK4* plants were generated by Dr Yiming Wang and Dr Ken Tsuda from MPIZ in Cologne and in collaboration the metabolite accumulation after induction of the plants was studied. MKK4 is a MAP kinase kinase, which is responsible for activation of MPK3 and MPK6 after perception of flg22 (Asai *et al*., 2002). By engineering an inducible promoter in front of the gene encoding MKK4, it is possible to induce the signalling cascade in the absence of a pathogen by treating plants with the inducing agent, in this case dexamethasone.

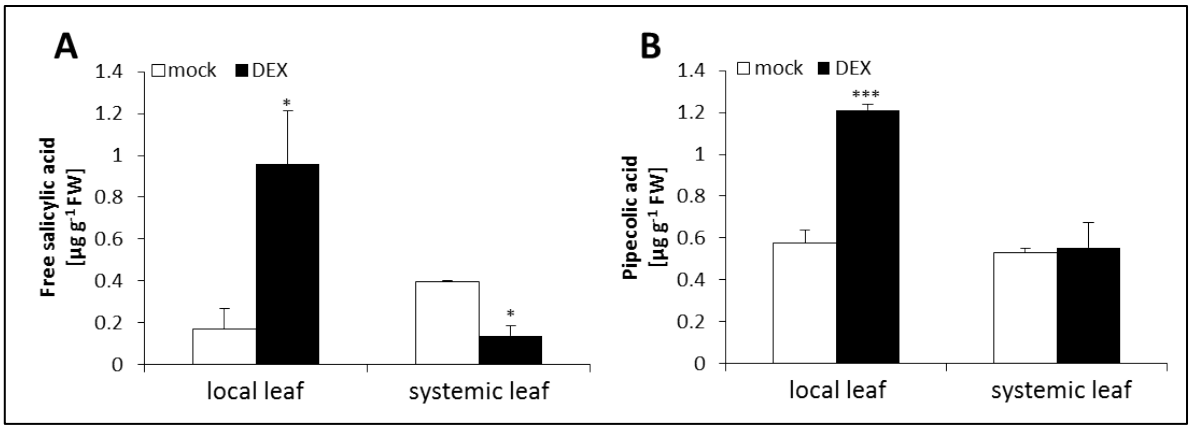

Figure 32. Induction of local SA- and Pip-accumulation by activation of MPK3 and MPK6.

A DEX-inducible *MKK4* line was treated with either water or dexamethasone and local and systemic leaves taken for analysis of metabolites. Bars represent the mean ±SD of three replicate samples, asterisks above the bars denote significant statistical differences between treatments (two-tailed *t* test; *, P< 0.05; **, P< 0.01; ***, P< 0.001). DEX, dexamethasone; FW, fresh weight. This experiment was done in collaboration with Dr Yiming Wang (MPIZ Cologne).

After induction, *MKK4-DEX* plants demonstrated moderate accumulation of free SA and Pip in local, but not in systemic leaves (Figure 32 A; Figure 32 B). Compared to *Psm*-infected plants, accumulation of SA and Pip was very low. SA accumulated in previous experiments to levels between 3 and 5 µg g^{-1} FW in leaves inoculated with *Psm* (Attaran *et al*., 2009) and Pip was shown to increase to levels more than 40 µg g^{-1} FW (Návarová *et al*., 2012). These results show that MAP kinases play only a minor role in SAR and defence priming and that activation of this signalling cascade alone is not enough to induce accumulation of defence-related compounds to similar high levels as observed in *Psm*-inoculated leaves.

6.4 Establishment of different pathosystems to study inducible immunity and Pip-induced resistance in *A. thaliana*

Additional to our studies concerning the interaction between *Arabidopsis thaliana* and *Pseudomonas syringae* pv. *maculicola,* we were interested to find out which similarities and differences might exist between distinct types of pathogens differing in their lifestyle and phylogenetic group. Therefore, pathosystems with the necrotrophic fungus *Botrytis cinerea* and the obligate biotrophic oomycete *Hyaloperonospora arabidopsidis* were established in our laboratory. By collaborating with Dr Volker Lipka and Dr Michaela Kopischke at Göttingen University, we were able to study the *Arabidopsis-Golovinomyces orontii* interaction as well. Investigations into various pathogen modes of infection included evaluation of disease symptoms, analyses of metabolite accumulation and studies concerning the possibility of Pip-induced resistance to different types of pathogens.

6.5 Changes in the metabolic profile of *A. thaliana* after infection with *B. cinerea,* a fungus of necrotrophic lifestyle

The first step in the analysis of the *Arabidopsis-Botrytis* interaction was to analyse accumulation of metabolites over a defined period of time.

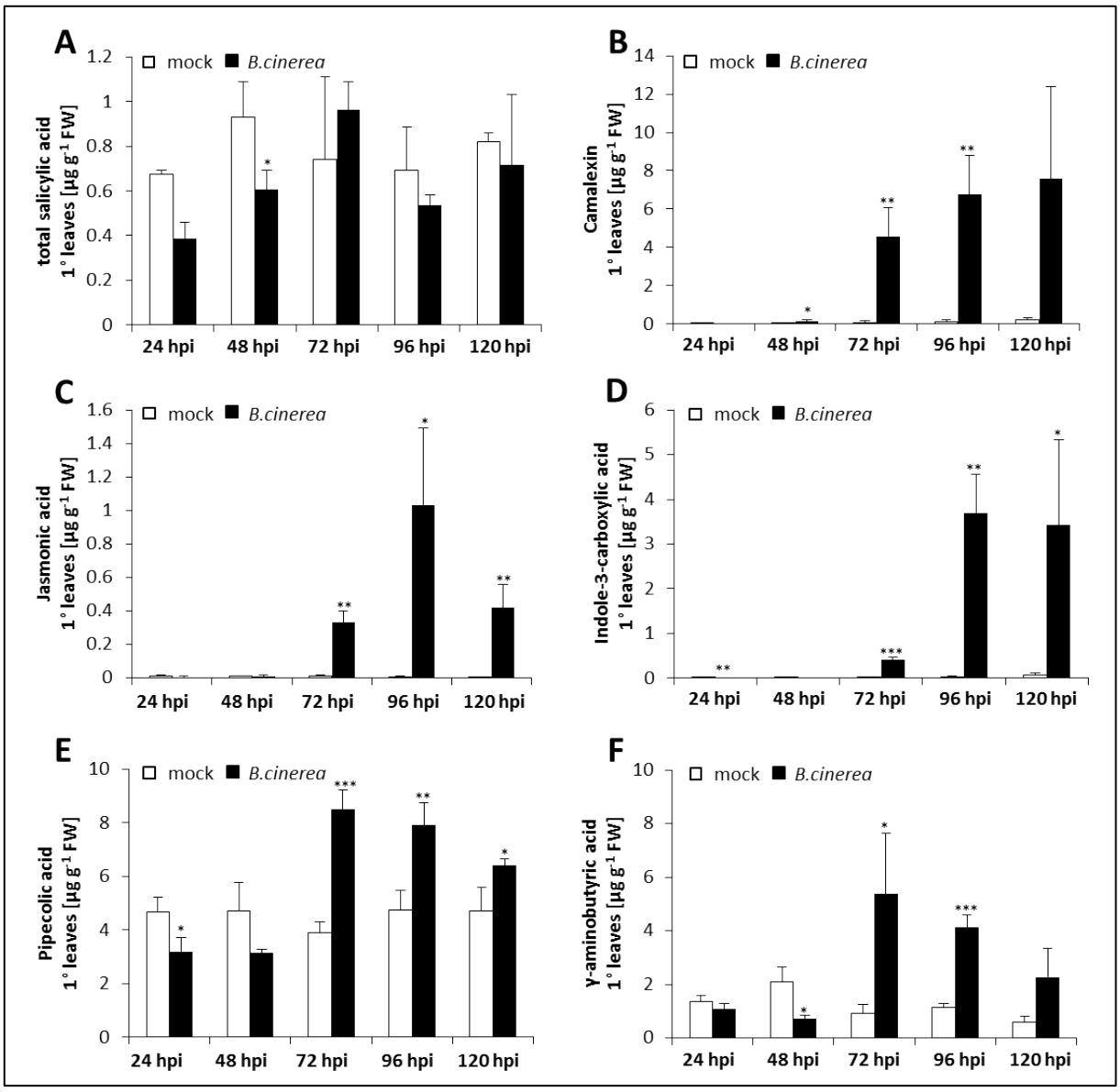

Figure 33. Accumulation of numerous defence-related metabolites after infection of *Arabidopsis thaliana* with the necrotrophic fungus *Botrytis cinerea*.

Time course of total SA- (sum of free and conjugated SA) (A), camalexin- (B), JA- (C), indole-3-carboxylic acid- (D), Pip- (E), and γ-aminobutyric acid- (F) accumulation in *Arabidopsis* leaves infected with *B. cinerea*. Plants were infected with 4 drops á 3 µl of pregerminated *B. cinerea* spores per leaf on 3 leaves per plant, kept in high air humidity for the indicated amount of time and analysed for accumulation of defence compounds. Bars represent the mean ±SD of three replicate samples and asterisks above the bars show significant statistical differences between non-infected and infected plants (two-tailed *t* test; *, P< 0.05; **, P< 0.01; ***, P< 0.001). FW, fresh weight.

6.5 Changes in the meatbolic profile of *A. thaliana* after infection with *B. cinerea*

Time points chosen for sampling were 24, 48, 72, 96, and 120 hpi. Distinct disease symptoms, namely water soaked lesions, started to become visible at 48 hpi, grew very pronounced at 72 hpi, with a complete maceration at 96 hpi, and almost complete destruction of leaves at 120 hpi (data not shown). Analysis of total SA-content showed no significant SA-accumulation in *Arabidopsis* after *B. cinerea* infection (Figure 33 A). Levels of SA ranged between 0.4 and 1 µg g^{-1} FW in non-infected leaves and no significant increases in SA-levels were observed in *B. cinerea*-infected leaves. In contrast to this, the indolic defence-related metabolites camalexin (Figure 33 B) and indole-3-carboxylic acid (ICA) (Figure 33 D) exhibited a strong accumulation at 72 hpi with an increase from 0.06 µg g^{-1} FW in control samples to 4 µg g^{-1} FW in infected leaves for camalexin and 0.01 µg g^{-1} FW in non-infected to about 0.5 µg g^{-1} FW in infected leaves for ICA, respectively. At later time points camalexin levels reached amounts of approximately 8 µg g^{-1} FW upon infection with the fungus and ICA was found to accumulate to a maximum of 3.5 µg g^{-1} FW at 96 hpi. Elevated levels of the oxylipin-derivative JA, a metabolite found to accumulate in plants after wounding and in interactions with necrotrophs, were first detected at 72 hpi (Figure 33 C) with basal levels of 0.01 µg g^{-1} FW, which increased to 0.3 µg g^{-1} FW in infected leaves, and maximum levels of 1 µg g^{-1} FW at 96 hpi. At 120 hpi JA-levels decreased again, presumably due to severe necrosis of leaf tissue (Figure 33 C). Among metabolites found to accumulate after *B. cinerea*-infection were also Pip and *γ*-aminobutyric acid (GABA) (Figure 33 E; Figure 33 F). Pip showed unusually high basal levels in this experiment, with 5 µg g^{-1} FW in non-infected leaves, which increased to 8 µg g^{-1} FW at 72 hpi and this amount seemed to be the peak accumulation as it did not accumulate to comparatively high levels at later time points (Figure 33 E). Basal levels for GABA were about 2 µg g^{-1} FW and accumulated to approximately 6 µg g^{-1} FW upon infection with *B. cinerea* (Figure 33 F). Similar to JA and Pip, GABA levels decreased at time points later than 72 hpi, which correlates with the progression of tissue necrosis (Figure 33 F). Analysis of metabolite accumulation in *A. thaliana* after *B. cinerea*-infection yielded not only known defence-related metabolites, but also a number of unknown ones (Table 2). One striking metabolite was named “unknown 13” and found only in the *Arabidopsis-Botrytis* interaction (Figure 34; Table 5). This substance, obtained via amino acid extraction, had a retention time of 18.10 minutes and a mass spectrum with the prominent masses of 70 and 112 (Figure 34 A). This presumed amino acid or amino acid derivative was not detected in mock-treated leaves and found to increase more than 500-fold in *B. cinerea*-infected leaves at 72 hpi (Figure 34 B). Levels of this compound increased further at later time points, making it a very interesting candidate to study in the *Arabidopsis-Botrytis* interaction.

In order to shed more light on defence mechanisms against *B. cinerea*, metabolite accumulation in several *Arabidopsis* mutant lines 72 h after *Botrytis* infection was monitored.

6.5 Changes in the meatbolic profile of *A. thaliana* after infection with *B. cinerea*

Plant lines used in this experiment were the Pip-deficient mutant *ald1*, the SAR-deficient *fmo1*, the ethylene receptor mutant lines *ein2-1* and *etr1-1*, the JA-receptor mutant *coi1*, as well as the camalexin-deficient lines *pad2* and *pad3*, and the SA-deficient line *sid2*. Basal levels between 0.3 and 0.5 µg g^{-1} FW were detected for total SA in Col-0, *ald1, pad2*, and *pad3*, which did not increase upon *B. cinerea* infection (Figure 35 A).

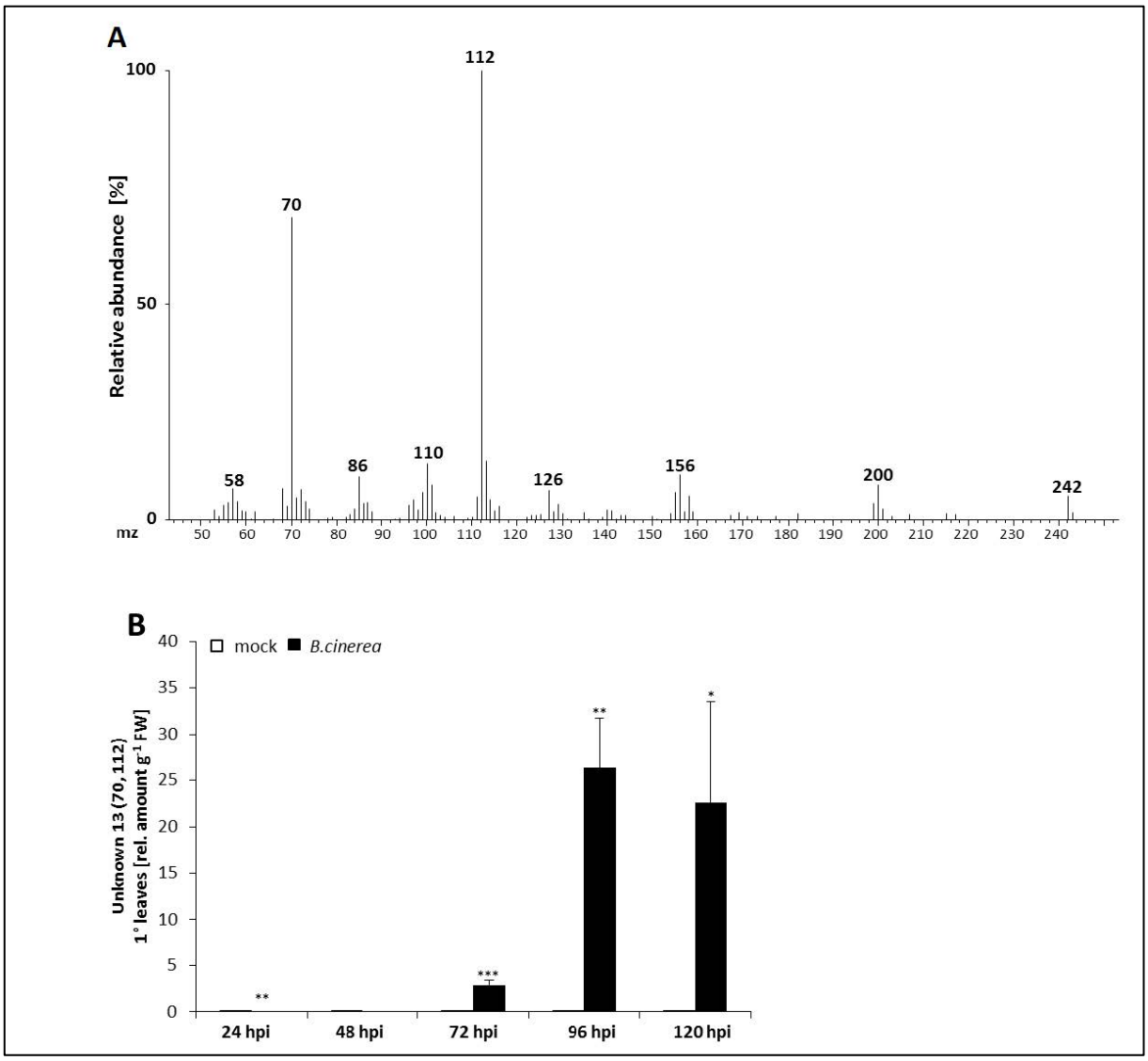

Figure 34. Infection of *Arabidopsis thaliana* Col-0 with the necrotrophic fungus *B. cinerea* leads to the accumulation of a number of unknown metabolites.

Plants were treated as described in figure 33, kept in high air humidity for 3 days and analysed for accumulation of defence compounds. Mass spectrum (A) of the unknown amino acid or amino acid derivative with the distinct ions 70 and 112, which accumulated to high amounts in *Arabidopsis* after infection with *B. cinerea* (B). The content of this substance in leaf samples is given as relative amount per g FW, as no correction factor is established yet and was therefore assumed 1. Bars show the mean ±SD of at least three replicates, asterisks above the bars denote significant statistical differences between non-infected and infected plants (two-tailed *t* test; *, P< 0.05; **, P< 0.01; ***, P< 0.001). FW, fresh weight.

Basal SA-levels in *sid2* were with 0.1 µg g^{-1} FW below WT-levels and also did not increase during infection. A slight increase in total SA was observed in *coi1, etr1-1,* and *fmo1,* which

showed already elevated basal amounts of 0.5 µg g^{-1} FW in *coi1*, 1.3 µg g^{-1} FW in *etr1-1*, and 0.4 µg g^{-1} FW in *fmo1*, respectively (Figure 35 A). The highest basal levels of SA (4.2 µg g^{-1} FW) was measured for the ET-insensitive mutant *ein2-1*, with approximately five-fold higher amounts of SA than in Col-0, which decreased upon *Botrytis*-infection (Figure 35 A).

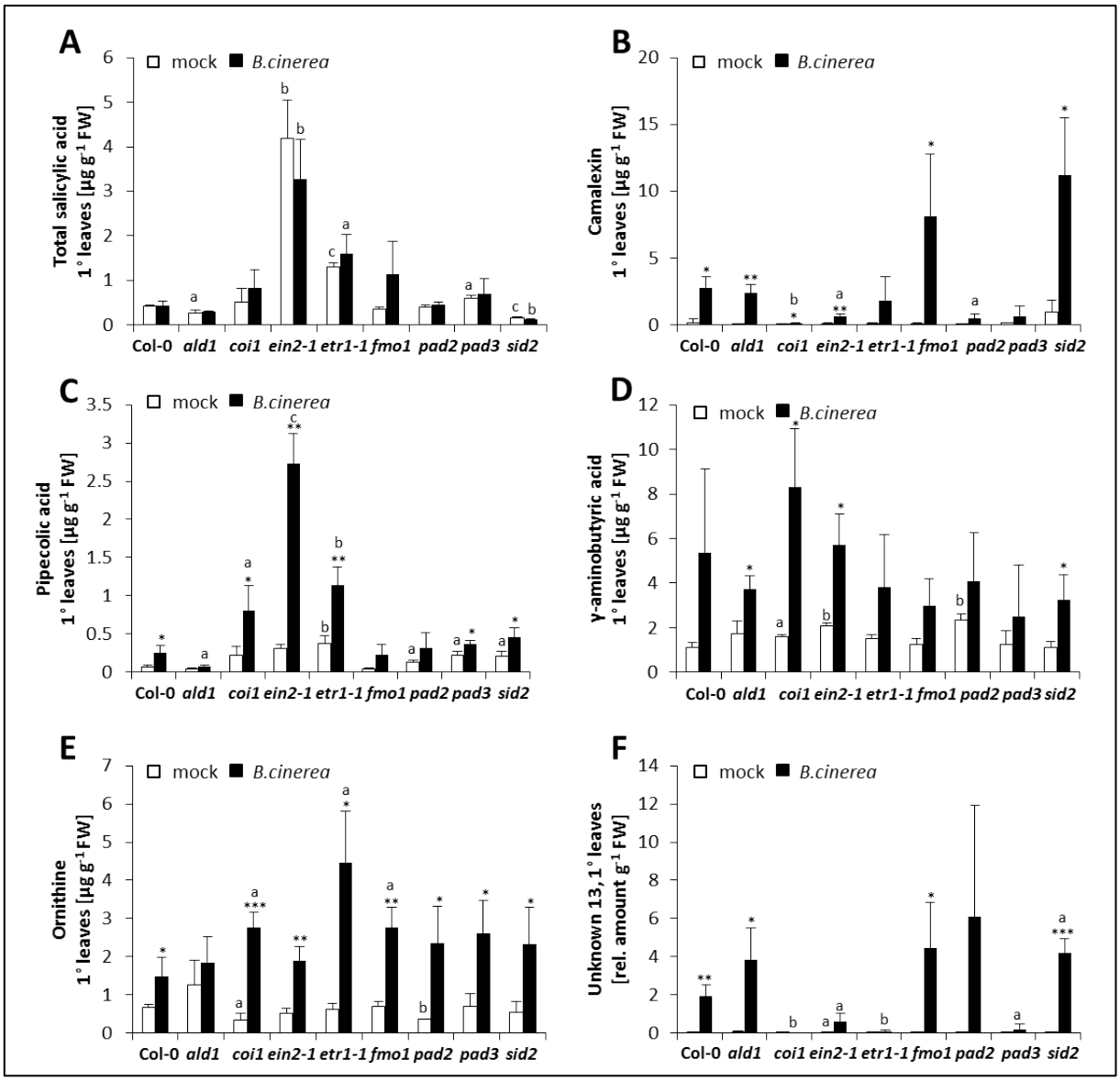

Figure 35. Defence signalling in the *Arabidopsis-Botrytis* interaction.

Plants were treated as described in figure 34. Accumulation of total SA (sum of free and conjugated SA) (A), camalexin (B), Pip (C), GABA (D), ornithine (E), and the unknown compound 13 (70, 112) (F) in *Arabidopsis* plants after *B. cinerea*-infection. Bars represent the mean ±SD of three replicate samples and significant statistical differences between non-infected and infected, as well as between wild type control and mutant plants are indicated by asterisks and letters, respectively, above the bars (two-tailed *t* test; * a, P< 0.05; ** b, P< 0.01; *** c, P< 0.001). The unknown substance 13 was analysed as described in figure 34. *Arabidopsis* mutant lines *coi1, ein2, etr1*, and *pad2* were used once in this kind of experiment, the rest of the mutants were used in at least three independent biological experiments with similar results. FW, fresh weight.

In this experiment, camalexin levels showed an increase from 0.2 µg g^{-1} FW in Col-0 and from 0.02 µg g^{-1} FW in *ald1,* to about 4 µg g^{-1} FW in both lines (Figure 35 B). Camalexin levels in *etr1-1* were slightly lower than in WT (0.1 µg g^{-1} FW) and did not increase as

strongly as observed in Col-0 (1.8 µg g^{-1} FW). *Arabidopsis* lines *coi1, ein2-1, pad2*, and *pad3* contained very little camalexin in uninfected leaves (0.04-0.1 µg g^{-1} FW) and also did not accumulate this phytoalexin as much as in *Botrytis*-infected Col-0 plants. The mutant lines *fmo1* and *sid2*, on the other hand, exhibited overaccumulation of camalexin from basal levels comparable to Col-0 levels to almost 10 µg g^{-1} FW upon infection with *B. cinerea* (Figure 35 B). However, because of the high standard deviation for *fmo1* and *sid2* samples in this experiment, this camalexin overaccumulation most likely is not significant. Another metabolite analysis using *B. cinerea*-infected plants, could not support these findings (Supplemental figure 13). Accumulation of Pip was found to be different than observed in the time course experiment (Figure 33 E) with basal levels of 0.07 µg g^{-1} FW that increased to 0.3 µg g^{-1} FW, marking a three-fold upregulation of Pip in *B. cinerea*-infected leaves. This discrepancy between the two experiments may be explained by differences in experimental procedure or conditions. Pip-accumulation in *fmo1, pad2, pad3*, and *sid2* was comparable to levels found in Col-0 and no Pip was detectable in *ald1* (Figure 35 C). Slightly elevated Pip-levels showed *coi1* and *etr1-1* and more than two-fold higher Pip-levels were discovered in infected *ein2-1* leaves (Figure 35 C). Analysis of GABA-accumulation showed basal levels of 1-2 µg g^{-1} FW that increased to approximately 5 µg g^{-1} FW in Col-0 and the mutant lines and slightly higher GABA-levels in infected *coi1* leaves (Figure 35 D). The non-protein amino acid ornithine exhibited an increase from 0.3-1 µg g^{-1} FW in non-infected leaves to around 1.5 µg g^{-1} FW in Col-0, *ald1,* and *ein2-1*, with slightly higher levels in *coi1, fmo1, pad2, pad3*, and *sid2* and very high levels of approximately 4 µg g^{-1} FW in *etr1-1* (Figure 35 E). Interestingly, the compound “unknown 13” accumulated more than 1000-fold in *Botrytis*-infected Col-0 and *sid2* plants, and even 2000-fold in *fmo1* compared to uninfected controls (Figure 35 F). In *ein2-1* and *ein2* this substance increased 100- and 600-fold, respectively, and a less than 100-fold increase was observed in plant lines *ald1, etr1-1*, and *pad3*. In the phytoalexin- and glucosinolate-deficient *pad2* mutant line an almost 500-fold increase of this compound was detected in infected leaves compared to uninfected ones. The JA-receptor mutant *coi1* did not exhibit any accumulation of this substance in *B. cinerea*-infected leaves at all. As it was not to possible to detect “unknown 13” in *coi1,* and levels for this compound were very low in *etr1-1*, and *pad3*, it appears plausible that either JA/ET-mediated signalling is involved in the biosynthesis of this compound, or that “unknown 13” and camalexin share a common biosynthesis pathway (Figure 35 F). These results demonstrate that camalexin accumulation –in contrast to that of SA– seems to play a major role in defence in the interaction between *Arabidopsis* and *Botrytis*. It also shows that infection with this necrotroph induces Pip-accumulation, albeit not to similar high levels as in the *Arabidopsis-Psm* interaction.

6.6 Reduction of *B. cinerea*-caused disease symptoms by exogenous Pip-treatment

As Pip-levels were found to increase upon infection with the necrotrophic fungus *B. cinerea*, the ability of exogenously applied Pip to induce resistance to this pathogen was tested analogously to the Pip-induced resistance (Pip-IR) experiments performed with the hemibiotrophic bacterium *Psm*. For this experiment the same plant lines were used as in the analysis of metabolite accumulation.

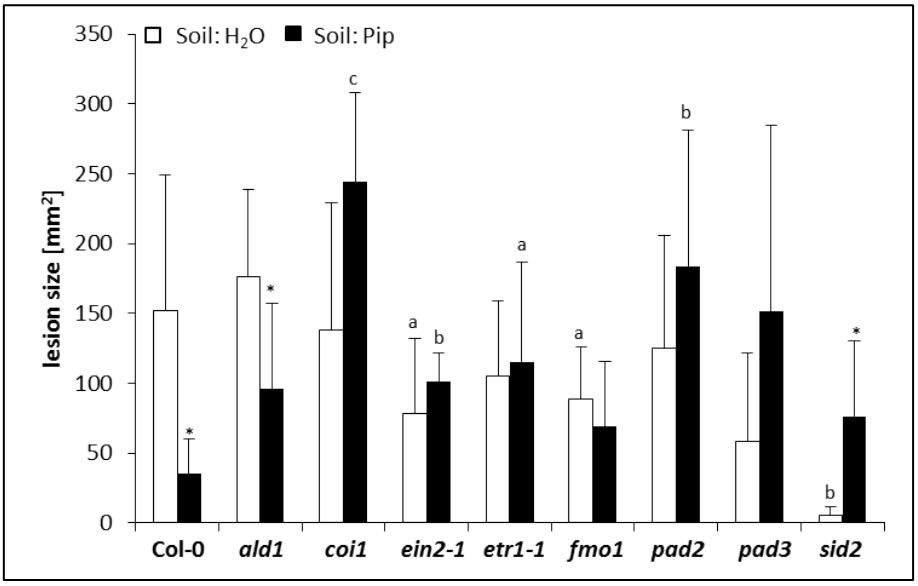

Figure 36. Pip-induced resistance against the necrotrophic fungus *B. cinerea*.

Plants were supplied with 10 ml water or 10 ml 1 mM (10 µmol) Pip per pot 1 day prior to infection with 4 drops á 3 µl of pregerminated *B. cinerea* spores per leaf on 3 leaves per plant. Plants were kept in high air humidity for 3 days and disease symptoms were evaluated by measuring lesion size. Statistical significant differences between water- and Pip-treated plants (asterisks above the bars) and between Col-0 and mutant plants (letters above the bars) were assessed using a two-tailed *t* test (* a, P< 0.05; ** b, P< 0.01; *** c, P<0.001).

Plants were treated with 10 µmol Pip one day prior to infection with *B. cinerea* and disease symptoms and lesion size documented were at 3 dpi (Figure 36; Figure 37). Pip induced resistance to *B. cinerea* in Col-0 and to a lesser degree in *ald1*. A very weak, but insignificant, induction of defence was observed in *fmo1* and no significant difference in water- and Pip-treated plants was seen in *ein2-1* and *etr1-1* (Figure 36; Figure 37). The camalexin-deficient lines *pad2* and *pad3* showed severe disease symptoms in water- and Pip-treated leaves. In stark contrast to Col-0, treatment of plants with Pip prior to *B. cinerea* infection aggravated disease symptoms in *coi1* and *sid2* with large and more numerous lesions (Figure 36; Figure 37) and almost complete leaf destruction.

6.6 Reduction of *B. cinerea*-caused disease symptoms by exogenous Pip-treatment

Figure 37. Pip induces resistance to *B. cinerea* in Col-0, but exacerbates symptoms in the mutant lines *coi1, pad2*, and *sid2*.

Plants were supplied with 10 ml water or 10 ml 1 mM (10 µmol) Pip per pot 1 day prior to infection with 4 drops á 3 µl of pregerminated *B. cinerea* spores per leaf on 3 leaves per plant and kept in high air humidity for 3 days.

This is especially interesting, since the SA-biosynthesis impaired *sid2* mutant exhibited high basal resistance in water-treated leaves (Figure 36). This experiment reflects earlier findings with *Psm*, as exogenously applied Pip is able to induce resistance against *B. cinerea* in Col-0

and also in part in *ald1*, but not in *fmo1*, which is hypothesised to be responsible for processing the resistance-inducing signal derived from Pip. These results also show that JA/ET-mediated signalling and the presence of camalexin are crucial factors in resistance against this necrotrophic fungus, and that Pip alone is not able to reduce disease symptoms in lines impaired in these processes.

6.7 Metabolic profile of *A. thaliana* after infection with a biotrophic oomycete

After examining metabolite accumulation in *Arabidopsis* in a hemibiotrophic (*Psm*) and in a necrotrophic (*B. cinerea*) interaction, metabolic profiles of plants in an interaction with the biotrophic oomycete *Hyaloperonospora arabidopsidis* were investigated (Figure 38). For this experiment the *Hpa* strain Noco2 was used, which is virulent to *A. thaliana* ecotype Col-0. A slight increase in free SA-levels from 0.05 µg g^{-1} FW to about 0.5 µg g^{-1} FW was observed in Col-0 infected with this pathogen (Figure 38 A). In the mutant lines *ald1* and *fmo1* accumulation of free SA was slightly weaker than in Col-0, with SA-levels around 0.2 µg g^{-1} FW in infected leaves (Figure 38 A). The SA-deficient *sid2* and the SA- and Pip-deficient *sid2 ald1* double mutant did not accumulate free SA upon infection with the virulent *Hpa* isolate. Basal amounts of 0.01 µg g^{-1} FW for camalexin, which moderately increased to roughly 2 µg g^{-1} FW were detected in infected leaves of Col-0, *sid2*, and *sid2 ald1* (Figure 38 B). Similarly to accumulation of free SA, camalexin levels in infected *ald1* and *fmo1* plants were lower than in Col-0 (0.8-1 µg g^{-1} FW). Analysis of ICA showed basal levels of 0.004 µg g^{-1} FW and with 0.1 µg g^{-1} FW quite low levels in Col-0 after infection with this virulent oomycete (Figure 38 C). In *ald1* and *fmo1,* basal ICA-levels were slightly higher than in Col-0 (0.008 µg g^{-1} FW), but ICA-accumulation in *Hpa*-infected leaves was comparable to the WT control. The lines *sid2* and *sid2 ald1* both showed higher ICA-levels than in Col-0, with basal amounts of 0.01 µg g^{-1} FW for *sid2* and 0.02 µg g^{-1} FW for *sid2 ald1*, which increased to 0.2 µg g^{-1} FW in both plant lines (Figure 38 C). In this interaction of *Arabidopsis* with a biotrophic oomycete an unknown compound, termed “unknown 28”, was found (Figure 38 D; Table 2). This compound was present in very low levels in uninfected leaves of Col-0, *ald1*, *fmo1*, and *sid2 ald1*, increased approximately tenfold in infected leaves and was only detectable in the interaction with this pathogen (Table 5). Elevated basal levels of this compound were detected in *sid2* and increased 14-fold in infected leaves. The *sid2 ald1* double mutant exhibited similar levels of this compound as in Col-0, but showed a more than 20-fold increase of this metabolite in infected plants (Figure 38 D). Basal levels of Pip were slightly elevated compared to previous findings (approx. 1 µg g^{-1} FW *vs* 0.6 µg g^{-1} FW as published in Návarová *et al*., 2012) and increased upon infection to levels of 8 µg g^{-1} FW and 6 µg g^{-1} FW in Col-0 and *fmo1*, respectively (Figure 38 E).

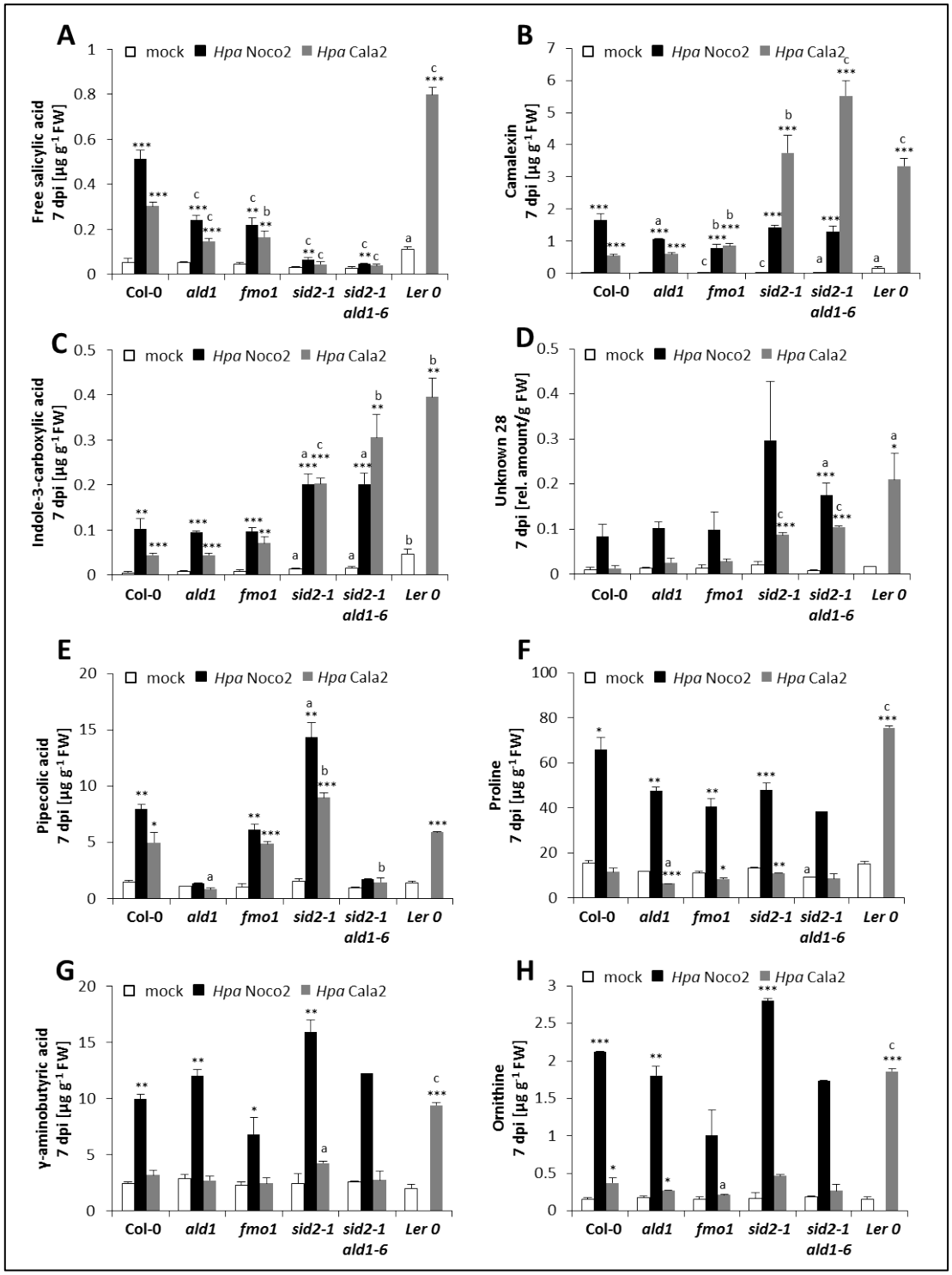

Figure 38. Distinct differences in defence metabolite accumulation upon infection of *Arabidopsis* with a virulent *(*Noco2) and an avirulent (Cala2) *Hpa* strain.

Arabidopsis Col-0, as well as select mutant, plants were spray-infected with *Hpa* strains Noco2 or Cala2 ($5x10^4$ spores ml^{-1}; kept in high air humidity for 7 days) and accumulation of free SA (A), camalexin (B), ICA (C), "unknown 28" (D), Pip (E), Pro (F), GABA (G), and Orn (H) was analysed in three replicate samples. Significant statistical differences between non-infected and infected, as well as between Col-0 and mutant, plants are marked with asterisks and letters, respectively, above the bars (two-tailed *t* test; * a, P< 0.05; ** b, P< 0.01; *** c, P< 0.001). For accumulation of metabolites in Ler-0 only the compatible interaction with *Hpa* Cala2 was included. Results following the study of the interaction of *A. thaliana* with the avirulent *Hpa* isolate Cala2 are described in section 6.10. FW, fresh weight. Generation of the *sid2 ald1* mutant line by Dr Friederike Bernsdorff.

6.7 Metabolic profile of *A. thaliana* after infection with a biotrophic oomycete

No increases in Pip-levels were measured in the Pip-biosynthesis-impaired mutant lines *ald1* and *sid2 ald1*. In *sid2* mutants an even stronger increase in Pip-levels (1.6 µg g^{-1} FW in non-infected leaves *vs* 14 µg g^{-1} FW in *Hpa*-infected leaves) compared to WT was observed upon infection (Figure 38 E). In contrast to plants infected with the bacterium *Psm*, infection with the virulent *Hpa* Noco2 induced a strong accumulation of the proteinogenous amino acid proline (Pro) from basal levels of averagely 10 µg g^{-1} FW to more than 60 µg g^{-1} FW in Col-0 and 40-50 µg g^{-1} FW in the analysed mutant lines (Figure 38 F). Similar to plants infected with the fungus *B. cinerea*, the non-protein amino acids GABA and ornithine (Orn) also accumulated in *Hpa*-infected plants (Figure 38 G; Figure 38 H). GABA-levels increased in Col-0, *ald1*, and *sid2 ald1* from 2 µg g^{-1} FW in non-infected to 10-12 µg g^{-1} FW in infected leaves (Figure 38 G). This amino acid showed an even stronger increase in *sid2* to 15 µg g^{-1} FW and accumulated to lower levels in *fmo1* (7 µg g^{-1} FW). Orn showed similar levels in Col-0 as well as in the mutant lines with basal levels of 0.2 µg g^{-1} FW in non-infected and 1-2 µg g^{-1} FW in *Hpa*-infected leaves (Figure 38 H). These results indicate an interaction of Pip- and SA-mediated signalling in regulation of defence metabolite accumulation. In *ald1*, which is unable to synthesize Pip, and in *fmo1*, which presumably does not process the Pip-derived signal, SA-accumulation after infection with *Hpa* Noco2 was found to be reduced. Pip and its processing by FMO1 seems to be important for camalexin accumulation as well, but not for accumulation of ICA, as *ald1* and *fmo1* plants showed reduced levels of camalexin, but similar ICA-levels as detected in infected Col-0 leaves. On the other hand, ICA-accumulation seemed to benefit from the absence of SA, as ICA-accumulation was enhanced in *sid2* and *sid2 ald1* plants. The hypothesis of Pip having no role in ICA-accumulation upon infection with this oomycete was also strengthened by ICA-levels in *ald1*, which were similar to those found in Col-0 and ICA-levels in *sid2 ald1* being similar to *sid2*. Further differences in amino acid accumulation between *ald1, fmo1*, and *sid2* were also observed, with the most striking disparities observed in *fmo1* (see table 7 in the appendix). For instance, accumulation of isoleucine seemed to be Pip-dependent, as it showed only a two-fold accumulation in *fmo1* and *ald1* in contrast to a four-fold increase in Ile levels in Col-0 (Table 7). Similar results were also observed for leucine, lysine, and phenylalanine, all of which were found to increase less in *fmo1* than in Col-0 (Table 7). Interestingly, for tyrosine and the lysine derivative α-aminoadipic acid (Aad), higher levels than in WT were found in infected leaves of *sid2* and for Aad in *ald1*, respectively (Table 7). It is conceivable that the metabolite overaccumulation observed in *sid2* correlates with enhanced disease symptoms, but in order to answer this hypothesis more studies on the relationship between *sid2* and *Hpa* would be necessary.

6.8 Pip-induced resistance against the virulent *Hpa* isolate Noco2

To analyse the host-pathogen relationship between *A. thaliana* and *Hpa,* a set of various *Arabidopsis* lines impaired in Pip- and SA-mediated signalling processes or biosynthesis were chosen. In addition to *ald1, fmo1, sid2*, and *sid2 ald1* described before in this work, the MATE transporter mutant *eds5* (*sid1*), which is an essential component of SA-mediated defence signalling, was used. A double knockout line for both isochorismate 1 and 2 (*ics1 ics2*) and the SA-signalling and -receptor mutant *npr1* were utilised as well. Disease symptoms of *Hpa*-infected plants were analysed on the one hand by staining hyphae on infected leaves with lactophenol/trypanblue (TB), followed by surveying the leaves via light microscopy (Figure 39, Figure 40), and on the other hand by counting oomycete spores 7 days after infection (Figure 41). For TB-stained leaves a disease rating according to Ton *et al.* (2005) was performed to give an extensive overview of all stained leaves and not only a small selection. This rating technique includes four classes of disease severity: class I (no conidiophores visible on leaf surface), class II (less than 50% of the leaf area covered in conidiophores), class III (more than 50% of leaf surface covered in conidiophores), and class IV (densely covered in conidiophores, with additional chlorosis).

Figure 39 A shows the disease rating for *A. thaliana* leaves infected with *Hpa* Noco2, harvested 7 days after spray-infection and stained with lactophenol/trypanblue. It becomes apparent that in water-treated Col-0 plants the majority of leaves show class II disease symptoms and a smaller percentage of leaves class I and III symptoms. The disease rating for the Pip-deficient *ald1* mutant also revealed disease symptoms of these three classes, with a large percentage of leaves showing predominantly symptoms of class III. In *fmo1,* leaves uniformly showed symptoms of class II, which was also predominant in *sid2* with small percentages of leaves showing disease symptoms of classes I and III. For *sid2 ald1*, which accumulates neither SA nor Pip, a small percentage of leaves showed class III disease symptoms, the remaining leaves exhibited class I and II disease symptoms. In *eds5, ics1 ics2*, and *npr1*, approximately half of the analysed leaves showed class II symptoms and the other half symptoms of class III. As Pip was shown to accumulate in plants infected with *Hpa* Noco2 (Figure 38 E), Pip-IR was analysed by treating plants with 10 ml 1 mM (=10 µmol) Pip 1 day before spray-infection with the pathogen and scoring disease symptoms 7 days after infection. Disease rating of Col-0 TB-stained leaves showed that Pip-treatment of plants significantly reduced the severity of the infection to approximately 30 per cent of analysed leaves showing growth and sporulation of the oomycete (class II) and 70 per cent of leaves exhibiting no disease symptoms (Figure 39 A). In *ald1* exogenously applied Pip also induced resistance to the oomycete, albeit not as strong as in Col-0.

6.8 Pip-induced resistance against the virulent *Hpa* isolate Noco2

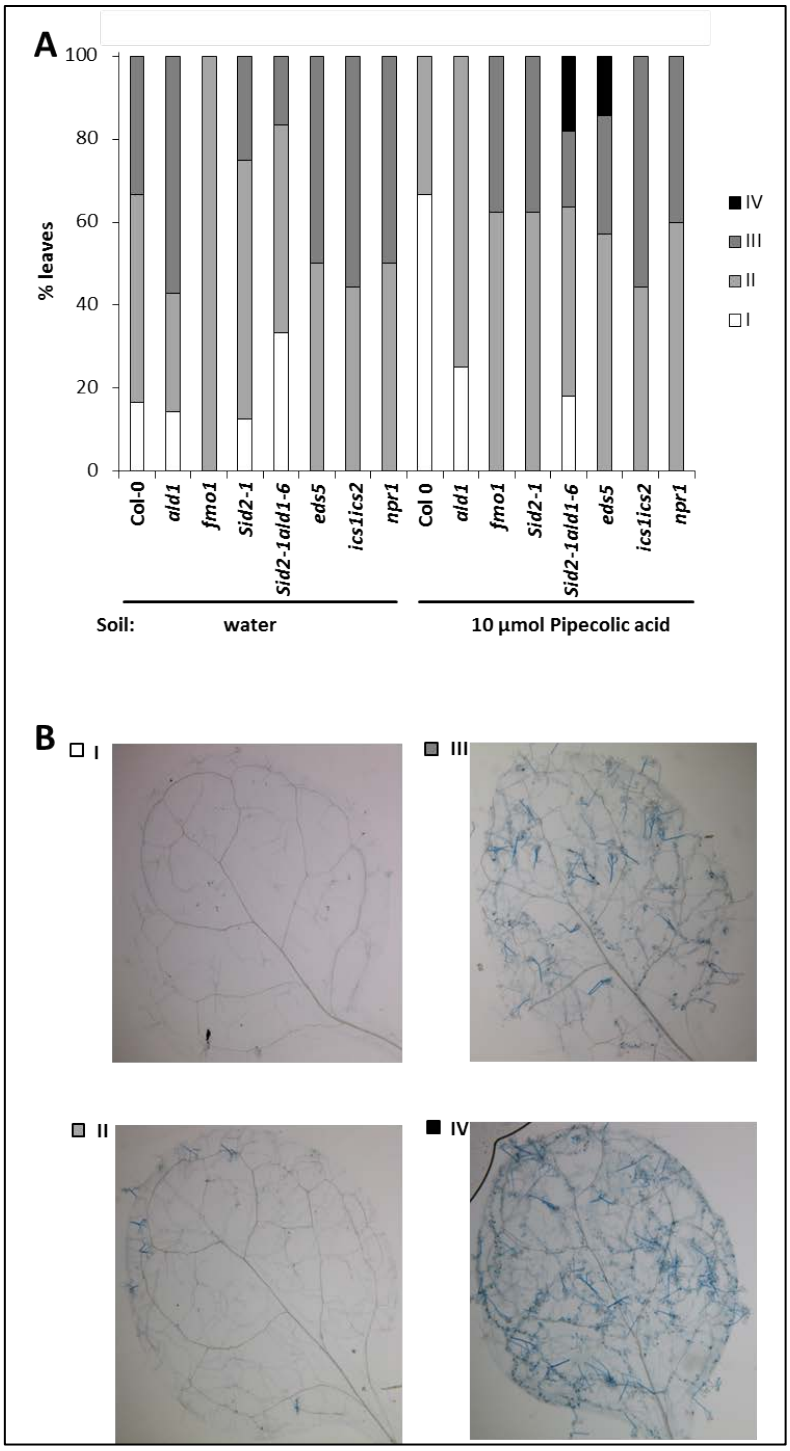

Figure 39. Visibly reduced disease symptoms in *Arabidopsis* plants infected with *Hpa* Noco2 after exogenous Pip-application.

Two week old *Arabidopsis* seedlings were supplied with water or 10 µmol Pip 1 day before spray-infection with a spore solution of $5x10^4$ spores ml^{-1} and kept in high air humdity for 7 days. (A) Leaves were stained with lactophenol/trypanblue solution and disease severity was assessed via microscopy analysis. (B) Disease rating is expressed according to Ton *et al*. (2005) as percentages of leaves in disease classes I (no conidiophores visible on leaf surface), II (less than 50% of the leaf area covered in conidiophores), class III (more than 50% of leaf surface covered in conidiophores), and class IV (densely covered in conidiophores, with additional chlorosis). With the exception of *eds5, ics1 ics2*, and *npr1*, the mutant lines were used in at least two independent biological experiments with similar results. The *sid2 ald1* double mutant line was generated by Dr Friederike Bernsdorff.

6.8 Pip-induced resistance against the virulent *Hpa* isolate Noco2

Analysis of *fmo1, sid2, sid2 ald1*, and *eds5* showed that Pip-treatment seemed to have impaired resistance against the oomycete in these lines. In *fmo1* and *sid2*, the majority of Pip-treated leaves showed symptoms of class II and a smaller number of leaves symptoms of class III. In Pip-treated *sid2 ald1* plants, disease symptoms of classes I-III were observed, with a small percentage of leaves showing dense coverage in conidiophores and even beginning chlorosis (class IV). The SA-transporter mutant *eds5*, which showed disease symptoms of classes II and III in water-treated leaves, exhibited class IV symptoms in a small percentage of Pip-treated plants as well. In *ics1 ics2* and *npr1,* no significant difference of resistance to *Hpa* was observed between water- and Pip-treated plants.

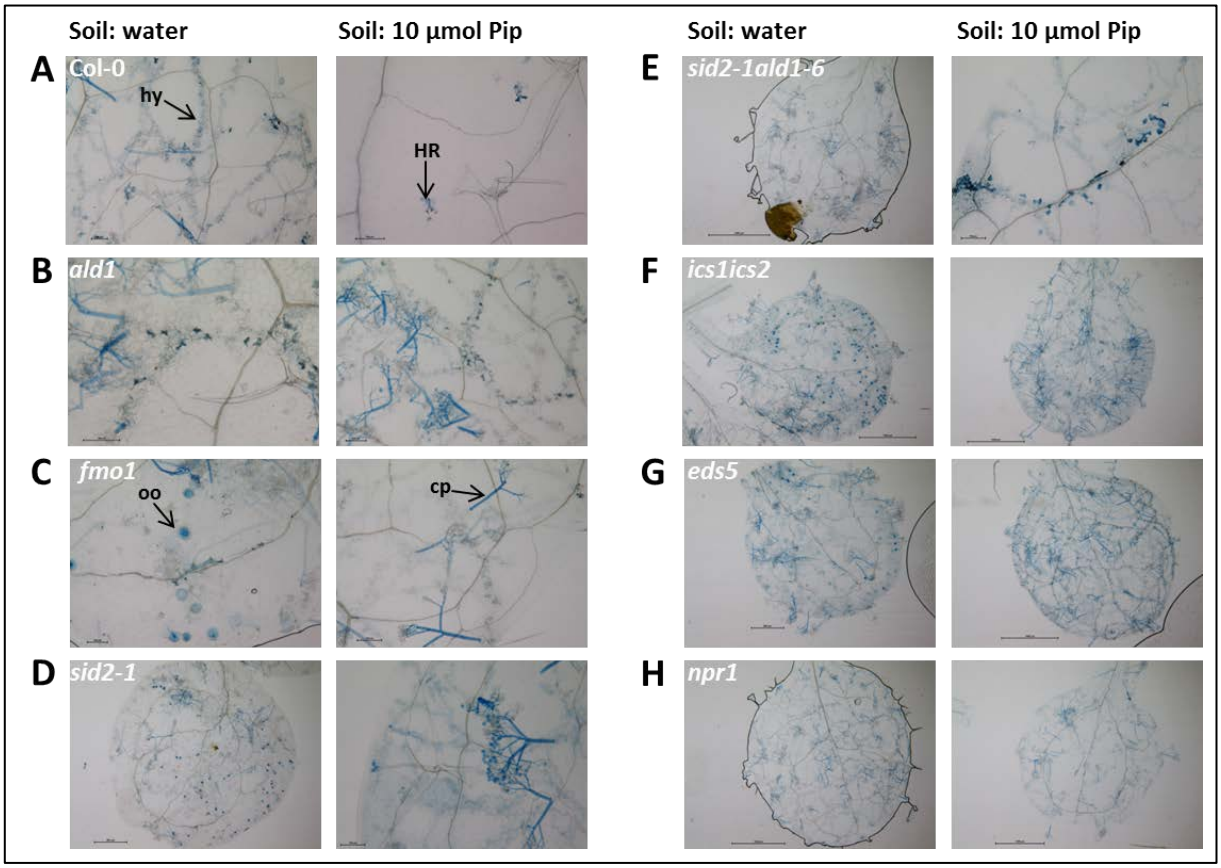

Figure 40. Pip-induced resistance against *Hpa* Noco2 in *A. thaliana* Col-0.

Plants were treated and analysed as described in figure 39. Shown are representative detail views of *A. thaliana* Col-0 (A) and the mutant lines *ald1* (B), *fmo1* (C), *sid2* (D), the double mutants *sid2 ald1* (E) and *ics1 ics2* (F), as well as *eds5* (G) and *npr1* (H). For mutant lines with no detail picture available, a representative overview shot is shown. The *sid2 ald1* mutant was generated by Dr Friederike Bernsdorff. Cp, conidiophore; HR, hypersensitive response; hy, hyphae; oo, oospore.

Closer inspection of individual representative TB-stained water-treated leaves infected with *Hpa* Noco2 showed that in Col-0 the oomycete hyphae pervaded the whole leaf accompanied by trailing necroses (TN) and a moderate amount of conidiophores and oospores (Figure 40 A, left side). In stark contrast to this, Pip-treated Col-0 leaves did not carry hyphae or conidiophores and only a few dead cells (HR) were visible (Figure 40 A, right

side). The Pip-biosynthesis mutant *ald1* showed more severe symptoms in TB-stained leaves with most of the leaf area covered in hyphae and conidiophores (Figure 40 B, left side). Even after Pip-treatment, TB-stained leaves showed a large area covered by oomycete hyphae and conidiophores (Figure 40 B, right side). Mutant lines for *fmo1, sid2, sid2 ald1, ics1 ics2, npr1*, and *eds5* all exhibited enhanced susceptibility towards *Hpa* Noco2 compared to Col-0, with leaf areas pervaded by hyphae and covered with conidiophores and sexual oospores (Figure 40). Except for *sid2 ald1* and *npr1*, no significant reduction of disease symptoms by Pip-treatment was apparent.

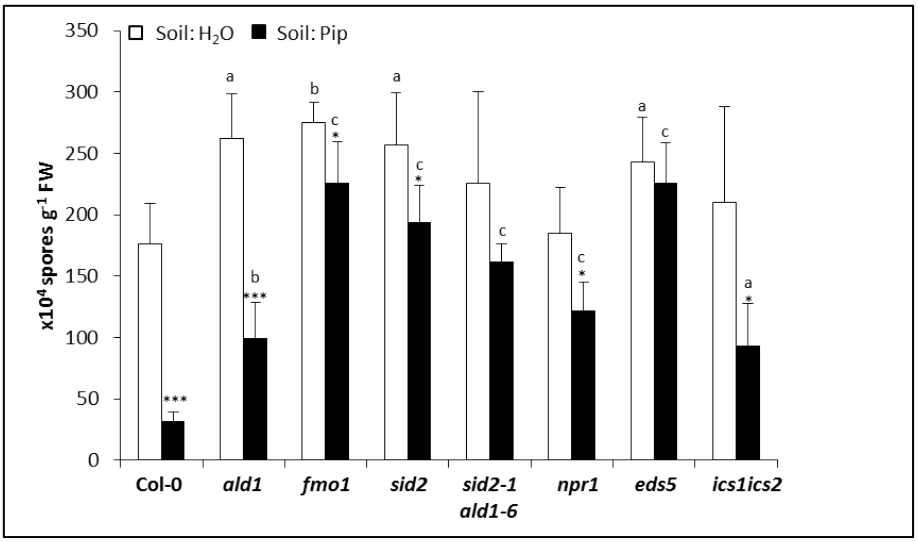

Figure 41. Pip-induced resistance against the virulent *Hpa* isolate Noco2.

Pip (10 ml, 1 mM) was applied to 2 week old plants via soil drench 1 day prior to spray-infecting the plants with a solution of 5 x 10^4 spores ml^{-1}. Plants were kept in high air humidity for 7 days and growth of the oomycete was determined by counting spores. *Arabidopsis* mutant lines *npr1, eds5*, and *ics1 ics2* were used once in this kind of experiment, all other lines were used in at least three independent biological experiments with similar results. The double mutant *sid2 ald1* was generated by Dr Friederike Bernsdorff. Statistical significant differences between water- and Pip-treated plants (asterisks above the bars), as well as Col-0 wild type and mutant plants (letters above the bars), were assessed using a two-tailed *t* test (*a, P< 0.05; **b, P< 0.01; ***c, P<0.001). FW, fresh weight.

As microscopy analysis of TB-stained leaves is a quite limited and qualitative method to assess Pip-induced reduction of *Hpa*-induced disease, the quantitative method of counting conidiospores 7 days after infection was employed. In water-treated Col-0 plants, a conidiospore number of approximately 170 x 10^4 spores g^{-1} FW were counted (Figure 41). Pretreatment of plants with Pip significantly reduced spore numbers to less than 50 x 10^4 spores g^{-1} FW, demonstrating the effectiveness of Pip to induce resistance against the oomycete *Hpa* in Col-0. The Pip-biosynthesis mutant *ald1* hosted more than 250 x 10^4 spores g^{-1} FW on water-treated leaves, showing enhanced susceptibility to *Hpa* Noco2 compared to Col-0 (Figure 41). Pip-treatment prior to infection partly reduced the conidiospore number to approximately 100 x 10^4 spores g^{-1} FW, showing that resistance against *Hpa* can be restored to some extent by exogenous application of Pip in *ald1*.

Surprisingly, in *ics1 ics2* exogenous Pip-application reduced conidiospore numbers also by half from over 200 x 10^4 spores g^{-1} FW in water-treated to 90 x 10^4 spores g^{-1} FW in Pip-treated plants (Figure 41). The SA-signalling mutant *npr1* hosted approximately the same amount of spores as Col-0 on water-treated leaves, but Pip-treatment induced only a very slight reduction of disease symptoms (Figure 41). In *fmo1, sid2, sid2 ald1,* and *eds5* the increased susceptibility towards *Hpa* Noco2 became apparent with very high spore numbers quantified in water-treated leaves (Figure 41). Pip-treatment prior to infection reduced symptoms only slightly or not at all (Figure 41).

Results from this set of experiments suggest that resistance against the virulent oomycete *Hpa* Noco2 depends on the combined results of SA- and Pip-mediated signalling in plants. Analysis of basal resistance, either qualitatively by microscopy or quantitatively by counting spores, showed that plant lines impaired in Pip-biosynthesis (*ald1*) and -signalling (*fmo1*) were much more susceptible to *Hpa* than Col-0. The same was true for lines impaired in SA biosynthesis (*sid2, eds5, ics1 ics2*) and signalling (*npr1*), but no additive effects of Pip- and SA-deficiency was observed, as the *sid2 ald1* double mutant exhibited a disease pattern similar to the parental lines. As observed for interactions with *Psm* and *B. cinerea*, exogenously applied Pip induced resistance against *Hpa* in Col-0 and partly in *ald1*, but not in *fmo1*, which shows again that processing of the Pip-mediated signal by *FMO1* is crucial for induction of defence responses. Priming of SA-accumulation appears to be an essential factor of Pip-induced resistance against this oomycete, which explains why Pip-treatment did not induce resistance in *sid2* and *eds5* plants. In *npr1*, SA-accumulation is not disturbed, which seemed to enable a partial defence induction by Pip. Conflicting results were obtained for *ics1 ics2*, which did not exhibit a reduction of disease symptoms by treatment with Pip via microscopic analysis, but showed a partial Pip-induced defence response after counting of spores. It could be assumed for this plant line that exogenous Pip-application would not be able to induce resistance comparable to *sid2*, because *ics1 ics2* is not only impaired in the expression of the pathogen-inducible gene, *ICS1*, but also the second *Arabidopsis ICS2* gene. As this mutant line was used only one time so far, future experiments will have to be conducted to allow for more solid conclusions.

6.9 Resistance to *Hpa* Noco2 mediated by *Psm*-induced SAR

It is often discussed that induction of the SAR response in *Arabidopsis* by one pathogen (e.g. *Psm*) confers resistance to a broad spectrum of pathogens (Durrant & Dong, 2004). To verify this statement, a SAR experiment was carried out by using *Psm* as SAR-inducing pathogen and *Hpa* for the challenge infection. Lower leaves of 5 week old naive plants were infiltrated with either 10 mM $MgCl_2$ (mock) or *Psm* (OD_{600}=0.005).

6.9 Resistance to *Hpa* Noco2 mediated by *Psm*-induced SAR

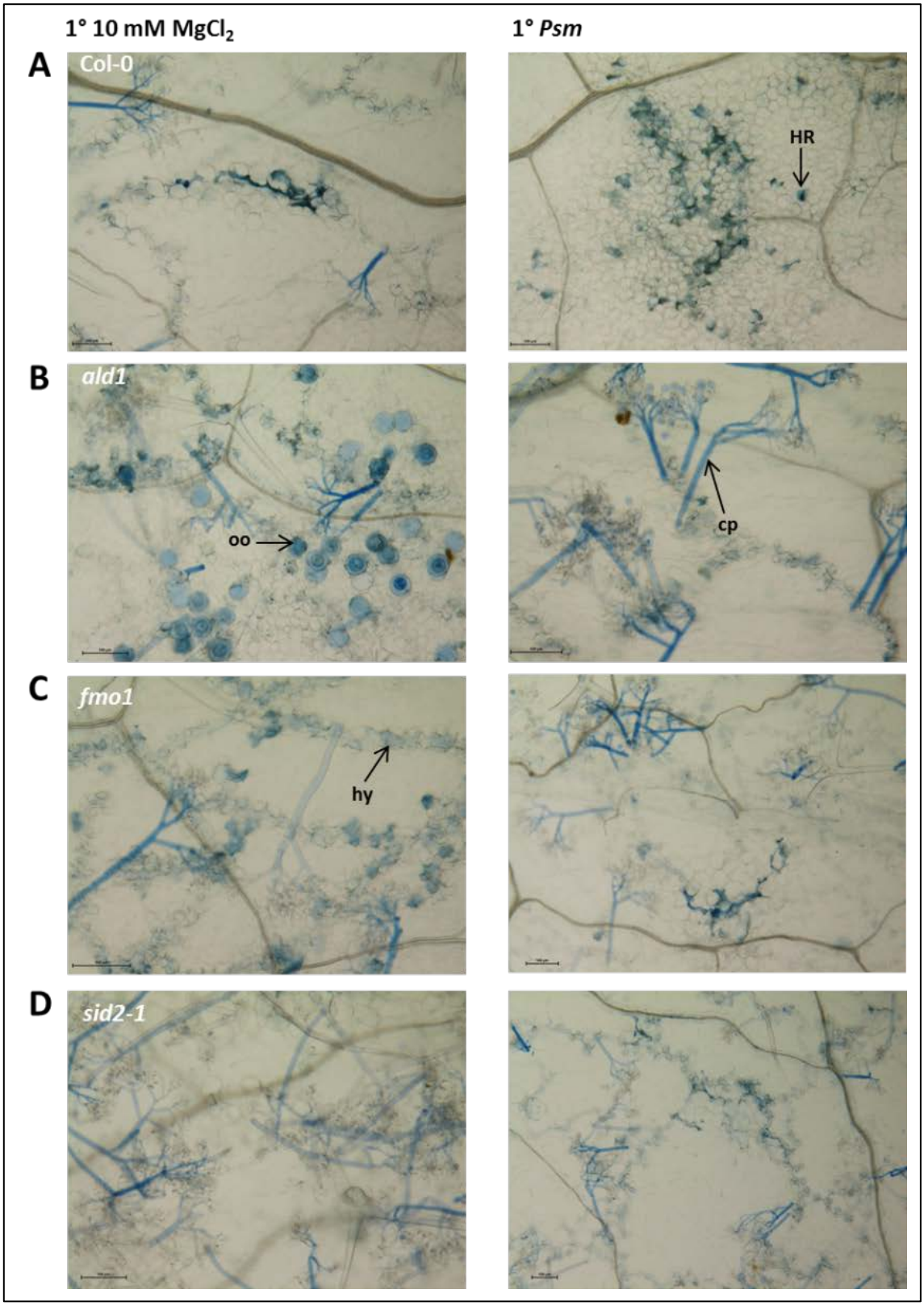

Figure 42. Protection of Col-0, but not *ald1, fmo1*, or *sid2* against subsequent infection by *Hpa* Noco2 by *Psm*-induced SAR.

Plants were infiltrated in three lower leaves with either 10 mM $MgCl_2$ or *Psm* (OD_{600}=0.005) and challenge infected 2 days later by spray-infection with a spore solution of *Hpa* Noco2 ($5x10^4$ spores ml^{-1}). Oomycete hyphae and dead plant cells were TB-stained and disease severity analysed by light microscopy. Representative detailed pictures of Col-0 (A), *ald1* (B), *fmo1* (C), and *sid2* (D) are shown. Cp, conidiophore; HR, hypersensitive response; hy, hyphae; oo, oospore.

6.9 Resistance to *Hpa* Noco2 mediated by *Psm*-induced SAR

Two days after 1° infiltration, plants were spray-infected with a spore solution of *Hpa* Noco2 (5 x 10^4 spores ml^{-1}) and kept in high humidity for one week. To assess the SAR response, spore production on the plants was quantified (Figure 43), and TB-stained leaves were studied under the microscope (Figure 42).

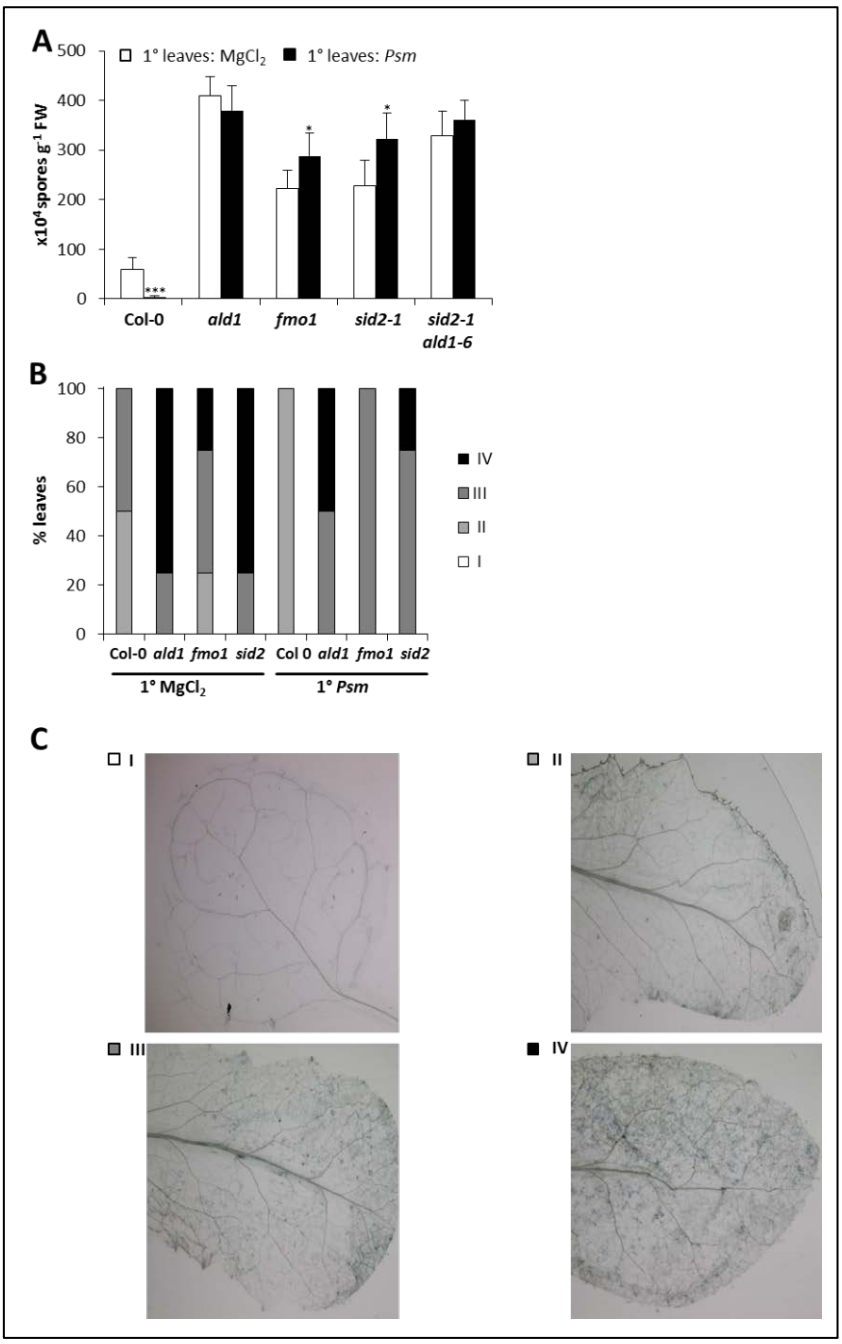

Figure 43. *Psm* infection induces SAR against *Hpa* Noco2.

Plants were treated as described in figure 42 and disease severity assessed by counting spores (A) as well as microscopy analysis (B). Asterisks above the bars denote significant statistical differences between SAR-noninduced and SAR-induced plants (two-tailed *t* test; *, P< 0.05; **, P< 0.01; ***, P< 0.001). (C) Disease rating as delineated in figure 39. The *sid2 ald1* plants used in this experiment were generated by Dr Friederike Bernsdorff.

Mock-treated Col-0 leaves supported strong hyphal growth of the oomycete with conidiophores covering a large part of the leaf surface (Figure 42 A, left side). In *Psm*-treated leaves, more incidents of HR and less conidiophores were visible (Figure 42 A, right side). Quantification of spores resulted in approximately 100 x 10^4 spores g^{-1} FW in 1° mock-treated plants and a huge reduction of spore numbers to 3 x 10^4 spores g^{-1} FW in 1° *Psm* treated plants (Figure 43 A). The SAR-impaired mutant lines *ald1* and *fmo1* showed more severe disease symptoms in 1° mock- and *Psm*-treated leaves than Col-0 after analysis of TB-stained leaves, with most of the leaf area pervaded by hyphae and conidiophores, as well as a lot of sexual oospores, covering most of the leaf surfaces (Figure 42 B; Figure 42 C). Quantification of conidiospores demonstrated that the Pip-biosynthesis mutant *ald1* allowed much stronger proliferation of the oomycete, compared to Col-0, with about four times more spores in 1° $MgCl_2$-treated leaves and no significant reduction in spore numbers in 1° *Psm* treated leaves (Figure 43 A). In *fmo1,* quantification of oomycete spores yielded about 2 times more spores than in Col-0 in 1° mock infiltrated leaves and no reduction in spore number in 1° *Psm* inoculated leaves (Figure 43 A). Microscopy analysis of *Hpa*-infected *sid2* 1° mock- and *Psm*-treated plants showed leaves covered densely in conidiophores and a large area traversed by hyphae (Figure 42 D). Quantification of spores gave similar results as for *fmo1* (Figure 43 A). The *sid2 ald1* double mutant also showed a high amount of spores in mock-infiltrated leaves (ca 300 x 10^4 spores g^{-1} FW) and no SAR response in 1° *Psm*-treated plants (Figure 43 A). In addition to representative microscopy images shown in Figure 42, a disease rating was performed. Figure 43 B shows a reduction of disease severity in 1° *Psm*-treated Col-0 plants compared to 1° mock-treated plants, which shows the SAR response of Col-0. There was no SAR effect discernable for *ald1*, but *fmo1* and *sid2* showed a slight induction of SAR in this experiment. These results show that Pip-accumulation and its processing by *FMO1*, as well as an increase in SA levels in systemic leaves upon infection with the bacterium *Psm* is crucial for SAR against *Hpa* Noco2.

6.10 The metabolic profile of *Arabidopsis* plants infected with the avirulent *Hpa* isolate Cala2 differs from plants infected with the virulent *Hpa* isolate Noco2

In addition to the interaction of *A. thaliana* with the virulent *Hpa* Noco2 strain, the *Hpa* isolate Cala2 was used, which is avirulent to Col-0 and virulent to Ler-0 that served as a positive control. Infection of Col-0 with the avirulent *Hpa* Cala2 led to accumulation of slightly less free SA than with the virulent isolate, from basal levels of 0.05 µg g^{-1} FW to approximately 0.3 µg g^{-1} FW in infected leaves (Figure 38 A). The mutant lines *ald1* and *fmo1* exhibited basal free SA-levels similar to Col-0, but accumulated lower amounts of free SA in *Hpa*-infected leaves, with 0.15 µg g^{-1} FW in *ald1* and 0.16 µg g^{-1} FW in *fmo1*, respectively (Figure

38 A). A comparatively strong increase in free SA from basal levels of 0.1 µg g^{-1} FW to almost 1 µg g^{-1} FW was observed in the virulent interaction between *A. thaliana* ecotype Ler-0 and *Hpa* Cala2. The SA-biosynthesis impaired mutant *sid2* and the *sid2 ald1* double mutant did not accumulate free SA after infection with the avirulent oomycete. *Hpa* Cala2-infection elicited weaker accumulation of the phytoalexin camalexin in Col-0*, ald1*, and *fmo1* than observed with the virulent isolate Noco2. Basal levels of 0.01 µg g^{-1} FW were detected for camalexin in these three plant lines and levels increased to 0.6 µg g^{-1} FW in Col-0 and *ald1*, and to 0.9 µg g^{-1} FW in *fmo1*, respectively (Figure 38 B). In *sid2* and *sid2 ald1* on the other hand, camalexin levels increased from 0.02 µg g^{-1} FW in non-infected to respective 4 µg g^{-1} FW in *sid2* and 6 µg g^{-1} FW in *sid2 ald1* in *Hpa* Cala2-infected leaves (Figure 38 B). Similar to free SA, the *Arabidopsis* ecotype Ler-0 showed elevated basal levels for camalexin of 0.2 µg g^{-1} FW that increased to 3 µg g^{-1} FW after infection with *Hpa* Cala2 (Figure 38 B). ICA-analysis showed a comparably weak accumulation from 0.005-0.008 µg g^{-1} FW in non-infected to 0.04 µg g^{-1} FW in Col-0 and *ald1* and respective 0.07 µg g^{-1} FW in *fmo1* in *Hpa* Cala2-infected leaves (Figure 38 C). For the SA-deficient *sid2* and SA- and Pip-deficient *sid2 ald1* elevated basal levels of respective 0.01 and 0.02 µg g^{-1} FW were detected for ICA, which increased to 0.2 µg g^{-1} FW in *sid2* and 0.3 µg g^{-1} FW in *sid2 ald1*, respectively (Figure 38 C). The highest ICA-amount with 0.4 µg g^{-1} FW was detected in *Hpa* Cala2-infected leaves of Ler-0, which already showed comparatively high ICA-levels of 0.05 µg g^{-1} FW in non-infected leaves (Figure 38 C). The unknown compound 28 (table 2), which increased almost tenfold in Col-0 plants infected with the virulent *Hpa* Noco2, did not accumulate in Col-0 upon infection with the avirulent oomycete (Figure 38 D). In *ald1* and *fmo1* a weak, approximately two-fold, increase of this substance was detected (Figure 38 D). In contrast to this, in *sid2* a four-fold increase and in *sid2 ald1* a 13-fold increase of this compound were quantified in *Hpa*-Cala2 infected leaves (Figure 38 D). This strong increase in levels of this substance was also observed in Ler-0, which is susceptible to *Hpa* Cala2 (Figure 38 D). Analysis of Pip-accumulation upon infection with the avirulent *Hpa* Cala2 showed an increase in Pip-levels from approximately 1 µg g^{-1} FW in non-infected to 5 µg g^{-1} FW in infected leaves of Col-0 and *fmo1* (Figure 38 E). The SA-biosynthesis impaired line *sid2* showed an even stronger increase in Pip-levels from 1.6 µg g^{-1} FW in non-infected to 9 µg g^{-1} FW in *Hpa*-infected leaves (Figure 38 E). The mutant lines *ald1* and *sid2 ald1* demonstrated no increase of Pip-levels upon infection with *Hpa* Cala2 (Figure 38 E). In the *Hpa* Cala2-susceptible ecotype Ler-0, basal levels for Pip were comparable to Col-0 and increased to approximately 6 µg g^{-1} FW in infected leaves (Figure 38 E). No increase of Pro, which accumulated to high levels in leaves infected with the virulent *Hpa* Noco2, was observed in Col-0, *ald1, fmo1, sid2*, and *sid2 ald1* after infection with the avirulent Cala2 isolate (Figure 38 F). In contrast, in Ler-0 *Hpa* Cala2 was able to elicit a strong increase of Pro from 15 µg g^{-}

^{1} FW in non-infected to 75 µg g^{-1} FW in infected leaves (Figure 38 F). A similar picture unfolds for the accumulation of GABA and Orn after infection with the avirulent oomycete (Figure 38 G; Figure 38 H). After treatment with *Hpa* Noco2, levels of GABA and Orn showed a strong increase in Col-0, *ald1, sid2*, and *sid2 ald1* that were not detectable after treatment with the avirulent isolate Cala2. In Ler-0, on the other hand, a respective increase from 2 µg g^{-1} FW to 9 µg g^{-1} FW was observed for GABA and 0.2 µg g^{-1} FW to 1.9 µg g^{-1} FW for Orn upon infection with *Hpa* Cala2 (Figure 38 G; Figure 38 H). Analysis of amino acid accumulation in Col-0 plants infected with the avirulent *Hpa* Cala2 showed a generally lower increase in amino acid levels compared to plants infected with *Hpa* Noco2(see table 6 in the appendix). The results from metabolite analyses in *A. thaliana* in interaction with an avirulent *Hpa* strain show that recognition of the pathogen by *RPP* genes and the ensuing HR-generated cell death is the most potent plant defence against this biotroph and that high accumulation of defence-related metabolites are –if at all– only of very minor importance. However, SA-mediated signalling is an important part of the HR process. The significant increases in the indolic compounds camalexin and ICA in the SA-deficient lines *sid2* and *sid2 ald1* allow the speculation that the oomycete, which is avirulent on the background line Col-0, might become more virulent to these lines.

6.11 Analysis of the interaction of *A. thaliana* with the avirulent *Hpa* isolate Cala2

As described for the interaction between *A. thaliana* and the virulent *Hpa* Noco2, disease symptoms were analysed in plants infected with the avirulent Cala2 isolate as well. For this experiment the same mutant lines were employed as for the studies with *Hpa* Noco2: the Pip-deficient line *ald1*, the SAR-impaired line *fmo1*, the SA biosynthesis mutant lines *sid2, eds5*, and *ics1 ics2*, the SA- and Pip-deficient mutant *sid2 ald1*, and the SA-signalling mutant *npr1*. This oomycete isolate did not produce spores on the majority of analysed plant lines so that only qualitative microscopy analysis of TB-stained leaves was performed. For microscopy analysis a disease rating was performed as described in Ton *et al*. (2005) (Figure 44 B). Analysis of TB-stained leaves followed by a disease rating showed that no disease symptoms were discernible on Col-0, *ald1*, and *fmo1* leaves, allowing the conclusion that the avirulent isolate of this oomycete was not able to grow and proliferate on these plant lines (Figure 44 A, left side). In the SA-deficient *sid2* mutant, half of the analysed leaves showed weak growth and proliferation of *Hpa* Cala2, which was even more pronounced in the SA- and Pip-deficient *sid2 ald1* double mutant (Figure 44 A, left side). In the SA-biosynthesis mutant lines *eds5, ics1 ics2*, and the SA signalling mutant *npr1* no disease symptoms were visible (Figure 44 A, left side). In Pip-treated plants, no disease symptoms

were visible on leaves of Col-0, *ald1*, *fmo1* and *eds5*, and a lower percentage of *sid2* leaves showed successful sporulation of the oomycete (Figure 44 A, right side).

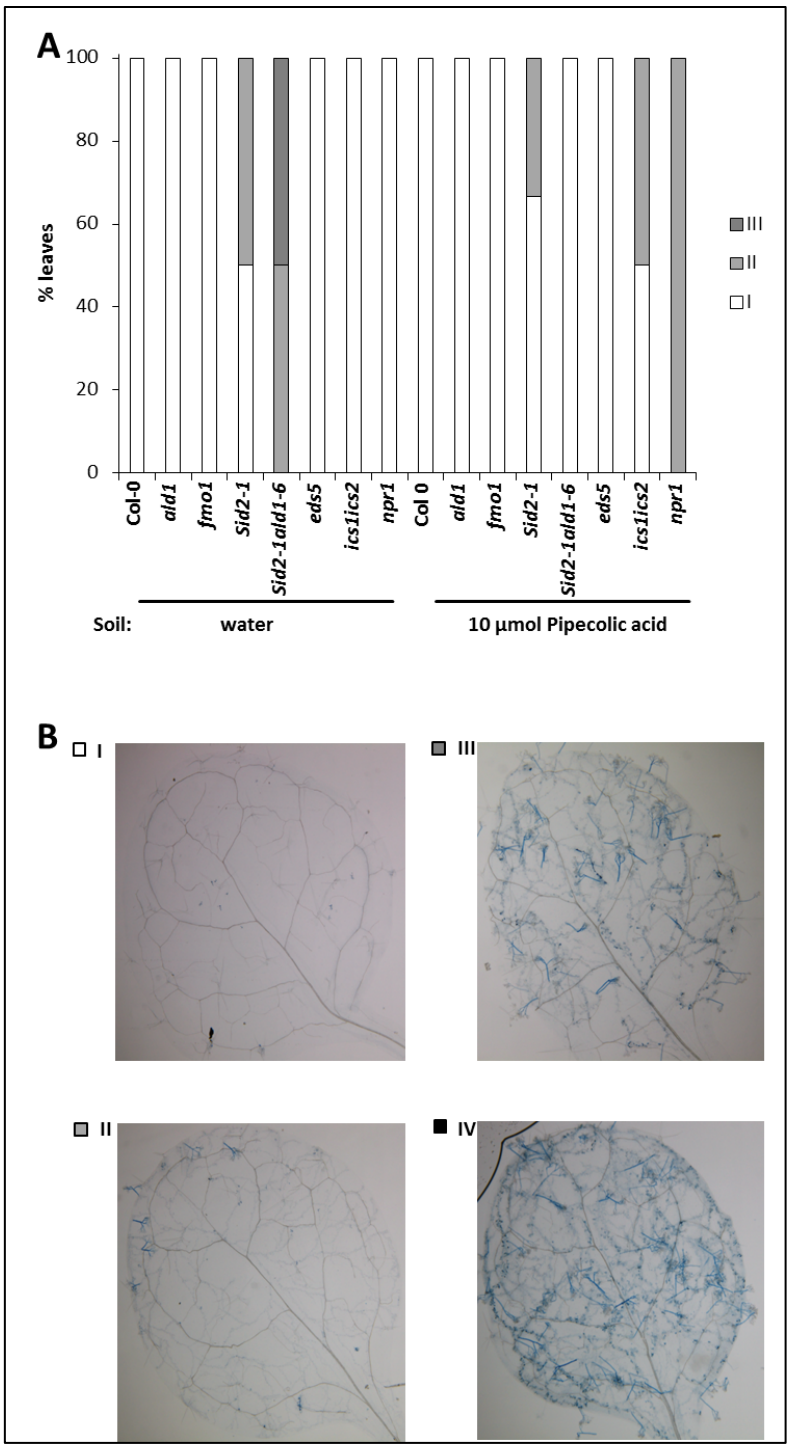

Figure 44. Pip-induced resistance against the avirulent *Hpa* isolate Cala2.

Plants were treated and analysed as described in figure 39. With the exception of *eds5, ics1ics2*, and *npr1*, the mutant lines were used in at least two independent biological experiments with similar results. The *sid2 ald1* double mutant line was generated by Dr Friederike Bernsdorff.

Furthermore, in *sid2 ald1* plants, treatment with Pip prior to infection with *Hpa* Cala2 protected plants from this oomycete (Figure 44 A, right side). Surprisingly, on *ics1 ics2* and *npr1* Pip-treatment seemed to enable the oomycete to partially grow and proliferate on leaves (Figure 44 A, right side). Additionally to classification of disease symptoms, representative TB-stained leaves were analysed to further study the interaction between *Arabidopsis* and the avirulent oomycete (Figure 45). Infection of water-treated Col-0 plants with *Hpa* Cala2 did not lead to observable disease symptoms, except for a few spots of HR on leaves (Figure 45 A). This oomycete was also not able to grow and proliferate on *ald1* (Figure 45 B), but analysis of infected *fmo1* leaves showed a few hyphae with trailing necroses visible in water-treated plants (Figure 45 C). Unlike Col-0, the SA-deficient *sid2* and the SA- and Pip-deficient *sid2 ald1* mutant lines supported growth of the avirulent oomycete on water-treated leaves (Figure 45 D). Neither growth nor sporulation on water-treated leaves of *eds5*, *ics1 ics2*, and *npr1* plants was visible (Figure 45 F; Figure 45 G; Figure 45 H).

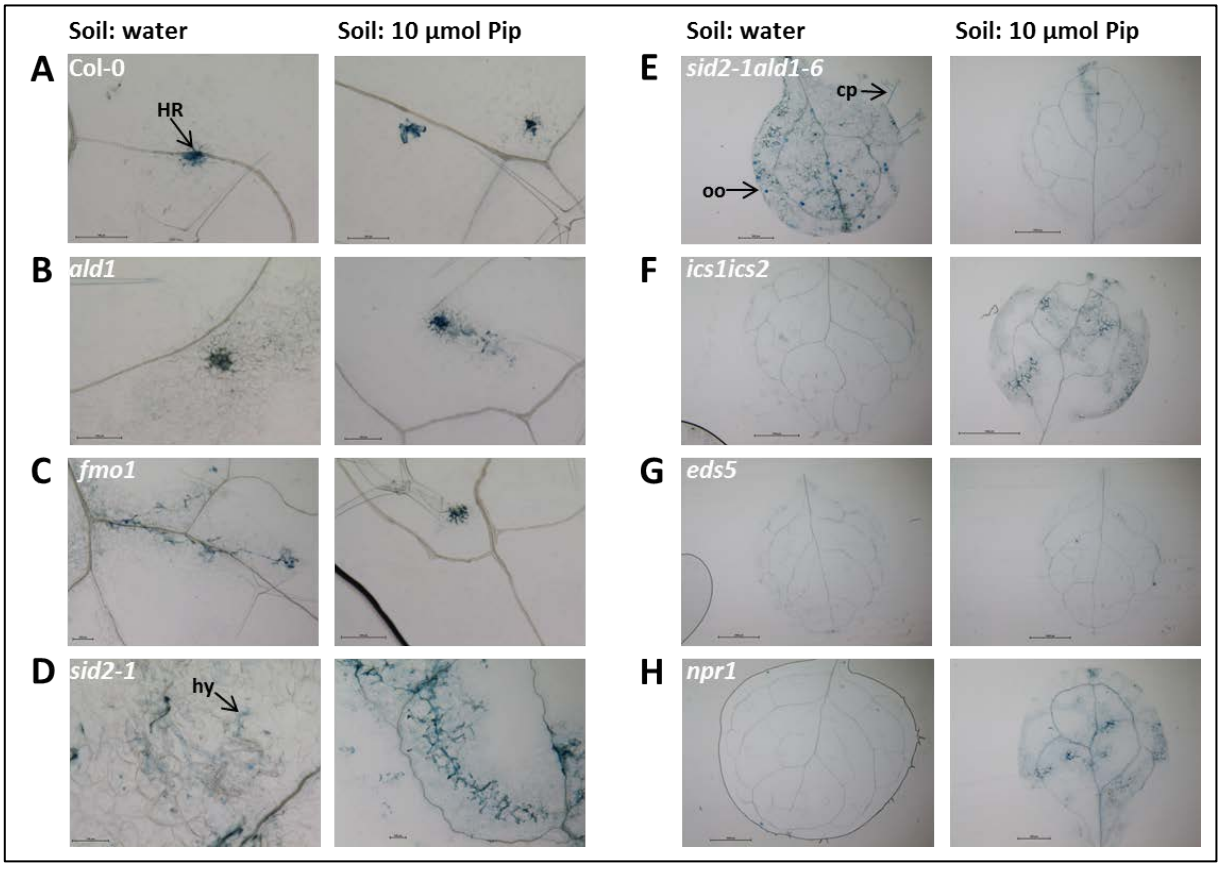

Figure 45. The avirulent *Hpa* Cala2 is able to grow and proliferate on *sid2* and *sid2 ald1*.

This experiment was done as specified in figure 39. Shown are representative detail views of *A. thaliana* Col-0 (A) and the mutant lines *ald1* (B), *fmo1* (C), *sid2* (D), the double mutants *sid2 ald1* (E) and *ics1 ics2* (F), as well as *eds5* (G) and *npr1* (H). For mutant lines with no detail picture available, a representative overview shot is shown. Generation of the *sid2 ald1* double mutant line was done by Dr Friederike Bernsdorff. Cp, conidiophore; HR, hypersensitive response; hy, hyphae; oo, oospore.

In plants treated with Pip prior to infection with *Hpa* Cala2 no disease symptoms were discernible for Col-0, *ald1, eds5*, and also *fmo1* (Figure 45 A; Figure 45 B; Figure 45 C; Figure 45 G). Pip-treatment did not induce resistance in *sid2*, which hosted hyphae and few conidiophores on leaves of Pip-treated plants, but reduced disease symptoms in *sid2 ald1*, which showed several spots of HR on analysed leaves. In *ics1 ics2* and *npr1*, surprisingly, Pip-treatment of plants prior to infection reduced resistance against the pathogen and allowed partial growth and proliferation of the oomycete (Figure 45 F, Figure 45 H). These analyses confirm the importance of SA for *RPP*-mediated resistance against an avirulent *Hpa* isolate already conjectured after analysis of metabolite profiles in infected leaves. In this avirulent interaction SA- and Pip-deficiency seems to add up, as the *sid2 ald1* double mutant shows more severe disease symptoms than the parental lines. It is surprising that in *sid2 ald1* resistance can be induced by exogenous Pip-application, which was not possible in *sid2*. Moreover, the other analysed plant lines impaired in SA-biosynthesis or -signalling initially show resistance against *Hpa* Cala2. It would be expected that at least the *ics1 ics2* double mutant, which is not able to synthesise any SA at all, and *eds5*, essential for SA-biosynthesis, showed equally severe disease symptoms as observed in *sid2*. Similarly confusing is the enhanced susceptibility of *ics1 ics2* and *npr1* induced by exogenous Pip-application. As the plant lines for *sid2 ald1, ics1 ics2, eds5*, and *npr1* were used one time so far in the analysis of the interaction of *Arabidopsis* with an avirulent oomycete strain, further experiments will be needed to strengthen the results and illuminate the mechanisms of this interaction.

6.12 Changes in defence metabolite profiles of A*. thaliana* after infection with the obligate biotrophic fungus *G. orontii*

To account for potential phylum-specific differences, another biotrophic pathogen, the fungal powdery mildew agent *Golovinomyces orontii* was chosen and accumulation of defence-related metabolites monitored over a defined period of time after infection. Five week old, unstressed *Arabidopsis thaliana* plants were treated with *G. orontii* spores and samples taken at different time points, untreated plants were used as control. Time points for sampling were chosen to match distinct stages in infection of *Arabidopsis* by *G. orontii*. According to Weßling and Panstruga (2012), spore germination and formation of the fungal appressorium can be detected at 2 to 5 hpi, haustoria formation starts around 1 dpi, formation of secondary hyphae and secondary feeding structures can be observed at 3 dpi and formation of new conidiophores at 4-7 dpi (Figure 19). As we were mainly interested in early accumulation of defence metabolites, the time points 4, 8, 24, 48, and 72 hpi were chosen. As can be seen in figure 46 A, levels for free SA were very low in non-infected as well as in *G. orontii*-infected plants. As only weak SA-accumulation was observed at 72 hpi

and those levels were even lower than in non-treated plants at earlier time points, the accumulation of free SA this early in the infection process can be considered negligible. In contrast to SA-levels, camalexin significantly increased from basal levels of under 0.005 µg g^{-1} FW to 0.03 µg g^{-1} FW in infected leaves at 72 hpi, but these levels were still much lower than after infection with *Psm* (Figure 46 B). Pip accumulated from basal levels of 0.1 µg g^{-1} FW to 0.4 µg g^{-1} FW in infected leaves 48 hours after infection and increased further to 0.9 µg g^{-1} FW at 72 hpi (Figure 46 C). A relatively high accumulation of the C_{20} fatty acid eicosanoic acid from approximately 0.05 µg g^{-1} FW in non-infected to almost 1 µg g^{-1} FW in infected leaves was observed at all selected time points (Figure 46 D). As levels for eicosanoic acid were very similar at all analysed time points, it can be concluded that this compound stems from the heavily infected plants used for spore propagation and infection of the plants in this experiment.

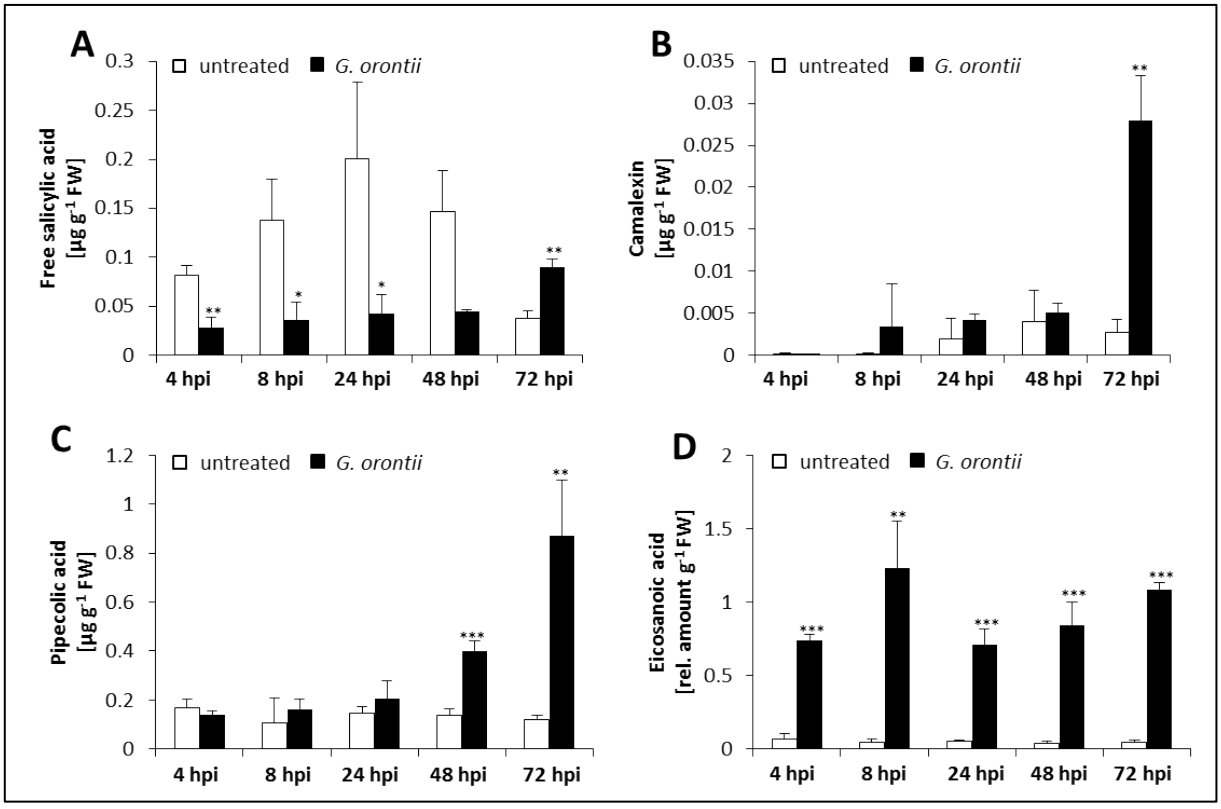

Figure 46. Camalexin and Pip-accumulation after infection of *Arabidopsis* with *G. orontii*.

Time course of free SA- (A), camalexin- (B), Pip- (C), and eicosanoic acid- (D) accumulation in *Arabidopsis* leaves infected with the powdery mildew *G. orontii*. Bars correspond to the mean ±SD of three replicate samples and asterisks above the bars show significant statistical differences between non-infected and infected plants (two-tailed *t* test; *, P< 0.05; **, P< 0.01; ***, P< 0.001). FW, fresh weight. This experiment was done in collaboration with Dr Michaela Kopischke (University Göttingen; now TSL).

These analyses show on the one hand that after infection with the powdery mildew *Golovinomyces orontii* the defence-related metabolites camalexin and Pip accumulate relatively early. On the other hand, these compounds did not increase to levels comparable to *Psm*-infected leaves.

6.13 Pip does not induce resistance against the powdery mildew *G. orontii*

Similarly to the analyses of pathosystems with *Botrytis cinerea* and *Hyaloperonospora arabidopsidis*, disease development in plants infected with *Golovinomyces orontii* and Pip-IR against this powdery mildew was analysed. In this study a diverse set of mutant lines was used: *ald1, fmo1, sid2*, and *npr1*, which were also used in experiments with *B. cinerea* and *Hpa*. In addition to those lines the *pad4* mutant line was used, which is impaired in expression of a positive regulator of SA-biosynthesis (Jirage *et al.,* 1999). The *edr1* (*enhanced disease resistance 1*) mutant line was shown to exhibit enhanced resistance against different powdery mildew strains (Frye and Innes, 1998) and was used as a control line for strong resistance against *G. orontii*. As an example for a very susceptible plant line the *pen2 pad4 sag101* triple mutant was used, which is impaired in penetration resistance conferred by the glycosyl hydrolase PEN2, shows disturbances in regulation of SA-biosynthesis, and SA-mediated signalling (Lipka *et al*., 2005). The *gl1* (*glabra1*; Marks and Feldmann, 1989) mutant line was used as a positive control for the triple mutant.

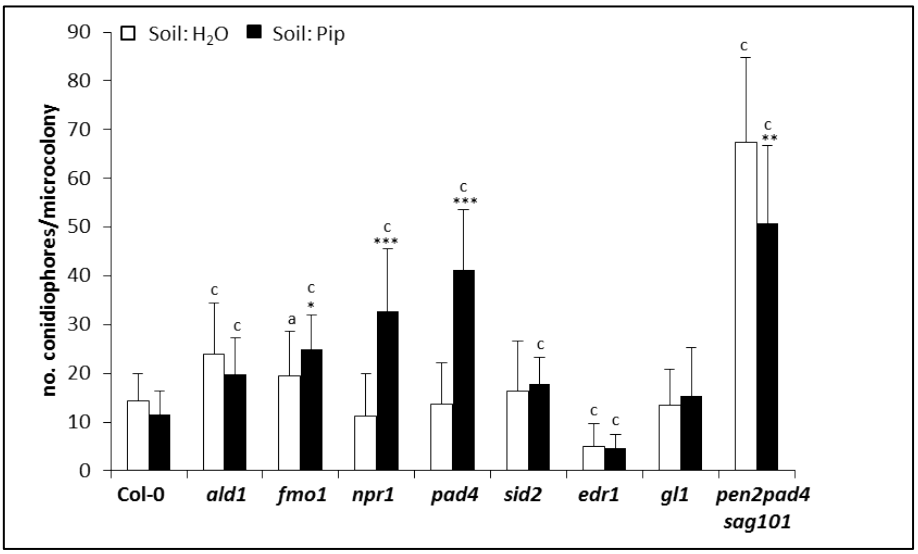

Figure 47. Growth of the powdery mildew *G. orontii* is not impaired by exogenously applied Pip.

A. thaliana plants were supplied with water or 1 mM Pip to the root system 1 day prior to brush-infection with the biotrophic fungus *G. orontii.* At 7 dpi, leaves were destained in ethanol and fungal colonies on the leaves stained with Coomassie Brilliant-blue. To ascertain severity of infection, 20 microcolonies per leaf were chosen and the number of conidiophores per microcolony counted. Experiments with *G. orontii* were conducted with the kind help of Dr Michaela Kopischke (University Göttingen; now TSL). Statistical significant differences between water- and Pip-treated plants (asterisks above the bars) were assessed, as well as differences between Col-0 and mutant plants (letters above the bars), using a two-tailed *t* test (* a, P< 0.05; ** b, P< 0.01; *** c, P<0.001).

On water-treated leaves of Col-0, *sid2*, and *gl1* plants, on average 15 conidiophores per microcolony were counted, which signifies a moderate spread of the powdery mildew fungus on the leaves (Figure 47). The mutant lines *ald1* and *fmo1* exhibited slightly more proliferation of *G. orontii* on water-treated leaves, with approximately 20 conidiophores per

microcolony. Both for the SA-signalling mutant *npr1* and the *pad4* line, impaired in regulation of SA biosynthesis, fewer conidiophores were counted than in Col-0 (Figure 47). The lowest numbers of conidiophores were counted on leaves of *edr1* and in contrast the triple mutant *pen2 pad4 sag101* hosted the highest number of conidiophores per microcolony (Figure 47). No significant induction of defence responses by Pip-treatment prior to infection with *G. orontii* was observed (Figure 47). Col-0 and *ald1* showed a slight decrease of disease symptoms, which could not be confirmed in a second experiment (see supplemental figure 19). In *fmo1,* and particularly in *npr1* and *pad4,* infection seemed to be stronger after Pip-treatment (Figure 47). No effect of Pip was observed in *sid2, edr1*, and *gl1*. The *pen2 pad4 sag101* line on the other hand showed a slight decrease of conidiophore numbers in plants treated with Pip prior to infection. These results show that an intact penetration resistance is highly important for defence against *G. orontii*. As long as pre- and postpenetration mechanisms are intact, Pip-treatment of plants does not enhance defence against this powdery mildew. The same seems to be true for SA-signalling pathways, which were not activated in plants with intact penetration resistance upon infection with *G. orontii*. As soon as pre- and postpenetration defence mechanisms are impaired, Pip seems to enable the plant to mount a better disease resistance.

6.14 Dependency of the metabolite accumulation pattern on the lifestyle of the attacking pathogen

Table 2 gives an overview of metabolites found to accumulate after infection with *Botrytis cinerea, Hyaloperonospora arabidopsidis,* or *Golovinomyces orontii*. For substances that showed an explicit entry in our GC-MS database the name is shown in the table, all other metabolites were called “Unknown” and numbered serially. In the table given are also the abundant ions of the mass spectra, the m/z value that was used for quantification, the retention time, and the pathogen interaction in which the substance was first detected in. Boldly marked substances were taken into account for analysis of the different plant-pathogen interactions, because these substances were more than three-fold upregulated in the studied interaction. The mass spectra of these metabolites can be found in the appendix.

Table 2. Overview of unknown compounds found in interactions of *Arabidopsis thaliana* with *B. cinerea*, *H. arabidopsidis*, and *G. orontii*.

Given are the names for metabolites that showed an entry in the GC/MS database and the number of unknown compounds, respectively. Prominent ions in the chromatogram are shown in bold letters, given are also the m/z which was used for analysis, as well as the retention time and pathosystem the compound was first discovered in.

Name	Ions	m/z	retention time [min]	first found in
2-Benzoylsuccinic acid	77**,105**,207	105	21.02	*Bc*
Eicosanoic acid	**74, 87**, 143, 283, **326**	74	26.6	*Go*
Hexacosanoic acid	55,74,97,143,410	410	30.45	*Hpa*
Hydroxyterephthalic acid	119,127,**147,178**,210	178	18.1	*Bc*
Isophthalic acid	135,**163**,194	163	16.6	*Bc*
Neophytadien	55,67,**68,82,95**,109,**123**,226	68	21.17	*Bc*
Phytol	73, **75, 143**	143	24.82	*Bc*
Tetracosanoic acid	57,74,87,143,339,382	382	29.57	*Hpa*
trans-Phytol	55,67,68,69,**81,95**,109,**123**,278	81	21.7	*Bc*
Unknown 1	**55,83,97,111**,222,264,265,296	55	24.4	*Bc*
Unknown 2	54,**67,81,82,95**,109,123	67	24.3	*Bc*
Unknown 3	83, 125, 149, **210, 234**	210	24.17	*Bc*
Unknown 4	55,**74**,97,143,**494**	494	33.37	*Bc*
Unknown 5	**55,81,263**,322	263	26.15	*Bc*
Unknown 6	264**,265**,281	265	26.22	*Bc*
Unknown 8	**59**, 68, 83, 95, **127**, **151**, 154, 168	151	14.96	*Bc*
Unknown 9	**91, 230**	230	22.48	*Bc*
Unknown 10	91, **105, 119**, 132, **133**, 161	105	26.56	*Bc*
Unknown 11	**105, 133**, 145, **161, 188**, 220	105	29.49	*Bc*
Unknown 12	51,78**,106**	106	21.53	*Bc*
Unknown 13	**70,112**	112	18.16	*Bc*
Unknown 15	156	156	15.58	*Bc*
Unknown 16	95,181,268	268	17.44	*Bc*
Unknown 17	105,106,123,163	123	6.37	*Bc*

6.14 Dependency of the metabolite accumulation pattern on the lifestyle of the attacking pathogen

Name	Ions	m/z	retention time [min]	first found in
Unknown 18	105,106,123,163	123	6.69	*Bc*
Unknown 19	95, 215	215	13.7	*Go*
Unknown 20	132	132	16.05	*Go*
Unknown 22	**61**, 73, 83, 102, 115, 295, 313, **354**	354	28	*Go*
Unknown 23	73, 473, **488**	488	30.69	*Go*
Unknown 24	53, 59, 85, 113	113	6.9	*Hpa*
Unknown 25	73, 75, 103, 119, 121,161	161	9.58	*Hpa*
Unknown 26	84	84	14.5	*Hpa*
Unknown 27	55,67,72,122,136	136	14.77	*Hpa*
Unknown 28	57,68,81,83,95,123,155,278	123	30.55	*Hpa*

In order to get deeper insight into the differences between modi of infection of analysed pathogens, metabolite accumulation in plant tissue after infection with *P. syringae* pv. *maculicola, B. cinerea, H. arabidopsidis* Noco2, and *G. orontii* was analysed and summarized in tables 3 (defence metabolites), 4 (amino acids), and 5 (unknown compounds)

6.14 Dependency of the metabolite accumulation pattern on the lifestyle of the attacking pathogen

Table 3. Comparison of defence metabolite accumulation in *Arabidopsis* after infection with different pathogens.

Metabolite accumulation in *A. thaliana* after infection with *P. syringae, B. cinerea, H. arabidopsidis*, and *G. orontii* was analysed and fold-change ratio for each metabolite determined. Significant statistical differences between non-infected and infected plants are marked by asterisks (two-tailed t test; *, P< 0.05; **, P< 0.01; ***, P< 0.001). SM, Sabour & Maltose medium; nt, not treated; FW, fresh weight.

Pathogen	*Psm*-inoculated leaves (2 dpi)			*B. cinerea*-inoculated leaves (3 dpi)			*Hpa*-sprayed leaves (7 dpi)			*G. orontii*-infected leaves (3 dpi)		
	µg g^{-1} FW		ratio	µg g^{-1} FW		ratio	µg g^{-1} FW		ratio	µg g^{-1} FW		ratio
Metabolite	$MgCl_2$	*Psm*	P/M	SM	*Bc*	PM	H_2O	*Hpa*	P/M	nt	*Go*	P/M
Salicylic acid	0.27 ± 0.07	5.0 ± 1.9	18.6 *	0.26 ± 0.1	0.38 ± 0.07	1.5	0.05 ± 0.02	0.51 ± 0.04	9.8 ***	0.04 ± 0.01	0.09 ± 0.01	2.4 **
Pipecolic acid	0.6 ± 0.2	42.2 ± 15.8	65.3 ***	0.07 ± 0.02	0.25 ± 0.08	3.4 *	0.46 ± 0.1	2.9 ± 0.6	6.2 **	0.12 ± 0.01	0.87 ± 0.2	7.2 **
Camalexin	0.09 ± 0.01	69.3 ± 6.2	741.2 ***	0.06 ± 0.07	4.6 ± 1.2	76.1 **	0.01 ± 0.001	1.7 ± 0.2	307.2 ***	0.002 ± 0.001	0.03 ± 0.004	10.4 **
Indole-3-carboxylic acid	0.01 ± 0.001	6.92 ± 1.3	676.0 **	0.01 ± 0.01	0.42 ± 0.04	34.9 ***	0.005 ± 0.002	0.10 ± 0.02	21.7 **	0.006 ± 0.00	0.01 ± 0.00	2.6 ***
Indole-3-carbaldehyde	0.03 ± 0.004	0.12 ± 0.03	4.6 *	0.007 ± 0.00	0.01 ± 0.002	1.5	0.002 ± 0.002	0.02 ± 0.004	7.9 *	0.005 ± 0.00	0.005 ± 0.00	1.0
Jasmonic acid	0.08 ± 0.02	1.74 ± 0.4	21 **	0.01 ± 0.001	0.33 ± 0.06	22.4 **	not detected			0.03 ± 0.01	0.03 ± 0.005	0.9

> 100	> 20	5-20	3-5	1.6-3	0.5-0.8	≤ 0.5

Table 4. Comparison of amino acid accumulation in *Arabidopsis* after infection with different pathogens.

Amino acid accumulation in *A. thaliana* after infection with *P. syringae, B. cinerea, H. arabidopsidis*, and *G. orontii* was analysed and fold-change ratio for each metabolite determined. Significant statistical differences between non-infected and infected plants are marked by asterisks (two-tailed t test; *, P< 0.05; **, P< 0.01; ***, P< 0.001). SM, Sabour & Maltose medium; nt, not treated; FW, fresh weight.

Pathogen	*Psm*-inoculated leaves (2 dpi)			*B. cinerea*-inoculated leaves (3 dpi)			*Hpa* Noco2-sprayed leaves (7 dpi)			*G. orontii*-infected leaves (3 dpi)		
Amino acid	µg g^{-1} FW		ratio P/M	µg g^{-1} FW		ratio PM	µg g^{-1} FW		ratio P/M	µg g^{-1} FW		ratio P/M
	$MgCl_2$	*Psm*		SM	*Bc*		H_2O	*Hpa*		nt	*Go*	
Ala	78.4 ± 7.3	141.0 ± 32.5	1.8 **	7.2 ± 0.4	18.9 ± 7.2	2.6	9.7 ± 1.00	30.0 ± 5.9	3.1 **	88.8 ± 0.4	96.0 ± 9.8	1.1
Lys	5.1 ± 1.1	28.8 ± 11.7	5.7 **	6.4 ± 0.8	10.5 ± 1.8	1.6 *	0.90 ± 0.3	7.8 ± 3.4	8.7 *	0.44 ± 0.009	0.87 ± 0.4	2.0
Gly	12.8 ± 1.0	21.7 ± 5.4	1.7 *	3.6 ± 0.3	11.3 ± 6.3	3.2	2.03 ± 0.3	7.5 ± 2.4	3.7 *	39.2 ± 2.3	11.4 ± 2.2	0.3 **
Glu	277.0 ± 63.9	282.5 ± 95.1	1.0	119.4 ± 12.2	105.4 ± 17.4	0.9	134.0 ± 28.1	208.6 ± 40.2	1.6	453.0 ± 13.4	362.4 ± 19.2	0.8 **
Gln	254.1 ± 65.2	374.5 ± 72.0	1.5	3.1 ± 1.3	10.8 ± 3.5	3.5 *	15.2 ± 7.9	105.0 ± 37.7	6.9 *	95.3 ± 1.7	70.1 ± 20.8	0.7
Phe	3.7 ± 0.2	20.3 ± 4.9	5.5 *	7.3 ± 0.7	8.6 ± 1.5	1.2	1.2 ± 0.03	4.4 ± 0.7	3.7 **	3.5 ± 0.05	3.6 ± 0.6	1.0
Tyr	3.3 ± 1.0	23.9 ± 4.5	7.3 ***	2.0 ± 0.06	2.7 ± 1.3	1.3	0.3 ± 0.05	3.9 ± 0.9	11.9 **	0.3 ± 0.02	0.5 ± 0.1	1.5
Trp	2.7 ± 0.7	24.7 ± 11.7	9.2 **	0.3 ± 0.04	0.5 ± 0.2	1.6	0.09 ± 0.02	1.5 ± 0.6	17.5 *	0.1 ± 0.004	0.1 ± 0.03	1.1
Val	7.9 ± 1.3	54.4 ± 27.1	6.9 **	12.6 ± 0.8	12.9 ± 3.3	1.0	2.3 ± 0.2	13.2 ± 3.2	5.7 **	6.4 ± 0.3	5.4 ± 0.8	0.8
Leu	3.3 ± 0.6	49.2 ± 26.7	14.8 **	17.6 ± 1.5	14.3 ± 3.6	0.8	1.0 ± 0.1	7.9 ± 2.3	7.8 *	1.4 ± 0.06	1.7 ± 0.5	1.2
Ile	2.6 ± 0.4	31.4 ± 16.0	12.0 **	7.1 ± 0.3	7.0 ± 1.7	1.0	0.8 ± 0.03	4.7 ± 1.3	5.6 *	1.5 ± 0.04	1.4 ± 0.3	0.9
Thr	58.9 ± 13.0	98.5 ± 33.7	1.7	13.3 ± 0.3	16.6 ± 3.9	1.2	10.6 ± 0.7	21.1 ± 6.6	2.0	26.4 ± 0.4	27.5 ± 5.2	1.0
Pro	11.1 ± 1.5	10.0 ± 3.0	0.9	11.8 ± 1.5	13.5 ± 3.6	1.1	9.0 ± 1.1	44.0 ± 11.7	4.9 *	70.3 ± 8.0	22.7 ± 4.7	0.3 **
Ser	127.5 ± 17.8	230.5 ± 46.4	1.8 *	19.7 ± 1.4	20.3 ± 4.2	1.0	13.3 ± 0.4	33.3 ± 10.8	2.5	26.6 ± 2.4	29.9 ± 8.5	1.1
Asn	28.1 ± 4.3	78.9 ± 22.3	2.8 **	6.1 ± 1.0	6.9 ± 1.0	1.1	8.3 ± 1.2	23.1 ± 9.3	2.8	31.7 ± 2.3	22.1 ± 4.0	0.7 *
Met	0.2 ± 0.02	1.0 ± 0.1	5.6 ***	0.06 ± 0.02	0.20 ± 0.08	3.6	not detected			not detected		
Asp	160.0 ± 46.6	91.7 ± 30.7	0.6 *	76.7 ± 6.6	102.9 ± 16.6	1.3	192.4 ± 27.4	325.0 ± 77.3	1.7	333.7 ± 22.8	271.0 ± 38.9	0.8
Aad	0.4 ± 0.1	25.6 ± 6.6	71.2 ***	0.1 ± 0.02	0.6 ± 0.4	5.3	0.06 ± 0.02	1.6 ± 0.4	26.1 **	0.05 ± 0.005	0.2 ± 0.03	3.4 **
Cys	0.09 ± 0.01	0.25 ± 0.03	2.9 *	0.07 ± 0.007	0.1 ± 0.04	2.1 *	0.1 ± 0.02	0.4 ± 0.09	3.3 **	0.09 ± 0.01	0.09 ± 0.006	1.0
Orn	0.7 ± 0.1	1.1 ± 0.2	1.6 *	0.7 ± 0.07	1.5 ± 0.4	2.2	0.1 ± 0.02	1.2 ± 0.5	10.9 *	0.09 ± 0.009	0.1 ± 0.03	1.3
GABA	6.5 ± 0.5	25.1 ± 6.5	3.8 **	1.1 ± 0.2	5.4 ± 3.1	4.9	2.4 ± 0.1	9.9 ± 0.4	4.1 **	not detected		

6.14 Dependency of the metabolite accumulation pattern on the lifestyle of the attacking pathogen

> 100	> 20	5-20	3-5	1.6-3	0.5-0.8	≤ 0.5

Table 5. Accumulation of unknown metabolites in *Arabidopsis* after infection with different pathogens.

Accumulation of unknown metabolites in *A. thaliana* after infection with *P. syringae, B. cinerea, H. arabidopsidis*, and *G. orontii* was analysed and fold-change ratio for each metabolite determined. As no correction factors for the unknown substances were identified yet, a correction factor of 1 was assumed and the relative amount per g FW calculated. Significant statistical differences between non-infected and infected plants are marked by asterisks (two-tailed t test; *, P< 0.05; **, P< 0.01; ***, P< 0.001). SM, Sabour & Maltose medium; nt, not treated; FW, fresh weight.

Pathogen	***Psm*-inoculated leaves (2 dpi)**			***B.cinerea*-inoculated leaves (3 dpi)**			***Hpa*-sprayed leaves (7 dpi)**			***G.orontii*-infected leaves (3 dpi)**		
	µg g^{-1} FW		**ratio**	**µg g^{-1} FW**		**ratio**	**µg g^{-1} FW**		**ratio**	**µg g^{-1} FW**		**ratio**
Metabolite	**$MgCl_2$**	***Psm***	**P/M**	**SM**	***Bc***	**P/M**	**H_2O**	***Hpa***	**P/M**	**nt**	***Go***	**P/M**
Unknown 1	0.3 ± 0.05	1.0 ± 0.2	3.7 **	0.3 ± 0.07	0.7 ± 0.2	2.5	0.4 ± 0.02	0.8 ± 0.2	2.2 *	not detected		
Unknown 2	0.1 ± 0.007	0.5 ± 0.08	3.8 **	0.09 ± 0.01	0.5 ± 0.2	6.0 *	0.2 ± 0.04	0.34 ± 0.08	1.6	not detected		
Unknown 3	not detected			0.001 ± 0.0004	0.1 ± 0.01	94.5 ***	not detected			not detected		
Neophytadien	0.6 ± 0.1	11.5 ± 1.4	17.7 ***	0.3 ± 0.04	0.5 ± 0.1	1.7	1.2 ± 0.5	2.5 ± 0.4	2.1	3.5 ± 0.3	3.6 ± 0.5	1.0
Hydroxy-terephthalic acid	1.4 ± 0.3	4.5 ± 0.2	3.2 ***	1.6 ± 0.4	3.9 ± 0.2	2.4 **	0.02 ± 0.03	0.1 ± 0.03	5.0	0.1 ± 0.01	0.2 ± 0.05	1.9
Unknown 9	not detected			0.0004 ± 0.0001	0.2 ± 0.05	559.3 **	not detected			not detected		
Unknown 13	not detected			0.005 ± 0.004	2.9 ± 0.5	559.4 ***	not detected			not detected		
Unknown 15	not detected			0.06 ± 0.04	0.3 ± 0.08	4.3 *	not detected			not detected		
Eicosanoic acid	0.1 ± 0.01	0.3 ± 0.05	2.3 *	0.1 ± 0.04	0.1 ± 0.02	1.2	0.04 ± 0.007	0.1 ± 0.008	2.8 ***	0.04 ± 0.01	1.1 ± 0.04	24.3 ***
Unknown 22	0.01 ± 0.002	0.05 ± 0.008	4.0 **	0.002 ± 0.0006	0.001 ± 0.0002	0.7	not detected			0.003 ± 0.0002	0.02 ± 0.003	5.7 **
Unknown 28	not detected			not detected			0.009 ± 0.006	0.08 ± 0.03	9.5 *	not detected		

6.14 Dependency of the metabolite accumulation pattern on the lifestyle of the attacking pathogen

The metabolite profiles of plants infected with the hemibiotrophic bacterium *Psm* and the biotrophic oomycete *Hpa* Noco2 were very similar, with very strong increases observed in levels of SA, camalexin, and Aad (table 3; table 4). Furthermore, levels for Pip, ICA, and indole-3-carbaldehyde (table 3), as well as a large number of amino acids including Lys and Orn (table 4) were strongly elevated in both plant-pathogen interactions. In contrast to plants infected with *Psm*, an increase in Pro-levels was detected in *Hpa*-infected plants (table 4), as well as a number of as yet unidentified metabolites (table 5). Plants infected with the necrotrophic grey mould fungus *B. cinerea* showed similar accumulation of camalexin, ICA, and JA as observed in *Psm*-infected plants (table 3), but induced only a comparatively weak increase in amino acid levels (table 4). This fungus elicited a strong accumulation of not yet identified substances, which were only detectable in *B. cinerea*-infected plants (table 5). Of the analysed interactions, plants infected with the biotrophic powdery mildew fungus *G. orontii* induced the least changes in metabolite levels. Moderate increases were observed for Pip, camalexin, Aad, and a few unidentified compounds (table 3; table 4; table 5). Apart from that especially the amino acid content seemed to be reduced upon infection with this pathogen (table 4). These differences in fold-change of metabolite accumulation highlight the distinct *modus operandi* of the studied pathogens and also reflect the experimental procedure for infection with pressure infiltration of bacteria into the apoplast *vs* infection of epidermal cells by distributing spores on leaves.

7 Discussion

7.1 Unravelling the regulation of defence priming in *A. thaliana*

A very important and interesting aspect of plant defence and SAR is priming, which enables the plant to react faster and significantly stronger to a threat by pathogens following an earlier attack (Bruce *et al*., 2007; Conrath, 2011; Návarová *et al*., 2012). Priming of plants can also be triggered artificially by the SA-analogues INA and BTH (Conrath *et al*., 2001), the non-protein amino acid BABA (Ton *et al*., 2005), which does not occur naturally in *Arabidopsis*, and the naturally occurring non-protein amino acid Pip (Návarová *et al*., 2012). Plants in the primed state exhibit pre-activated metabolite pathways (Gruner *et al*., 2013), preformed but dormant enzymes participating in MAPK signalling (Beckers *et al*., 2009), as well as chromatin modifications, marking genes for fast expression (Jaskiewicz *et al*., 2011). Analysis of a set of genome-wide microarrays concerning the regulation of the SAR response in *Arabidopsis* (Gruner *et al.,* 2013) yielded the possibility to arrange SAR-genes in the categories of SA-dependent, -independent, and partially SA-dependent genes. For a more detailed understanding of priming in plants, a set of 67 genes was chosen and expression analyses in Col-0, *ald1*, and *fmo1* were performed (Figure 24; Figure 25; Figure 26; Table 1). Genes exhibiting primed expression (genes in bold font SA-independent) can be classified as involved in detoxification (*2OGD1,* ***2OGD2****,* ***ACD11L****, BGLU31,* ***CYP81G1****, GRXS13*), defence signalling (***AIG1****,* ***ALD1****,* ***FMO1****, FRK1, GRXS13, NPR4, PR1,* ***PR3****, UGT76B1,* ***UGT85A1****, RKL1-12*), cell wall-related processes (*AGP5,* ***CXE17, CXE20****,* ***PMEa****, XHT10*), defence metabolism (***ANACO42****,* ***CYP710A1****,* ***CYP71A13****, MYB122,* ***PAD3***), biotic/abiotic stress responses (***ACD11L****, BGLU31, PER58,* ***UGT74E2****,* ***CHI1****,* ***UGT73B2, UGT73B3***), cell death (***KTI1****,* ***SAG13***), primary and secondary metabolism (*ARD3,* ***BGLU45****,* ***CXE17****,* ***GH3.3****, NCED5,* ***TPPD****, UGT85A1*), and others (*ATPase1,* ***MAPKKK18****,* ***ZCF37***) (Figure 27 C). Only a very small number of genes with primed expression in the analysed set encode proteins not directly involved in defence, for example the trehalose-6-phosphate phosphatase TPPD (Eastmond *et al*., 2003), which is involved in sugar metabolism, or the MAP kinase kinase kinase 18 (MAPKKK18), which might play a role in cell signalling. A more diverse classification of functions emerged for genes not showing primed expression (genes in bold font SA-dependent). Genes found to be not primed are mostly involved in cell signalling (*ASK7, C2D1,* ***LHY****, NPR1, NPR3,* ***PBS3****, PRB1, SDR4, WRKY38*), primary and secondary metabolism (***At5g39090****, BAHD1, GH3.4, IPT7, LAC7, UGT73D1,* ***BSMT1****,* ***GPAT5***), defence metabolism (*PBS3*), ROS-production or -scavenging (***At1g26420****, RBOHA*), development (*KNAT1*), cell wall-related processes (*COBL4,* ***RABA1i***), detoxification (***GSTU1***), and others (*MRP7, At1g03660*) (Figure 27 D). Among this group are only a few defence-related genes

like the SA-receptors *NPR1* (Wu *et al*., 2012) and *NPR3* (Fu *et al*., 2012), the defence-related *PBS3*, which was reported to conjugate amino acids to benzoates (Okrent *et al*., 2009) and *RABA1i,* which was shown to be involved in cell wall-modification processes (Vernoud *et al*., 2003). It does make sense to find a majority of genes involved in defence-related processes primed, as this enables plants to react faster to subsequent threats without having to synthesize all needed components of defence *de novo* upon infection. Among strongly primed genes several genes involved in camalexin biosynthesis and cell wall-modification can be found, which gives credit to the hypothesis of broad-spectrum resistance conferred by SAR. On the other hand, it is not very surprising that products of many non-primed genes are involved in processes more related to growth and cell signalling. As mentioned above, a large number of primed genes exhibit SA-independent expression, for instance critical defence regulators like the Pip-biosynthesis gene *ALD1* (Návarová *et al*., 2012) and the flavin-dependent monooxygenase *FMO1* (Mishina and Zeier, 2006), or the camalexin biosynthesis genes *CYP71A13* (Nafisi *et al.,* 2007) and *PAD3* (Schuhegger *et al*., 2006). This enables the plant to react very fast to the subsequent threat, before accumulation of high SA-amounts, which is a quite slow process compared to Pip-accumulation. Many non-primed genes, on the other hand, are SA-dependent with the exception of genes not involved in any defence-related process like *At5g39090*, which is involved in anthocyanin biosynthesis (Luo *et al*., 2007) or *LHY*, an integral regulator in the circadian clock (Alabadi *et al*., 2001), respectively. In the mutant lines *ald1* and *fmo1* no priming of gene expression was detected, except for *ASK7 and UGT85A1* in *ald1* and *GSTU1 and TPPD* in *fmo1*, respectively (Table 1). These findings support our theory and earlier findings that *ALD1* and *FMO1* are critical regulators of SAR and the priming response in plants (Návarová *et al*., 2012). We were able to show that Pip-accumulation in local leaves and the ensuing generation of a mobile signal leads to Pip-accumulation in leaves distal from the infection site, setting in motion a feedback amplification loop in which both *ALD1* and *FMO1* are key components to establish SAR in plants (Figure 6; Návarová *et al*., 2012). Also, exogenous Pip-application primed gene expression of *ALD1* and *FMO1*, as well as camalexin accumulation. Several different approaches can be followed in future experiments to further dissect defence priming in *Arabidopsis*. Gene expression tested in the biological priming experiment presented in this work would have to be re-tested, as the experiment was done only once due to the high cost of quantitative real-time PCR. A larger set of mutant lines could be used in this experiment, for example *sid2* and *sid2 ald1* in addition to *ald1* and *fmo1*, as well as *npr1* and *pad4*, which have been implicated to play a role in priming before (Conrath *et al*., 2001). Using *sid2* and the *sid2 ald1* double mutant would also shed further light on the regulation of SA-independent and partially SA-dependent genes in priming. Furthermore, it would be interesting to analyse Pip-induced priming of the set of genes tested

so far to see to what extent defence priming and Pip-induced priming of gene expression overlap, this might also lead to discovering more SA-dependent genes primed in *ald1* by exogenously supplied Pip.

7.2 Pip as essential component for priming of SA-independent and -dependent gene expression

In our previous experiments, we found a partial SAR response in the SA-biosynthesis impaired mutant *sid2*, which apparently is a result of a SA-independent process. To analyse this phenomenon more closely with respect to defence and Pip-induced priming, experiments with *sid2, ald1*, and the *sid2 ald1* double mutant were carried out and gene expression of select genes was analysed (Figure 28). The SA-independent genes *ALD1* and *FMO1* showed a strong priming response in Col-0 and *sid2*, but not in *ald1* or *sid2 ald1*, respectively. Expression of the SA-dependent *PR-1* gene was primed in WT plants, but abolished in all three mutant lines. The strong priming response of *ALD1* and *FMO1* in *sid2*, which was even stronger than in Col-0 for *FMO1* in the biological priming experiment (Figure 28 B) and for *ALD1* and *FMO1* in Pip-induced priming (Figure 28 D; Figure 28 E), and the complete abolishment of this response in *ald1* and the *sid2 ald1* double mutant show clearly that *ALD1* is an absolutely necessary regulator of the priming response and SA is needed for priming of SA-dependent genes. Exogenously applied Pip induced strong priming of *ALD1* and *FMO1* expression in Col-0 and *sid2*, but not in the Pip-deficient *ald1* and the Pip- and SA-deficient *sid2 ald1* (Figure 28 D; Figure 28 E). Priming of *PR-1* expression even reached almost WT-levels in *ald1* plants exogenously supplied with Pip, but not in the *sid2 ald1* double mutant (Figure 28 F). This shows that in *ald1* plants provided with Pip, primed expression of the SA-dependent *PR-1* gene can be partially restored. These data allow the conclusion that Pip is essential for defence priming of both the majority of SA-independent and -dependent defence-related genes, whereas SA-accumulation is necessary for primed expression of SA-dependent genes. These data also show that for primed expression of certain SA-independent genes, for instance *FMO1*, the amount of exogenously applied Pip seems to be insufficient and needs to be boosted by the feedback amplification loop consisting of *ALD1, FMO1*, and *ICS1* (Figure 6). To shed more light on the role of interplay between Pip and SA in priming, a larger set of genes should be analysed in *ald1, sid2* and *sid2 ald1* in future experiments. This can be achieved by including *sid2* and *sid2 ald1* into the set of mutant lines analysed in defence and Pip-induced priming.

7.3 The flavin-dependent monoxygenase FMO1 is a crucial regulator of Pip-induced priming of gene expression and camalexin accumulation

The flavin-dependent monooxygenase FMO1 can be established as the second critical regulator, besides *ALD1*, for defence priming in *Arabidopsis*. This function can be explained by the hypothesis that Pip is a substrate of FMO1, leading to a modified and thus activated form of Pip (Zeier, 2013). As Pip was able to restore priming of *PR-1* expression in *ald1*, the possibility to restore Pip-induced priming in *fmo1* was analysed as well (Figure 29). Supplying *fmo1* plants with Pip did not restore priming of gene expression of the SA-independent genes *ALD1* (Figure 29 A) and *SAG13* (Figure 29 C), as well as the SA-dependent gene *PR-1* (Figure 29 B), respectively. Pip-induced priming of camalexin accumulation was also not possible in *fmo1* plants (Figure 29 E). These results strengthen the theory that *FMO1* translates the Pip-generated signal into the actual priming response, as this process is no longer possible in the *fmo1* mutant line. An important question to find answers for in future experiments besides the role of Pip- and SA-mediated signalling in defence priming, is how the priming signal is stored in plant cells to be released so fast upon subsequent pathogen attack. Recently, attention moved more and more towards epigenetic changes to ensure a longer alert state for the plant than conferred by metabolic changes (Bruce *et al*., 2007). An example for such epigenetic changes without changing the DNA sequence is chromatin modification and remodelling (Conrath, 2011; Jaskiewicz *et al*., 2011). Genetic information in a cell is tightly packed in chromatin, with the basic chromatin structure being the nucleosome, a protein structure of eight histone proteins the DNA is associated with. These histone proteins can be modified by acetylation of Lys- and methylation of Lys- and Arg-residues in the protein structure. Acetylation and triple methylation of Lys-residues was shown previously to be associated with active genes (Eberharter and Becker, 2002; Ruthenburg *et al*., 2007; Jaskiewicz *et al*., 2011). Genes showing these kinds of chromatin modification can be "marked" for fast transcription upon perception of pathogen-elicited signals by the plant cell (Jaskiewicz *et al*., 2011). It was also shown that epigenetic changes can be transferred vertically over several plant generations (Luna *et al.,* 2012). Analysis of epigenetic changes in defence priming and Pip-induced priming in Col-0, *ald1, fmo1, sid2*, and *sid2 ald1* would grant valuable insight into the mechanism of storing the priming signal. Singh *et al*. (2014) were also able to show that epigenetic markers on primed genes are modulated in a HISTONE ACETYLTRANSFERASE1-dependent manner and can influence defence mechanisms in that way. To find out if this mechanism also plays a role in Pip-dependent priming or Pip-induced defence priming, the *hac1-1* (*histone acetyltransferase1-1*) mutant could be included in future studies.

7.4 A minor role for MAPK signalling in defence priming

In 2009 Beckers *et al*. published results showing that MPK3 and MPK6 are required for full priming in *Arabidopsis*. They showed that mRNA for and inactive proteins of MPK3 and MPK6 accumulate after BTH-treatment, that priming of defence-related gene expression (*PR-1* and *PAL1*) and BTH-induced resistance are completely lost in *mpk3* and *mpk6*, and that SAR is abolished in *mpk3*. In experiments done for this work, the same mutant lines as in the Beckers *et al.* (2009) publication and additionally the *mpk3 mpk6* (+/-) double mutant were used. A first step in the analyses concerning the role of MAPKs in priming was to test the SAR response and Pip-induced resistance in these lines. SAR was not impaired in *mpk3* or *mpk6* and only slightly reduced in *mpk3 mpk6* (Figure 30 A). Analysis of Pip-IR yielded no differences between Col-0 and the three mutant lines at all (Figure 30 B). Next, priming of defence-related gene expression and metabolite accumulation was studied. Pip was found to be strongly primed in *mpk6* and *mpk3 mpk6* and accumulated to high levels also in *mpk3* (Figure 30 C). It was not possible to see priming of Pip accumulation in *mpk3* in the first experiment, because the mutant line showed high Pip-levels in systemic leaves (1°*Psm*/2°$MgCl_2$). A second experiment showed that Pip-accumulation is primed in *mpk3* as well (see supplemental figure 11). Analysis of camalexin accumulation showed strong priming in *mpk3*, more than WT-levels and priming in *mpk6*, and slightly decreased but primed levels in *mpk3 mpk6* (Figure 30 D). MPK3 and MPK6 have been reported as activators of camalexin biosynthesis upon infection of plants with the fungus *B. cinerea,* the authors´ results showing impaired camalexin accumulation in *mpk3* and complete abolishment in *mpk3 mpk6* (Ren *et al*., 2008). These results differed from camalexin accumulation measurements in MAPK mutant lines upon infection with the bacterium *Psm* presented in this work, as camalexin was found to accumulate to WT-levels in *mpk3* and *mpk3 mpk6*, and to levels even higher than in WT in *mpk6*, and this camalexin production was also found to be primed in all three lines (Figure 30 D).

For the analysis of gene expression, the priming regulators *ALD1* and *FMO1* were chosen. Priming of *ALD1* expression was observed in Col-0, to a comparable degree in *mpk3*, and even stronger in *mpk6* and *mpk3 mpk6* (Figure 30 E). Priming of *FMO1* expression was similar in Col-0, *mpk6*, and *mpk3 mpk6* and slightly weaker (approximately half as strong as in Col-0) in *mpk3* (Figure 30 F). Closer perusal of the publication by Beckers *et al.* (2009) showed several differences in the experimental setup. The same mutant lines were used for the experiments, but the authors used *P. syringae* pv. *tomato avrRpt2* (*Pst*) as trigger for the SAR response and *Pst* DC3000 for the challenge infection, while in the experiments presented here, the virulent *Psm* strain was used that triggers a robust SAR response at 2 dpi in *Arabidopsis* (Mishina and Zeier, 2007) for both infections.

Also the challenge infection was done 48 hrs after the first infiltration in the experiments for this work, in contrast to 3 days between inoculations used in the publication by Beckers *et al*. (2009). These differences in experimental execution might be responsible for the discrepancies between published results and those presented here. Especially the pathogen chosen for first infiltration seems to be very important for MAPK signalling, as Tsuda *et al*. showed in 2013. The authors provided data that showed a much more robust and longer MAPK activation if ETI was triggered by *Pst avrRpt2,* compared to the PTI triggered by *Pst* containing an empty vector. In plants treated with *Pst avrRpt2,* MAPK activation was detectable for up to 12 hours after treatment, whereas MAPK activity after treatment with *Pst* lasted only approximately an hour (Tsuda *et al*., 2013). Glazebrook and Ausubel also described differences in camalexin accumulation depending on the pathogen used for inoculation. Plants inoculated with virulent *Psm* and avirulent *Psm* strains *avrRpm1* and *Psm avrRpt2*, respectively, showed no differences in camalexin accumulation. However, camalexin accumulation was more rapid in plants inoculated with avirulent *Pst* DC3000 *avrRpt2* than with virulent *Pst* DC3000 (Glazebrook and Ausubel, 1994). The best way to solve this problem would be to repeat the SAR-, Pip-IR-, and priming-experiments using not only *Psm* but also *Psm avrRpm1* and/or *Pst avrRpt2* as inducing pathogens. Involvement of MPK3 and MPK6 in plant innate immunity signalling was analysed by Asai and colleagues (2002), who presented data describing activation of MPK3 and MPK6 upon flg22 perception in protoplasts of *Arabidopis*. If MAPK activation played a major role in defence and priming, activation of MAPKs upon infection with either virulent or avirulent bacteria would be expected, as well as a changed activation pattern in *ald1* and *fmo1*. Detection of MAPK activity was possible in local leaves of Col-0, *ald1* and *fmo1* 6 hours after infection with *Psm avrRpm1* and 48 hours after infection with *Psm* and *Psm avrRpm1* (Figure 31). Activation of MPK3 and MPK6 seemed to be slightly less pronounced in *ald1* and *fmo1*. Except for *ald1* treated with *Psm avrRpm1*, no systemic activation of MAPKs was detected. It was also not possible to detect systemic accumulation of free SA and Pip in transgenic plants expressing MKK4, the MAP kinase kinase responsible for phosphorylation and subsequent activation of MPK3 and MPK6, under the control of a DEX-inducible promoter (Figure 32). These results back up our hypothesis that MAPK signalling is not as strongly involved in defence priming as claimed in earlier publications (Asai *et al*., 2002; Beckers *et al*., 2009). To be able to confirm our results that MAPK signalling is not involved in defence priming, several other experiments come to mind. As MAPK activation is one of the earliest responses in plants upon infection, a time course with more and earlier time points would be a possibility to test MAPK activation in local and systemic leaves of Col-0, *ald1, fmo1, sid2*, and *sid2 ald1* after infection with *Psm* and *Psm avrRpm1*. It would also make sense to include *Pst avrRpt2* in this experiment, as this pathogen was shown to stabilize MAPK activation in *Arabidopsis*

(Tsuda *et al*., 2013). The next step would be to test MAPK activation in defence priming by using the setup for the priming experiment as described, but take samples for analysis of MAPK activity at different time points after challenge infection (e.g. 2 hpi, 4 hpi, 6 hpi, 8 hpi, 12 hpi, 24 hpi, and 48 hpi) and not only at 10 hpi. Another important experiment still missing is the analysis of MAPK activation after Pip-treatment, a time course after Pip-feeding would serve this purpose well. Concerning further experiments to analyse defence priming in Col-0, *ald1*, and *fmo1*, gene expression analysis of *MPK3* and *MPK6* would be important to see if these two genes might play a role in priming or are being primed after infection.

7.5 The role of Pip in the interaction of *A. thaliana* with the necrotrophic fungus *B. cinerea*

The first step for studying the interaction of *Arabidopsis* with a pathogen following a necrotrophic lifestyle was a comparative analysis of metabolite accumulation after infection. To achieve this, a time course experiment was performed and metabolite accumulation quantified (Figure 33). As described before (Govrin and Levine, 2002), no significant induction of SA-accumulation was observed in plants after *B. cinerea*-infection at chosen time points (Figure 33 A). The tryptophan-derived camalexin and its intermediate ICA (Böttcher *et al*., 2014) on the other hand, showed strong accumulation from day three of infection on (Figure 33 B; Figure 33 D). Camalexin exhibits potent antifungal activity, as it was shown to limit lesion development in *Arabidopsis* infected with *B. cinerea* in a dose-dependent manner (Ferrari *et al*., 2003) and reveals a ten times lower inhibitory concentration for sensitive fungi than for Gram negative bacteria like *Psm* (Glawischnig, 2007). The importance of camalexin accumulation upon *Botrytis*-infection is also emphasised by the high susceptibility of the phytoalexin-deficient mutant lines *pad2* and *pad3* towards *Botrytis*-infection (Glazebrook and Ausubel, 1994; Ferrari *et al*., 2003). The oxylipin derivative JA was also found to accumulate in *Botrytis*-infected plants (Figure 33 C) simultaneously with ongoing destruction of leaf tissue. Plants infected with the fungus also exhibited moderate accumulation of Pip (Figure 33 E), GABA (Figure 33 F), and a number of not yet identified compounds at 3 dpi (Table 2). The results from this experiment show that Pip does not exclusively accumulate after infection with the bacterium *Psm*, but also with the fungus *B. cinerea*. This allows the conclusion that this critical compound is not only involved in defence against hemibiotrophic, but may also play a role in defence against necrotrophic pathogens. For GABA, a very important role in defence against necrotrophic pathogens was shown before: In ABA-deficient tomato (*Solanum lycopersicum*) *sitiens* plants, survival of cells around the pathogen-invaded tissue was preserved by changes in C:N metabolism via over-activation of the GS/GOGAT (Glutamine synthetase/glutamate synthase) cycle and GABA shunt, leading to a slowing-down of pathogen-induced senescence on the site of

primary invasion (Seifi *et al*., 2013). GABA-accumulation was shown to be induced by several biotic and abiotic stresses, which implies several roles for this compound, for example in regulation of cytosolic pH, protection against oxidative stress, and signalling (Roberts, 2007). In mammals, GABA is a very prominent neurotransmitter, which negatively regulates excitability of the nervous system. In insects it was shown to participate in both stimulating and repressing activities in regulation of muscle activity and of certain glands (Ffrench-Constant *et al*., 1993; Watanabe *et al*., 2002). It is possible that GABA plays a role in plant signalling as well, comparable to its role in animals. Infection of *A. thaliana* with *B. cinerea* not only lead to an increase in levels of known metabolites, but also induced accumulation of so far unidentified substances (Table 2). A few of these metabolites, namely "unknown 3", "unknown 9", and "unknown 13" (Figure 34) showed very high fold changes of accumulation, from barely detectable in mock-treated plants to comparatively high amounts in infected plants, and were not present in plants after infection with other pathogens analysed (Table 5).

After establishing 3 dpi –when plants show distinct lesions, but leaves are not macerated yet– as the most suitable time point for further experiments, metabolite analyses in Col-0 and a set of *Arabidopsis* mutants impaired in different signalling or biosynthesis pathways were conducted (Figure 35). No SA-accumulation in infected leaves was observed in Col-0, *ald1*, the phytoalexin-deficient *pad2* and *pad3*, the ethylene receptor mutant *etr1-1*, and also not in *sid2* (Figure 35 A). A slight increase in SA-levels exhibited the JA-insensitive *coi1* mutant and in *fmo1* a considerable increase was found for SA. The ethylene insensitive mutant *ein2-1* displayed four times more SA than Col-0 in mock-treated leaves and showed a decrease in SA-levels upon infection with *B. cinerea*. Previously, EIN3, in combination with EIL1, was shown to negatively regulate SA-biosynthesis by repressing *SID2* expression, and the *ein3-1 eil1-1* double mutant was also shown to constitutively accumulate SA in the absence of *Psm* (Chen *et al*., 2009). As *ein2-1* also accumulated high SA-amounts in the absence of *B. cinerea*, a similar role might be possible for this gene in the interaction of plants with necrotrophs. Camalexin accumulated to moderate levels in Col-0, *ald1, etr1-1*, and in *ein2-1* (Figure 35 B). No camalexin accumulation was observed for *coi1,* as well as for *pad2* and *pad3*, and significantly higher camalexin levels were quantified in *fmo1* and *sid2*. It was quite surprising to find camalexin not accumulating in *coi1* upon *Botrytis*-infection, as this mutant was not described as lacking camalexin before and *PAD3*-expression was found to be not impaired by *coi1*, resulting in *PAD3* expression being independent of JA-signalling in the *Arabidopsis-Botrytis* interaction (Ferrari *et al*., 2007). The ability of *coi1* to synthesize camalexin upon *Botrytis*-infection will have to be verified in future experiments. Analysis of Pip-accumulation yielded comparatively low increases in Col-0, *fmo1, pad2, pad3*, and *sid2*, and none in the Pip-biosynthesis mutant *ald1* (Figure 35 C). Interestingly, moderate to strong

Pip-accumulation was observed in *coi1*, *etr1-1* and *ein2-1* (Figure 35 C). This strong increase in Pip-levels in *coi1, etr1-1*, and especially in *ein2-1* after infection with *Botrytis* hint at negative regulation of Pip-biosynthesis by the ET/JA-signalling pathway. It was shown before that for expression of the *Botrytis*-induced defensin gene *PDF1.2* the functional components of ET-signalling, *EIN2* and *ETR1*, and JA-signalling, *COI1*, are needed and that those two pathways have to be activated in combination for successful induction of *PDF1.2* expression (Penninckx *et al*., 1998; Thomma *et al*., 1999). It is possible that a similar, possibly repressive, mechanism exists for regulation of Pip-function in *Arabidopsis* interactions with necrotrophic fungi. Basal levels for Pip were found to be quite high in the time course experiment and comparable to levels found in *B. cinerea*-infected leaves in the metabolite profliling using mutant lines. These are conflicting results and one logical explanation for these differences between the two experiments might lie in experimental conditions after infection. It is possible that the spore distribution on leaves later harvested for amino acid analysis was not as uniform as on leaves harvested for analysis of SA and camalexin. Furthermore, too little humidity might impair growth of the fungus, which needs very high air humidity to grow and proliferate on *Arabidopsis* and this high air humidity might influence Pip-levels in control plants. No significant differences in accumulation of GABA and Orn between Col-0 and mutant lines became apparent upon metabolite analysis (Figure 35 D; Figure 35 E), the conclusion being that GABA- and Orn-accumulation after *Botrytis*-infection are not regulated by Pip, JA, ET, or SA. As described above, possible roles for GABA-involvement in the interaction between plants and necrotrophs involve retaining viability of cells surrounding infected tissue, as well as participating in plant signalling. Orn can be decarboxylated by a Orn decarboxylase to form the polyamine putrescine, which in turn serves as precursor for other polyamines like spermine or spermidine (Zeier, 2013). Polyamines play a role in regulation of ROS-production in pathogen-challenged plants and were also shown to be able to induce ROS-production when applied exogenously. Production of ROS, followed by HR-induced cell death, is a strategy used by *B. cinerea* to facilitate infection. It was shown that the degree of *B. cinerea*-pathogenecity directly correlated with the level of ROS-production and that the fungus actively triggers a HR to aggravate infection (Govrin and Levine, 2000). Induction of Orn-accumulation and following conversion of the amino acid to polyamines to trigger ROS-production might be one way for *B. cinerea* to achieve facilitation of infection. The unknown compound 13 showed moderate accumulation after *B. cinerea*-infection in Col-0, *ald1, fmo1, pad2,* and *sid2* (Figure 35 F), was strongly reduced in *ein2-1* and not detectable in *coi1, etr1-1*, and *pad3*. This substance seems to be a very specific metabolite, as it was only detected in *B. cinerea*-infected plants (Table 5). From this metabolite being missing in *coi1* and *etr1-1* and greatly reduced in *ein2-1*, the conclusion can be drawn that the JA- and ET-signalling pathways, each alone or a

combination of both, might be required for biosynthesis of this compound. A most important step for elucidating the role of this compound in resistance of *Arabidopsis* to *B. cinerea* will be the identification and characterisation of this compound. After achieving substance identification, it would be very interesting to find out more about its chemical and physical properties and its ability to chemically induce resistance against *B. cinerea* in plants, as already demonstrated for a number of other amino acids (e.g. BABA).

7.6 Pip induces resistance against *B. cinerea* in Col-0 and *ald1*, but exacerbates disease in *sid2* and *coi1*

One of the substances shown to induce resistance against *B. cinerea* in *Arabidopsis* is the non-protein amino acid BABA, which does not occur naturally in *A. thaliana*. This amino acid induced resistance against different types of pathogens by enhancing plant resistance mechanisms and induction of priming (Zimmerli *et al*., 2001; Ton *et al*., 2005). We were able to demonstrate that BABA-IR against the bacterial pathogen *Psm* depends actually on Pip-activity, as firstly, both BABA and Pip can induce resistance, secondly, BABA did not induce resistance in *ald1*, and thirdly, a combination of BABA and Pip did not show additional effects (Návarová *et al*., 2012). As a considerable accumulation of Pip in *Botrytis*-infected plants was detected, the next step was to test whether Pip can induce resistance to the fungus (Figure 36; Figure 37). Defence against *B. cinerea* was induced by exogenously applied Pip in Col-0 and *ald1,* as could be determined by a reduction in lesion size in Pip-treated plants. No difference in water- and Pip-treated plants was observed in *ein2-1, etr1-1*, *fmo1, pad2,* and *pad3*. In *coi1* and *sid2* an aggravation of disease symptoms was seen, which was particularly grave for *sid2* (Figure 36). The SA-biosynthesis mutant *sid2-2* was previously shown to be less susceptible to infection with *Botrytis* (Ferrari *et al*., 2003) and the same holds true for *sid2-1* used in the experiments presented in this work. Water-treated *sid2-1* plants showed a very strong resistance phenotype with barely any visible lesions at 3 days post *B. cinerea*-infection. Pretreating plants with Pip, however, lead to enhanced susceptibility of *sid2* towards the fungus with development of large lesions culminating in the complete destruction of the leaf. The ICS1-mediated SA-biosynthesis was shown to be inducible by pathogen infection (Wildermuth *et al*., 2001), but another possible way for SA-biosynthesis is the often discussed phenylalanine ammonia-lyase (PAL-) pathway, which was thought to be the primary SA-biosynthesis pathway for a long time (Lee *et al*., 1995). It might be possible that Pip induces the PAL-pathway for SA-accumulation (Ferrari *et al*., 2003), but this seems highly unlikely, as no SA-accumulation was detected in Pip-treated *sid2* plants (data not shown). Gene expression of *GRXS13,* encoding a glutaredoxin, was shown to be induced by *Botrytis*-infection and is necessary for optimal infection of plants by the fungus (La Camera *et al.,* 2011). *GRXS13* can not only be induced by SA, but also by Pip (data not shown), which

might explain the observed symptoms in *sid2* as no SA-accumulation was observed. Comparable to other signalling molecules, Pip might not only be able to activate gene expression, but also to repress the expression of some genes. It was shown that *B. cinerea* secretes small RNAs into the plant to hijack the RNAi-system and selectively silence host immunity-related genes (Weiberg *et al*., 2013). The observed phenotype of disease aggravation in Pip-treated *sid2* plants might be the result of additive effects in disturbed signalling. A similar induction of susceptibilty by Pip was observed for *coi1*, which showed strong leaf maceration in Pip-treated and *B. cinerea*-infected leaves (Figure 36). The reason for this observation might be that in Pip-treated and *Botrytis*-infected *coi1* plants a strong accumulation of SA was detected (data not shown), which enabled the fungus to use *GRXS13* to aggaravate infection as described above. In future experiments the data gathered so far will have to be verified. To be able to get a more uniform infection of *Arabidopsis* leaves, the spore solution could be sprayed on the leaves instead of putting droplets onto the leaf surface and disease symptoms additionally analysed by TB-staining of infected leaves. Also, growth conditions for the fungus on agar plates will have to be optimized, as there were several experiments for which not enough spores could be obtained, making it impossible to carry out planned experiments. Additionally to metabolite and disease symptom studies, the analysis of gene expression (*ALD1, FMO1, GRXS13, PDF1.2, MPK3, MPK6*, others) would enable us to get an even better picture of the mechanism behind *B. cinerea*-infection of *A. thaliana*.

7.7 Changes in metabolite composition of *A. thaliana* plants infected with a virulent and an avirulent isolate of *Hpa*

In comparison to interactions of *Arabidopsis* with nectrophic (*B. cinerea*) and hemibiotrophic (*Psm*) pathogens, two obligate biotrophs were chosen to study interactions between plants and specialized biotrophic pathogens: the downy mildew oomycete *Hyaloperonospora arabidopsidis* and the powdery mildew fungus *Golovinomyces orontii* (7.10). Resistance in *A. thaliana* against *Hpa* is conferred by products of *RPP* (*RESISTANCE TO PERONOSPORA PARASITICA*) genes, cytoplasmatically localized proteins of the CC:NB:LRR (coiled-coil:nucleotide-binding:leucine rich repeat) class that are very diverse in the LRR domain (Allen *et al*., 2004; Nemri *et al*., 2010). This interaction is also characterised by accumulation of the defence metabolites SA and camalexin (Nawrath and Métraux, 1999). The first step in the studies of the *Arabidopsis*-interaction with *Hpa* was analysis of metabolite accumulation (Figure 38). As described before, SA accumulated to moderate levels in Col-0, *ald1* and *fmo1*, and only very slightly in *sid2* and the *sid2 ald1* double mutant after infection with the virulent *Hpa* Noco2 (Figure 38 A). Infection with *Hpa* Cala2, which is avirulent on Col-0, resulted in accumulation of approximately half the amount of SA than observed in the virulent

interaction. The tryptophan-derived phytoalexin camalexin accumulated in all analysed plant lines after *Hpa* Noco2-infection and, similarly to SA-accumulation, lower camalexin levels were observed after infection with the avirulent isolate. In *fmo1*, similar camalexin levels were detected in the virulent and the avirulent interaction (Figure 38 B). In *sid2* and *sid2 ald1*, on the other hand, *Hpa* Cala2-infection induced very strong camalexin accumulation (more than two-fold), comparable to levels detected in Ler-0 plants, which are susceptible to *Hpa* Cala2 (Figure 38 B). The strong response towards *Hpa* Cala2 shows that this avirulent oomycete induces stronger defence metabolite accumulation in *sid2* and *sid2 ald1* than in Col-0. A similar finding was published by Nawrath and Métraux in 1999, who reported higher camalexin levels in *sid2* plants inoculated with *Pst avrRpt2*. This finding demonstrates that biosynthesis of camalexin does not depend on SA, in contrast to priming of camalexin accumulation (Bernsdorff *et al*., submitted to The Plant Cell). Only a weak increase was found for the camalexin intermediate ICA, but a pattern similar to camalexin accumulation emerged (Figure 38 C). *A. thaliana* plants infected with this biotrophic oomycete demonstrated accumulation of an unknown compound, termed “unknown 28”, which was only detectable in this interaction (Figure 38 D; Table 2; Table 5). This substance was present in very low levels in uninfected leaves and increased approximately tenfold in leaves infected with the virulent *Hpa* Noco2, but not in *Hpa* Cala2-infected plants (Figure 38 D). Accumulation of “unknown 28” seems to be characteristic for the compatible interaction of *A. thaliana* with *Hpa*, as levels also increased in the interaction between the *Arabidopsis* ecotype Ler-0 and the *Hpa* isolate Cala2. Pip also accumulated to moderate levels in *Hpa* Noco2-infected, and to slightly lower levels in *Hpa* Cala2-infected, plants, respectively (Figure 38 E). In contrast to plants infected with the bacterium *Psm*, the amino acid Pro accumulated to very high levels in *Arabidopsis* infected with *Hpa* Noco2 (Figure 38 F), but showed no increasing levels after infection with the Cala2 isolate. This high Pro-accumulation is possibly a hallmark of the compatible plant-oomycete interaction comparable to increase in levels observed for “unknown 28”, as Pro was also found to accumulate to high levels in *Hpa* Cala2-infected Ler-0 plants. Accumulation of Pro was shown to be a typical response to osmotic stress, but Pro-levels were also found to increase upon infection of *Arabidopsis* with avirulent *Psm* strains (Fabro *et al*., 2004). The exact role of proline accumulation after infection of plants with virulent isolates of *Hpa* will have to be clarified in future experiments. Similarly to Pro-accumulation, increasing levels were detected for GABA and Orn after infection with the virulent *Hpa* Noco2, but not with the avirulent Cala2 (Figure 38 G; Figure 38 H). As described earlier, GABA plays a role in maintaining cell viability in the interaction with necrotrophs and is also a very important signalling molecule in mammals and insects. Accumulation of GABA was only observed in compatible interactions of *Arabidopsis* plants with *Hpa*. It is possible that this oomycete manipulates the plant´s C:N metabolism via

GABA to support its biotrophic lifestyle. It was shown before that *Hpa* introduces RXLR effectors into the cytoplasm to suppress PAMP-triggered immune responses and reprogram the host´s metabolism (Birch *et al*., 2006; Birch *et al*., 2008). These effectors all have the RXLR motif (Arg, any amino acid, Leu, Arg) in common and show a modular structure, with the N-terminus involved in secretion and host translocation of the effector protein and the C-terminus responsible for modulation of host defences inside plant cells (Win *et al*., 2007). Manipulation of the C:N metabolism by a pathogen was already observed for the interaction between *A. thaliana* and the powdery mildew *Golovinomyces cichoracearum* (Fabro *et al*., 2008) and might be a feature of highly specialized biotrophs. The accumulation of Orn after *Hpa*-infection is possibly connected to increasing levels observed for Pro, as Orn can function as a precursor for proline production (Zeier, 2013).

7.8 Pip-IR against *Hpa* is dependent on FMO1 and SA-accumulation

Pip was shown to induce resistance against the hemibiotrophic bacterial pathogen *Psm* (Návarová *et al*., 2012) and, as it also accumulated after infection with the biotrophic downy mildew pathogen *Hpa*, the next logical step was to test Pip-IR against a virulent (Figure 39; Figure 40; Figure 41) and an avirulent isolate of this oomycete (Figure 44; Figure 45). Analysis of TB-stained leaves showed strong growth of *Hpa* Noco2 on water treated Col-0 plants, with pervasion of leaves by hyphae and conidiophores as well as sexual oospores covering the leaf surface (Figure 40). Mutant lines for *ald1, fmo1*, *sid2, sid2 ald1, eds5, ics1 ics2,* and *npr1* were even more susceptible to *Hpa* Noco2, with major leaf areas covered in conidiophores and presence of sexual oospores on leaves (Figure 40). In Col-0, Pip-treatment greatly reduced disease symptoms, a large number of analysed leaves showed neither hyphal growth nor conidiophores present on the leaf surface, but clusters of cells that had undergone HR-induced cell death, the most effective defence against this biotrophic pathogen (Birch *et al*., 2006). This strong reduction of oomycete growth was not observed for mutant lines, which all showed hyphal growth and conidiophores on the leaf surface to some extent. Quantification of conidiospores at 7 dpi showed with significantly higher spore numbers enhanced susceptibility towards *Hpa* Noco2 in the analysed mutant lines compared to Col-0 (Figure 41). Treating plants with Pip 1 day prior to infection protected Col-0 effectively against this oomycete. To a lesser degree the Pip-deficient *ald1* and the SA-deficient *ics1 ics2* also showed enhanced resistance against *Hpa* after Pip-treatment. In *fmo1, sid2, sid2 ald1, eds5,* and *npr1* only a weak or no significant defence induction conferred by Pip was observed. As the mutant lines for *eds5, npr1*, and *ics1 ics2* were only used once in this kind of experiment so far, and because of the quite large standard deviations observed in this study, this experiment will have to be repeated to properly interpret the results. For now the conclusion can be drawn that resistance against *Hpa* is

strongly dependent on SA-accumulation, but seems to have a SA-independent component as well, as Pip was shown to slightly reduce spore numbers in *ics1 ics2*. However, the full Pip-induced defence response seems to require both SA-dependent and -independent processes, as well as amplification of Pip-production, as Pip-treated *ald1* plants did not show a full resistance response.

In addition to the virulent *Hpa* Noco2, Pip-induced resistance was also tested with the avirulent isolate Cala2 (Figure 44; Figure 45). In water- and Pip-treated plants of Col-0, *ald1*, and *eds5*, inoculation with *Hpa* Cala2 lead to the formation of HR-induced cell death, preventing oomycete growth and proliferation on the plant surface. In *fmo1, sid2,* and *sid2 ald1* plants exhibited different degrees of susceptibility towards *Hpa* Cala2, and disease symptoms were not significantly reduced by Pip-treatment, except in *sid2 ald1*. It was shown before that *sid2* is more susceptible to avirulent *Hpa* strains (Nawrath and Métraux, 1999; Bartsch *et al.,* 2006), but it was surprising to see a stronger resistance against *Hpa* Cala2 in *fmo1* than in *sid2*, as the mutation in *FMO1* was described as partially disabling *RPP2*-mediated resistance towards this isolate, making *fmo1* plants more susceptible than *sid2* (Bartsch *et al*., 2006). A decrease of resistance against *Hpa* Cala2 was observed in Pip-treated *ics1 ics2* and *npr1* plants, which showed a few spots of HR-induced cell death on water-treated leaves and hyphal growth followed by trailing necrosis in Pip-treated leaves. As those mutants were used in only one experiment with *Hpa* Cala2 so far, this result will have to be retested in future experiments. Future work should also include repetitions of the experiments presented in this work to verify the data obtained and enable a deeper understanding of the roles for SA, Pip, and the interplay between both in plant defence against this specialised biotroph. Additionally to analysis of disease symptoms, analysis of gene expression upon infection with virulent and avirulent *Hpa* isolates will have to be tested to get a better insight into the interaction between *A. thaliana* and this oomycete and how the large-scale manipulation of plant metabolism by the pathogen is executed. Furthermore, using a GUS-reporter line it was shown for the interaction between *A. thaliana* and the *Hpa* isolate Waco9 that the oomycete supresses *PR-1* expression in haustoriated cells, but not in non-invaded cells (Caillaud *et al*., 2013). A similar GUS-reporter line for *ALD1* might enable us to to elucidate if *Hpa* manipulates Pip-signalling in a similar way compared to SA-signalling.

7.9 Pip- and SA-dependency of *Psm*-induced SAR against *Hpa* Noco2

As previously reported (Nawrath and Métraux, 1999), *P. syringae*-induced SAR proved effective against *Hpa* Noco2 in Col-0. These results are strongly supported by those presented in this work: Analysis of the SAR response in Col-0 after first infection with *Psm* greatly reduced conidiospore numbers and showed growth and proliferation of the oomycete

on leaves to a much lower extent than observed in control plants (Figure 42; Figure 43). In mutant lines of *ald1, fmo1*, and *sid2* no SAR response was seen after quantification of spore numbers and a slight SAR response after analysis of TB-stained leaves. Microscopy analysis of TB-stained leaves was done in a qualitative manner, whereas the determination of conidiospores is a quantitative method, which could explain these differences in obtained results. To bypass this problem in future experiments, image-analysis supporting software like ImageJ or Photoshop could be used. Nevertheless, this study showed that comparably to SAR against *Psm*, Pip-production and amplification of the SAR signal conferred by Pip-mediated signalling to increase SA-levels in systemic leaves are essential for establishment of the SAR reaction against a virulent *Hpa* isolate. For further studies of broad spectrum-resistance conferred by SAR and the role of priming in this defence mechanism, the priming experiment could be done with *Psm* as the inducing pathogen and *Hpa* for the challenge infection. Analysis of gene expression and comparison to results presented in this thesis would give valuable insight into the SAR response and how it is regulated on the gene expression level.

7.10 Comparative metabolite profiling of *Arabidopsis* plants infected with the powdery mildew *G. orontii* focussing on Pip- and camalexin-accumulation in the early stages of infection

Infection of *Arabidopsis* with the biotrophic powdery mildew pathogen *Golovinomyces orontii* was studied as an additional example of a highly specialized interaction between a plant and a pathogen closely adapted to its host. Similar to studies on plant-pathogen interactions with *B. cinerea* and *Hpa*, changes in metabolite composition in *Arabidopsis* upon infection with *G. orontii* were analysed at different time points (4, 8, 24, 48, 72 hpi). It was reported previously that endogenous levels of SA and JA increase upon infection with powdery mildews (Fabro *et al*., 2008; Chandran *et al*., 2013), yet no significant increase in SA-levels was observed at chosen time points, except a slight increase at 72 hpi (Figure 46 A). Camalexin levels showed a moderate increase at 72 hpi (Figure 46 B) and Pip started to accumulate at 48 hpi, with an even stronger increase at 72 hpi (Figure 46 C). In general, metabolite levels were found to be very low and just a handful of metabolites increased upon infection with this fungus. The low levels of SA and camalexin for example, can be explained by only epidermal cells being affected by *G. orontii*. It is also possible that the chosen time points were too early in the infection cycle and more changes in metabolite composition would be observed at later stages of infection. This will have to be considered in future experiments with this powdery mildew. Treatment with exogenously applied SA was shown to enhance resistance against *G. orontii* in *Arabidopsis* by increasing expression of *RPW8* genes and subsequent HR-induced cell death, which limits the growth of the fungus (Xiao *et al*., 2003). The *Arabidopsis*

accession used for analysis of changes in metabolite accumulation was Col-0, which does not possess *RPW8* genes and exhibits susceptibility to *G. orontii*. This might be another reason why so little SA-accumulation was observed in this interaction. A compound found in comparatively high levels at all analysed time points was eicosanoic acid, a C_{20} fatty acid, which was described to be part of the *Arabidopsis* leaf cuticle composition (Franke *et al*., 2005). It is possible that this component of plant cuticles was brushed off heavily infected plants in the process of infecting fresh plants for this experiment, which might explain its presence in equal amounts at all analysed time points.

7.11 Lack of Pip-induced resistance against the powdery mildew *G. orontii*

It was possible to induce resistance in *A. thaliana* against *Psm, B. cinerea*, and *Hpa* by treating plants with exogenously applied Pip prior to infection. As Pip also showed moderate accumulation upon infection with *G. orontii*, it was tested if Pip can induce resistance against this fungus, too. The *G. orontii*-susceptible Col-0, as well as the mutant lines *ald1, fmo1, sid2, npr1, pad4, edr1, pen2 pad4 sag101*, and *gl1* were treated with either water or Pip one day prior to infection and disease symptoms were scored by analysing microcolony development on infected leaves (Figure 47). No difference between water- and Pip-treated plants was observed in Col-0, *ald1, fmo1, sid2*, and *gl1* plants, which showed similar levels of infection. In *npr1* and *pad4* a higher, but not significant, basal resistance to the powdery mildew was detected, which was compromised by pretreatment with Pip. *NPR1* and *PAD4* are important components for activation of resistance against *G. orontii* and are involved in SA-mediated signal amplification (Xiao *et al*., 2005). These results are in conflict with published results, as an enhanced susceptibility of *npr1* and *pad4* towards *G. orontii* was described previously. One possible reason for these results may lie in experimental conditions, as microscopy analysis of microcolonies can be prone to subjective errors. As a similar aggravation of symptoms was observed in Pip-treated *sid2* plants infected with *B. cinerea*, these findings may also hint at a very fine-tuned interaction of SA- and Pip-signalling in plant defence against fungal pathogens. Very high basal resistance to *G. orontii* was seen in *edr1*, in which pretreatment with Pip showed no changes in resistance. The *EDR1* gene encodes a conserved MAPKK kinase, which was described to act as a negative regulator of resistance against powdery mildews (Xiao *et al*., 2005). The triple mutant *pen2 pad4 sag101*, which is impaired in penetration resistance, as well as SA-signalling and regulation, exhibited very low basal resistance towards *G. orontii*, but was the only mutant line in which a significant resistance induction by exogenous Pip-treatment was observed. This finding shows that the first and foremost layer of defence against this powdery mildew pathogen is penetration resistance and all other defences affect post-penetration processes (Consonni *et*

al., 2006). In order to analyse the importance of *ALD1, FMO1*, and *SID2* in the plant-powdery mildew interaction, it would be necessary to generate mutant lines for these genes in the *pen2* background and repeat these studies.

7.12 The metabolic profile of *A. thaliana* depending on the lifestyle of the invading pathogen

Changes in metabolite accumulation after infection with different kinds of pathogens were compared to identify how differences in pathogenic lifestyles impact the metabolic profile of *A. thaliana* (Table 3; Table 4; Table 5). In the interaction between *Arabidopsis* and the hemibiotrophic bacterium *Psm*, levels of defence metabolites showed significant differences between mock- and pathogen-treated plants. Especially SA, Camalexin, ICA, Pip, and Lys accumulated to very high levels, as did aromatic amino acids and GABA. Infection with the necrotrophic fungus *B. cinerea* led to a significant increase of camalexin and ICA, as well as the yet unidentified substances 3, 9, and 13. Otherwise, metabolites levels showed fewer differences between mock- and pathogen-treated plants than in the *Arabidopsis-Psm* interaction. Analyses of interactions between plants and the oomycete *Hpa* and the fungus *G. orontii*, two pathogen species with a highly specialized lifestyle adapted to their host, show clear differences. Infection of *Arabidopsis* with the virulent *Hpa* Noco2 elicited moderate changes in metabolite composition, with a strong increase in camalexin and Aad levels and moderate increase in levels of assorted amino acids. Compared to these results, barely any changes were found in the interaction between *Arabidopsis* and the likewise biotrophic pathogen *G. orontii*. This powdery mildew induced moderate accumulation of camalexin and Pip, but scarcely changes in levels of other analysed substances. It is very important to note significant differences in infection protocols with these pathogens. While *Psm* bacteria are infiltrated into the apoplastic space, where they can multiply and get in close contact with a large number of cells, infection with spores of *B. cinerea, Hpa*, and *G. orontii* affects mainly epidermal cells. These differences in infection will have to be minimized in future experiments in order to get more comparable results. Nevertheless, these data distinctly show that the metabolite profile of *Arabidopsis thaliana* depends on the type of the attacking pathogen. While the metabolic profiles for plants infected with the hemibiotrophic bacterium *Psm* and the biotrophic oomycete *Hpa* were found to be quite similar, especially in the case of changes in amino acid accumulation, they differ markedly in plants infected with the fungi *B. cinerea* and *G. orontii,* which in turn were very different from each other. Moreover, accumulation of compounds very specific for each pathogen may point at differences in manipulation of the plant´s metabolism by each pathogen. Identification of the so far unknown compounds will give more insight into the origin of these substances and their role in infection by different types of microbes.

8 Conclusions and outlook

In this work it was shown that in *Arabidopsis thaliana*, a large number of genes primed for expression in the SAR response encode proteins that are mostly involved in defence metabolism, defence signalling and in cell wall-related processes. Furthermore, the defence-related genes *ALD1*, involved in Pip-biosynthesis, and *FMO1*, encoding a flavin-dependent monooxygenase required for Pip-induced resistance, were shown to be necessary for priming of gene expression. The role of *FMO1* in Pip-induced priming of gene expression and camalexin accumulation was shown to be essential, as these processes were not longer observed in the *fmo1* mutant line. In future experiments, the function of SA in priming can be further elucidated by studying priming of expression of a larger set of genes in the *sid2* and the *sid2 ald1* mutant lines. Another promising study would be a comparison of SAR-primed and Pip-primed gene expression to see if the same set of genes show primed expression or if there are differences. Moreover, a study of priming in gene expression on the whole genome level would give valuable insight of the extent of primed genes in the SAR reaction.

This thesis also provided evidence that MAPK signalling is not involved in SAR and defence priming to the extent previously described. Further studies to verify these results should include a repetition of the experiments presented and analysis of MAPK activity in plants exogenously treated with Pip. For studies concerning MAPK involvement in defence, the use of a broader range of *Pseudomonas syringae* strains might be advisable to see if the type of inducing pathogen might have an influence on MAPK signalling.

In studies with the necrotrophic fungus *Botrytis cinerea*, the biotrophic downy mildew oomycete *Hyaloperonospora arabidopsidis*, and the biotrophic powdery mildew fungus *Golovinomyces orontii,* evidence was provided that Pip not only accumulates in *A. thaliana* upon infection with these pathogens, but also that in the case of *B. cinerea* and *Hpa* exogenously applied Pip induces resistance against these microbes. Comparative metabolite profiling additionally provided a number of yet unknown compounds and highlighted specific patterns of metabolite accumulation for each interaction. In future experiments the focus should move to gene expression analysis in plants infected with these microbes. Another interesting angle would be a comparative analysis of primed gene expression in plants infected with *Psm*, *B. cinerea*, and *Hpa*.

9 Literature cited

Ahn, I.-P., Kim, S., Lee, Y.-H, and Suh, S.-C. (2007). Vitamin B1-Induced Priming Is Dependent on Hydrogen Peroxide and the *NPR1* Gene in Arabidopsis. Plant Physiol. **143:** 838–848.

Alabadi, D., Oyama, T., Yanovsky, M.J., Harmon, F.G., Más, P., and Kay, S.A. (2001). Reciprocal Regulation Between *TOC1* and *LHY*/*CCA1* Within the *Arabidopsis* Circadian Clock. Science **293:** 880-883.

Allen, R.L., Bittner-Eddy, P.D., Grenville-Briggs, L.J., Meitz, J.C., Rehmany, A.P., Rose, L.E., and Beynon, J.L. (2004). Host-Parasite Coevolutionary Conflict Between *Arabidopsis* and Downy Mildew. Science **306:** 1957-1960.

Amselem, J., Cuomo, C.A., van Kan, J.A.L., Viaud, M., Benito, E.P., Couloux, A., Coutinho, P.M., de Vries, R.P., Dyer, P.S., Fillinger, S., Fournier, E., Gout, L., Hahn, M., Kohn, L., Lapalu, N., Plummer, K.M., Pradier, J.-M., Quévillon, E., Sharon, A., Simon, A., ten Have, A., Tudzynski, B., Tudzynski, P., Wincker, P., Andrew, M., Anthouard, V., Beever, R.E., Beffa, R., Benoit, I., Bouzid, O., Brault, B., Chen, Z., Choquer, M., Collémare, J., Cotton, P., Danchin, E.G., Da Silva, C., Gautier, A., Giraud, C., Giraud, T., Gonzalez, C., Grossetete, S., Güldener, U., Henrissat, B., Howlett, B.J., Kodira, C., Kretschmer, M., Lappartient, A., Leroch, M., Levis, C., Mauceli, E., Neuvéglise, C., Oeser, B., Pearson, M., Poulain, J., Poussereau, N., Quesneville, H., Rascle, C., Schumacher, J., Ségurens, B., Sexton, A., Silva, E., Sirven, C., Soanes, D.M., Talbot, N.J., Templeton, M., Yandava, C., Yarden, O., Zeng, Q., Rollins, J.A., Lebrun, M.-H., and Dickman, M. (2011). Genomic Analysis of the Necrotrophic Fungal Pathogens *Sclerotinia sclerotiorum* and *Botrytis cinerea.* PLOS Genetics **7:** 1-27.

Anderson, J.C., Wan, Y., Kim, Y.-M., Pasa-Tolic, L., Metz, T.O., and Peck, S.C. (2014). Decreased abundance of type III secretion system-inducing signals in Arabidopsis mkp1 enhances resistance against Pseudomonas syringae. PNAS **111:** 6846–6851.

Asai, T., Tena, G., Plotnikova, J., Willmann, M.R., Chiu, W.L., Gomez-Gomez, L., Boller, T., Ausubel, F.M., and Sheen, J. (2002). MAP kinase signalling cascade in *Arabidopsis* innate immunity. Nature **415:** 977-983.

Attaran, E., Zeier, T.E., Griebel, T., and Zeier, J. (2009). Methyl Salicylate Production and Jasmonate Signaling Are Not Essential for Systemic Acquired Resistance in *Arabidopsis.* The Plant Cell **21:** 954–971.

Axtell, M.J. and Staskawicz, B.J. (2003). Initiation of *RPS2*-Specified Disease Resistance in *Arabidopsis* Is Coupled to the AvrRpt2-Directed Elimination of RIN4. Cell **112:** 369–377.

Bartsch, M., Gobbato, E., Bednarek, P., Debey, S., Schultze, J.L., Bautor, J., and Parker, J.E. (2006). Salicylic Acid–Independent ENHANCED DISEASE SUSCEPTIBILITY1 Signaling in *Arabidopsis* Immunity and Cell Death Is Regulated by the Monooxygenase *FMO1* and the Nudix Hydrolase *NUDT7.* The Plant Cell **18:** 1038–1051.

Baulcombe, D. (2013). Small RNA—the Secret of Noble Rot. Science **342:** 45-46.

Baxter, L., Tripathy, S., Ishaque, N., Boot, N., Cabral, A., Kemen, E., Thines, M., Ah-Fong, A., Anderson, R., Badejoko, W., Bittner-Eddy, P., Boore, J.L., Chibucos, M.C., Coates, M., Dehal, P., Delehaunty, K., Dong, S., Downton, P., Dumas, B., Fabro, G., Fronick, C., Fuerstenberg, S.I., Fulton, L., Gaulin, E., Govers, F., Hughes, L., Humphray, S., Jiang, R.H.Y., Judelson, H., Kamoun, S., Kyung, K., Meijer, H., Minx, P., Morris, P., Nelson, J., Phuntumart, V., Qutob, D., Rehmany, A., Rougon-Cardoso, A., Ryden, P., Torto-Alalibo, T., Studholme, D., Wang, Y., Win, J., Wood, J., Clifton, S.W., Rogers, J., Van den Ackerveken, G., Jones, J.D.G., McDowell, J.M., Beynon, J., and Tyler, B.M. (2010). Signatures of adaptation to obligate biotrophy in the *Hyaloperonospora arabidopsidis* genome. Science **330:** 1549–1551.

Beckers, G. J.M., Jaskiewicz, M., Liu, Y., Underwood, W.R., He, S.Y., Zhang, S., and Conrath, U. (2009). Mitogen-Activated Protein Kinases 3 and 6 Are Required for Full Priming of Stress Responses in *Arabidopsis thaliana*. The Plant Cell **21:** 944–953.

Bednarek, P., Piślewska-Bednarek, M., Svatoš, A., Schneider, B., Doubský, J., Mansurova, M., Humphry, M., Consonni, C., Panstruga, R., Sanchez-Vallet, A., Molina, A., and Paul Schulze-Lefert, P. (2009). A Glucosinolate Metabolism Pathway in Living Plant Cells Mediates Broad-Spectrum Antifungal Defense. Science **323:** 101-106.

Bender, C.L., Alarcón-Chaidez, F., and Gross, D. (1999). *Pseudomonas syringae* Phytotoxins: Mode of Action, Regulation, and Biosynthesis by Peptide and Polyketide Synthetases. MICROBIOLOGY AND MOLECULAR BIOLOGY REVIEWS **63:** 266–292.

Birch, P.R.J., Rehmany, A.P., Pritchard, L., Kamoun, S., and Beynon, J.L. (2006). Trafficking arms: oomycete effectors enter host plant cells. TRENDS in Microbiology **14:** 8-11.

Birch, P.R.J., Boevink, P.C., Gilroy, E.M., Hein, I., Pritchard, L., and Whisson, S.C. (2008). Oomycete RXLR effectors: delivery, functional redundancy and durable disease resistance. Current Opinion in Plant Biology **11:** 373–379.

Block, A., Toruño, T.Y., Elowsky, C.G., Zhang, C., Steinbrenner, J., Beynon, J., and Alfano, J.R. (2013). The *Pseudomonas syringae* type III effector HopD1 suppresses effector-triggered immunity, localizes to the endoplasmic reticulum, and targets the Arabidopsis transcription factor NTL9. New Phytologist **201:** 1358-1370.

Boller, T. and Felix, G. (2009). A Renaissance of Elicitors: Perception of Microbe-Associated Molecular Patterns and Danger Signals by Pattern-Recognition Receptors. Annu. Rev. Plant Biol. **60:** 379–406.

Böttcher, C., Chapman, A., Fellermeier, F., Choudhary, M., Scheel, D., and Glawischnig, E. (2014). The biosynthetic pathway of indole-3-carbaldehyde and indole-3-carboxylic acid derivatives in *Arabidopsis thaliana*. Plant Physiol. **165:** 841-853.

Bradford, M. M. (1976). A rapid and sensitive method for the quantitation of microgram quantities of protein utilizing the principle of protein - dye binding. Analytical Biochemistry **72:** 248 – 254.

Bruce, T.J.A., Matthes, M.C., Napier, J.A., and Pickett, J.A. (2007) Stressful ‘‘memories’’ of plants: Evidence and possible mechanisms. Plant Science **173:** 603–608.

Caillaud, M.-C., Asai, S., Rallapalli, G., Piquerez, S., Fabro, G., and Jones, J.D.G. (2013). A Downy Mildew Effector Attenuates Salicylic Acid–Triggered Immunity in Arabidopsis by Interacting with the Host Mediator Complex. PLoS Biol **11:** e1001732.

Cashman, J.R. (2004). The implications of polymorphisms in mammalian flavin-containing monooxygenases in drug discovery and development. Drug Discov. Today, **9:** 574–581.

Chandran, D., Rickert, J., Cherk, C., Dotson, B.R., and Wildermuth, M.C. (2013). Host Cell Ploidy Underlying the Fungal Feeding Site Is a Determinant of Powdery Mildew Growth and Reproduction. MPMI **26:** 537–545.

Chen, H., Xue, L., Chintamanani, S., Germain, H., Lin, H., Cui, H., Cai, R., Zuo, J., Tang, X., Li, X., Guo, H., and Zhou, J.-M. (2009). ETHYLENE INSENSITIVE3 and ETHYLENE INSENSITIVE3-LIKE1 Repress *SALICYLIC ACID INDUCTION DEFICIENT2* Expression to Negatively Regulate Plant Innate Immunity in *Arabidopsis.* The Plant Cell **21:** 2527–2540.

Chester, K.S. (1933). The problem of acquired physiological immunity in plants. Q. Rev. Biol. **8:** 275–324.

Chinchilla, D., Bauer, Z., Regenass, M., Boller, T., and Felix, G. (2006). The Arabidopsis Receptor Kinase FLS2 Binds flg22 and Determines the Specificity of Flagellin Perception. The Plant Cell **18:** 465–476.

Chinchilla, D., Zipfel, C., Robatzek, S., Kemmerling, B., Nürnberger, T., Jones, J.D.G., Felix, G., and Boller, T. (2007). A flagellin-induced complex of the receptor FLS2 and BAK1 initiates plant defence. Nature **448:** 497-501.

Coates, M.E. and Beynon, J.L. (2010). *Hyaloperonospora arabidopsidis* as a Pathogen Model. Annu. Rev. Phytopathol. **48:** 329–45.

Cohen, Y.R. (2002). β-Aminobutyric Acid-Induced Resistance Against Plant Pathogens. Plant Disease **68:** 448-457.

Conrath, U., Pieterse, C.M.J., and Mauch-Mani, B. (2001). Priming in plant–pathogen interactions. TRENDS in Plant Science **7:** 210-216.

Conrath, U. (2011). Molecular aspects of defence priming. TRENDS in Plant Science **16:** 524-531.

Consonni, C., Humphry, M.E., Hartmann, H.A., Livaja, M., Durner, J., Westphal, L., Vogel, J., Lipka, V., Kemmerling, B., Schulze-Lefert, P., Somerville, S.C., and Panstruga, R. (2006). Conserved requirement for a plant host cell protein in powdery mildew pathogenesis. Nature Genetics **38:** 716-720.

Cui, F., Wu, S., Sun, W., Coaker, G., Kunkel, B., He, P., and Shan, L. (2013). The *Pseudomonas syringae* Type III Effector AvrRpt2 Promotes Pathogen Virulence via Stimulating Arabidopsis Auxin/Indole Acetic Acid Protein Turnover. Plant Physiology **162:** 1018–1029.

Czechowski, T., Stitt, M., Altmann, T., Udvardi, M.K., and Scheible, W.R. (2005). Genome-Wide Identification and Testing of Superior Reference Genes for Transcript Normalization in Arabidopsis. Plant Physiology **139:** 5–17.

Da Cunha, L., McFall, A.J., and Mackey, D. (2006). Innate immunity in plants: a continuum of layered defenses. Microbes and Infection **8:** 1372-1381.

Dempsey, D.A., Vlot, A.C., Wildermuth, M.C., and Klessig, D.F. (2011). Salicylic Acid Biosynthesis and Metabolism. The Arabidopsis Book 1-24.

Durrant, W.E. and Dong, X. (2004). Systemic Acquired Resistance. Annu. Rev. Phytopathol. **42:**185–209.

Eastmond, P.J., Li, Y., and Graham, I.A. (2003). Is trehalose-6-phosphate a regulator of sugar metabolism in plants? Journal of Experimental Botany **54:** 533-537.

Eberharter, A. and Becker, P.B. (2002). Histone acetylation: a switch between repressive and permissive chromatin. EMBO reports **3:** 224-229.

Ellinger, D., Naumann, M., Falter, C., Zwikowics, C., Jamrow, T., Manisseri, C., Somerville, S.C., and Voigt, C.A. (2013). Elevated Early Callose Deposition Results in Complete Penetration Resistance to Powdery Mildew in Arabidopsis. Plant Physiology **161:** 1433–1444.

Ellis, C., and Turner, J. G. (2001). The *Arabidopsis* mutant *cev1* has constitutively active jasmonate and ethylene signal pathways and enhanced resistance to pathogens. Plant Cell **13:** 1025-1033.

Fabro, G., Kovács, I., Pavet, V., Szabados, L., and Alvarez, M. (2004). Proline Accumulation and *AtP5CS2* Gene Activation Are Induced by Plant-Pathogen Incompatible Interactions in *Arabidopsis.* MPMI **17:** 343–350.

Fabro, G., Di Rienzo, J.A., Voigt, C.A., Savchenko, T., Dehesh, K., Somerville, S., and Alvarez, M.E. (2008). Genome-Wide Expression Profiling Arabidopsis at the Stage of *Golovinomyces cichoracearum* Haustorium Formation. Plant Physiology **146:** 1421–1439.

Fan, J., Crooks, C., and Lamb, C. (2008). High-throughput quantitative luminescence assay of the growth in planta of *Pseudomonas syringae* chromosomally tagged with *Photorhabdus luminescens* luxCDABE. The Plant Journal **53:** 393–399.

Ffrench-Constant, R.H., Rocheleau, T.A., Steichen, J.C., and Chalmers, A.E. (1993). A point mutation in a *Drosophila* GABA receptor confers insecticide resistance. *Nature* **363:** 449 – 451.

Ferrari, S., Plotnikova, J.M., De Lorenzo, G., and Ausubel, F. (2003). *Arabidopsis* local resistance to *Botrytis cinerea* involves salicylic acid and camalexin and requires *EDS4* and *PAD2*, but not *SID2, EDS5* or *PAD4.* The Plant Journal **35:** 193-205.

Ferrari, S., Galletti, R., Denoux, C., De Lorenzo, G., Ausubel, F.M., and Dewdney, J. (2007). Resistance to *Botrytis cinerea* Induced in Arabidopsis by Elicitors Is Independent of Salicylic Acid, Ethylene, or Jasmonate Signaling But Requires *PHYTOALEXIN DEFICIENT3.* Plant Physiol. **144:** 367–379.

Feys, B.J., Moisan, L.J., Newman, MA., and Parker, J.E. (2001). Direct interaction between the *Arabidopsis* disease resistance signaling proteins, EDS1 and PAD4. EMBO J. **20:** 5400–11.

Flor, H.H. (1942). Inheritance of pathogenicity in Melampsora lini. Phytopathology **32:** 653–69.

Franke, R., Briesen, I., Wojciechowski, T., Faust, A., Yephremov, A., Nawrath, C., and Schreiber, L. (2005). Apoplastic polyesters in *Arabidopsis* surface tissues – A typical suberin and a particular cutin. Phytochemistry **66:** 2643–2658.

Frye, C.A. and Innes, R.W. (1998). An *Arabidopsis* Mutant with Enhanced Resistance to Powdery Mildew. The Plant Cell **10:** 947–956.

Fu, Z.Q., Yan, S., Saleh, A., Wang, W., Ruble, J., Oka, N., Mohan, R., Spoel, S.H., Tada, Y., Zheng, N., and Dong, X. (2012). NPR3 and NPR4 are receptors for the immune signal salicylic acid in plants. Nature **486:** 228-233.

Glawischnig, E. (2007). Molecules of interest-Camalexin. Phytochemistry **68:** 401–406.

Glazebrook, J. and Ausubel, F.M. (1994). Isolation of phytoalexin-deficient mutants of *Arabidopsis thaliana* and characterization of their interactions with bacterial pathogens. PNAS **91:** 8955-8959.

Glazebrook, J. (2005). Contrasting Mechanisms of Defense against Biotrophic and Necrotrophic Pathogens. Annu. Rev. Phytopathol. **43:** 205–227.

Gómez-Gómez, L. and Boller, T. (2000). FLS2: An LRR Receptor–like Kinase Involved in the Perception of the Bacterial Elicitor Flagellin in Arabidopsis. Molecular Cell **5:** 1003–1011.

Govrin, E.M. and Levine, A. (2000). The hypersensitive response facilitates plant infection by the necrotrophic pathogen *Botrytis cinerea.* Current Biology **10:** 751–757.

Govrin, E.M. and Levine, A. (2002). Infection of *Arabidopsis* with a necrotrophic pathogen, *Botrytis cinerea*, elicits various defense responses but does not induce systemic acquired resistance (SAR). *Plant Molecular Biology* **48:** 267–276.

Gruner, K., Griebel, T., Návarová, H., Attaran, E., and Zeier, J. (2013). Reprogramming of plants during systemic acquired resistance. Frontiers in Plant Science **4:** 1-28.

Gu, Y. Q., Wildermuth, M. C., Chakravarthy, S., Loh, Y. T., Yang, C., He, X., Han, Y., and Martin, G. B. (2002). Tomato transcription factors Pti4, Pti5, and Pti6 activate defense responses in *Arabidopsis*. Plant Cell **14:** 817-831.

Gupta, V., Willits, M.G., and Glazebrook, J. (2000). *Arabidopsis thaliana EDS4* Contributes to Salicylic Acid (SA)-Dependent Expression of Defense Responses: Evidence for Inhibition of Jasmonic Acid Signaling by SA. MPMI **13:** 503-511.

Hamel, L.P., Nicole, M.C., Sritubtim, S., Morency, M.J., Ellis, M., Ehlting, J., Beaudoin, N., Barbazuk, B., Klessig, D., Lee, J., Martin, G., Mundy, J., Ohashi, Y., Scheel, D., Sheen, J., Xing, T., Zhang, S., Seguin, A., and Ellis, B.E. (2006). Ancient signals: comparative genomics of plant MAPK and MAPKK gene families. Trends Plant Sci. **11:** 192-98.

Hansjakob, A., Riederer, M., and Hildebrandt, U. (2011). Wax matters: absence of very-long-chain aldehydes from the leaf cuticular wax of the *glossy11* mutant of maize compromises the prepenetration processes of *Blumeria graminis. Plant Pathology* **60:** 1151–1161.

Heese, A., Hann, D.R., Gimenez-Ibanez, S., Jones, A.M.E., He, K., Li, J., Schroeder, J.I., Peck, S.C., and Rathjen, J.P. (2007). The receptor-like kinase SERK3/BAK1 is a central regulator of innate immunity in plants. PNAS **104:** 12217–12222.

Ichimura, K., Shinozakia, K., Tena, G., Sheen, J., Henry, Y., Champion, A., Kreis, M., Zhang, S., Hirt, H., Wilson, C., Heberle-Bors, E., Ellis, B.E., Morris, P.C., Innes, R.W., Ecker, J.R., Scheel, D., Klessig, D.F., Machida, Y., Mundy, J., Ohashi, Y., and Walker, J.C. (2002). Mitogen-activated protein kinase cascades in plants: a new nomenclature. Trends Plant Sci. **7:** 301–8.

Jaskiewicz, M., Conrath, U., and Peterhänsel, C. (2011). Chromatin modification acts as a memory for systemic acquired resistance in the plant stress response. EMBO reports **12:** 50-55.

Jirage, D., Tootle, T.L., Reuber, T.L., Frost, L.N., Feys, B.J., Parker, J.E., Ausubel, F.M., and Glazebrook, J. (1999). *Arabidopsis thaliana PAD4* encodes a lipase-like gene that is important for salicylic acid signaling. PNAS **96:** 13583–13588.

Jones, J.D.G. and Dangl, J.L. (2006). The plant immune system. Nature **444:** 323-329.

Jung, H.W., Tschaplinski, T.J., Wang, L., Glazebrook, J., and Greenberg, J.T. (2009). Priming in Systemic Plant Immunity. Science **324:** 89-91.

Katsir, L., Schilmiller, A.L., Staswick, P.E., He, S.Y., and Howe, G.A. (2008). COI1 is a critical component of a receptor for jasmonate and the bacterial virulence factor coronatine. PNAS **105:** 7100–7105.

Kauss, H., Theisingerhinkel, E., Mindermann, R., and Conrath, U. (1992). Dichloroisonicotinic and salicylic acid, inducers of systemic acquired resistance, enhance fungal elicitor responses in parsley cells. Plant J. **2:** 655–60.

Kauss, H., Franke, R., Krause, K., Conrath, U., Jeblick, W., Grimmig, B., and Matern, U. (1993) Conditioning of parsley (*Petroselinum crispum* L.) suspension cells increases elicitor-induced incorporation of cell wall phenolics. Plant Physiol **102:** 459–466.

Kauss, H. and Jeblick, W. (1995). Pretreatment of parsley suspension cultures with salicylic acid enhances spontaneous and elicited production of H_2O_2. Plant Physiol **108:** 1171–1178.

Keogh, R. C., Deverall, B. J., and McLeod, S. (1980). Comparison of Histological and Physiological Responses to *Phakopsora pachyrhizi* in Resistant and Susceptible Soybean. Trans. Br, mycol, Soc. **74:** 329-333.

Kessmann, H., Staub, T., Hofmann, C., Maetzke, T., and Herzog, J. (1994). Induction of Systemic Acquired Disease Resistance in Plants by Chemicals. Annu. Rev. Phytopathol. **32:** 439-459.

King, E.O., Ward, M.K., Raney, D.E. (1954). Two simple media for the demonstration of pyocyanin and fluorescin. J. Lab. Clin. Med. **44:** 301-307.

Koch, M., Vorwerk, S., Masur, C., Sharifi-Sirchi, G., Olivieri, N., and Schlaich, N.L. (2006). A role for a flavin-containing mono-oxygenase in resistance against microbial pathogens in *Arabidopsis*. The Plant Journal **47:** 629–639.

Koo, A.J.K., Gao, X., Jones, A.D., and Howe, G.A. (2009). A rapid wound signal activates the systemic synthesis of bioactive jasmonates in Arabidopsis. The Plant Journal **59:** 974–986.

Koorneef, A. and Pieterse, C.M.J. (2008). Cross Talk in Defense Signaling. Plant Physiology **146:** 839–844.

Kuc, J., Williams, E. B., and Shay, J. R. (1957). Increase of resistance to apple scab following injection of host with phenylthiourea and Dphenylalanine. (Abstr.) Phytopathology **47:** 21-22.

Kuc, J., Barnes, E., Daftsios, A., and Williams, E. B. (1959). The effect of amino acids on susceptibility of apple varieties to scab. Phytopathology **49:** 313-315.

Kugler, F., Graneis, S., Schreiter, P.P.Y., Stintzing, F., and Carle, R. (2006). Determination of Free Amino Compounds in Betalainic Fruits and Vegetables by Gas Chromatography with Flame Ionization and Mass Spectrometric Detection. J. Agric. Food Chem. **54:** 4311-4318.

La Camera, S., L'Haridon, F., Astier, J., Zander, M., Abou-Mansour, E., Page, G., Thurow, C., Wendehenne, D., Gatz, C., Métraux, J.-P., and Lamotte, O. (2011). The glutaredoxin ATGRXS13 is required to facilitate *Botrytis cinerea* infection of *Arabidopsis thaliana* plants. The Plant Journal **68:** 507–519.

Lawton, M.P., Cashman, J.R, Cresteil, T., Dolphin, C.T., Elfarra, A.A., Hines, R.N., Hodgson, E., Kimura T., Ozols J. and Phillips I.R. (1994). A nomenclature for the mammalian flavin-containing monooxygenase gene family based on amino acid sequence identities. Arch. Biochem. Biophys. **308:** 254–257.

Lee, H.-I., Leon, J., and Raskin, I. (1995). Biosynthesis and metabolism of salicylic acid. PNAS **92:** 4076-4079.

Li, G., Froehlich, J.E., Elowsky, C., Msanne, J., Ostosh, A.C., Zhang, C., Awada, T., and Alfano, J.R. (2014). Distinct Pseudomonas type-III effectors use a cleavable transit peptide to target chloroplasts. The Plant Journal **77:** 310–321.

Lin, W., Li, B., Lu, D., Chen, S., Zhu, N., He, P., and Shan, L. (2014). Tyrosine phosphorylation of protein kinase complex BAK1/BIK1 mediates Arabidopsis innate immunity. PNAS **111:** 3632–3637.

Lipka, V., Dittgen, J., Bednarek, P., Bhat, R., Wiermer, M., Stein, M., Landtag, J., Brandt, W., Rosahl, S., Scheel, D., Llorente, F., Molina, A., Parker, J.E., Somerville, S., and Schulze-Lefert, P. (2005). Pre- and Postinvasion Defenses Both Contribute to Nonhost Resistance in *Arabidopsis*. Science **310:** 1180-1183.

Luo, J., Nishiyama, Y., Fuell, C., Taguchi, G., Elliott, K., Hill, L., Tanaka, Y., Kitayama, M., Yamazaki, M., Bailey, P., Parr, A., Michael, A.J., Saito, K., and Martin, C. (2007). Convergent evolution in the BAHD family of acyl transferases: identification and characterization of anthocyanin acyl transferases from *Arabidopsis thaliana.* The Plant Journal **50:** 678–695.

Luna, E., Bruce, T.J.A., Roberts, M.R., Flors, V., and Ton, J. (2012). Next-Generation Systemic Acquired Resistance. Plant Physiology **158:** 844–853.

Maor, R. and Shirasu, K. (2005). The arms race continues: battle strategies between plants and fungal pathogens. Current Opinion in Microbiology **8:** 399–404.

Marks, M.D. and Feldmann, K.A. (1989). Trichome Development in *Arabidopsis thaliana*. I. T-DNA Tagging of the *GLABROUS1* Gene. The Plant Cell **1:** 1043-1050.

Meng, X. and Zhang, S. (2013). MAPK Cascades in Plant Disease Resistance Signaling. Annu. Rev. Phytopathol. **51:** 245–266.

Micali, C., Gollner, K., Humphry, M., Consonni, C., and Panstruga, R. (2008). Pages 1-19 in: The Arabidopsis Book. American Society of Plant Biologists, Rockville, MD, U.S.A.

Mishina, T.E and Zeier, J. (2006). The Arabidopsis Flavin-Dependent Monooxygenase FMO1 Is an Essential Component of Biologically Induced Systemic Acquired Resistance. Plant Physiology **141:** 1666–1675.

Mishina, T.E. and Zeier, J. (2007). Pathogen-associated molecular pattern recognition rather than development of tissue necrosis contributes to bacterial induction of systemic acquired resistance in Arabidopsis. The Plant Journal **50:** 500–513.

Morgan, w. and Kamoun, S. (2007). RXLR effectors of plant pathogenic oomycetes. Current Opinion in Microbiology **10:** 332–338.

Mou, Z., Fan, W., and Dong, X. (2003). Inducers of Plant Systemic Acquired Resistance Regulate NPR1 Function through Redox Changes. Cell **113:** 935–944.

Mur, L.A.J., Naylor, G., Warner, S.A.J., Sugars, J.M., White, R.F., and Draper, J. (1996). Salicylic acid potentiates defence gene expression in tissue exhibiting acquired resistance to pathogen attack. Plant J. **9:** 559–71.

Murashige, T. and Skoog, F. (1962). A Revised Medium for Rapid Growth and Bio Assays with Tobacco Tissue Cultures. Physiologia Plantarum **15:** 473-497.

Mutka, A.M., Fawley, S., Tsao, T., and Kunkel, B.N. (2013). Auxin promotes susceptibility to *Pseudomonas syringae* via a mechanism independent of suppression of salicylic acid-mediated defenses. The Plant Journal **74:** 746–754.

Nafisi, M., Goregaoker, S., Botanga, C.J., Glawischnig, E., Olsen, C.E., Halkier, B.A., and Glazebrook, J. (2007). *Arabidopsis* Cytochrome P450 Monooxygenase 71A13 Catalyzes the Conversion of Indole-3-Acetaldoxime in Camalexin Synthesis. The Plant Cell **19:** 2039–2052.

Naumann, C., Hartmann, T., and Obe, D. (2002). Evolutionary recruitment of a flavin-dependent monooxygenase for the detoxification of host plant-acquired pyrrolizidine alkaloids in the alkaloid-defended arctiid moth *Tyria jacobaeae*. PNAS **99:** 6085-6090.

Návarová, H., Bernsdorff, F., Döring, A.C., and Zeier, J. (2012). Pipecolic Acid, an Endogenous Mediator of Defense Amplification and Priming, Is a Critical Regulator of Inducible Plant Immunity. The Plant Cell **24:** 5123–5141.

Nawrath, C. and Métraux, J.-P. (1999). Salicylic Acid Induction–Deficient Mutants of *Arabidopsis* Express *PR-2* and *PR-5* and Accumulate High Levels of Camalexin after Pathogen Inoculation. The Plant Cell **11:** 1393–1404.

Nemri, A, Atwell, S., Tarone, A.M., Huang, Y.S., Zhao, K., Studholme, D.J., Nordborg, M., and Jones, J.D.G. (2010). Genome-wide survey of *Arabidopsis* natural variation in downy mildew resistance using combined association and linkage mapping. PNAS **107:** 10302–10307.

Nishimura, M.T., Stein, M., Hou, B.-H., Vogel, J.P., Edwards, H., and Somerville, S.C. (2003). Loss of a Callose Synthase Results in Salicylic Acid–Dependent Disease Resistance. Science **301:** 969-972.

Okrent, R.A., Brooks, M.D., and Wildermuth, **M.C.** (2009). *Arabidopsis* GH3.12 (PBS3) Conjugates Amino Acids to 4-Substituted Benzoates and Is Inhibited by Salicylate. THE JOURNAL OF BIOLOGICAL CHEMISTRY **284:** 9742–9754.

Pajerowska-Mukhtar, K.M., Emerine, D.K., and Mukhtar, M.S. (2013). Tell me more: roles of NPRs in plant immunity. Trends in Plant Science **18:** 402-411.

Park, J.-E., Park, J.-Y., Kim, Y.-S., Staswick, P.E., Jeon, J., Yun, J., Kim, S.-Y., Kim, J., Lee, Y.-H., and Park, C.-M. (2007). GH3-mediated auxin homeostasis links growth regulation with stress adaptation response in Arabidopsis. J. Biol. Chem. **282:** 10036-10046.

Pedley, K.F. and Martin, G.B. (2005). Role of mitogen-activated protein kinases in plant immunity. Curr. Opin. Plant Biol. **8:** 541–47.

Penninckx, I.A.M.A., Thomma, B.P.H.J., Buchala, A., Métraux, J-P., and Broekaert, W.F. (1998). Concomitant Activation of Jasmonate and Ethylene Response Pathways Is Required for Induction of a Plant Defensin Gene in Arabidopsis. The Plant Cell **10:** 2103–2113.

Petersen, M., Brodersen, P., Naested, H., Andreasson, E., Lindhart, U., Johansen, B., Nielsen, H.B., Lacy, M., Austin, M.J., Parker, J.E., Sharma, S.B., Klessig, D.F., Martienssen, R., Mattsson, O., Jensen, A.B., and Mundy, J. (2000). Arabidopsis MAP kinase 4 negatively regulates systemic acquired resistance. Cell **103:** 1111–20.

Pitzschke, A., Schikora, A., and Hirt, H. (2009). MAPK cascade signalling networks in plant defence. Curr. Opin. Plant Biol. **12:** 421–26.

Rauhut, T. and Glawischnig, E. (2009). Evolution of camalexin and structurally related indolic compounds. Phytochemistry **70:** 1638–1644.

Rehmany, A.P., Gordon, A., Rose, L.E., Allen, R.L., Armstrong, M.R., Whisson, S.C., Kamoun, S., Tyler, B.M., Birch, P.R.J., and Beynon, J.L. (2005). Differential Recognition of Highly Divergent Downy Mildew Avirulence Gene Alleles by *RPP1* Resistance Genes from Two Arabidopsis Lines. The Plant Cell **17:** 1839–1850.

Ren, D., Liu, Y., Yang, K.Y., Han, L., Mao, G., Glazebrook, J., and Zhang, S. (2008). A fungal-responsive MAPK cascade regulates phytoalexin biosynthesis in *Arabidopsis.* PNAS **105:** 5638-5643.

Reuber, T. L., Plotnikova, J. M., Dewdney, J., Rogers, E. E., Wood, W., and Ausubel, F. M. (1998). Correlation of defense gene induction defects with powdery mildew susceptibility in Arabidopsis enhanced disease susceptibility mutants. Plant J. **16:** 473-485.

Roberts, M.R. (2007). Does GABA Act as a Signal in Plants?-Hints from Molecular Studies. Plant Signaling & Behavior **2:** 408-409.

Rodriguez, M.C., Petersen, M., and Mundy, J. (2010). Mitogen-activated protein kinase signaling in plants. Annu. Rev. Plant Biol. **61:** 621–49.

Ruthenburg, A.J., Allis, C.D., and Wysocka, J. (2007). Methylation of lysine 4 on histone H3: intricacy of writing and reading a single epigenetic mark. Mol Cell **25:** 15–30.

Schmelz, E.A., Engelberth, J., Tumlinson, J.H., Block, A., and Alborn, H.T. (2004). The use of vapor phase extraction in metabolic profiling of phytohormones and other metabolites. The Plant Journal **39:** 790–808.

Schuhegger, R., Nafisi, M., Mansourova, M., Petersen, B.L., Olsen, C.E., Svatoš, A., Halkier, B.A., and Glawischnig, E. (2006). CYP71B15 (PAD3) Catalyzes the Final Step in Camalexin Biosynthesis. Plant Physiology **141:** 1248–1254.

Seifi, H.S., Curvers, K., De Vleesschauwer, D., Delaere, I., Aziz, A., and Höfte, M. (2013). Concurrent overactivation of the cytosolic glutamine synthetase and the GABA shunt in the ABA-deficient sitiens mutant of tomato leads to resistance against *Botrytis cinerea.* New Phytologist **199:** 490–504.

Singh, P., Yekondi, S., Chen, P.-W., Tsai, C.-H., Yu, C.-W., Wu, K., and Zimmerli, L. (2014). Environmental History Modulates *Arabidopsis* Pattern-Triggered Immunity in a HISTONE ACETYLTRANSFERASE1–Dependent Manner. The Plant Cell **26:** 2676–2688.

Skipp, R.A. and Deverall, B.J. (1973). Studies on cross-protection in the anthracnose disease of bean. Physiol. Plant Pathol. **2:** 357–74.

Spanu, P.D., Abbott, J.C., Amselem, J., Burgis, T.A., Soanes, D.M., Stüber, K., van Themaat, E.V.L., Brown, J.K.M., Butcher, S.A., Gurr, S.J., Lebrun, M.-H., Ridout, C.J., Schulze-Lefert, P., Talbot, N.J., Ahmadinejad, N., Ametz, C., Barton, G.R., Benjdia, M., Bidzinski, P., Bindschedler, L.V., Both, M., Brewer, M.T., Cadle-Davidson, L., Cadle-Davidson, M.M., Collemare, J., Cramer, R., Frenkel, O., Godfrey, D., Harriman, J., Hoede, C., King, B.C., Klages, S., Kleemann, J., Knoll, D., Koti, P.S., Kreplak, J., López-Ruiz, F.J., Lu, X., Maekawa, T., Mahanil, S., Micali, C., Milgroom, M.G., Montana, G., Noir, S., O'Connell, R.J., Oberhaensli, S., Parlange, F., Pedersen, C., Quesneville, H., Reinhardt, R., Rott, M., Sacristán, S., Schmidt, S.M., Schön, M., Skamnioti, P., Sommer, H., Stephens, A., Takahara, H., Thordal-Christensen, H., Vigouroux, M., Weßling, R., Wicker, T., and Panstruga, R. (2010). Genome Expansion and Gene Loss in Powdery Mildew Fungi Reveal Tradeoffs in Extreme Parasitism. Science **330:** 1543-1546.

Spoel, S.H., Koornneef, A., Claessens, S.M.C., Korzelius, J.P., Van Pelt, J.A., Mueller, M.J., Buchala, A.J., Métraux, J.-P., Brown, R., Kazan, K., Van Loon, L.C., Dong, X., and Pieterse, C.M.J. (2003). NPR1 Modulates Cross-Talk between Salicylate- and Jasmonate-Dependent Defense Pathways through a Novel Function in the Cytosol. The Plant Cell **15:** 760–770.

Spoel, S.H. and Dong, X. (2012). How do plants achieve immunity? Defence without specialized immune cells. Nature Reviews Immunology **12:** 89-100.

Staswick, P.E., Tiryaki, I., and Rowe, M.L. (2002). Jasmonate response locus *JAR1* and several related Arabidopsis genes encode enzymes of the firefly luciferase superfamily that show activity on jasmonic, salicylic, and indole-3-acetic acids in an assay for adenylation. Plant Cell **14:** 1405-1415.

Sticher, L., Mauch-Mani, B., and Métraux, J.-P. (1997). Systemic Acquired Resistance. Annu. Rev. Phytopathol. **35:** 235–270.

Stuttmann, J., Hubberten, H.-M., Rietz, S., Kaur, J., Muskett, P., Guerois, R., Bednarek, P., Hoefgen, R., and Parker, J.E. (2011). Perturbation of *Arabidopsis* Amino Acid Metabolism Causes Incompatibility with the Adapted Biotrophic Pathogen *Hyaloperonospora arabidopsidis*. The Plant Cell **23:** 2788–2803.

Suh, J.-K., Poulsen, L.L., Ziegler, D.M., and Robertus, J.D. (1999). Yeast flavin-containing monooxygenase generates oxidizing equivalents that control protein folding in the endoplasmic reticulum; PNAS **96:** 2687–2691.

Tena, G., Boudsocq, M., and Sheen, J. (2011). Protein kinase signaling networks in plant innate immunity. Curr. Opin. Plant Biol. **14:** 519–29.

Thomma, B.P.H.J., Eggermont, K., Penninckx, I.A.M.A., Mauch-Mani, B., Vogelsang, R., Cammue, B.P., Broekaert, W.F. (1998). Separate jasmonate-dependent and salicylate-dependent defense-response pathways in *Arabidopsis* are essential for resistance to distinct microbial pathogens. PNAS **95:** 15107–11.

Thomma, B.P.H.J., Eggermont, K., Tierens, K.F.M.-J., and Broekaert, W.F. (1999). Requirement of Functional *Ethylene-Insensitive 2* Gene for Efficient Resistance of Arabidopsis to Infection by *Botrytis cinerea.* Plant Physiology **121:** 1093–1101.

Thordal-Christensen, H. (2003). Fresh insights into processes of nonhost resistance. Current Opinion in Plant Biology **6:** 351–357.

Thulke, O. and Conrath, U. (1998). Salicylic acid has a dual role in the activation of defense-related genes in parsley. Plant J **14:** 35–42.

Ton, J. and Mauch-Mani, B. (2004). ß-amino-butyric acid-induced resistance against necrotrophic pathogens is based on ABA-dependent priming for callose. The Plant Journal **38:** 119-130.

Ton, J., Jakab, G., Toquin, V., Flors, V., Iavicoli, A., Maeder, M.N., Métraux, J.P., and Mauch-Mani, B. (2005). Dissecting the ß-Aminobutyric Acid–Induced Priming Phenomenon in Arabidopsis. The Plant Cell **17:** 987–999.

Tsai, C.-H., Singh, P., Chen, C.-W., Thomas, J., Weber, J., Mauch-Mani, B., and Zimmerli, L. (2011). Priming for enhanced defence responses by specific inhibition of the Arabidopsis response to coronatine. The Plant Journal **65:** 469–479.

Tsuda, K., Mine, A., Bethke, G., Igarashi, D., Botanga, C.J., Tsuda, Y., Glazebrook, J., Sato, M., and Katagiri, F. (2013). Dual Regulation of Gene Expression Mediated by Extended MAPK Activation and Salicylic Acid Contributes to Robust Innate Immunity in *Arabidopsis thaliana.* PLOS Genetics **9:** 1-14.

Underwood, W., Zhang, S., and He, S.Y. (2007). The *Pseudomonas syringae* type III effector tyrosine phosphatase HopAO1 suppresses innate immunity in *Arabidopsis thaliana.* The Plant Journal **52:** 658–672.

Van Andel, O. M. (1958). Investigations on plant chemotherapy II. Influence of amino acids on the relation plant-pathogen. Tijdschr. Planteziekten **64:** 307-327.

Van Damme, M., Zeilmaker, T., Elberse, J., Andel, A., de Sain-van der Velden, M., and van den Ackerveken, G. (2009). Downy mildew resistance in *Arabidopsis* by mutation of HOMOSERINE KINASE. Plant Cell **21:** 2179–2189.

Van Peer, R., Niemann, G.J., and Schippers, B. (1991) Induced resistance and phytoalexin accumulation in biological control of fusarium wilt of carnation by *Pseudomonas* sp. strain WCS417r. Phytopathology **81:** 728–734.

Vernooij, B., Friedrich, L., Morse, A., Reist, R., Kolditz-Jawhar, R., Ward, E., Uknes, S., Kessmann, H., and Ryals, J. (1994). Salicylic Acid 1s Not the Translocated Signal Responsible for Inducing Systemic Acquired Resistance but 1s Required in Signal Transduction. The Plant Cell **6:** 959-965.

Vernoud, V., Horton, A.C., Yang, Z., and Nielsen, E. (2003). Analysis of the Small GTPase Gene Superfamily of Arabidopsis. Plant Physiol. **131:** 1191-1208.

Vlot, A.C., Dempsey, D.A., and Klessig, D.F. (2009). Salicylic Acid, a Multifaceted Hormone to Combat Disease. Annu. Rev. Phytopathol. **47:** 177–206.

Wang, H., Chevalier, D., Larue, C., Ki Cho, S., and Walker, J.C. (2007). The protein phosphatases and protein kinases of Arabidopsis thaliana. Arabidopsis Book **5:** e0106.

Wang, H., Ngwenyama, N., Liu, Y., Walker, J.C., and Zhang, S. (2007 b). Stomatal development and patterning are regulated by environmentally responsive mitogen-activated protein kinases in *Arabidopsis.* Plant Cell **19:** 63–73.

Wang, W., Zhang, Y., Wen, Y., Berkey, R., Ma, X., Pan, Z., Bendigeri, D., King, H., Zhang, Q., and Xiao, S. (2013). A Comprehensive Mutational Analysis of the Arabidopsis Resistance Protein RPW8.2 Reveals Key Amino Acids for Defense Activation and Protein Targeting. The Plant Cell 25**:** 4242–4261.

Wang, X., Sager, R., Cui, W., Zhang, C., Lu, H., and Lee, J.-Y. (2013 b). Salicylic Acid Regulates Plasmodesmata Closure during Innate Immune Responses in *Arabidopsis*. Plant Cell **25:** 2315-29.

Watanabe, M., Maemura, K., Kanbara, K., Tamayama, T., and Hasayaki, H. (2002). GABA and GABA Receptors in the Central Nervous System and Other Organs. International Review of Cytology **213:** 1-47.

Weiberg, A., Wang, M., Lin, F.-M., Zhao, H., Zhang, Z., Kaloshian, I., Huang, H.-D., and Jin, H. (2013) Fungal Small RNAs Suppress Plant Immunity by Hijacking Host RNA Interference Pathways. Science **342:** 118-123.

Weßling, R. and Panstruga, R. (2012). Rapid quantification of plant-powdery mildew interactions by qPCR and conidiospore counts. Plant Methods **8:** 2-10.

Widmann, C., Gibson, S., Jarpe, M.B., and Johnson, G.L. (1999). Mitogen-activated protein kinase: conservation of a three-kinase module from yeast to human. Physiol. Rev. **79:** 143–80.

Wildermuth, M.C., Dewdney, J., Wu, G. and Ausubel, F.M. (2001). Isochorismate synthase is required to synthesize salicylic acid for plant defence. Nature **414:** 562-565.

Win, J., Morgan, W., Bos, J., Krasileva, K.V., Cano, L.M., Chaparro-Garcia, A., Ammar, R., Staskawicz, B.J., and Kamoun, S. (2007). Adaptive Evolution Has Targeted the C-Terminal Domain of the RXLR Effectors of Plant Pathogenic Oomycetes. The Plant Cell **19:** 2349–2369.

Wu, Y., Zhang, D., Chu, J.Y., Boyle, P., Wang, Y., Brindle, I.D., De Luca, V., and Després, C. (2012). The *Arabidopsis* NPR1 Protein Is a Receptor for the Plant Defense Hormone Salicylic Acid. Cell Reports **1:** 639–647.

Xiao, S., Brown, S., Patrick, E., Brearley, C., and Turner, J.G. (2003). Enhanced Transcription of the Arabidopsis Disease Resistance Genes *RPW8.1* and *RPW8.2* via a Salicylic Acid–Dependent Amplification Circuit Is Required for Hypersensitive Cell Death. The Plant Cell **15:** 33–45.

Xiao, S., Calis, O., Patrick, E., Zhang, G., Charoenwattana, P., Muskett, P., Parker, J.E., and Turner, J.G. (2005). The atypical resistance gene, *RPW8*, recruits components of basal defence for powdery mildew resistance in Arabidopsis. The Plant Journal **42:** 95–110.

Yan, J., Zhang, C., Gu, M., Bai, Z., Zhang, W., Qi, T., Cheng, Z., Peng, W., Luo, H., Nan, F., Wang, Z., and Xie, D. (2009). The *Arabidopsis* CORONATINE INSENSITIVE1 Protein Is a Jasmonate Receptor. The Plant Cell **21:** 2220–2236.

Yan, S. and Dong, X. (2014). Perception of the plant immune signal salicylic acid. Current Opinion in Plant Biology **20:** 64–68.

Zeier, J. (2013). New insights into the regulation of plant immunity by amino acid metabolic pathways. Plant, Cell and Environment **36:** 2085-2103.

Zeng, W., Melotto, M., and He, S.Y. (2010). Plant stomata: a checkpoint of host immunity and pathogen virulence. Curr. Opin. Biotechnol. **21:** 599–603.

Zhang, Z., Li, Q., Li, Z., Staswick, P.E., Wang, M., Zhu, Y., and He, Z. (2007). Dual regulation role of GH3.5 in salicylic acid and auxin signaling during *Arabidopsis-Pseudomonas syringae* interaction. Plant Physiol. **145:** 450-464.

Zhang, S. (2008). Mitogen-activated protein kinase cascades in plant intracellular signaling. In Annual Plant Reviews, **Vol. 33:** Intracellular Signaling in Plants, ed. Z Yang, pp. 100–136. Oxford:Wiley-Blackwell.

Zhou, N., Tootle, T.L., and Glazebrook, J. (1999). Arabidopsis *PAD3*, a Gene Required for Camalexin Biosynthesis, Encodes a Putative Cytochrome P450 Monooxygenase. The Plant Cell **11:** 2419–2428.

Ziegler, D.M. and Pettit, F.H. (1964). Formation of an intermediate N-oxide in the oxidative demethylation of N,N-dimethylaniline catalyzed by liver microsomes. Biochem. Biophys. Res. Commun. **15**: 188–193.

Zimmerli, L., Jakab, G., Métraux, J.-P., and Mauch-Mani, B. (2000) Potentiation of pathogen-specific defense mechanisms in *Arabidopsis* by b-aminobutyric acid. PNAS **97:** 12920–12925.

Zimmerli, L., Métraux, J.-P., and Mauch-Mani, B. (2001). ß-Aminobutyric Acid-Induced Protection of *Arabidopsis* against the Necrotrophic Fungus *Botrytis cinerea*. Plant Physiology **126:** 517–523.

Zimmerli, L., Stein, M., Lipka, V., Schulze-Lefert, P., and Somerville, S. (2004). Host and non-host pathogens elicit different jasmonate/ethylene responses in *Arabidopsis.* Plant J. **40:** 633–46.

10 Appendix

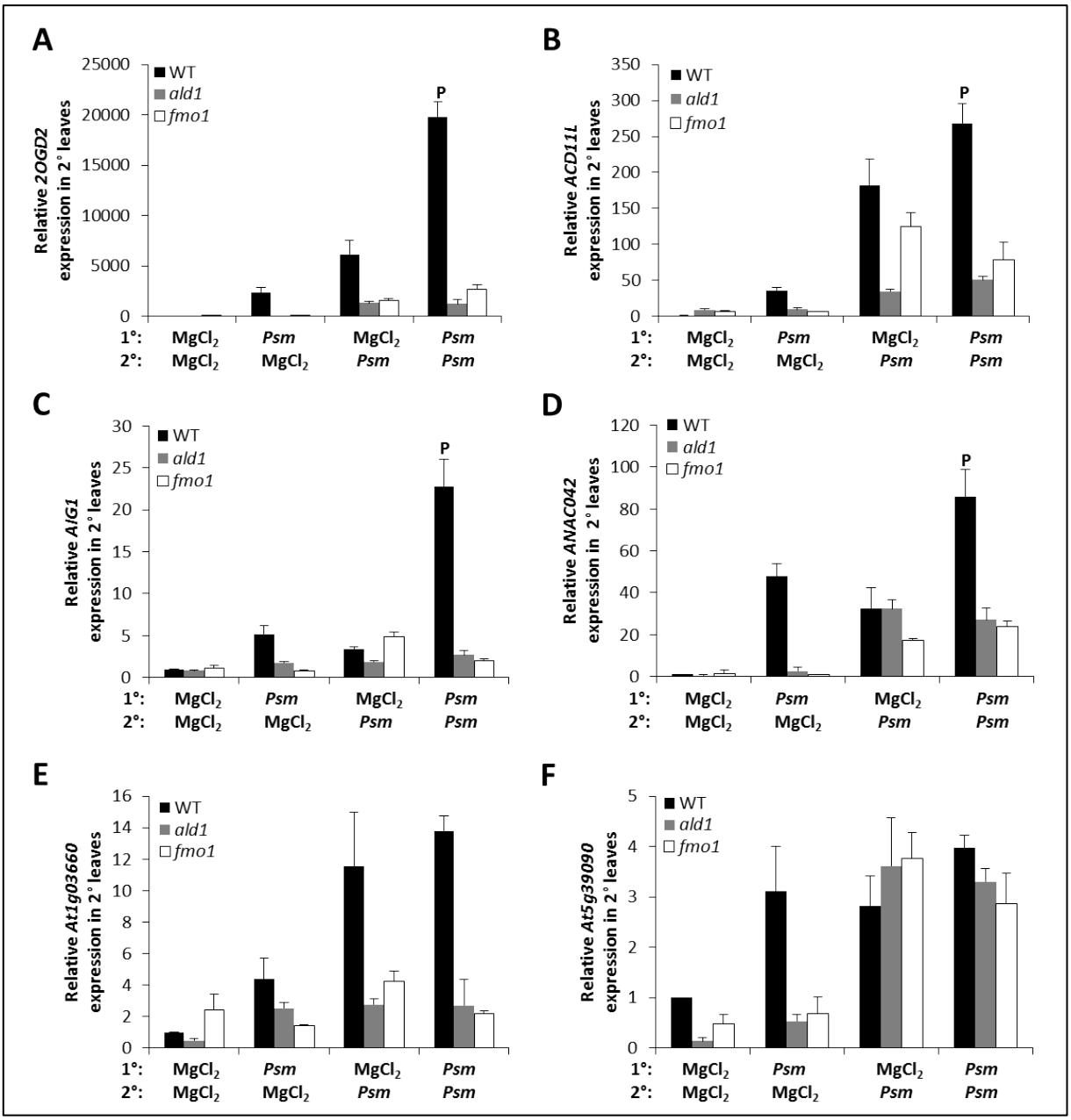

Supplemental figure 1. Analysis of defence priming in *Arabidopsis thaliana*.

Plants were double inoculated to analyse defence priming during SAR in Col-0, *ald1* and *fmo1*. Plants were treated in lower (1°) leaves with either 10 mM $MgCl_2$ or *Psm* (OD_{600}=0.005); 2 days later, upper leaves were infiltrated with either 10 mM $MgCl_2$ or *Psm* (OD_{600}=0.005) and scored for gene expression analysis 10 h post inoculation. Four different cases, a control situation (1° $MgCl_2$/2° $MgCl_2$), a systemic response (1° *Psm*/2°$MgCl_2$), a local response (1° $MgCl_2$/2° *Psm*), and a combination of systemic and local responses to the pathogen, can be discerned with this experimental setup. Relative expression of *2OGD2* (A), *ACD11L* (B), *AIG1* (C), *ANAC042* (D), *At1g03660* (E), and *At5g39090* (F) at 10 hours after 2° treatment. Transcript levels were determined by quantitative real-time PCR analysis, are given as means ±SD of three replicate samples, and are expressed relative to the respective mock control value. Statistical differences in transcript abundance upon 2° *Psm* infection between SAR-noninduced and SAR-induced plants were analysed using two-tailed *t* test (P, primed gene). Due to the large number of genes analysed, the experiment was done one time.

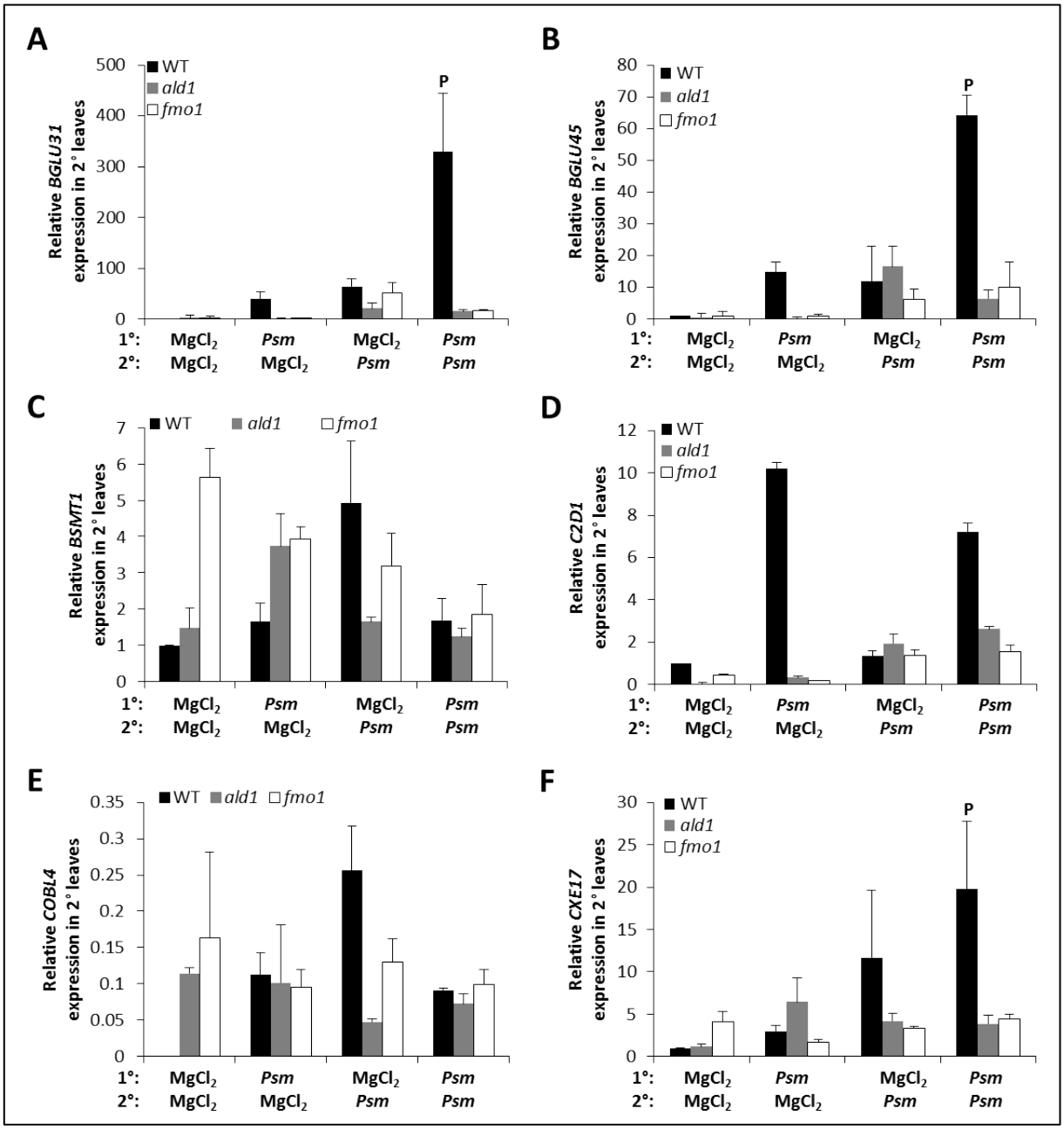

Supplemental figure 2. Analysis of defence priming in *A. thaliana* (continued).

Plants were treated as described in supplemental figure 1. Relative expression of *BGLU31* (A), *BGLU45* (B), *BSMT1* (C), *C2D1* (D), *COBL4* (E), and *CXE17* (F) at 10 hours after 2° treatment. Transcript levels were determined by quantitative real-time PCR analysis, are given as means ±SD of three replicate samples, and are expressed relative to the respective mock control value. Statistical differences in transcript abundance upon 2° *Psm* infection between SAR-noninduced and SAR-induced plants were analysed using two-tailed *t* test (P, primed gene). Due to the large number of genes analysed, the experiment was done one time.

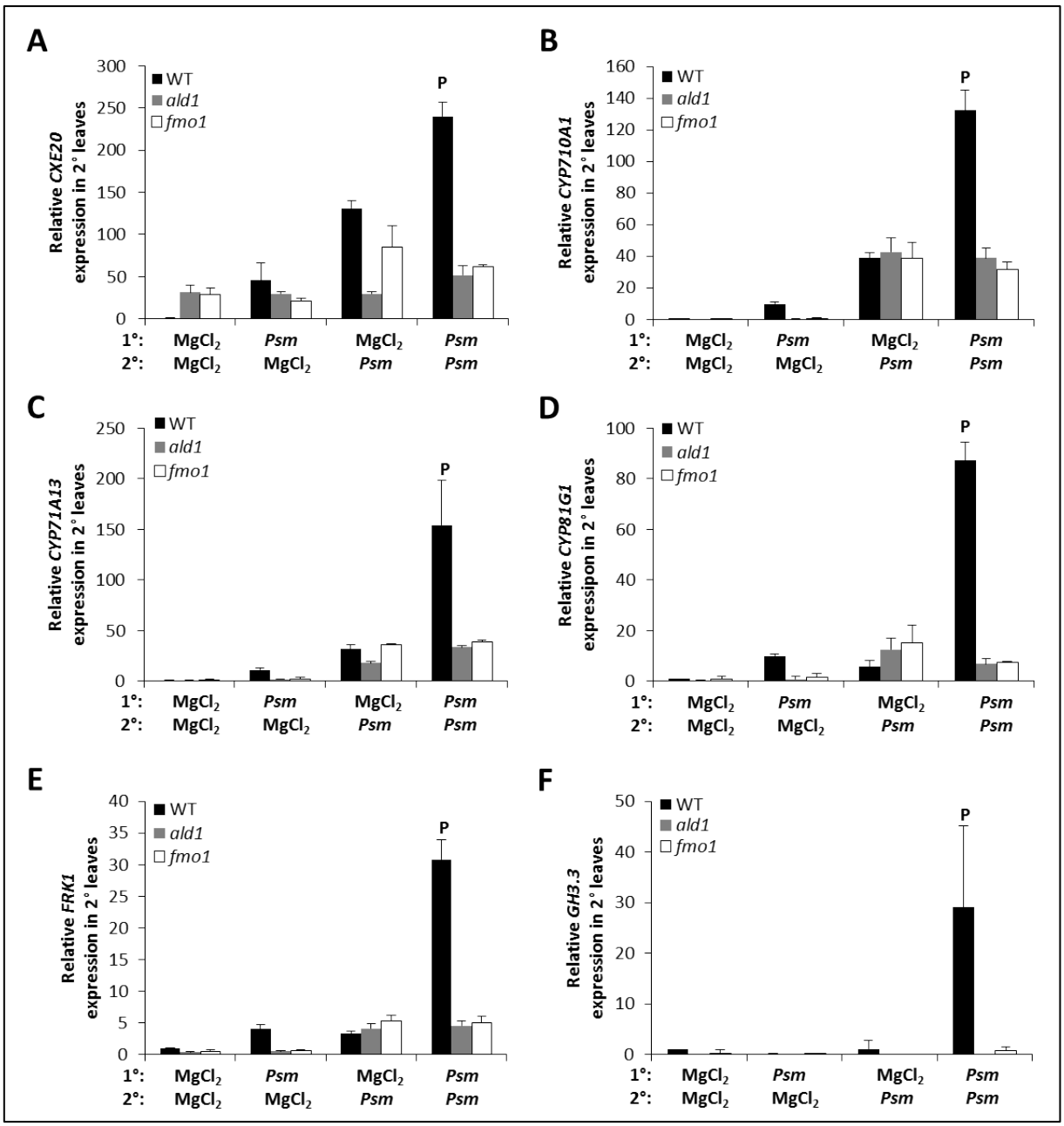

Supplemental figure 3. Analysis of defence priming in *A. thaliana* (continued).

Plants were treated as described in supplemental figure 1. Relative expression of *CXE20* (A), *CYP710A1* (B), *CYP71A13* (C), *CYP81G1* (D), *FRK1* (E), and *GH3.3* (F) at 10 hours after 2° treatment. Transcript levels were determined by quantitative real-time PCR analysis, are given as means ±SD of three replicate samples, and are expressed relative to the respective mock control value. Statistical differences in transcript abundance upon 2° *Psm* infection between SAR-noninduced and SAR-induced plants were analysed using two-tailed *t* test (P, primed gene). Due to the large number of genes analysed, the experiment was done one time.

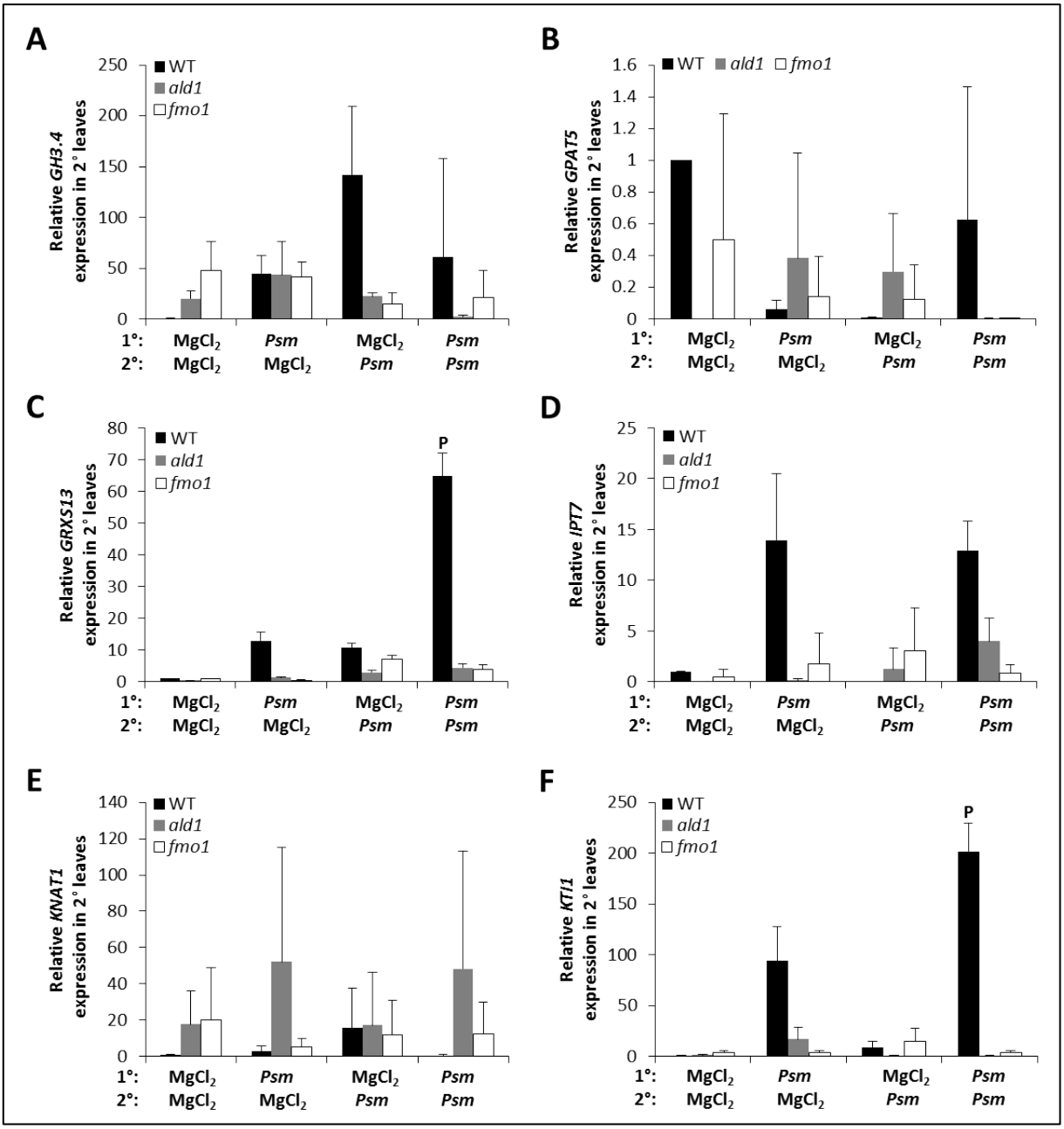

Supplemental figure 4. Analysis of defence priming in *A. thaliana* (continued).

Plants were treated as described in supplemental figure 1. Relative expression of *GH3.4* (A), *GPAT5* (B), *GRXS13* (C), *IPT7* (D), *KNAT1* (E), and *KTI1* (F) at 10 hours after 2° treatment. Transcript levels were determined by quantitative real-time PCR analysis, are given as means ±SD of three replicate samples, and are expressed relative to the respective mock control value. Statistical differences in transcript abundance upon 2° *Psm* infection between SAR-noninduced and SAR-induced plants were analysed using two-tailed *t* test (P, primed gene). Due to the large number of genes analysed, the experiment was done one time.

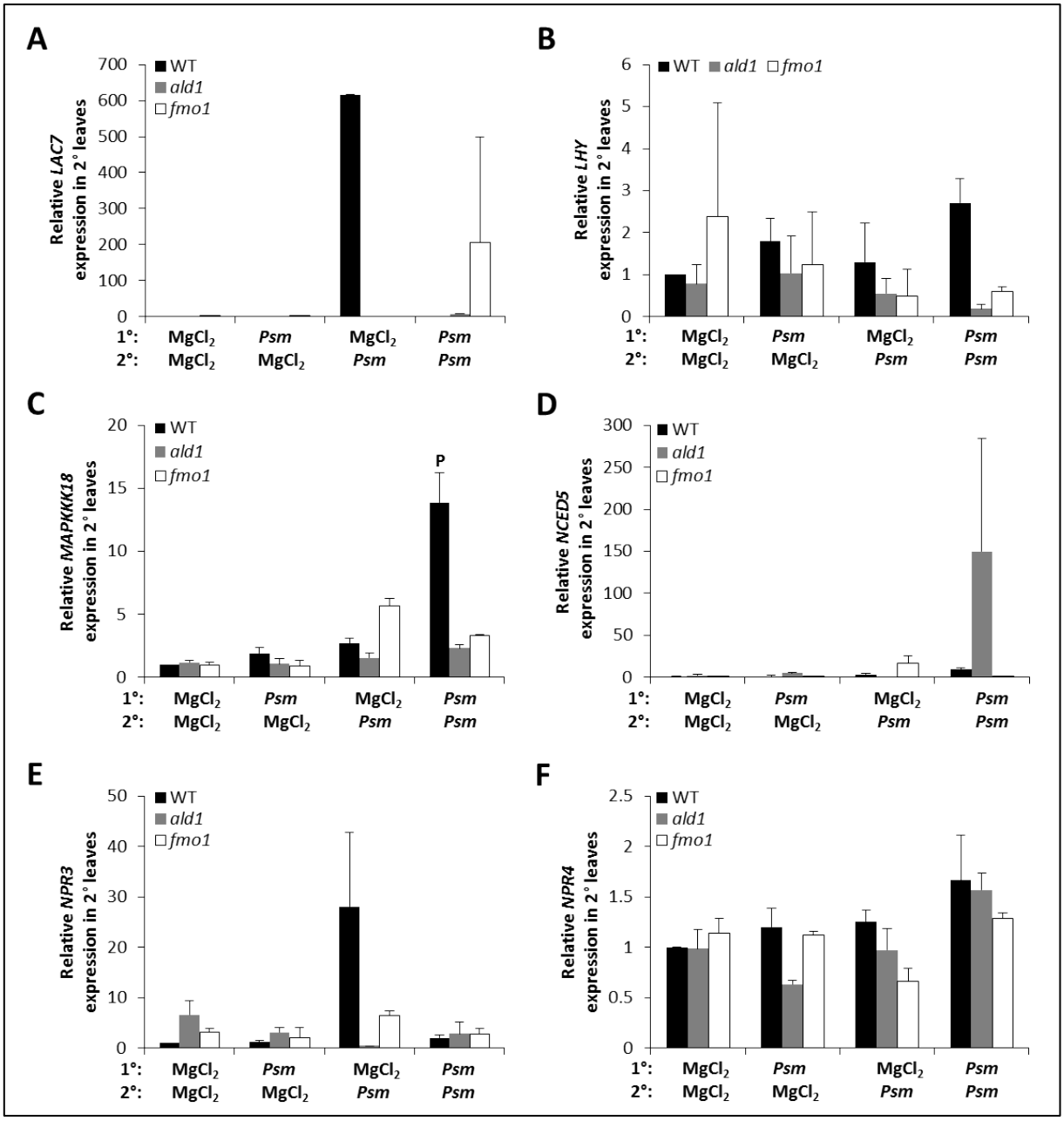

Supplemental figure 5. Analysis of defence priming in *A. thaliana* (continued).

Plants were treated as described in supplemental figure 1. Relative expression of *LAC7* (A), *LHY* (B), *MAPKKK18* (C), *NCED5* (D), *NPR3* (E), and *NPR4* (F) at 10 hours after 2° treatment. Transcript levels were determined by quantitative real-time PCR analysis, are given as means ±SD of three replicate samples, and are expressed relative to the respective mock control value. Statistical differences in transcript abundance upon 2° *Psm* infection between SAR-noninduced and SAR-induced plants were analysed using two-tailed *t* test (P, primed gene). Due to the large number of genes analysed, the experiment was done one time.

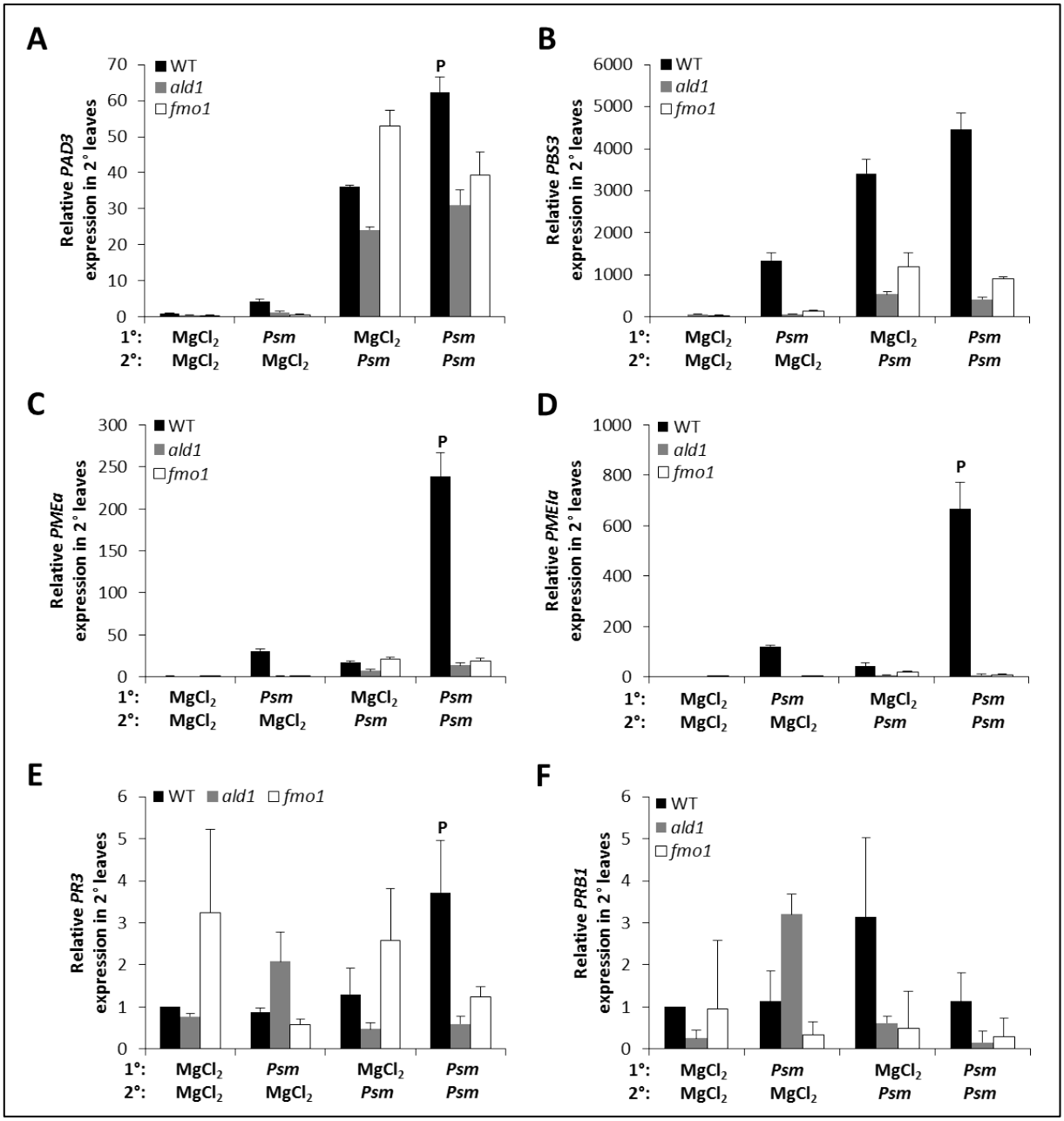

Supplemental figure 6. Analysis of defence priming in *A. thaliana* (continued).

Plants were treated as described in supplemental figure 1. Relative expression of *PAD3* (A), *PBS3* (B), *PMEα* (C), *PMEIα* (D), *PR3* (E), and *PRB1* (F) at 10 hours after 2° treatment. Transcript levels were determined by quantitative real-time PCR analysis, are given as means ±SD of three replicate samples, and are expressed relative to the respective mock control value. Statistical differences in transcript abundance upon 2° *Psm* infection between SAR-noninduced and SAR-induced plants were analysed using two-tailed *t* test (P, primed gene). Due to the large number of genes analysed, the experiment was done one time.

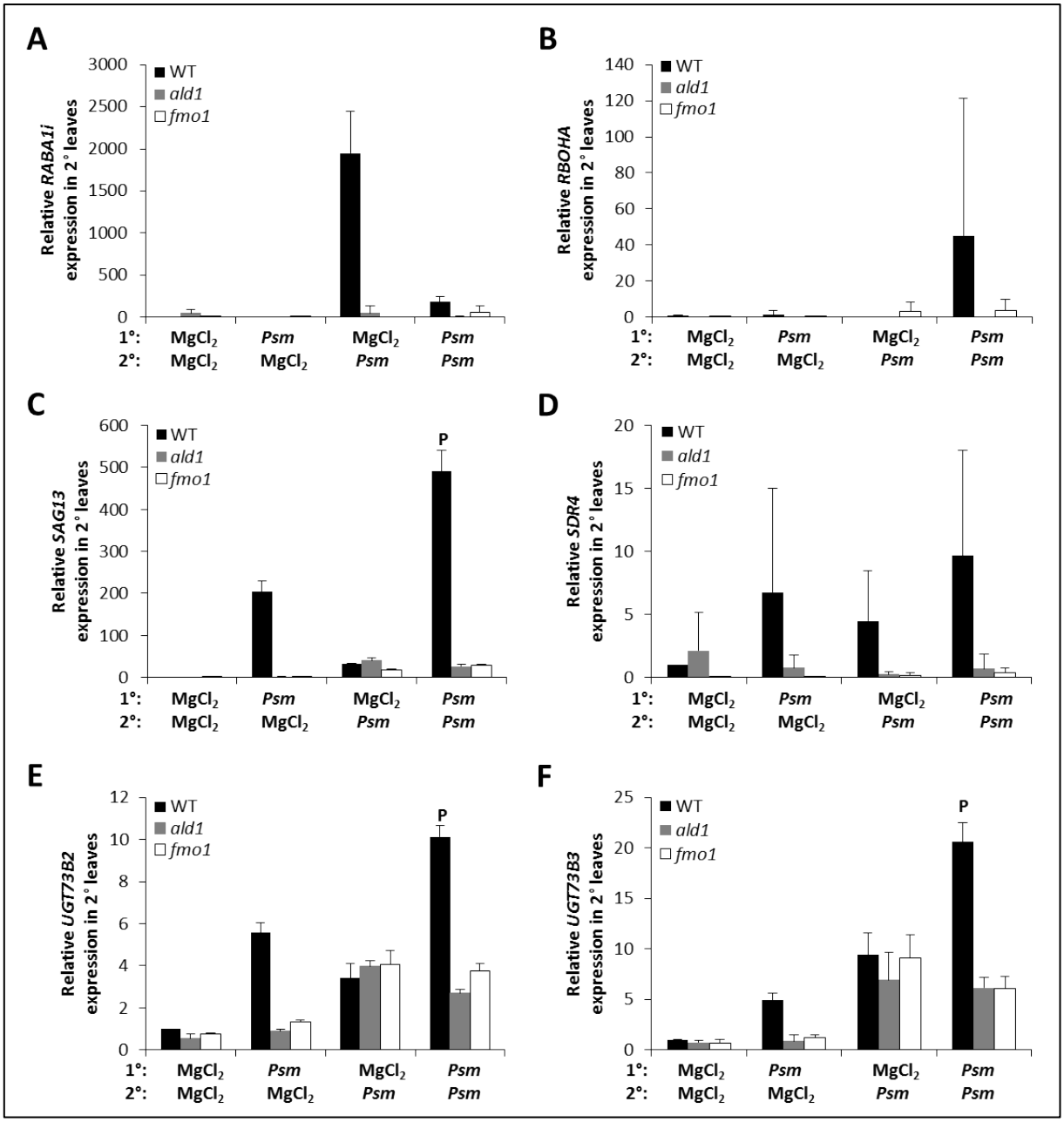

Supplemental figure 7. Analysis of defence priming in *A. thaliana* (continued).

Plants were treated as described in supplemental figure 1. Relative expression of *RABA1i* (A), *RBOHA*(B), *SAG13* (C), *SDR4* (D), *UGT73B2* (E), and *UGT73B3* (F) at 10 hours after 2° treatment. Transcript levels were determined by quantitative real-time PCR analysis, are given as means ±SD of three replicate samples, and are expressed relative to the respective mock control value. Statistical differences in transcript abundance upon 2° *Psm* infection between SAR-noninduced and SAR-induced plants were analysed using two-tailed *t* test (P, primed gene). Due to the large number of genes analysed, the experiment was done one time.

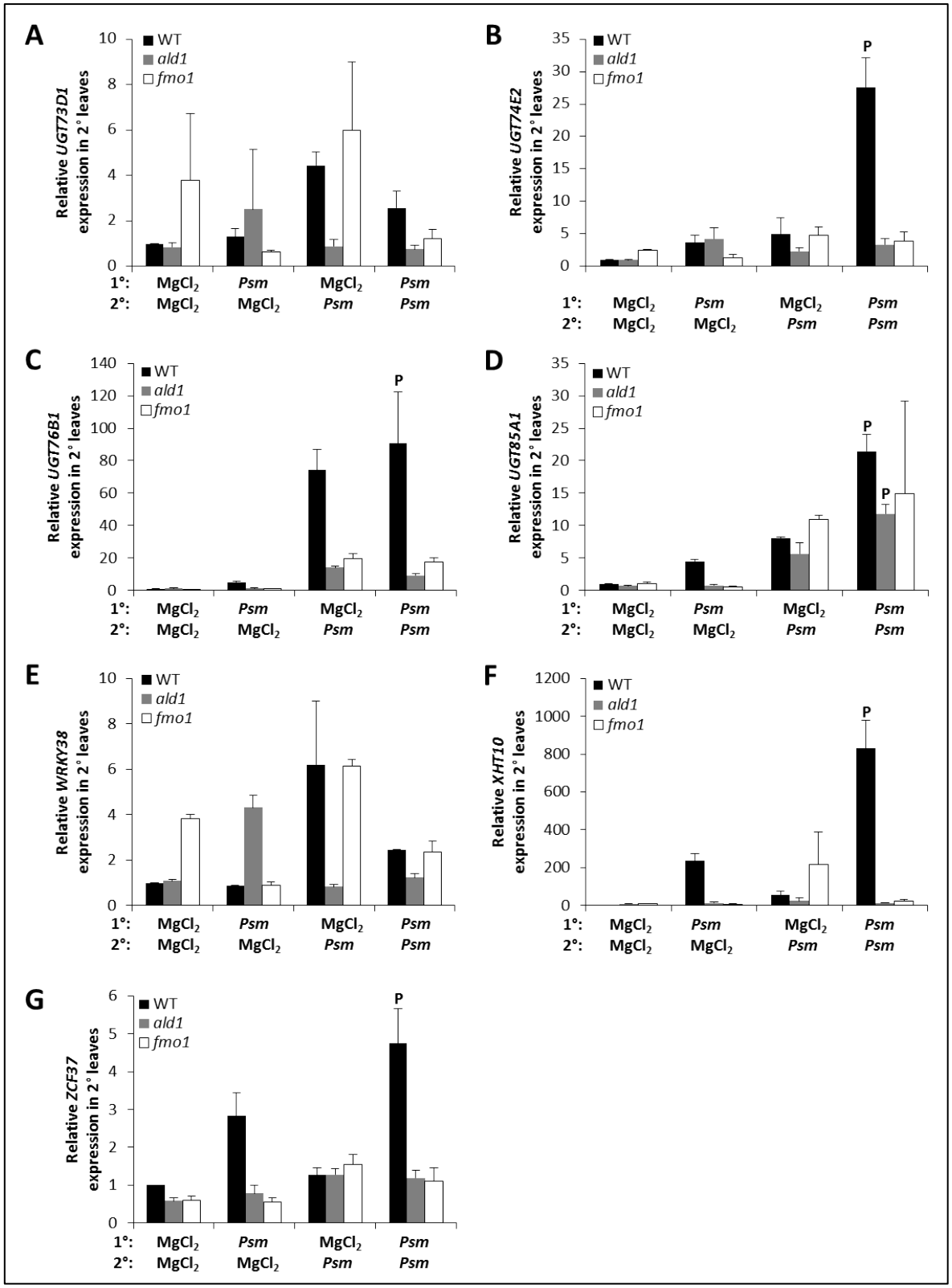

Supplemental figure 8. Analysis of defence priming in *A. thaliana* (continued).

Plants were treated as described in supplemental figure 1. Relative expression of *UGT73D1* (A), *UGT74E2* (B), *UGT76B1* (C), *UGT85A1* (D), *WRKY38* (E), *XHT10* (F), and *ZCF37* (G) at 10 hours after 2° treatment. Transcript levels were determined by quantitative real-time PCR analysis, are given as means ±SD of three replicate samples, and are expressed relative to the respective mock control value. Statistical differences in transcript abundance upon 2° *Psm* infection between SAR-noninduced and SAR-induced plants were analysed using two-tailed *t* test (P, primed gene). Due to the large number of genes analysed, the experiment was done one time.

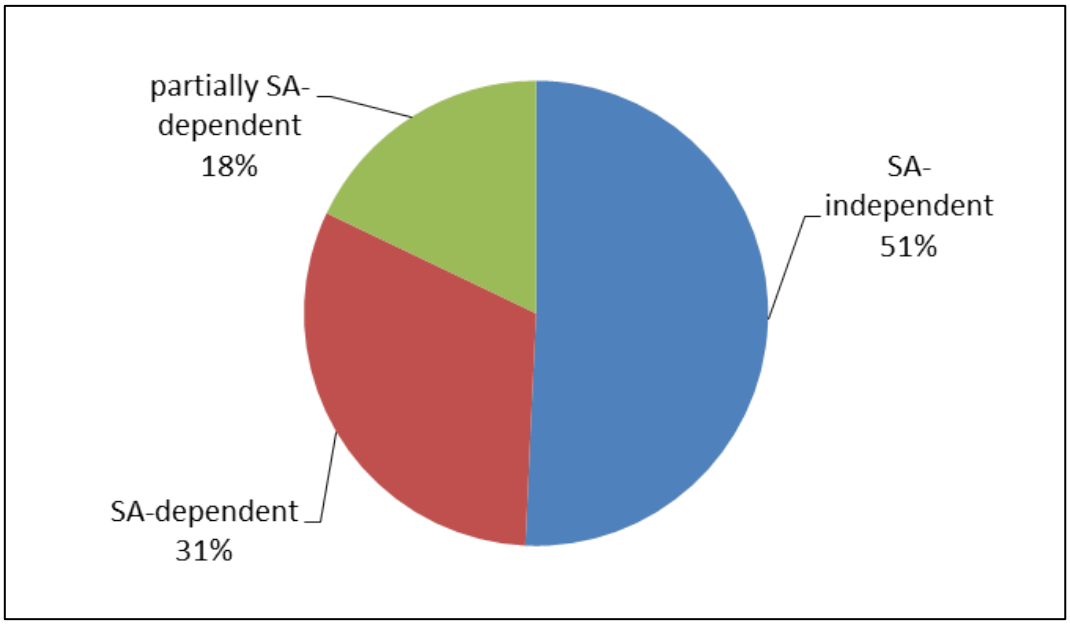

Supplemental figure 9. SA-dependency of genes analysed for defence priming.

The majority of genes analysed for primed expression during SAR were SA-independent.

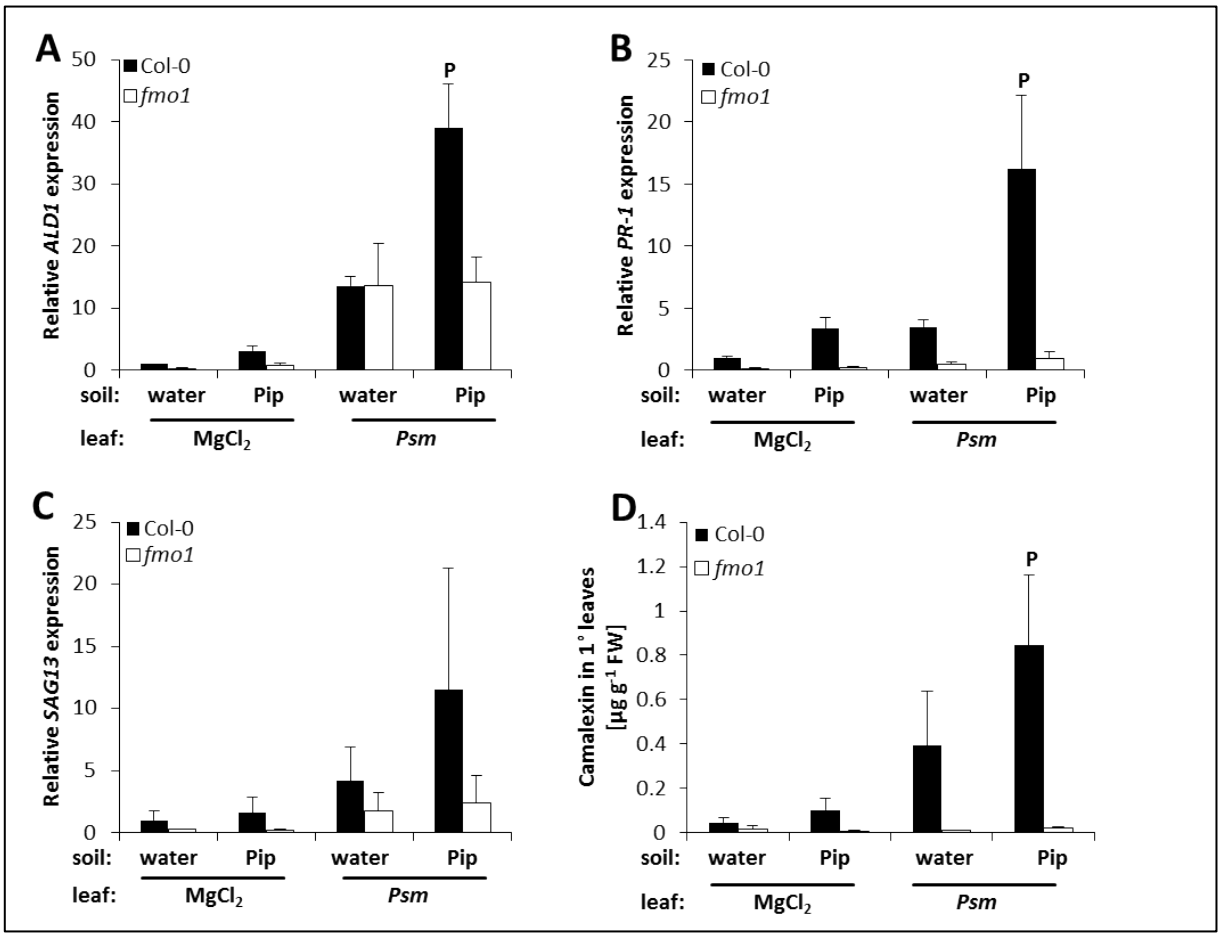

Supplemental figure 10. Primed gene expression and camalexin accumulation by exogenously applied Pip is abolished in *fmo1*.

Plants were treated and samples analysed as described in figure 29. P, primed gene expression. This experiment was done in collaboration with Dr Friederike Bernsdorff and Katrin Gruner.

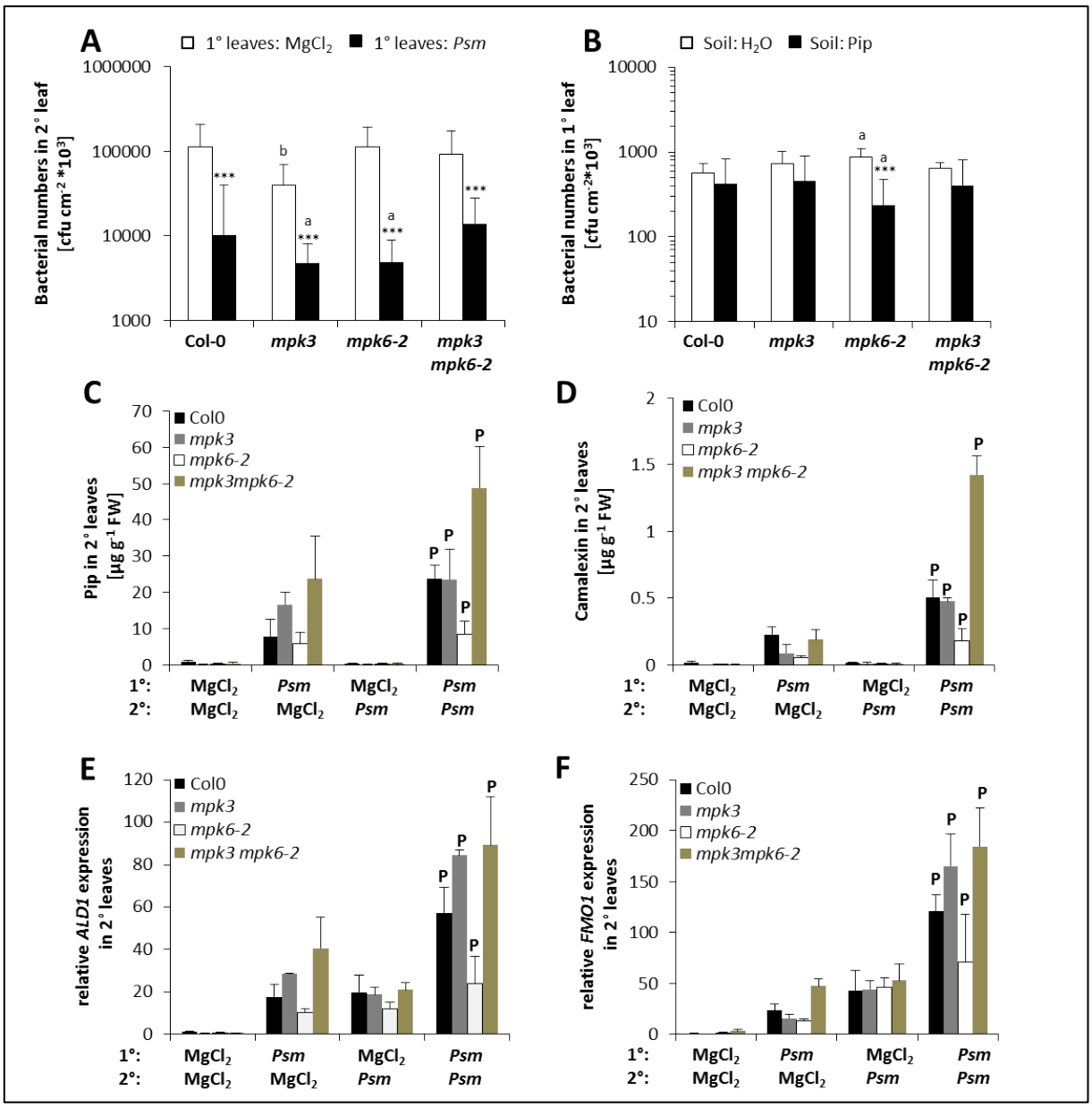

Supplemental figure 11. MPK3 and MPK6 are not involved in defence priming.

Plants were treated and samples analysed as delineated in figure 30. Analysis of SAR (A) and Pip-induced resistance (B) in *Arabidopsis* Col-0 as well as *mpk3, mpk6*, and *mpk3 mpk6*. Accumulation of defence compounds Pip (C) and camalexin (D) and expression of defence-related genes *ALD1* (E) and *FMO1* (F) were studied in respect of defence priming in Col-0, *mpk3, mpk6*, and *mpk3 mpk6*. Seeds for *mpk3, mpk6*, and *mpk3 mpk6* were provided by Dr Ken Tsuda (MPIZ Cologne). P, primed response.

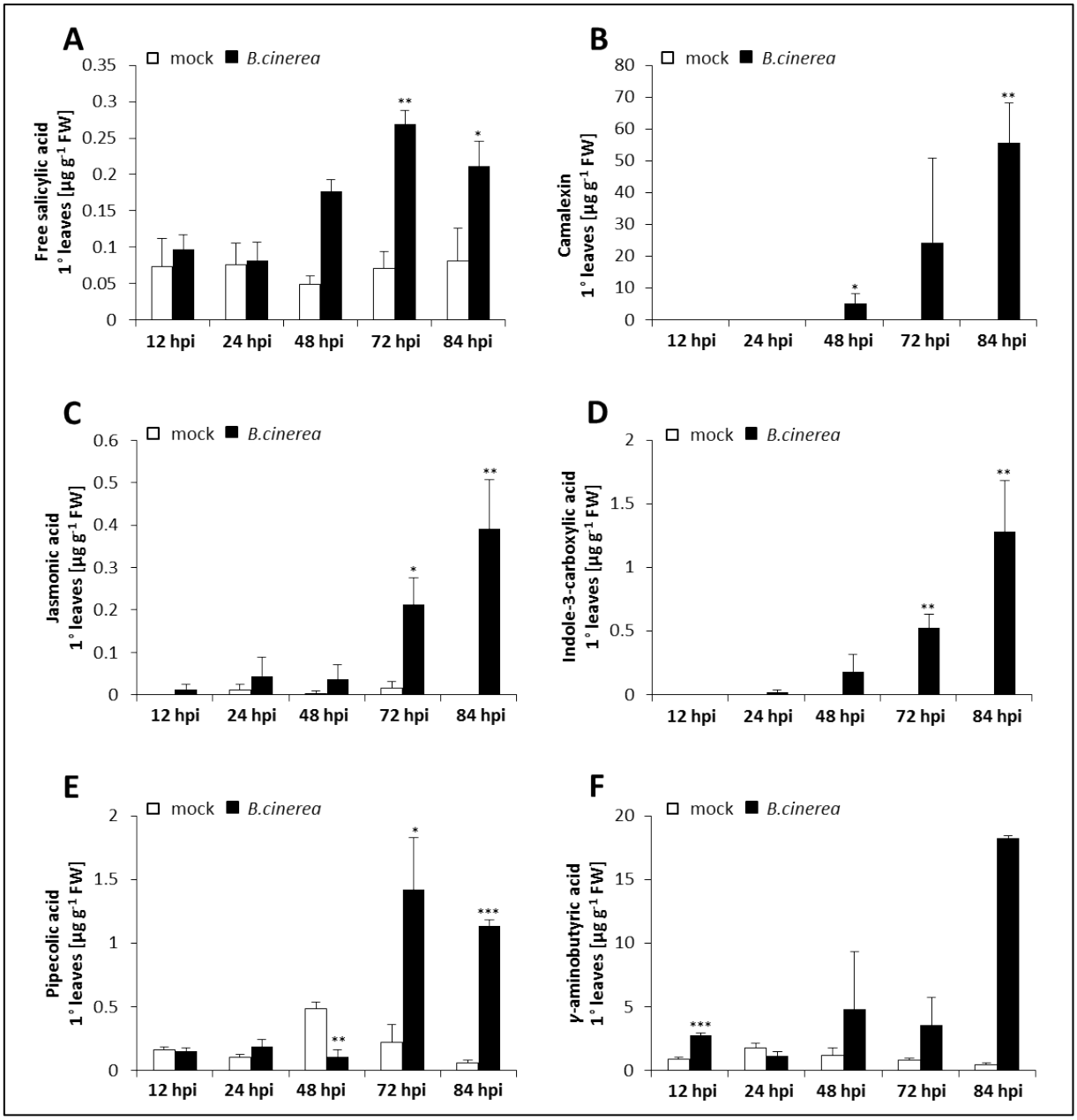

Supplemental figure 12. Metabolic profile of *A. thaliana* plants infected with the necrotroph *B. cinerea*.

Plants were treated and analysed as described in figure 33. Accumulation of free SA (A), camalexin (B), JA (C), ICA (D), Pip (E), and GABA (F). Bars represent the mean ±SD of three replicate samples and asterisks above the bars show significant statistical differences between non-infected and infected plants (two-tailed *t* test; *, P< 0.05; **, P< 0.01; ***, P< 0.001). FW, fresh weight. This experiment was done in cooperation with Verena Gruber, B.Sc..

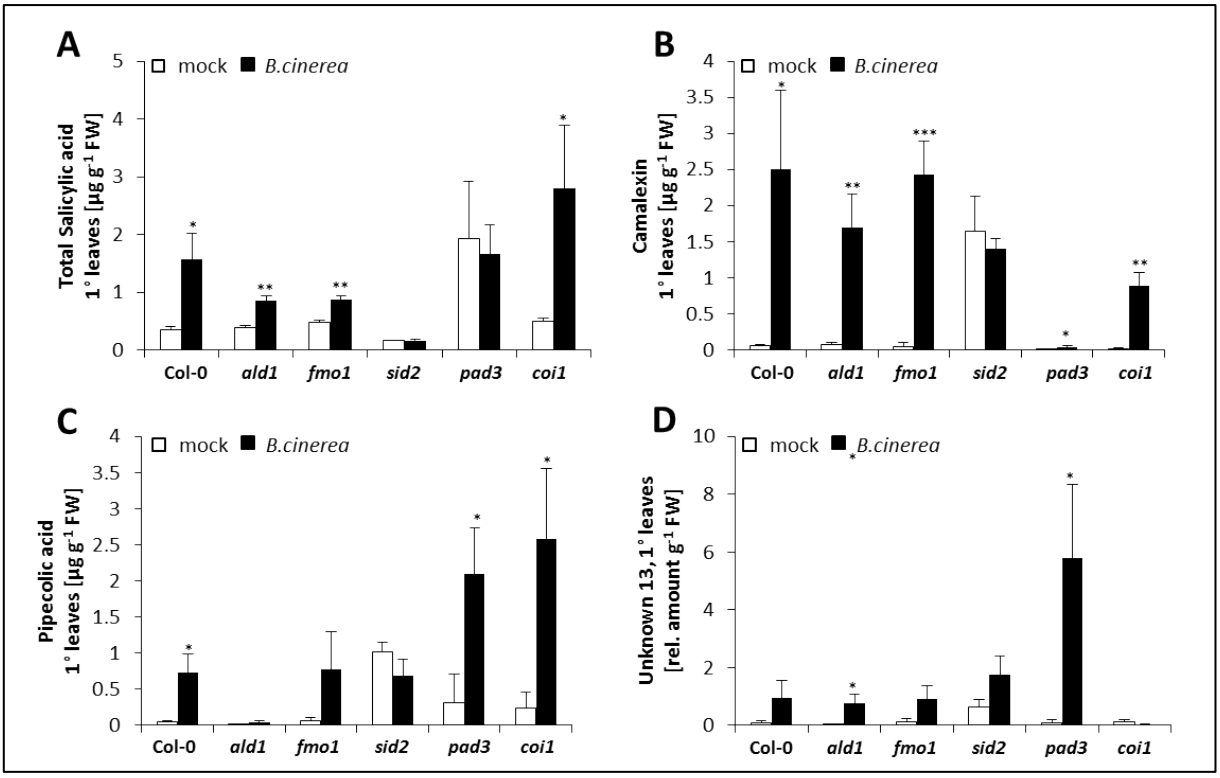

Supplemental figure 13. Defence signalling in the *Arabidopsis-Botrytis* interaction.

Analysis of metabolite accumulation in *Arabidopsis* plants after infection with the necrotrophic fungus *B. cinerea* as delineated in figure 35. Accumulation of total SA (sum of free and conjugated SA) (A), camalexin (B), Pip (C), and the unknown compound 13 (D). Bars represent the mean ±SD of three replicate samples and asterisks above the bars show significant statistical differences between non-infected and infected plants (two-tailed *t* test; *, P< 0.05; **, P< 0.01; ***, P< 0.001). FW, fresh weight.

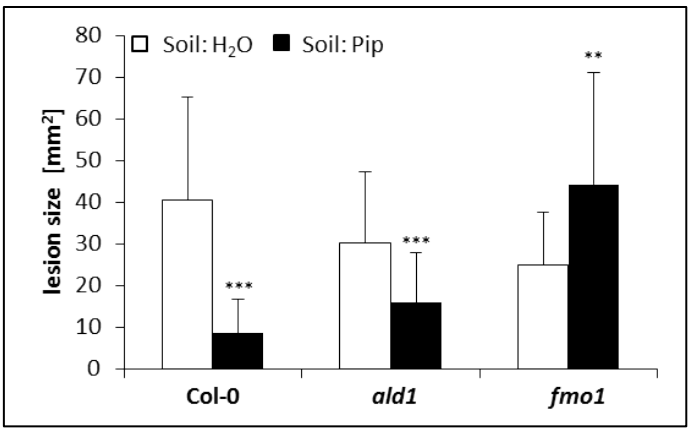

Supplemental figure 14. Exogenous Pip induces resistance against *B. cinerea*.

Plants were treated and samples analysed as described in figure 37. Asterisks above the bars show significant statistical differences between non-infected and infected plants (two-tailed *t* test; *, P< 0.05; **, P< 0.01; ***, P< 0.001).

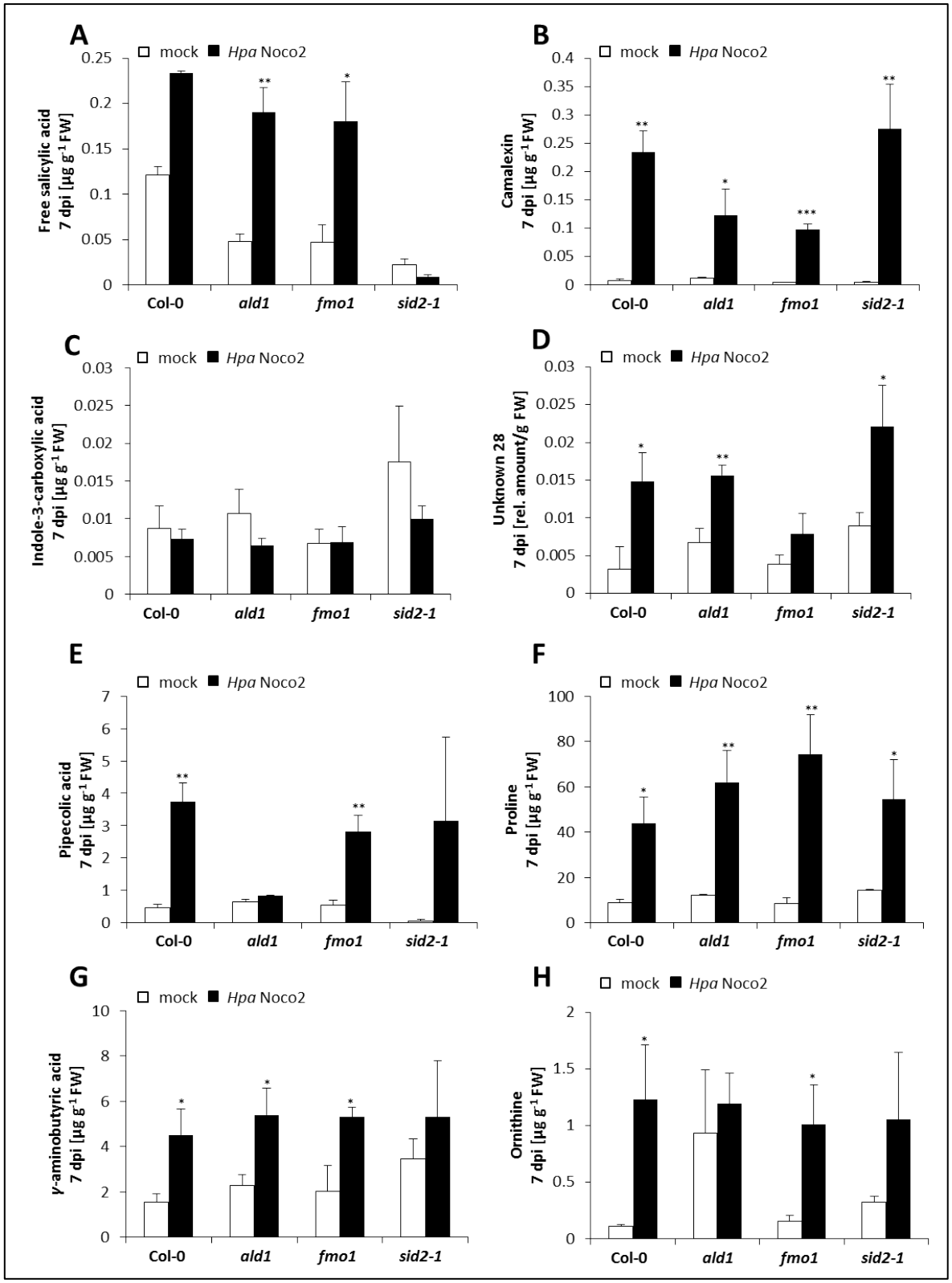

Supplemental figure 15. Metabolite profiling of *Arabidopsis* plants infected with the virulent *Hpa* Noco2.

Treatment and metabolite analyses as detailed in figure 38, but in this experiment only the virulent *Hpa* isolate Noco2 was used. Accumulation of free SA (A), camalexin (B), ICA (C), "unknown 28" (D), Pip (E), Pro (F), GABA (G), and Orn (H). Asterisks above the bars show significant statistical differences between non-infected and infected plants (two-tailed *t* test; *, P< 0.05; **, P< 0.01; ***, P< 0.001).

Table 6. Analysis of amino acid accumulation in *A. thaliana* Col-0 plants infected with the virulent *Hpa* isolate Noco2 and the avirulent isolate Cala2.

Amino acid content in water- and pathogen-treated plants was analysed and fold-change ratio for each amino acid determined. Significant statistical differences between non-infected and infected plants are marked by asterisks (two-tailed *t* test; *, P< 0.05; **, P< 0.01; ***, P< 0.001). FW, fresh weight.

Amino acid	*H. arabidopsidis*-sprayed leaves (7dpi)				
	µg g^{-1} FW			ratio P/M	ratio P/M
	water	*Hpa* Noco2	*Hpa* Cala2	*Hpa* Noco2	*Hpa* Cala2
Alanine	31.0 ± 2.54	64.5 ± 3.16	38.4 ± 5.92	2.1 *	1.2
Asparagine	17.0 ± 0.61	55.9 ± 6.68	34.4 ± 4.07	3.3 *	2.0 *
Aspartic acid	311.4 ± 16.75	345.2 ± 11.05	255.1 ± 34.76	1.1	0.8
Cysteine	0.2 ± 0.0008	0.6 ± 0.03	0.3 ± 0.05	3.0 **	1.5
Glutamic acid	245.4 ± 14.11	288.2 ± 19.44	205.3 ± 24.60	1.2	0.8
Glutamine	42.3 ± 5.84	276.5 ± 19.13	98.7 ± 12.10	6.5 **	2.3 *
Glycine	22.4 ± 2.16	12.4 ± 0.91	4.4 ± 0.62	0.6	0.2 **
Isoleucine	3.9 ± 0.24	14.3 ± 1.23	8.5 ± 1.41	3.7 *	2.2 *
Leucine	4.4 ± 0.3	18.3 ± 0.64	9.1 ± 1.68	4.2 **	2.1
Lysine	4.5 ± 0.47	22.0 ± 0.57	12.6 ± 2.34	4.9 **	2.8 *
Ornithine	0.2 ± 0.02	2.1 ± 0.01	0.41 ± 0.07	10.5 ***	2.1 *
Phenylalanine	2.8 ± 0.29	10.9 ± 0.49	7.7 ± 1.38	3.9 **	2.8 *
Pipecolic acid	1.5 ± 0.12	8.0 ± 0.46	5.0 ± 0.88	5.3 **	3.3 *
Proline	15.3 ± 1.10	66.1 ± 5.29	11.5 ± 1.68	4.3 *	0.8
Serine	38.7 ± 6.44	73.2 ± 0.77	57.6 ± 7.22	1.9 *	1.5
Threonine	34.1 ± 4.76	47.2 ± 1.00	41.3 ± 5.70	1.4	1.2
Tryptophane	0.3 ± 0.13	5.0 ± 0.26	1.2 ± 0.22	16.7 **	4.0 *
Tyrosine	1.4 ± 0.19	11.9 ± 0.48	3.6 ± 0.67	8.5 **	2.6 *
Valine	7.6 ± 0.73	32.5 ± 2.34	16.4 ± 0.9	4.3 **	2.2 **
α-aminoadipic acid	0.2 ± 0.02	5.2 ± 0.35	1.1 ± 0.13	26.0 **	5.5 **
γ-Aminobutyric acid	2.4 ± 0.12	9.9 ± 0.44	3.2 ± 0.44	4.1 **	1.3

> 100	> 20	5-20	3-5	1.6-3	0.5-0.8	≤ 0.5

Table 7. Analysis of amino acid accumulation in wild type and mutant *Arabidopsis thaliana* plants infected with the virulent *Hpa* isolate Noco2.

Amino acid content in water- and pathogen-treated Col-0, *ald1, fmo1, sid2*, and *sid2 ald1* plants was analysed and fold-change ratio for each amino acid determined. Significant statistical differences between non-infected and infected plants are marked by asterisks (two-tailed *t* test; *, P< 0.05; **, P< 0.01; ***, P< 0.001). GABA, *γ*-aminobutyric acid; Aad, *α*-aminoadipic acid; FW, fresh weight.

> 100	> 20	5-20	3-5	1.6-3	0.5-0.8	≤ 0.5

Amino acid	*Hyaloperonospora arabidopsidis*-sprayed leaves (7 dpi)																	
	Col0				*ald1*				*fmo1*				*sid2*					
	µg g^{-1} FW			ratio	µg g^{-1} FW			ratio	µg g^{-1} FW			ratio	µg g^{-1} FW			ratio		
	water		*Hpa*	P/M	water		*Hpa*	P/M	water		*Hpa*	P/M	water		*Hpa*	P/M		
Ala	31	± 3	64 ± 3	2 *	15	± 2	22 ± 4	1	11	± 1	24 ± 9	2	21	± 9	12 ± 1	1		
Asn	17	± 1	56 ± 7	3 *	23	± 1	47 ± 4	2 *	21	± 2	38 ± 7	2	26	± 8	115 ± 7	4 **		
Asp	311	± 17	345 ± 11	1	349	± 32	271 ± 20	1	339	± 52	202 ± 59	1	411	± 129	531 ± 15	1		
Cys	0.2	± 0.001	1 ± 0.03	4 **	0.2	± 0.02	1 ± 0.04	3 *	0.2	± 0.04	1 ± 0.1	3	0.2	± 0.05	2 ± 0.1	8 **		
GABA	2	± 0.1	10 ± 0.4	4 **	3	± 0.3	12 ± 1	4 **	2	± 0.2	7 ± 1	3 *	2	± 1	16 ± 1	6 **		
Gln	42	± 6	277 ± 19	7 **	77	± 12	275 ± 11	4 **	55	± 5	200 ± 86	4	67	± 30	435 ± 47	7 **		
Glu	245	± 14	288 ± 19	1	244	± 38	221 ± 17	1	252	± 51	170 ± 45	1	283	± 108	466 ± 31	2		
Gly	22	± 2	12 ± 1	1	16	± 2	13 ± 1	1	23	± 2	10 ± 1	0.5	12	± 1	10 ± 0.4	1 ***		
Ile	4	± 0.2	14 ± 1	4 *	3	± 0.1	8 ± 0.03	2 ***	3	± 0.3	6 ± 0.5	2 **	4	± 0.2	10 ± 1	3 **		
Leu	4	± 0.3	18 ± 1	4 **	4	± 0.1	11 ± 0.3	3 **	4	± 0.3	8 ± 1	2 *	4	± 0.4	14 ± 1	4 ***		
Lys	5	± 0.5	22 ± 1	5 **	5	± 1	21 ± 2	4 *	5	± 1	11 ± 4	2	6	± 2	30 ± 0.3	5 **		
Orn	0.2	± 0.02	2 ± 0.01	13 ***	0.2	± 0.02	2 ± 0.1	10 **	0.2	± 0.03	1 ± 0.3	6	0.2	± 0.1	3 ± 0.03	16 ***		
Phe	3	± 0.3	11 ± 0.5	4 **	3	± 0.2	8 ± 1	3 *	3	± 0.4	7 ± 2	2	3	± 1	19 ± 0.1	6 ***		
Pip	1	± 0.1	8 ± 0.5	5 **	1	± 0.1	1 ± 0.1	1	1	± 0.3	6 ± 0.5	6 **	2	± 0.2	14 ± 1	9 **		
Pro	15	± 1	66 ± 5	4 *	12	± 0.04	48 ± 2	4 **	11	± 1	41 ± 4	4 **	13	± 0.5	48 ± 3	4 ***		
Ser	39	± 6	73 ± 1	2 *	44	± 5	45 ± 3	1	44	± 6	32 ± 10	1	54	± 23	82 ± 3	2		
Thr	34	± 5	47 ± 1	1	38	± 5	30 ± 2	1	34	± 6	20 ± 7	1	41	± 16	56 ± 2	1		
Trp	0.3	± 0.1	5 ± 0.3	16 **	0.5	± 0.04	5 ± 0.2	11 **	0.5	± 0.01	4 ± 2	8	0.4	± 0.2	8 ± 0.4	19 ***		
Tyr	1	± 0.2	12 ± 0.5	9 **	1	± 0.1	13 ± 1	9 **	1	± 0.2	11 ± 3	7	2	± 0.5	30 ± 1	20 ***		

10 Appendix

Amino acid	*Hyaloperonospora arabidopsidis*-sprayed leaves (7 dpi)																	
	Col0				*ald1*				*fmo1*				*sid2*					
	µg g^{-1} FW			ratio P/M	µg g^{-1} FW			ratio P/M	µg g^{-1} FW			ratio P/M	µg g^{-1} FW			ratio P/M		
	water		*Hpa*		water		*Hpa*		water		*Hpa*		water		*Hpa*			
Val	8	± 1	33	± 2	4 **	5	± 0.3	16	± 2	3 *	5	± 0.4	16	± 3	3 *	6	± 1	14	± 1	2 *
Aad	0.2	± 0.02	5	± 0.3	**29** **	0.2	± 0.01	7	± 0.5	**41** **	0.2	± 0.04	5	± 1	**26** *	0.2	± 0.1	10	± 1	**50** ***

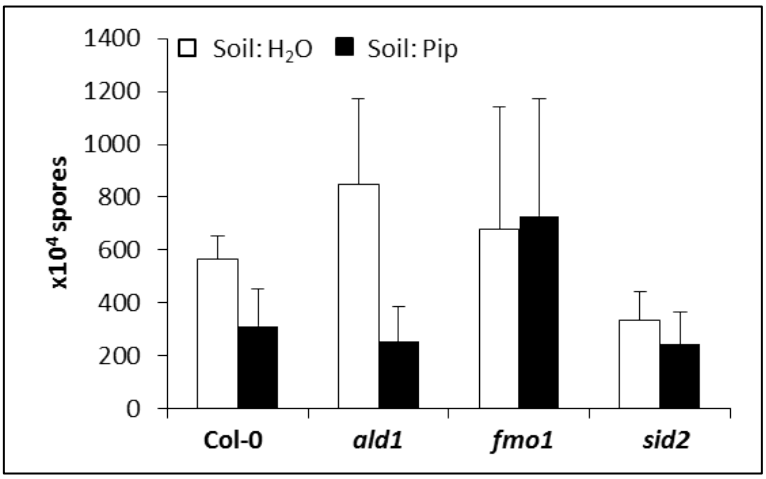

Supplemental figure 16. Exogenously applied Pip induces resistance against the virulent *Hpa* isolate Noco2 in Col-0 and *ald1*, but not in *fmo1* and *sid2*.

Plants were treated and analysed as described in figure 41.

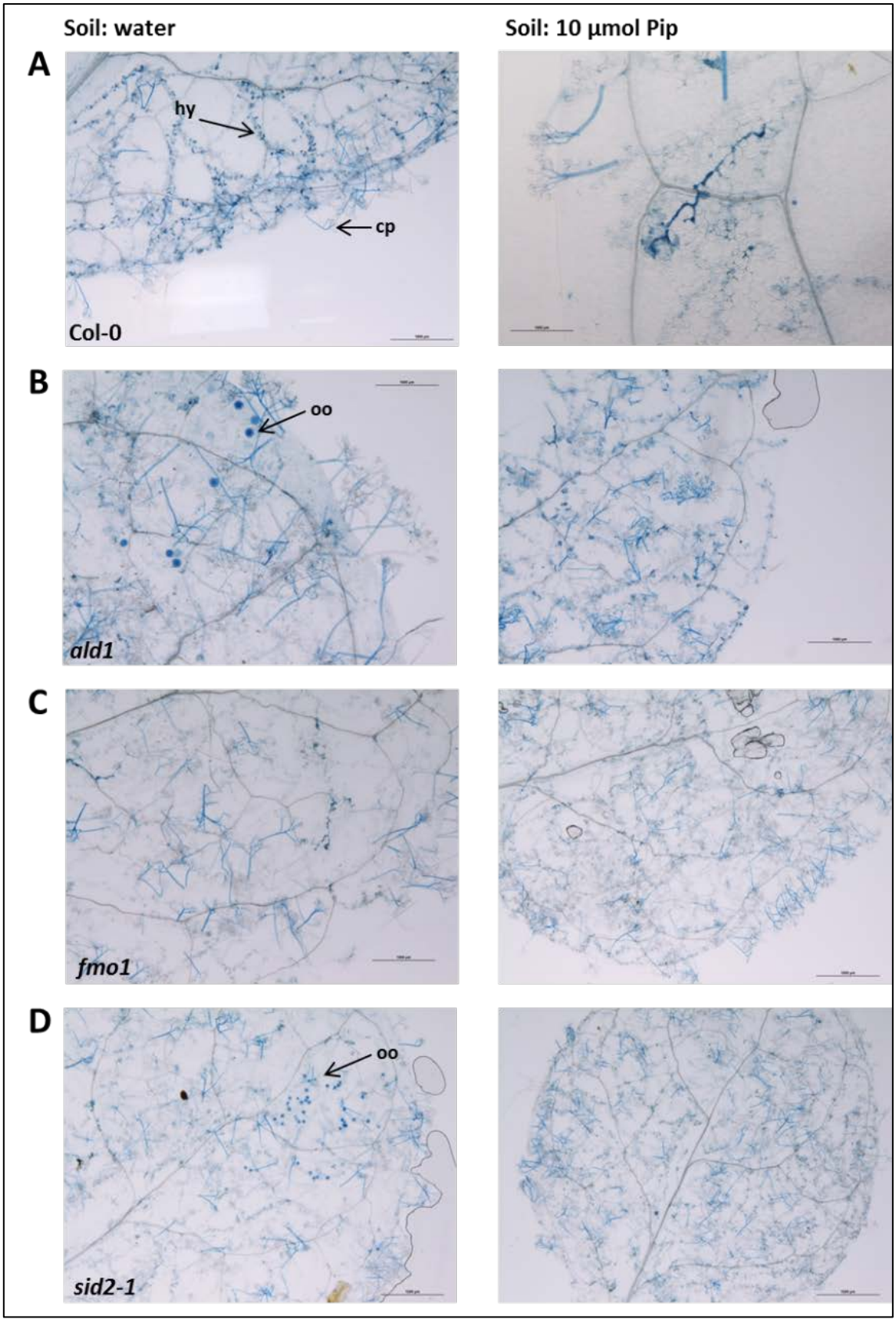

Supplemental figure 17. Pip-induced resistance against *Hpa* Noco2.

Plants were treated and analysed as described in figure 39. Shown are representative detail views of *A. thaliana* Col-0 (A) as well as the mutant lines *ald1* (B), *fmo1* (C), and *sid2* (D). Cp, conidiophore; HR, hypersensitive response; hy, hyphae; oo, oospore.

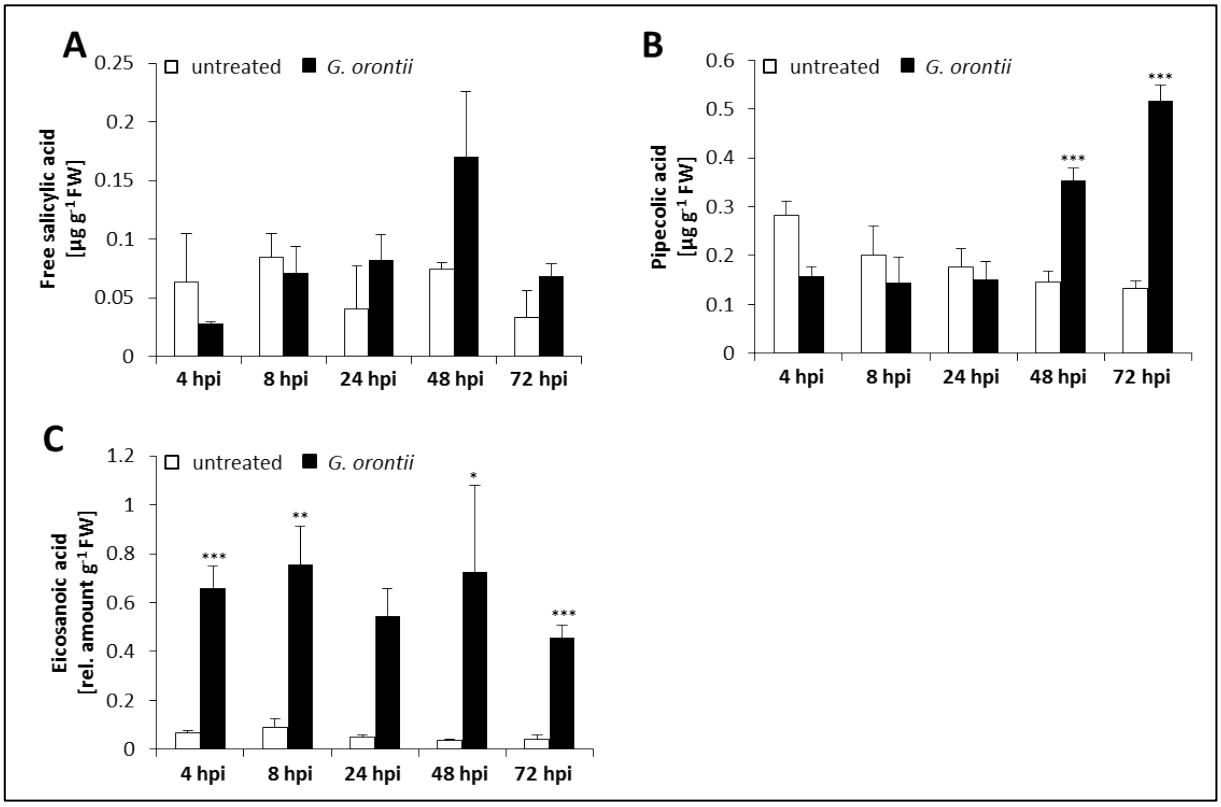

Supplemental figure 18. Metabolic profile of *Arabidopsis* plants infected with the powdery mildew fungus *G. orontii*.

The experimental setup was similar to the one described in figure 46. Accumulation of free SA (A), Pip (B), and eicosanoic acid (C). Asterisks above the bars show significant statistical differences between non-infected and infected plants (two-tailed *t* test; *, P< 0.05; **, P< 0.01; ***, P< 0.001). In contrast to the experiment depicted in figure 46, camalexin accumulation was not detected in this experiment. This experiment was done in collaboration with Dr Michaela Kopischke (University Göttingen; now TSL).

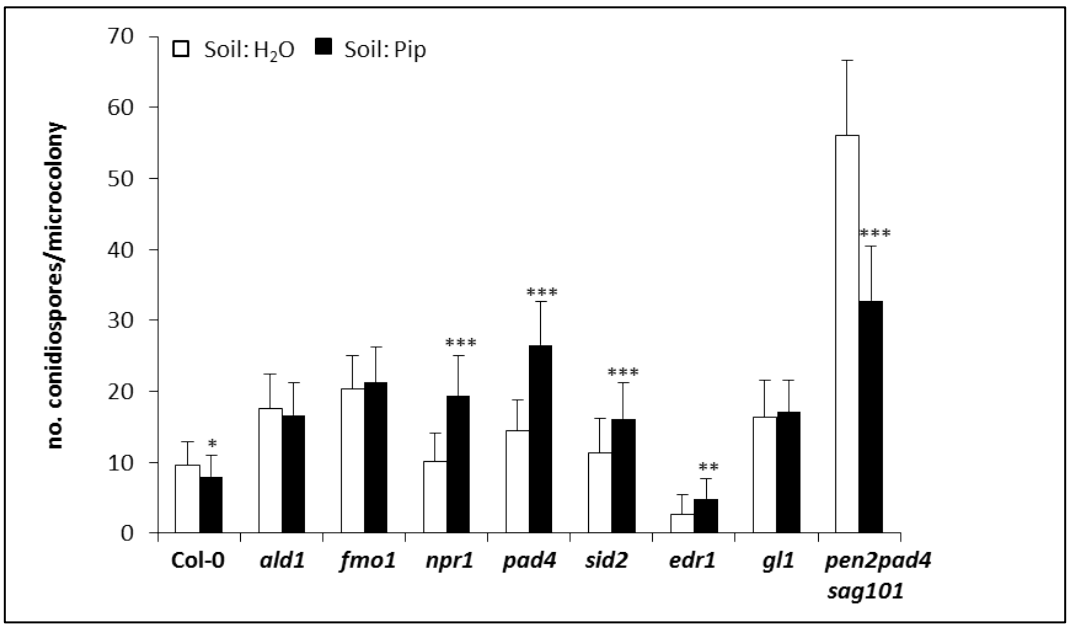

Supplemental figure 19. Exogenously applied Pip induces resistance against *G. orontii* in plants impaired in penetration resistance and SA-signalling.

Analysis of Pip-induced resistance against *G. orontii* was performed as delineated in figure 47. Asterisks above the bars show significant statistical differences between non-infected and infected plants (two-tailed *t* test; *, P< 0.05; **, P< 0.01; ***, P< 0.001). This experiment was done in collaboration with Dr Michaela Kopischke (University Göttingen; now TSL).

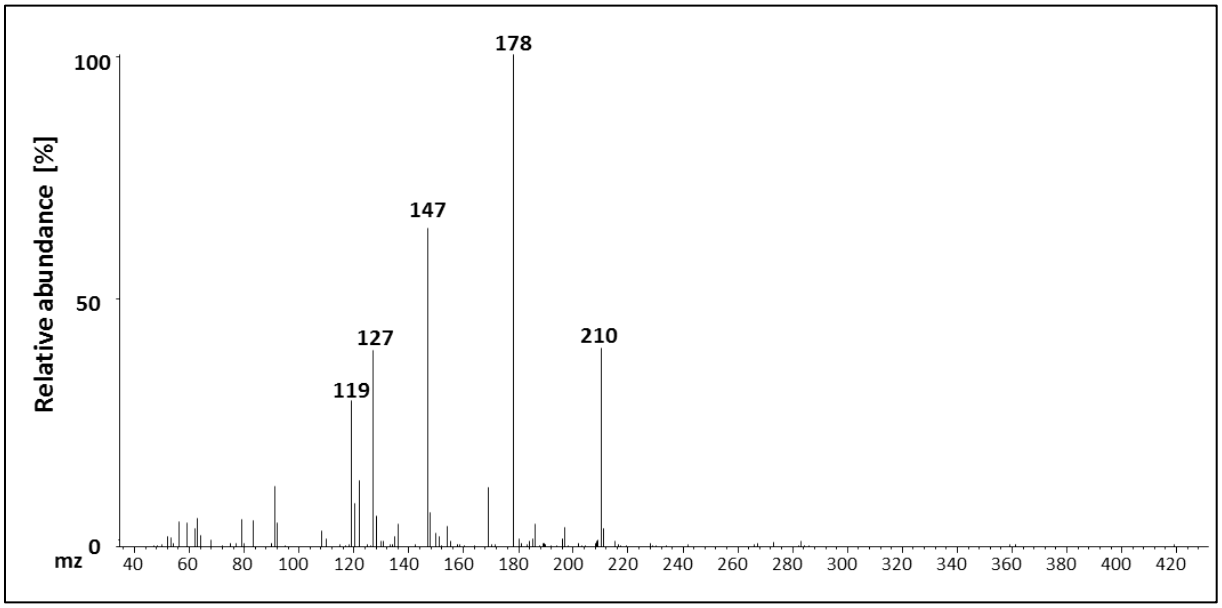

Supplemental figure 20. Mass spectrum for hydroxyterephthalic acid.

This substance was first detected in extracts from *B. cinerea*-infected *A. thaliana* plants. The extraction was done with the VPE method, the substance had a retention time of 18.10 minutes and as internal standard for quantification dihydrojasmonic acid was used.

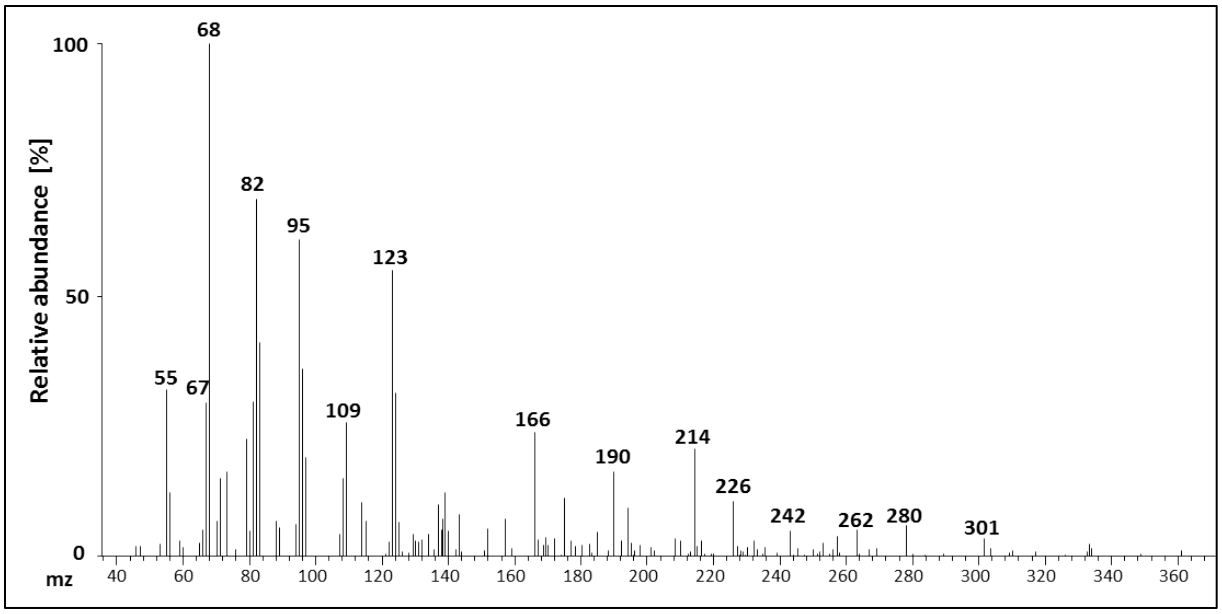

Supplemental figure 21. Mass spectrum for neophytadien.

This substance was first detected in *B. cinerea*-infected *A.thaliana* samples, extracted with the VPE method. The retention time was 21.17 minutes and as internal standard for quantification IPA was used.

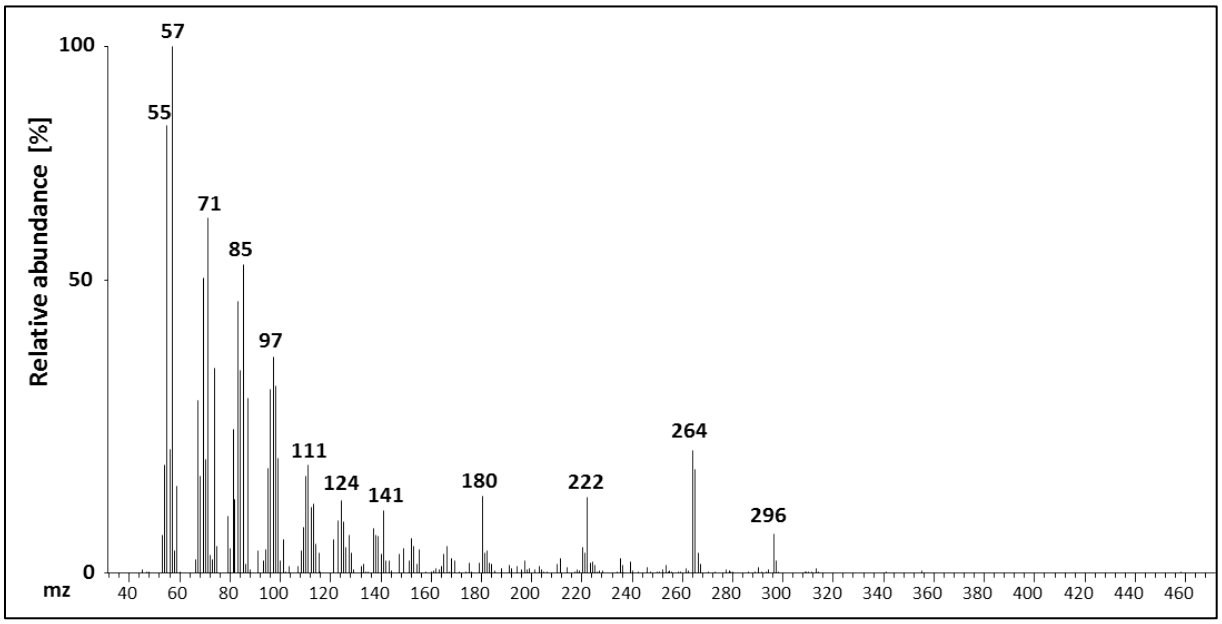

Supplemental figure 22. Mass spectrum for "unknown 1".

This substance was extracted first from *B. cinerea*-infected *Arabidopis* plants, had a retention time of 24.40 minutes and IPA was used as internal standard for quantification of the substance.

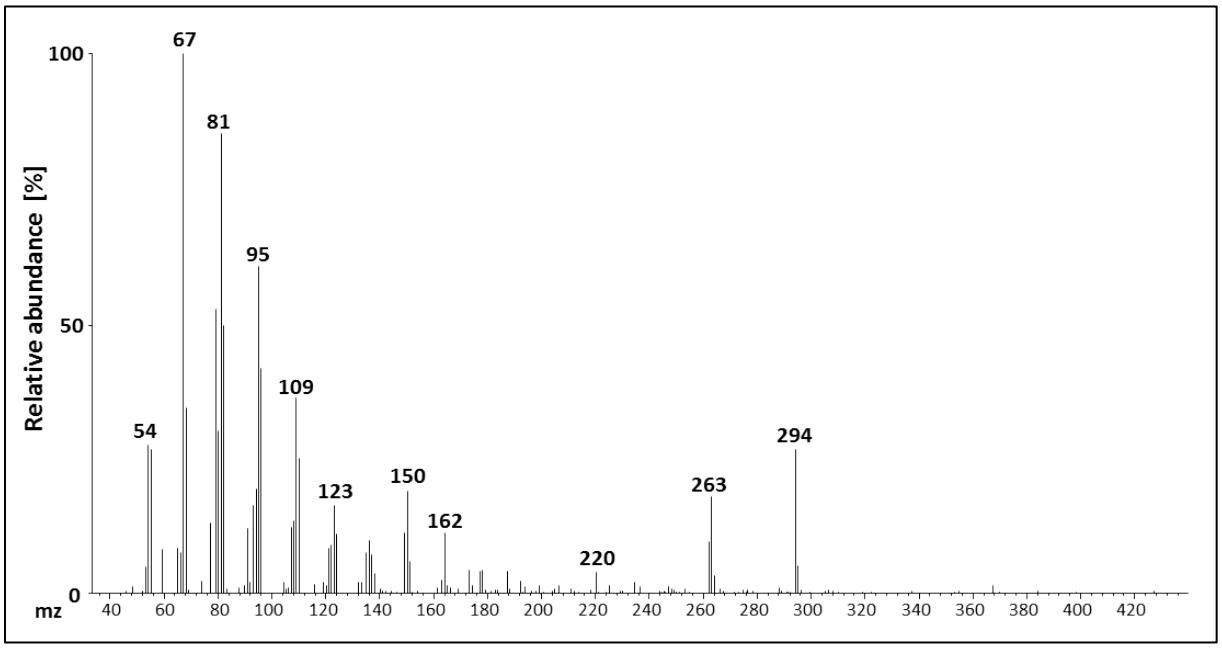

Supplemental figure 23. Mass spectrum for "unknown 2".

First detected in VPE extracts of *B. cinerea*-infected *A. thaliana* plants. The retention time for this substance was 24.30 minutes and IPA was used as internal standard for quantification.

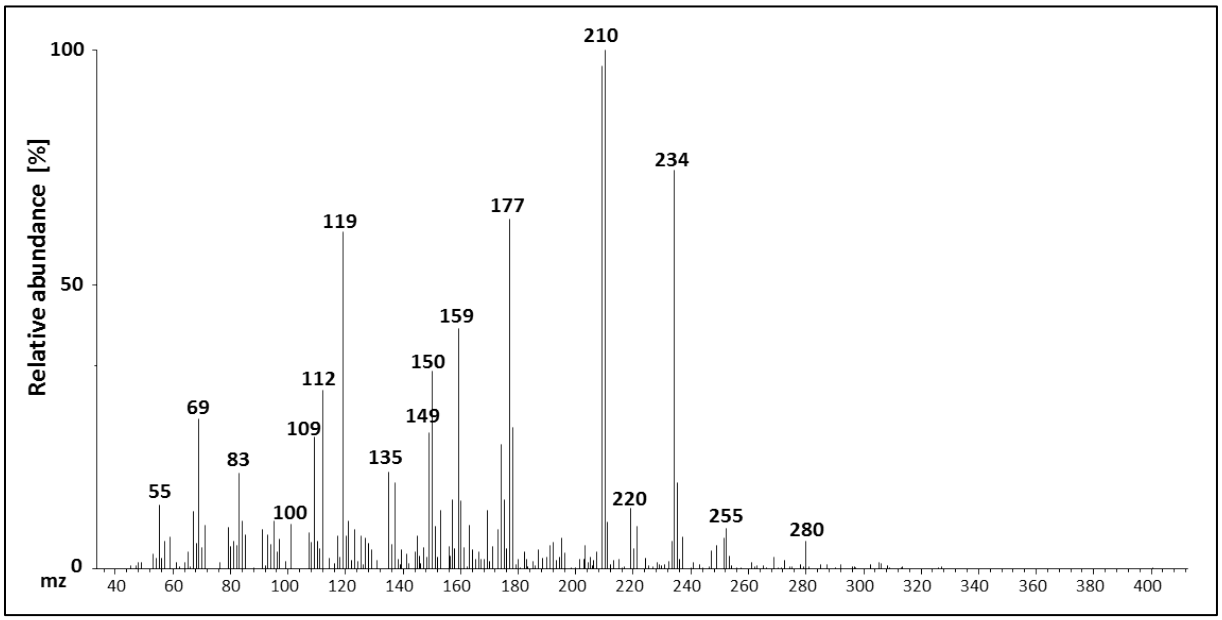

Supplemental figure 24. Mass spectrum for "unknown 3".

Detected in vapour phase-extracted *A. thaliana* leaves infected with *B. cinerea*. The substance had a retention time of 24.17 minutes and IPA was used as internal standard for quantification.

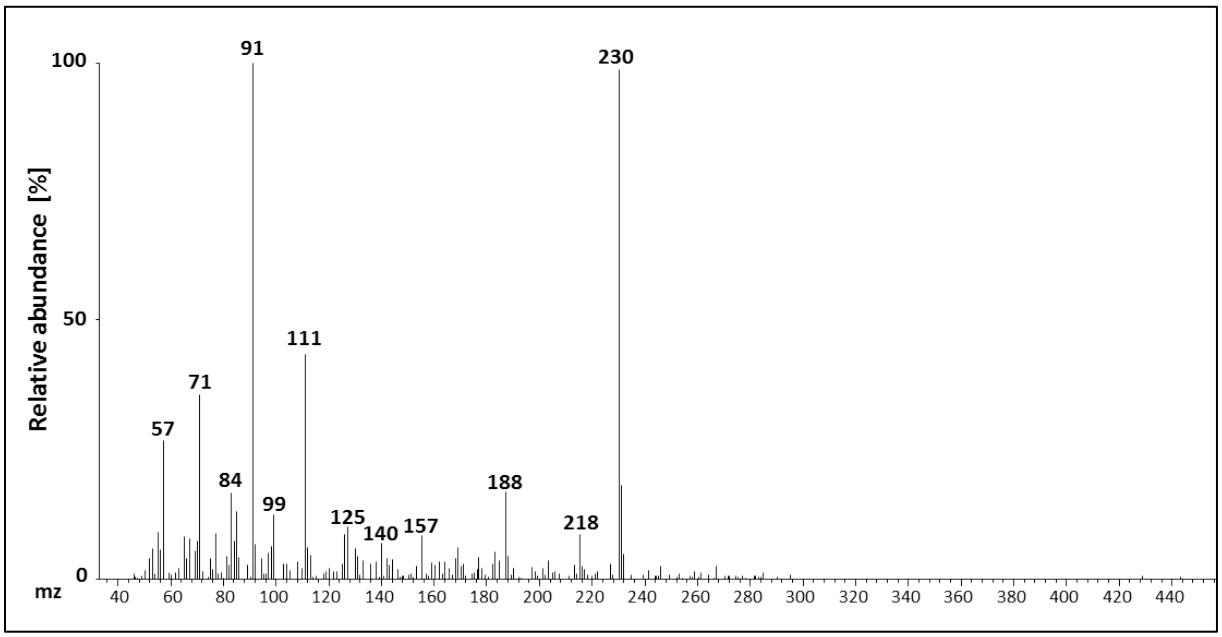

Supplemental figure 25. Mass spectrum for "unknown 9".

This substance was first identified in vapour phase-extracted samples of *B. cinerea*-infected *Arabidopsis* plants, had a retention time of 22.48 minutes and was quatnified using IPA as internal standard.

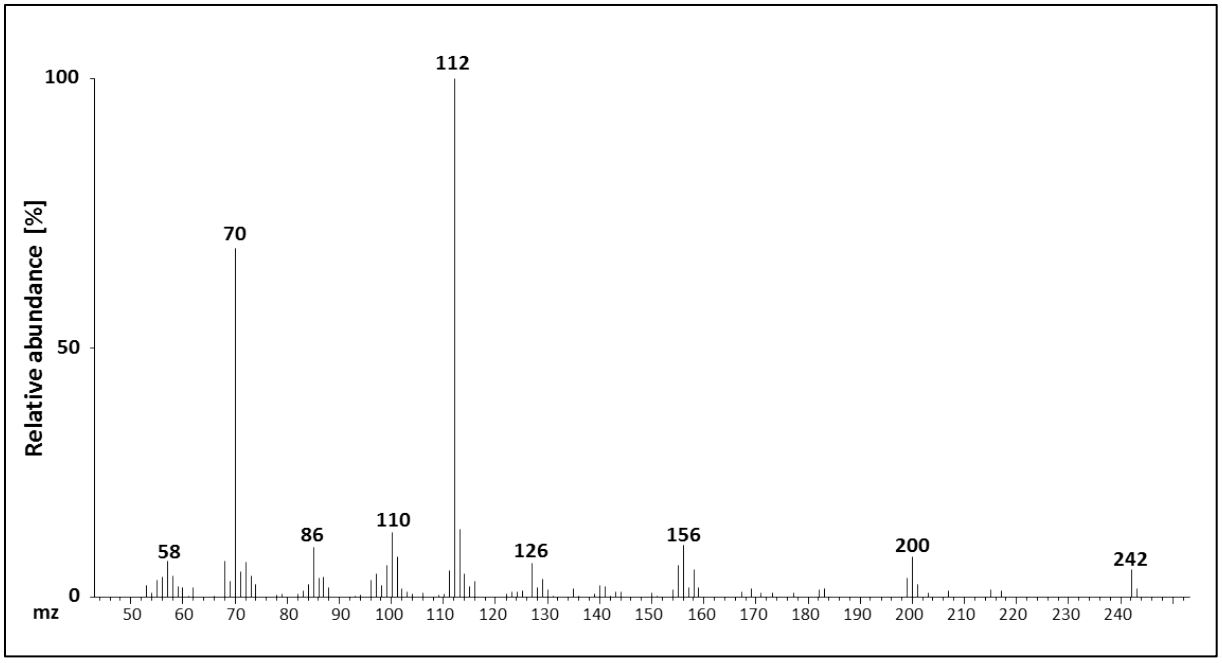

Supplemental figure 26. Mass spectrum for "unknown 13".

This compound was gained by extracting *B. cinerea*-infected *A. thaliana* leaves with the EZ:faast extraction kit for free physiological amino acids. The retention time for this substance was 18.16 minutes.

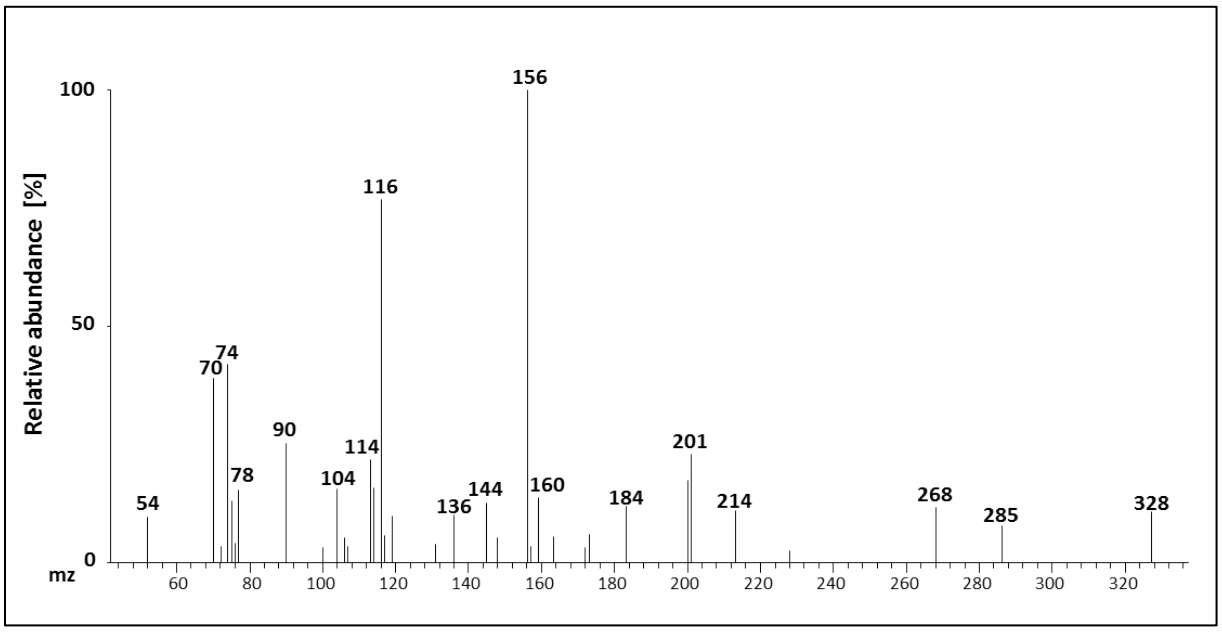

Supplemental figure 27. Mass spectrum for "unknown 15".

This metabolite was first found in *B. cinerea*-infected *Arabidopsis* leaf extracts gained with the EZ:faast amino extraction kit. This metabolite had a retention time of 15.58 minutes.

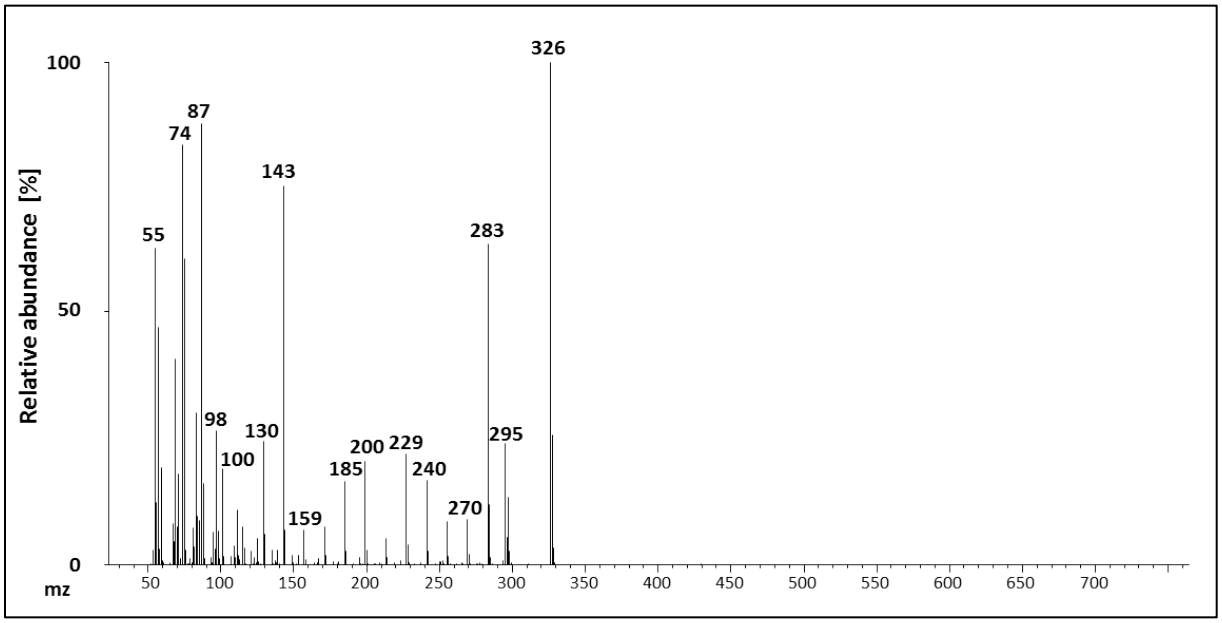

Supplemental figure 28. Mass spectrum of eicosanoic acid.

First found in vapour phase-extracted *A. thaliana* leaf samples infected with *G. orontii*. This substance had a retention time of 26.60 minutes and was quantified using IPA as internal standard.

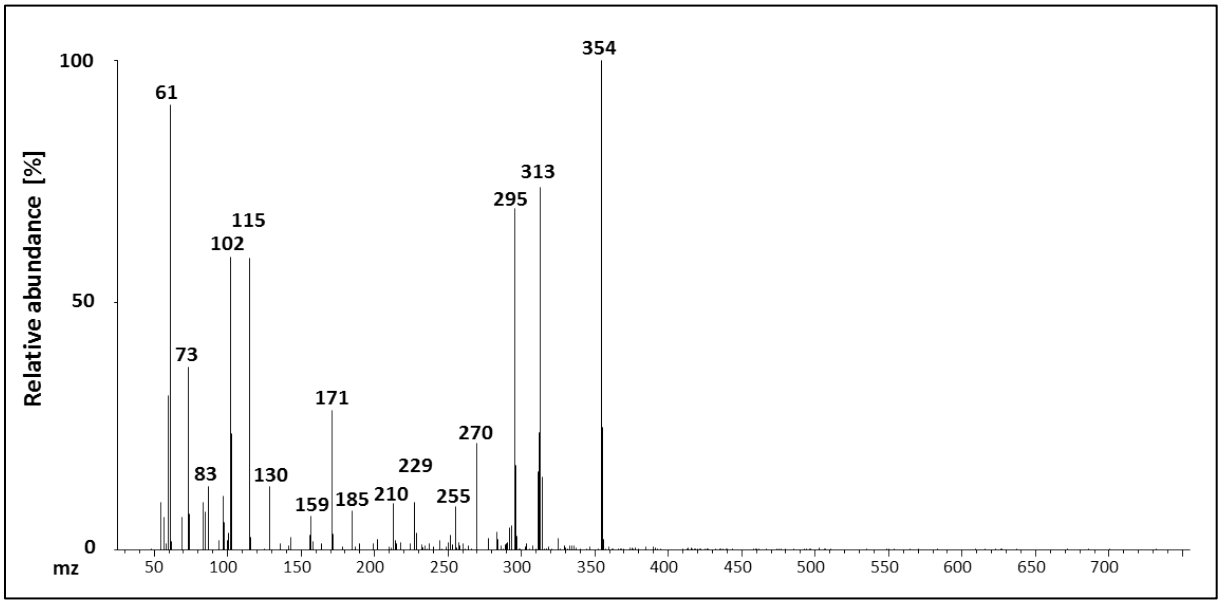

Supplemental figure 29. Mass spectrum for "unknown 22".

Unknown 22 was first vapour phase extracted from *G. orontii*-infected *A. thaliana* leaf samples. The retention time for this substance was 28.00 minutes and IPA was used as internal standard for quantification.

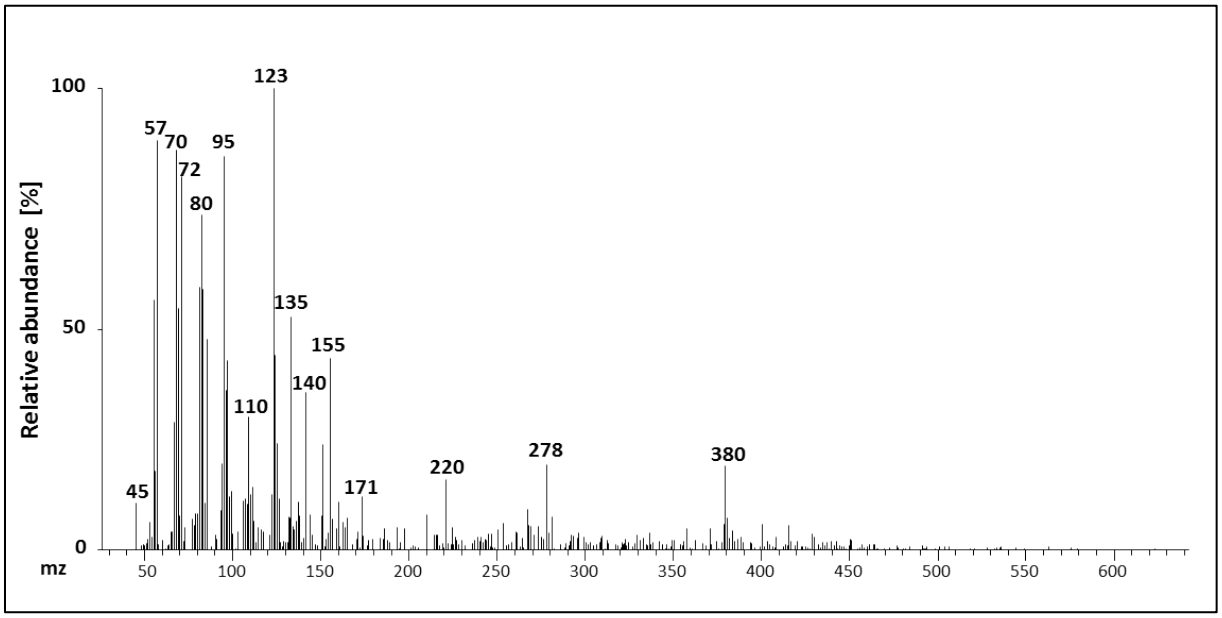

Supplemental figure 30. Mass spectrum for "unknown 28".

First identified in leaf samples of *Hpa*-infected *Arabidopsis* plants and extracted with the VPE method. This metabolite had a retention time of 30.55 minutes and was quantified using IPA as internal standard.

11 Acknowledgements

Ich möchte mich bei allen, die mich während der Promotionszeit, sei es im Labor oder daheim, unterstützt haben, sehr herzlich bedanken.
Ich danke meinem Doktorvater, Prof. Dr. Jürgen Zeier, für die Möglichkeit, in diesem spannenden Themengebiet zu promovieren, sowie für die interessanten Projekte und seine Anleitung in labortechnischen und akademischen Fragen.
Außerdem möchte ich Herrn Prof. Dr. Michael Feldbrügge sehr herzlich für die Übernahme des Koreferats danken.
Mein besonderer Dank gilt vor allem auch meinen Kollaborationspartnern, Prof. Dr. Volka Lipka und Dr. Michaela Kopischke in Göttingen, mit deren Hilfe etwas Licht in die Rolle von Pip in Pflanze-Mehltau-Interaktionen gebracht werden konnte. In Zusammenarbeit mit Dr. Kenichi Tsuda und Dr. Yiming Wang vom MPIZ Köln konnte die Rolle von MAP Kinasen in pflanzlicher Abwehr und Priming ein Stück weiter aufgeklärt werden und ich möchte mich ganz herzlich für die Hilfe und Unterstützung bedanken.
Dr. Stefan Schuck danke ich für die sorgfältige Lektüre meines Manuskriptes und der wirklich hilfreichen Korrekturvorschläge. Vielen Dank ebenfalls an Dr. Michael Hartmann für viele hilfreiche Ratschläge zum Thema Mikroskopie.
Eine einzelne Person kann noch so gut in ihrem Fachbereich sein, wenn das geeignete Umfeld nicht vorhanden ist, ist es sehr schwierig, gute Arbeit zu leisten. Ich danke meinen Kollegen Rike, Elia, Ziba, Stefan, Hanka, Michael, Stefan, Nicola und Tatyana für die freundliche und entspannte Arbeitsatmosphäre, sowie lebhafte Diskussionen und gegenseitige Hilfe bei arbeitsrelevanten und nicht so -relevanten Themen. Unserer TA, Karin, gilt mein ganz besonderer Dank, da sie als gute Fee ihr Bestes für einen reibungslosen Ablauf unseres Institutes gibt und immer ein offenes Ohr für Fragen, Anregungen und, ja auch Klagen, hat.
Für eine gute Arbeit sind Freunde außerhalb des Arbeitsumfeldes von ganz besonderer Bedeutung, da sie es schaffen, für Ablenkung und Erholung zu sorgen. Danke an Cori, Marc, Philip, Mathias, Vanessa, Alex, Claudia, Claus, Ede, Simone, Sven und alle, die ich hier aus Platzgründen nicht aufzählen kann.
Eine sehr große Unterstützung während der Promotionszeit war Familie Steimel, denen ich ebenfalls ganz herzlich danken möchte.
Mein größter Dank gilt meinem Gefährten Jochen Steimel, der mich während dieser oft auch anstrengenden Zeit nach Kräften unterstützt und auch wieder eine Zeit lang Fernbeziehung in Kauf genommen hat. Ich liebe dich!

12 *Curriculum vitae*

Anne-Christin Döring
Born July 21st, 1985 in Aschersleben (Germany)

Education

January 2011-September 2015 PhD, Heinrich-Heine-University Düsseldorf
October 2008-September 2010 Master of Science Biology, Ruhr-University Bochum
October 2005-June 2008 Bachelor of Science Biology, Ruhr-University Bochum
August 1998-June 2005 Theodor-Körner School (degree: Abitur), Bochum
August 1996-June 1998 Albert-Einstein School, Bochum
August 1992-June 1996 Fahrendeller primary school, Bochum

Publications

Bernsdorff, F., Döring, A.C., Gruner, K., Bräutigam, A., Schuck, S., and Zeier, J.: "Pipecolic acid orchestrates plant systemic acquired resistance and defense priming via salicylic acid-dependent and independent pathways";
Submitted to The Plant Cell

Návarová, H.; Bernsdorff, F.; Döring, A.C.; Zeier, J. (2012): "Pipecolic Acid, an Endogenous Mediator of Defense Amplification and Priming, Is a Critical Regulator of Inducible Plant Immunity"; The Plant Cell Vol 24, pp. 5123-5141;
www.plantcell.org/cgi/doi/10.1105/tpc.112.103564

Conferences

Botanikertagung 2013, September 29th-October 4th 2013; Oral presentation: "Pipecolic acid is an essential regulator of systemic acquired resistance and defence priming in plants"

Collaborations

August 2013-September 2014: Analysis of MAP kinase signalling in plant immunity in collaboration with Dr Yiming Wang and Dr Kenichi Tsuda (Max-Planck-Institute for plant breeding, Cologne)

April 2013: Analysis of *Arabidopsis*-powdery mildew interaction in collaboration with Dr Michaela Kopischke and Dr Volker Lipka (Georg-August-University Göttingen)

Experience

PhD thesis: "Exploring the role of pipecolic acid in defence priming and inducible immunity in *Arabidopsis thaliana*"

Master thesis: "Studies on *CIRCADIAN CLOCK ASSOCIATED 1* in *Arabidopsis thaliana* and *Arabidopsis halleri*"

Internship in microbiology: "Characterisation of the phycobiliprotein PC630 from *Chroomonas* sp. M1312"

Bachelor thesis: "Characterisation of the tyrosine aminotransferase 7 in *Arabidopsis thaliana*"

Teaching

November 2013-July 2014: Supervision of a Bachelor student; project: “Metabolite analyses in *Arabidopsis* interactions with fungal and oomycete pathogens” (HHU)
Winter semesters 2012/2013 and 2013/2014: Supervision of Bio120 (introduction into botany workshop) for first semester students (HHU)
August-October 2012: Supervision of project workshop of a master student; project: “Analysis of root exudates from *Arabidopsis thaliana*” (HHU)
Summer semesters 2011, 2012, 2013: Supervision of M-Module “Pflanze-Umwelt-Interaktionen: Gene, Proteine, Sekundärmetabolite“ for master students (HHU)
Winter semester 2011: Supervision of plant pathology workshop for bachelor students (HHU)
Summer semesters 2008, 2009, 2010: Supervision of plant physiology workshop (RUB)

Laboratory skills

Analysis of plant metabolites via gas chromatography (GC) and high-performance liquid chromatography (HPLC); Infection of plants with bacteria (*Pseudomonas syringae)*, fungi (*Botrytis cinerea, Golovinomyces orontii*) and oomycetes (*Hyaloperonospora arabidopsidis)*; RT-PCR; quantitative real-time PCR; lactophenol/trypanblue staining; enzyme assays (kinetic and analysis of final products); heterologous expression of proteins; SDS-PAGE and Western Blot; cloning of plant genes; analysis of bacterial growth by plating bacteria and counting colonies; preparation of insects; basic microscopy skills; Analysis of T-DNA insertion lines

13 Erklärung

Ich versichere an Eides statt, dass die Dissertation mit dem Titel „Exploring the role of pipecolic acid in defence priming and inducible immunity in *Arabidopsis thaliana* (L.) Heynh.“ von mir selbstständig und ohne unzulässige fremde Hilfe unter Beachtung der „Grundsätze zur Sicherung guter wissenschaftlicher Praxis an der Heinrich-Heine-Universität Düsseldorf“ erstellt worden ist. Ich habe keine anderen als die von mir angegebenen Quellen und Hilfsmittel verwendet. Diese Dissertation hat weder in gleicher noch ähnlicher Form einer anderen Institution vorgelegen. Ich habe bisher keine erfolglosen Promotionsversuche unternommen.

Bochum, den 14.05.2015

Anne-Christin Döring